Facoltà di Ingegneria Civile e Industriale

Dipartimento di Ingegneria Strutturale e Geotecnica

Dottorato di ricerca – XXX Ciclo

QUANTITATIVE FIRE RISK ASSESSMENT OF ROAD TUNNELS THROUGH ADVANCED CONSEQUENCE ANALYSIS

Candidate: Giordana Gai

Advisor: Prof. Enzo Cartapati

Co-Advisor: Ing. Michele Mazzaro

Dissertazione presentata per il conseguimento

del titolo di Dottore di ricerca

A.A. 2017/2018

To my family

Acknowledgements

I would like to express my gratitude to Prof. Enzo Cartapati for his scientific contribution during the development of my thesis.

I also thank the previous and current coordinators of the Ph.D. activities, Prof. Achille Paolone and Prof. Franco Bontempi, for their effort in supervising and improving my work.

My gratitude goes to the Italian National Fire Brigade, particularly to Michele Mazzaro, Chief of the Fire Investigation Unit, for placing his trust in me and helping me with his precious contribution. The fire officers Piergiacomo Cancelliere, Roberto Emmanuele and Fabio Alaimo Ponziani are also gratefully acknowledged for their daily suggestions and continuous support.

A special thank is addressed to my best friends Luisa, Marta, Mary and Roberta, for their loyal friendship and sincere encouragement during the most difficult times.

Finally, my deepest thank goes to my family, whose unconditional love and trust have always been the reason for my strength and my determination.

SYNTHESIS OF THE WORK

TABLE OF CONTENT

SYNTHESIS

SYNTHESIS OF THE WORK

Table of content

Synthesis

Abstract

The thesis is focused on the fire risk in road tunnels and its numerical estimation through quantitative risk analysis (QRA) supported by fire and evacuation modelling.
According to the in-force regulations concerning the Trans-European Road Network, the quantitative risk assessment is a mandatory step for existing tunnels that do not comply with the minimum structural safety requirements. When the risk does not reach the acceptability threshold, alternative configurations and mitigation strategies must be designed to reduce the residual risk under a suitable level, and again the QRA is useful to evaluate which choice is the best considering the actual risk reduction, in terms of Expected Value (EV) per year and cost-benefit ratio.
The thesis is divided in three macro-sections, which are intended to provide, on the one hand, an overall view of the complexity of road tunnel systems and, on the other hand, the possibility of a precise estimation of the consequences of a fire event through advanced modelling, in line with the state of the art of the fire safety engineering (FSE).
The first section introduces the reader to the topic of fire risk in road tunnels by the characterisation of their main features (traffic, systems, etc.), the statistics and the regulations which impose the QRA. In the second section, a detailed description of background aspects of tunnel fire safety is conducted; in addition, parametric studies aimed to assess the capabilities of models in a tunnel context are illustrated. The third section details the proposed methodology for QRA, which is finally applied to two cases studies of unidirectional and bidirectional tunnels.

Keywords

Quantitative Risk Analysis; Fire Safety Engineering; Road Tunnels; CFD modelling; Agent-Based Modelling; Ventilation Strategies; Pressurisation Strategies; Risk Assessment; Risk Mitigation; Frequency Analysis; Consequence Analysis; Human Behaviour.

Selected publications

Journal papers

1. G. Gai, P. Cancelliere, "Design of a pressurized smokeproof enclosure: CFD analysis and experimental tests", Safety 2017.

Conference papers

2. P. Cancelliere, M. Lombardi, L. Ponticelli, E. Gissi, G. Gai, M. Caciolai. "Italian Hybrid Fire Prevention Code", Proceedings of SAFE 2017 - 7th International Conference on Safety and Security Engineering, Rome, Italy.

3. G. Gai, P. Cancelliere, E. Carattin, E. Cartapati. "Numerical evaluation of RSET for road tunnels", Proceedings of IFireSS 2017, 7-9 june, Naples, Italy.

4. G. Gai, P. Cancelliere, M. Mazzaro, E. Cartapati. "Tuning procedure for evacuation models based on egress drills", Proceedings of IFireSS 2017, 7-9 june, Naples, Italy.

5. P. Cancelliere, L. Ponticelli, G. Gai, E. Gissi, M. Caciolai. "The new Italian fire code: a more perfomance-based approach to fire safety design", Proceedings of FireSS 2017, 7-9 june, Naples, Italy.

6. F. A. Ponziani, G. Gai, E. Cartapati, P. Cancelliere, M. Mazzaro, D. De Bartolomeo, M. Caciolai. "Comparison between experimental tests and computer models of a smokeproof enclosure safety vestibule", Proceedings of Interflam 2016, Windsor, UK.

7. G. Gai, E. Cartapati, P. Cancelliere, F. A. Ponziani, M. Mazzaro, D. De Bartolomeo, M. Caciolai. "Validation of premovement time distribution for evacuation modelling using real data from evacuation drill", Proceedings of Interflam 2016, Windsor, UK.

8. G. Gai, F. Gentili, "Influence of panic on human behaviour during emergency egress for tunnel fires", Proceedings of IF CRASC '15, 2015.

INTRODUCTION

1. INTRODUCTION

Chapter 1

Introduction

1.1. Road tunnels and fire risk assessment

The interest in studying tunnel fires has significantly increased in the last twenty years due to some major events that caused fatalities, injuries and damages. Mont Blanc, Tauern and St Gotthard tunnels are sadly known for the disastrous major fires from 1999-2001, highlighting the fragility of tunnels against fire hazard (Ingason, 2008). In fact, although the frequency of fires in tunnels is relatively low compared to accidents in open roads, the consequences of the events can be much more severe, mainly due to geometrical confinement, difficult smoke management and large travel distance for the evacuees.

Differently from what happens in railway tunnels, the human component is of primary importance in road tunnels (Shields, 2012). Before being evacuees, in fact, the occupants of the tunnels are drivers and passengers, which is important for fire and accident prevention (bad behaviour can be the cause of collisions) and potentially able to mitigate the consequences of a fire event in the very first phases (with extinguishing operations and/or signalling the alarm through SOS stations).

However, among the reported causes of fires, collisions are not the most important ones: the contribution of mechanical defects in the vehicles and electrical faults in the tunnel equipment are much more significant (Gehandler, 2015). Indeed, similarly to

railway tunnels, road tunnels are a complex environment, where a wide range of engineering aspects are deeply linked and contribute to its level of safety. For instance, from the geometrical point of view, a tunnel is a transition element of the road network, with the longitudinal dimension much longer than the lateral ones. It is a closed, confined environment, sometimes with poor visibility and people, even when frequent travellers, do not perceive this as a familiar element. People inside long tunnels are psychologically stressed and report feelings of boredom, monotony and claustrophobia. In other terms, their level of alertness can be high due to stress, but the environment (tunnel and vehicles) acts as a constraint on the occupants, whose behaviour can be extremely variable, making predictions uncertain.

Considering also the negative interaction between the tunnel and the human behaviour, the primary objective of the fire safety design should be to facilitate the evacuation process and of course guarantee tenable conditions along the escape routes for a safe evacuation. Prevention and protection play both a crucial role in this sense.

Preventive strategies help reduce the frequency of fire events. For this, the geometrical configuration is probably the most influential factor and with "geometrical" it is meant, for example, the shape of the cross section, the length of the tunnel, sense of travel (unidirectional or bidirectional), number of lanes, the longitudinal inclination, anomalies in the layout. Technical installations such as lighting panels, signage and paintings can be also considered as preventive additional measures, helping the drivers to find their way around a "familiar" environment, apart from being an assistance for the occupants in the evacuation phase (protective function) (Galea, 2014).

Protective strategies of the fire safety design aim to reduce the fatalities in case of a fire event and can be pursued through mechanical systems, primarily ventilation systems, pressurisation and fire-extinguishing systems with water.

The safety level of tunnels is very variable from country to country: if new tunnels can be "easily" designed providing a homogeneous safety level, for existing tunnels prove to be much more complicated. They have been built across long periods during which minimum requirements, that were imposed by the regulations, have significantly changed and where the refurbishment can be achieved with different practical solutions, with the agreement and the approval of designers, owners, stakeholders and jurisdictional authorities.

The attention of these factors is magnified when dealing with tunnel safety. On the one hand, fatalities and catastrophic events must be avoided, due to major fires from 1999-2001, that was followed by a dramatic increase in the risk perception against tunnel fires among society. On the other hand, considering that tunnels can be very long structures, the refurbishment through their entire length is generally extremely expensive in monetary terms and the fear might be if the cost is comparable to an equivalent benefit in terms of safety. Risk assessment and QRA try to answer that question.

The output of QRA is, in fact, a numerical estimation of risk of the adopted configuration in a tunnel (as built, reference or as designed), which can be negligible, acceptable or unacceptable depending on its magnitude. Therefore, a correct numerical estimation is the very first requirement when QRA is performed.

There is still no unique standard on how to effectively perform QRA in road tunnels. PIARC (2012) is currently the most used platform in Europe to gather data on risk evaluation, where the need of a "systemic approach" is recognised which takes into account the multiple components of human behaviour, traffic, operation and structure. Nevertheless, every Member State adopts a different procedure, not rarely based on very simplified analytical relationships between fire propagation and evacuation calculations, in spite of the "quantitative risk analysis" denomination. CFD models are

sometimes used to support these calculations; however, the use of simplified models seems obsolete considering the current computational power and the three dimensional effects in fire dynamics inside a confined environment (turbulence effects, high temperatures, interaction with ventilation flow). Furthermore, the monetary impact on society of the decisions made by the authorities among the proposed, and quantified, engineered solutions is significant; hence, the accuracy in the calculations may support cost optimisation and higher efficiency.

For this reason, it should be considered that the strength of using QRA lies especially in the context of the risk assessment of existing tunnels; that is in the possibility of comparing different mitigating strategies and engineered solutions in order to be able to make an aware decision driven by evidence of risk reduction and cost-benefit analysis. As it will be shown in the Chapter 9 and 10, by using QRA based on advanced models the effect of the safety measure (preventive or protective) can be represented in the FN diagram, where F is the back-cumulated frequency and N is the number of fatalities. This graphical representation allows to immediately read which measure is the most effective in reducing the overall risk or decreasing the expected number of fatalities for low-frequency events.

In this context, the attention of researchers in studying tunnel fires through advanced computer models and quantitative risk analysis can be understood and justified.

In the following section, the aim of the thesis and its content are described.

1.2. Aim of the thesis

The aim of the thesis is to highlight the possibility of conducting QRA through the combined use of CFD and evacuation modelling in order to obtain a detailed

description of the consequences of a tunnel fire in terms of fatalities and, possibly, injuries.

The process is divided into three macro-sections whose content is described below.

The first section is named "Fire risk for road tunnels" and is composed by three chapters (2, 3 and 4) intended to introduce the reader to the topic of tunnel fires, with a special focus on European and Italian context.

Chapter 2 contains a description of the recurring features of road tunnel systems that contribute to the overall complexity. This includes traffic characteristics, safety systems, ventilation and pressurisation strategies, all aspects that must be considered if one wants to carry out a systemic analysis of tunnels.

Chapter 3 consists of statistics of past accidents and fires and includes a review of case history which lead to the development of the in-force regulations such as the European Directive 2004/54 (EC) and the NFPA 502 (US). The case history is important to understand why the fires generally occur and develop and in which conditions the damages are likely to be severe in terms of lives and economic losses. The chapter contains also a section dedicated to the Italian context, with data acquired from the Fire Department of the yearly fire fighting operations on road tunnels in the period 2011-2016, which confirm that tunnels are potentially risky systems.

Chapter 4 is focused on the concept of risk, risk analysis and risk assessment. It includes, for example, the difference between individual risk (IR) and societal risk (SR), among qualitative, semi-quantitative and quantitative risk analysis as well as the acceptance criteria and thresholds currently used in some Member States.

The second section is named "Background aspects of tunnel fire safety" and is composed by three chapters (5, 6 and 7) which respectively focus on fire action, materials and structural behaviour and evacuation in tunnels.

Chapter 5 is aims to review full-scale tests performed in Northern Europe and the US, which for the first time gave the chance to measure the maximum temperature reached in tunnels and to establish reference values for back layering, critical velocity, fire load and the expected Heat Release Rate (HRR). Then, recommendations on fire scenarios based on literature and engineering evidence are provided (position, HRR and duration of the fire). Finally, a wide section is dedicated to fire modelling, from the nominal curve to the zone and field models; specifically, Fire Dynamics Simulator (FDS) is described in its main features. In addition, the results of an independent parametric study are reported, considering some of the parameters commonly used for tunnel fires and generally in the FSE approach (grid resolution, HRR, fire source dimensions, soot yield, material type, presence of vehicles, length of the external boundary, longitudinal inclination, initial temperature).

Chapter 6 is dedicated to the behaviour and resistance of all types of materials that can be found in road tunnels: from non-structural materials (signage, components of ventilation systems and so on) to the prevalent structural material used in tunnels, which is reinforced concrete. Considerations on the spalling phenomena at high temperatures are also made.

Chapter 7 is focused on the emergency evacuation and human behaviour in tunnels. Recommendations are made for the parameters normally used to describe the behavioural scenarios, together with a description of the tenability criteria, which are to be used in case of verifications of safe evacuation during fires. The challenge and the limitations of the modelling evacuation phenomena are also presented by describing the state of the art in the field and classifying the models internationally recognised. Sensitivity analysis is conducted for FDS+Evac and Pathfinder, as a preliminary assessment of the models before using them in the tunnel domain.

The third section is named "Proposed procedure and applications" and is composed by three chapters (8, 9 and 10) which focus on the description of each step of the methodology proposed for the QRA and highlight its potentialities through the numerical application to two case studies.

Chapter 8 provides a detailed description of the methodology used to conduct QRA using advanced models of fire and evacuation. Information on fire and evacuation scenarios is given as well as the hypothesis made for the choice of the length of the tunnel model.

Chapter 9 contains the quantitative risk analysis carried out for a 2.7 km long double tube - unidirectional road tunnel, based on an existing tunnel. The tunnel does not comply with the requirements of the European Directive concerning the maximum distance between two consecutive escape routes. No additional emergency exits can be added to the tunnel, therefore alternative measures are studied and evaluated in terms of Expected Value (EV) and back-cumulated frequency – fatalities (FN) curves.

Chapter 10 has the same structure of Chapter 9 but the case study is represented by two bidirectional road tunnels (1.367 km and 0.6 km), connected through two rockfall tunnels (with lateral openings along one side) and one central short tunnel. The peculiarity of this case study is that the five tunnels (overall length is 2.410 km) are connected from the point of view of the egress system, because no emergency exits are present in the actual configuration, but might be disconnected in thermo-fluid dynamics terms thanks to the lateral openings of the rockfall tunnels. QRA is performed for the tunnels in the initial configurations with additional measures designed to mitigate the risk.

Appendix A contains an in-depth analysis of the pressurisation of a small enclosure, with its experimental and numerical characterisation.

Appendix B and C describe respectively the governing equations of FDS and the complete results of the parametric study introduced in Chapter 5.

Finally, Appendix D contains a sensitivity analysis of the QRAM software.

SECTION 1: FIRE RISK FOR ROAD TUNNELS

Chapter 2

Overview on the characteristics of road tunnels

2.1 Factors of complexity

In the fire safety field, a generic system is considered "complex" in relation to the intensity of the fire hazard, the geometrical layout of the building and the occupant load. For road tunnels, other factors can be added to the previous list (PIARC, 2007): for example, traffic conditions, vehicles interaction, mechanical equipment and so on (Beard et al, 2012).

Fire hazard in tunnels is high (Carvel, 2004). The fire load of the vehicles in transit can account for several GJ and fire growth rate is generally fast or ultrafast, with peaks of Heat Release Rate (HRR) variable between 6 to 200 MW, most of the times reached within 10-15 minutes from the ignition time (PIARC, 2017). Moreover, apart from vehicles, electrical systems contribute to fire hazard. In Chapter 3 the statistical data on accidents and a review of case history of major tunnel fires will be detailed.

Compared to multi-storey buildings or multi-connected and irregular compartments, the geometrical layout of tunnels is, apparently, simple. However, the long extension of the tunnel together with the confinement act by the structure on the inside can facilitate the smoke propagation in the longitudinal direction, where most of the evacuation process takes place (Carvel, 2005; Carvel et al, 2016).

Considering the occupant load, it must be noted that the number of people who can be involved in a fire evacuation is variable depending on the position of the tunnel in the road network and the period of reference. For example, if one considers the traffic fluctuations over the course of a year, an extremely large traffic volume and a long queue can be noticed in the period of holidays in parts of the road network that are much less congested during the rest of the year. Normally, the adoption of the AADT (Annual Average Daily Traffic) as a reference value for traffic volume avoids choosing exaggeratedly conservative or underestimated values. In addition, the vicinity of the tunnel to touristic attractions gives information on the prevalent characteristics of the occupants (for example, young groups or buses of elderly for holiday trips).
In the following paragraphs, further information is provided considering the vehicle, human, infrastructure and operational factors in relation to fire events.

2.1.1 Vehicle factor

The technical characteristics of vehicles, with regards to the material composition, the performance of the mechanical system and the reliability of the safety devices play a crucial role in two aspects of fire prevention. In fact, vehicles can determine the occurrence of a fire accident due to collisions with other vehicles or to the failure of mechanical parts (engine problems or overheating of the braking system). In addition, the increasing percentage of plastic materials in modern vehicles affect the average fire load of traffic volume resulting in a higher expected HRR (Collier, 2011).
Considering heavy goods vehicles (HGVs), with average experienced drivers, their presence in the traffic volume affects negatively the motion of the vehicles, acting as a constraint to the normal flow. Moreover, it is no coincidence that all major fires involved at least one or more HGVs, which can lead to very severe fires, with a heat release rate up to 100-200 MW and a duration of hours (see Chapter 3). For safety

reasons, the drivers of HGVs should carry a fire extinguisher, but in case of collision, it could be difficult to stop the growth of the fire and extinguish it.

The transport of dangerous goods is disciplined by specific regulations (European Agreement concerning the International Carriage of Dangerous Goods by Road, briefly called ADR) and will not be treated in the thesis.

2.1.2 Infrastructure factor

The term "infrastructure" includes many relevant aspects of tunnels: geometry, equipment, traffic load, safety systems and more. All these aspects, in different ways, are influential for the prevention and the protection against accidents and fires.

For existing tunnels, a large variability can be found among the geometrical and functional layouts from tunnel to tunnel. The evolution of these standards (national and European) can be easily observed through different characteristics of tunnels: modern and new layouts are in contrast with old and inadequate sections that need refurbishment.

Considering traffic conditions, road tunnels can be unidirectional or bidirectional depending on the number of tubes chosen in the design phase: the choice is not free and depends on the predictions on traffic volume in the following 15 years. If it exceeds 10000 vehicles per lane per day, two tubes are necessary according to the geometrical requirements of the European regulations. The two possibilities (double or single tube for bidirectional traffic) lead to different scenarios in terms of probability of collision and stress of drivers.

Regarding the geometry of the cross section and the carriageway, the shape of the former largely influences the comfort of drivers. In addition, another geometrical factor that contributes to the risk of an overheating engine and brakes is the longitudinal slope that, generally, is detrimental for the quality of driving conditions.

The safety equipment and the mechanical systems can compensate the deficiency of the geometry in some ways. For instance, a good lighting system could be helpful to contrast the effect of constraint that drivers report in tunnels, other than helping people to orientate correctly in case of fire and smoke propagation. The ventilation system (detailed in section 2.3), in normal operations, is also an answer to obscuration due to pollution, thus it helps to maintain a good level of visibility conditions.

2.1.3 Human factor

As previously mentioned, the human factor significantly contributes to the complexity of the road tunnel systems. The presence of people is both negatively and positively influential for some aspects of tunnel safety:

1. incorrect behaviour of drivers can represent the cause of an accident;
2. the overall evacuation time is determined by the amount of people, their level of alertness and their distribution within the tunnel;
3. the occupants of the tunnel can potentially start firefighting operations with the use of fire extinguishers and by transmitting the alarm.

The first aspect is related to fire prevention and behaviour of drivers, which is strongly determined by cultural and social aspects (overtaking frequency, maintenance of the safety distance among the preceding vehicle, obeying road signals, etc.). The second aspect will be addressed in Chapter 7. The third aspect is related to fire protection but is strictly linked to previous experiences and personal attitudes of the occupants (Galea, 2015).

The geometry of the tunnel can affect positively or negatively the behaviour of drivers. In fact, frequent users of the tunnels may be familiar with its geometry and safety equipment, but generally, drivers and passengers do not pay attention to them, although their behaviour may unconsciously change regarding open sections.

Some geometrical critical points are impossible to eliminate in road tunnels like, for example, the irregularity of visibility conditions at the portals (Figure 2.1), which are often responsible for anomalies in the traffic flow (see section 3.1). Similarly, the lateral confinement of the walls is responsible for deviations of the vehicle's trajectory from their original pattern. This is an effect of the drivers-tunnel interaction, related to psychological stress.

In Chapter 7, the peculiarity of the evacuation from road tunnels will be detailed.

Figure 2.1. Irregular visibility conditions at portals (google search)

2.1.4 Operational factor

The operational conditions of the tunnels depend mainly on the appropriateness of the maintenance, which include several activities going from the management of traffic volume and equipment to tests, verifications and interventions of refurbishment (PIARC, 2008). The normal operation is as important as the emergency operation: the former, in fact, acts as a preventive measure, aimed to avoid failures of the tunnel's equipment, while the latter is crucial to limit the severity of the consequences for people, structure and environment.

The Mont Blanc tunnel is an example of how the mix of an absence of refurbishment, obsolete means of egress design and, finally, inadequacy of safety management was the

triggering event that led to 39 fatalities and huge structural and economic losses in a major fire that occurred in 1999. The event has been widely studied by researchers and authorities but still the information is contradictory when it comes to responsibilities of French and Italian management. Certainly, there was a lack in coordination between the two countries, which, thanks to the lesson learned, is something that now is particularly taken into account for tunnels connecting different countries. In Figures 2.2 and 2.3 (A-B) some pictures of the Mont Blanc tunnel are reported, respectively for the old and the new design: a modern and well visible design of the means of egress replaced the refuges, which are now forbidden for both existing and new tunnels.

Figure 2.2. Old configuration of Mont Blanc tunnel

Figure 2.3A-B. New design of the Mont Blanc tunnel

2.2 The safety equipment

The safety measures differ from tunnel to tunnel, mainly depending on three characteristics: length, number of tubes (unidirectional or bidirectional traffic conditions) and traffic volume (congested or not).

The safety measures consist of escape routes, distance between emergency exits, SOS stations and lay-by but also ventilation, detection, alarm and lighting system. Sprinklers and air curtains are specific protective measures in long tunnels, useful to control the fire and to limit the propagation of the effects along the tunnel.

While for new road tunnels the safety requirements are well specified and the achievement of a good standard is possible, a large number of existing road tunnels present a significant lack in one or some safety measures, due to inadequate design or compliance with old (and now obsolete) regulations.

Filling these holes in the fire safety design is not always possible due to geometrical constraints or because it is not convenient according to cost benefit analysis. For each specific case, other alternative measures must be designed with the objective of mitigating the residual risk. In Chapter 9 and 10 two case studies of existing road tunnels that only partially comply with the regulations will clarify this aspect.

In the following paragraphs, passive and active fire protection systems will be briefly described.

2.2.1 Passive fire protection systems

The passive fire protection measures must be integrated in the tunnel system.

Fire requirements of the structural and non-structural components regard the fire behaviour and resistance. Considering the latter, normally fire resistance of a tunnel lining must be guaranteed for a range of 60-120 minutes of the design fire.

The escape routes are another fundamental protective measure: they can be direct exits, by-pass to the other tube (Figure 2.4) or a suitable emergency tunnel, escape routes leading outside (no refuges are permitted).

Figure 2.4. Emergency exit of the Mrazovka (Praga) tunnel

2.2.2 Active fire protection systems

The active fire protection system may involve several technological equipment depending on the type of tunnel.

They involve, for instance, hydrants, sprinklers, mechanical ventilation (emergency mode).

In the field of fire control and extinguish systems, many innovative and highly technological solutions are being developed. Some of them are unique systems and already part of the existing tunnels, like the system recently inserted in the Gran Sasso tunnel (Figure 2.5).

Figure 2.5. The active fire protection system of the Gran Sasso tunnel

2.3 Ventilation strategies

Ventilation is necessary in road tunnels for two reasons. In normal conditions the ventilation, natural or mechanical, is needed to keep a good quality of air. In fact, the emissions of toxic gases must be controlled and diluted for the health of users and the maintenance of the visibility conditions within safe levels. On the other hand, in case of a fire, the ventilation must be able to control the spread of hot smoke, without destroying the stratification for a certain period useful for people escaping, but diluting toxic gases in order to minimise damages to structures, installations, equipment and other vehicles.

For short tunnels and when traffic is not congested, natural ventilation induced by the so-called "piston effect" might be able to guarantee safety conditions for users. This effect is sometimes guaranteed in short tunnels (no more than 500 m) with unidirectional traffic flow at least of 50 km/h. Otherwise, mechanical ventilation systems must be correctly designed considering the unique characteristics of the tunnel with the purpose of being operative in two modes (normal and emergency). In addition, the design of the mechanical ventilation should consider the meteorological conditions at the portals, which can cause difference of pressure between the entrance and the exit portal especially for very long tunnels (Borchiellini et al, 2009).

The European regulations and guidelines (RABT, 2006; PIARC, 2012) provide recommendations and best practice for the design of ventilation systems.

In the following paragraphs, the operating principles of some ventilation systems are described, from the most common to the most innovative solutions.

2.3.1 Longitudinal ventilation systems

A longitudinal ventilation system is aimed to establish a stable longitudinal flow of air along the tunnel. This can be created by local speed-up of air along the tunnel through jet fans (Fig. 2.6 A) or introducing fresh air through large axial fans (Fig. 2.6 B).

The most used solution is based on a series of jet fans, suspended from the ceiling level and blowing high-velocity air, thus establishing a steady flow through the whole tunnel. This longitudinal flow should, for example, be able to prevent a backlayering formation in case of a fire (this condition is generally considered to be verified if the average velocity on the cross section of the tunnel exceeds the critical velocity v_{cr}). Fresh air is introduced only by the entrance portal while exhaust air, with pollutants or smoke, is discharged outside through the exit portal.

Other solutions are based on large central fans injecting fresh air immediately after the entrance portal or at the middle of the tunnel and discharging exhaust air through the opposite portal or exhaust airshafts.

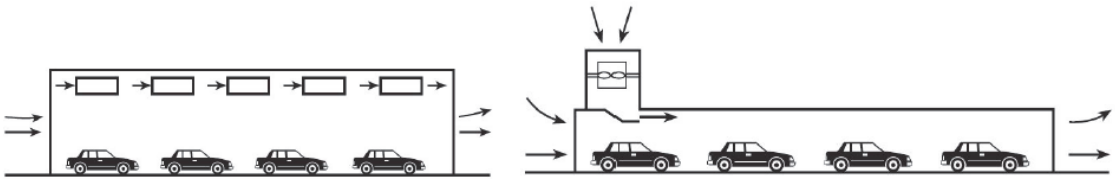

Figure 2.6 A-B. Longitudinal ventilation systems (NFPA 502, 2011)

The jet-fan solution seems to be the most convenient to establish a stable longitudinal airflow along the whole tunnel without requiring large amounts of space to insert central axial fans. Nevertheless, in case of a fire, some negative effects can occur. For example, it has been tested experimentally and confirmed numerically that jet fans placed next to the fire source should be disabled to avoid mixing phenomena between smoke and fresh air that might facilitate the growth of the fire source.

Longitudinal ventilation systems provide usually good solutions for medium length, unidirectional, non urban tunnels with free flowing traffic. Smoke is mechanically exhausted in the direction of the traffic circulation so that clear tenable conditions to escape are obtained upwind the fire.

The concept of critical velocity is crucial when designing the number of jet fans for a given tunnel. Roughly, it is often considered that the critical velocity for a tunnel is 3 m/s, ignoring the fact that this is not a fixed threshold. In fact, the critical velocity is a function of the geometry of the tunnel (height and area of the cross section, longitudinal slope), the heat release rate of the fire in addition to the characteristics of the incoming air, in terms of density, specific heat and temperature. The following equations 2.1 and 2.2 (NFPA 502, 2011) allow to iteratively do simple calculations to obtain the value of the critical velocity at steady state conditions. The results are plotted in Figures 2.7 A-B and 2.8.

$$V_{cr} = K_1 K_g \left(\frac{gHQ}{\rho C_p A T_f} \right)^{\frac{1}{3}} \tag{2.1}$$

$$T_f = \left(\frac{Q}{\rho C_p A \, V_{cr}} \right) + T \tag{2.2}$$

In Figure 2.7 A it is shown that fixing the height of the tunnel to a hypothetical value (e.g. 6 m) the critical velocity increases by diminishing the area of the cross section (that is, the width of the tunnel). This, in fact, implies a higher velocity of the hot smoke considering the same level of HRR (more dispersion is provided with large sections).

Figure 2.7 B instead shows that by fixing the area of the tunnel (e.g. 80 m^2) the critical velocity increases with the height of the tunnel (less than linearly). In other terms, it increases by decreasing the width of the tunnel.

From Figure 2.8 it appears that the longitudinal slope has little influence on the critical velocity, especially for low HRR. The negative longitudinal slope corresponds to the

development of a chimney effect in the opposite direction of the ventilation flow, whose performance should be, therefore, higher compared to that of zero slope. It is noticed that to be conservative, for positive longitudinal slopes the critical velocity is kept as for a zero slope.

The higher the critical velocity is, the higher the volume flow that jet fans or axial fans should provide in order to contrast backlayering for the selected HRR.

CFD simulations can be used if one needs a more detailed and reliable evaluation of the critical velocity.

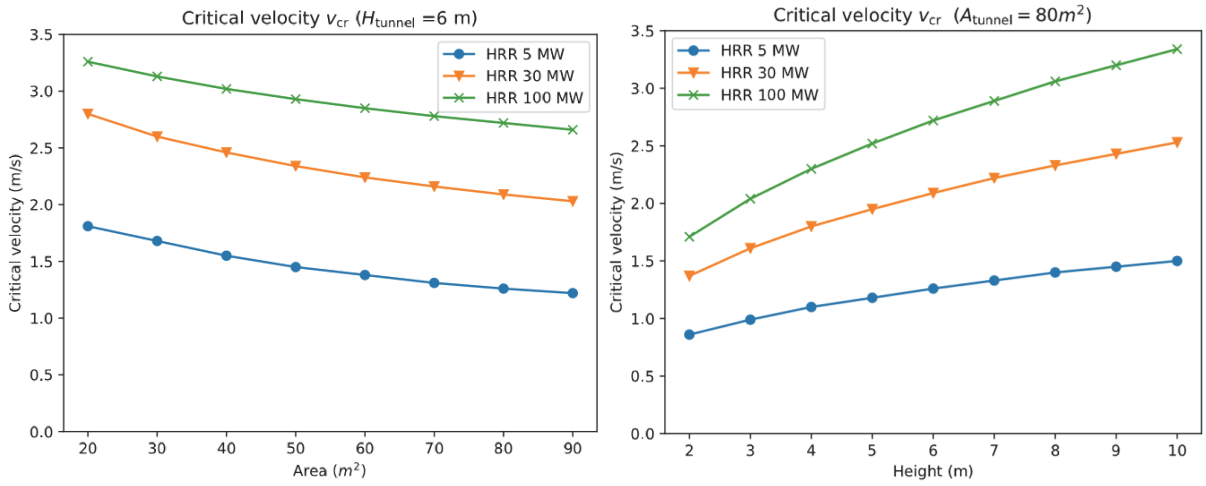

Figure 2.7 A-B. Critical velocity for different HRR by increasing area and height of the tunnel

2.3.2 Transverse ventilation systems

Fully transverse ventilation systems are equipped with supply and exhaust air ducts throughout the length of the tunnel roadway (Figure 2.9). When a fully transverse system is deployed, the majority of the pollutants or smoke discharges through stacks, with a minor portion exiting through the portals. In this case, the longitudinal direction of the velocity is coupled with a vertical component induced mainly by smoke extractors.

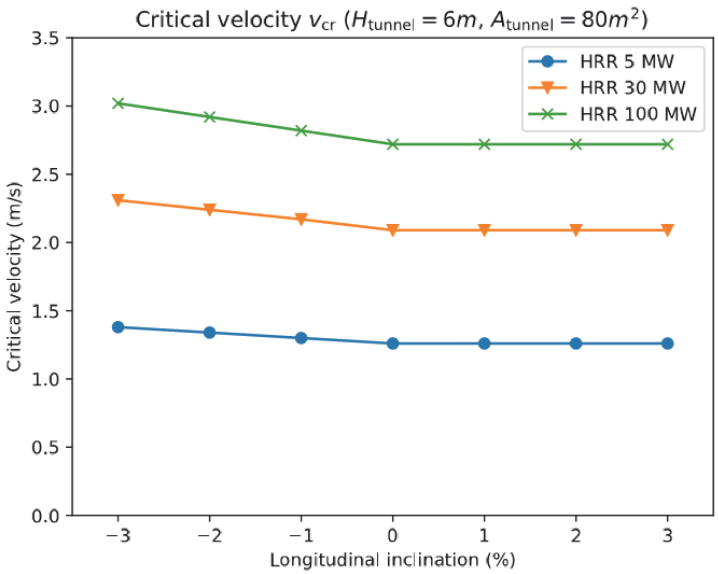

Figure 2.8. Critical velocity for different HRR by varying the longitudinal slope

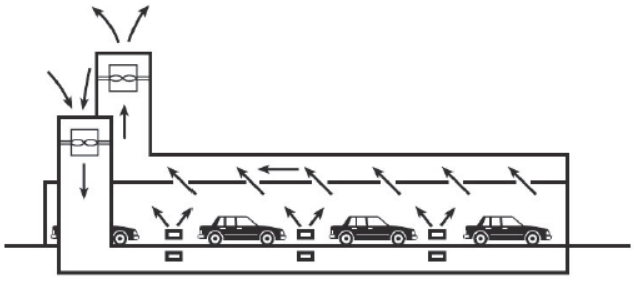

Figure 2.9. Transverse ventilation system (NFPA 502, 2011)

A fully transverse ventilation system can be either balanced (exhaust equals supply) or unbalanced (exhaust is greater than supply). The position of the air ducts is defined during the design phase: usually the injection and extraction of the air is obtained at the ceiling level, where there is a plenum, but, in some cases, a similar system is positioned at the side wall. However, there are cases with a supply of fresh air at the floor level and extraction at the ceiling.

2.3.3 Semi-transverse ventilation systems

Semi-transverse systems are equipped with only supply or exhaust elements (Figure 2.10 A-B). The exhaust from the tunnel is discharged at the portals or through exhaust stacks. In order to optimise the ventilation system in case of fire, a single point extraction can be easily implemented with the help of control dampers. The localised exhaust near the fire site is achieved through the activation of the control dampers at the extraction opening nearest to the fire source upon detection and confirmation of the existence of a fire within the tunnel. The control dampers nearest to the fire site remain open while the other control dampers are closed, allowing the system to maximise the exhaust air flow adjacent to the fire site. Fully or semi transverse systems are particularly efficient for long, bidirectional, urban tunnels with congested traffic, leaving clear tenable escape conditions on both sides of a fire.

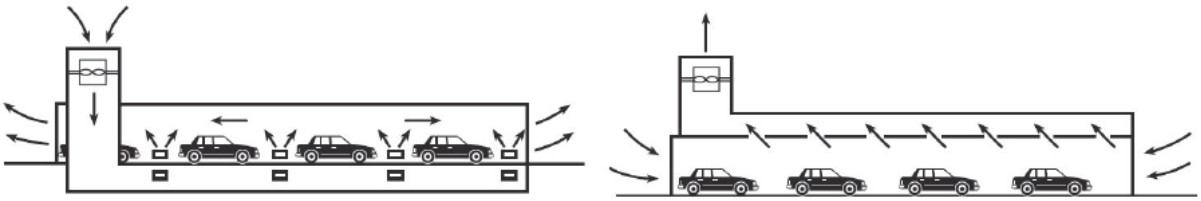

Figure 2.10 A-B. Semi-transverse ventilation systems (NFPA 502, 2011)

Considering the velocity along the longitudinal direction, in the case of a transverse (fully or semi) ventilation system the objective is to minimise the smoke propagation upwind and downwind from the fire source. A steady situation of zero velocity near the fire source should be achieved and the stratification should be maintained as long as the evacuation of the occupants is completed.

In Figure 2.11, this effect (sketched in Fig. 2.10 B) is highlight through a CFD simulation with FDS with an example: one side is near zero velocity (right side, where the fire is positioned) while the opposite side provides fresh air coming from the portal.

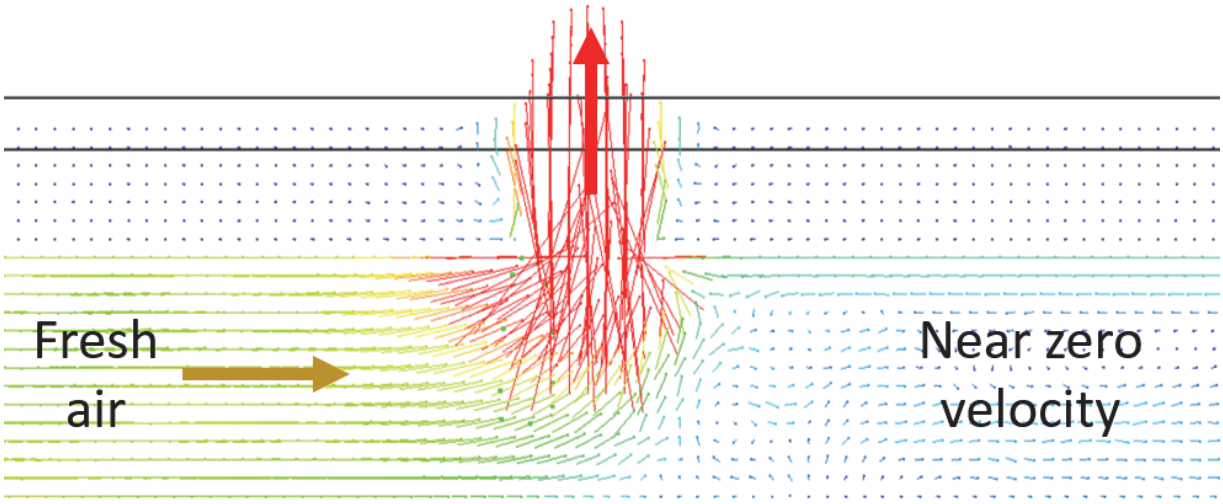

Figure 2.11. Vector-velocity field near the smoke extractor (blue and red are 0 and 5 m/s)

2.3.4 Alternative solutions

Several different solutions can be found in existing or under construction tunnel systems, depending on geometrical boundary conditions, geographical constraints and choices of design engineers.

For example, jet-fan based ventilation systems can be coupled with exhaust semi-transverse system if it is preferable not to discharge toxic gases through the exit portal because of the vicinity of buildings, preferring instead a dispersion stack (Figure 2.12).

Other innovative solutions are represented by air curtains used as barriers for heat and smoke (Figure 2.13). The aim of this kind of system is to isolate the fire zone from the rest of the tunnel with a supply of air from the ceiling, whose direction could be vertical or inclined towards the fire.

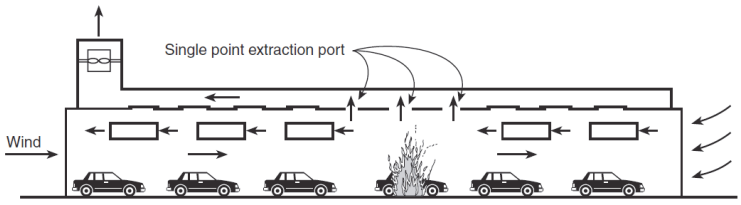

Figure 2.12. Single point extraction and jet fans ventilation system (NFPA 502, 2011)

Figure 2.13. Vertical and inclined air curtains as barrier of fire propagation (Krajewski, 2015)

2.4 Pressurisation strategies

Pressurisation strategies are normally included in the design of the means of egress system. They are part, from the general point of view, of the smoke management systems because their aim is to prevent the entrance of smoke and maintain tenable conditions along the escape routes. The escape routes can be in this case by-passes, routes leading outside or emergency tunnels.

In Figure 2.14, an example of the evacuation process from a road tunnel equipped with a pressurised bypass is shown. The occupants in the right tube where the fire develops need to evacuate the tunnel by going towards their entrance portal, with the risk of being exposed to fire and smoke effluents, or entering the by-pass that leads to the left tube. Once the occupants enter the pressurised environment, they are considered to be in a "safe place" and evacuation is considered as ended (then people could finalise the evacuation by exiting the left tube, clear of smoke, or wait for rescuers in the same left tube).

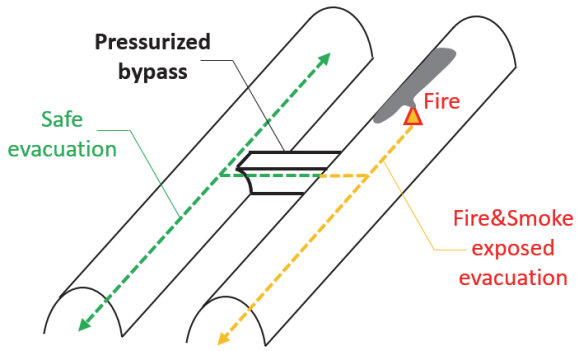

Figure 2.14. Sketch of the evacuation from a road tunnel equipped with pressurised bypass

In Figure 2.15, a zoom in on the configuration of the bypass is made. The configuration adopted for the bypass is generally that of a small smokeproof enclosure, able to guarantee an overpressure ΔP up to 30-50 Pa, depending on its design.

Generally, the smokeproof enclosures are confined fire compartments with two or more doors where only one door is released at a time in order to prevent continuous passage and leakage. These systems are often used, for instance, to protect the main vertical means of egress like stairs and fire elevators, or refuge areas, where the occupants can wait for help if unable to leave the building independently (hospitals, nursing home, etc.). These kind of systems, in general, might represent a good alternative to pressurisation of large volumes like whole stairwells, because, due to their limited extension, they require less powerful fans.

However, the operating principle of the smokeproof enclosure is not easily coupled with the evacuation. In fact, the action of opening the entrance door of the pressurised environment is responsible for an airflow exiting the door that should contrast the entrance of smoke. Meanwhile, differential pressure inevitably decreases due to the direct contact of the internal and external volumes. Then the door closes and the mechanical ventilation must be able to restore the initial overpressure conditions quickly before the door will be opened again. If the level of overpressure does not increase in a short time, in case of a fire, the smoke might enter the compartment through the first entrance door and exit through the second exit door, reaching exactly the opposite effect in preventing the entrance of smoke.

These uncertainties in the effectiveness of the smokeproof enclosures during fire evacuation are in agreement with Lay's work (Lay, 2014) that doubted the correctness of the operating conditions of pressurisation systems.

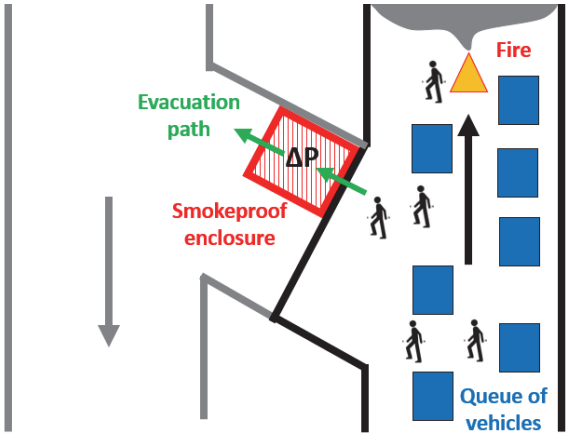

Figure 2.15. Zoom on the vicinity of the pressurised bypass

Considering the restoration of the initial overpressure conditions, fixing the characteristics of the fan, the velocity of the process depends mainly on the ratio between the volume of the compartment and the dimensions of the door. The smaller is the ratio, the quicker are the transient phases of decreasing and increasing of the overpressure, respectively at the opening and closing of a door. For larger value of the ratio between pressurised volume and door area the dynamics of the system change. In case of pressurised stairwells for example, depending on the flow of people (usually measured in people/seconds), a minimum differential pressure is likely to be still guaranteed even at the opening of a door. However, restoring the initial differential pressure might be much more difficult and expensive since the volume is much larger than the dimension of the door.

Considering that the operating conditions of the smokeproof enclosure in case of fire can affect the overall mechanism of self-evacuation, some tests of a full-scale pressurised enclosure, typical of the Italian fire safety design, have been conducted.

In Appendix A the phenomenological characterisation of the smokeproof enclosure through experimental tests and numerical analysis is reported.

Chapter 3

The European context

3.1 Statistics and accidental rates

The section is intended as a literature review of accidents and fires in road tunnels, including relevant statistical data, prediction models and case history.

3.1.1 Accidents in road tunnels

Accidents related to traffic are generally expressed in terms of 100 million of vehicles per kilometre and are basically related to the collision of a vehicle with another one or with the lateral walls of the tunnel. In this paragraph, the accident may or may not degenerate into a fire.

The comparison between the number of accidents inside the tunnel and the overall road network (mostly, open sections) shows different results if the database is limited to severe events or not. In fact, if all accidents are taken into consideration, statistical data affirms that only 50-60% of the accidents occur in tunnel sections (PIARC, 1995; Nussbaumer, 2007). In accordance with this, in Italy, the values recorded in 2011 were 4.63 and 9 accidents per 108 vehicles km respectively per tunnel and open sections (Commissione Permanente Gallerie, 2012).

However, the opposite trend is obtained if the analysis is restricted only to events with fatalities and injuries (SAFESTAR, 2002; SWOV, 2009; Caliendo et al, 2012) because accidents in tunnels are on average characterised by more severe consequences.

Considering the distribution of accidents along the tunnel, this is not homogenous and depends on the distance from the portals. In fact, statistics affirm that a higher number of accidents (up to three times) interests the sections next to the portals as opposed to the central part of the tunnel. This feature is probably due to the rapid change of visibility conditions from the external to the internal environment (Amundsen et al, 2009). Moreover, anomalies and irregularities can be also caused by the difference in the geometry of the carriageway, the lateral confinement and the reduction of a drivers' visual field as well.

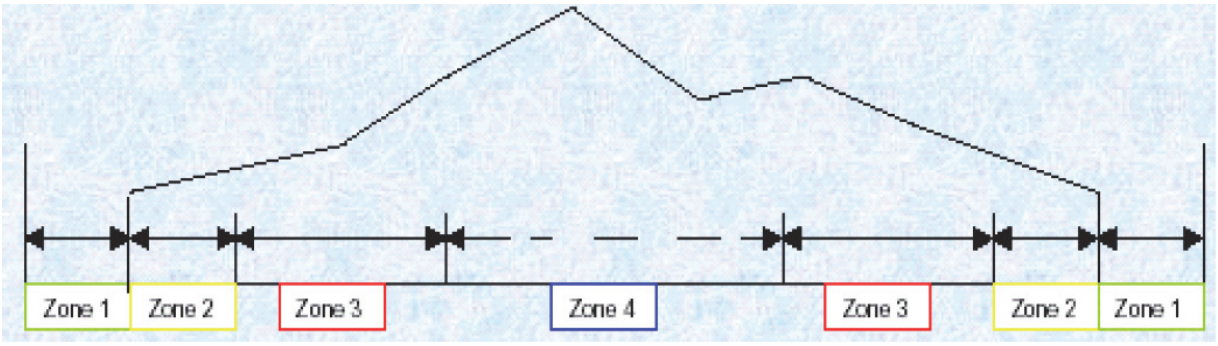

Figure 3.1. Trend of luminescence in the tunnel (De Guglielmo, 2007)

Other aspects that emerge from statistical reports are the following:

- considering the traffic volume, the presence of HGVs is responsible for increasing severity of the accidents (Salvisberg, 2004);

- considering the type of road, urban tunnels are much more prone to accidents compared to non-urban ones and accidents are likely to be severe (PIARC, 1995; Amunden, 2009);

- considering the traffic flow, accidents in bidirectional tunnels are approximately 1.4 times higher than those of unidirectional tunnels (Salvisberg, 2004; Amunden, 2009);

- considering the length, this parameter is generally treated as an intrinsic measure of risk in prediction models (the longer the tunnel, the higher the likelihood of an accident). However, this is not in agreement with the evidence collected through

surveys, which highlight that short tunnels are more dangerous because drivers are affected by fluctuating conditions between external and internal environment and, in addition, pay less attention to the layout (Lemke, 2000; Salvisberg, 2004);

- the slope, the lateral verge, the number of lanes, the speed limit are sometimes considered also as risk factors.

3.1.2 Accident prediction models

Some models are available and can be used to determine the expected number of accidents for a given tunnel. These models are based on statistical data, which are analysed through significant parameters using regression analysis.

UPI (Switzerland) developed the following relation (3.1) based on the analysis of the accidental rates on the Swiss national road network between 1992 and 1999.

$$N_{UPI} = e^{(-19.51+0.77lnL+0.59n+1.61lnTGM+0.12lnVP-0.82lnL_b)} \quad (3.1)$$

where N_UPI is the number of accidents, L the length of the tunnel, n the number of tubes, TGM bidir is the AADT, VP is the % HGVs and Lb is the width of the right verge.

This relationship has been compared to the Italian accidental rates: the UPI model slightly overestimates the predicted accidents, but can be used for the Italian network with a calibration factor of 0.939 (Domenichini et al, 2016).

Another model based on the Italian statistical database was developed (Caliendo et al, 2013) based on 260 unidirectional motorway tunnels for non severe (3.2) and severe (3.3) accidents. Further studies were done with random variables.

$$N_{UPI_{NS}} = e^{(3.6406+0.65747LogL+1.4538LogTGM+0.30106D1-0.17063D2+1.04928LogVP+0.6975NC+0.06850M)} \quad (3.2)$$

$$N_{UPI_S} = e^{(2.59513+0.4756LogL+2.08129LogTGM+0.61642D1-0.63012D2+0.69250LogVP+0.29956NC-0.0790M)} \quad (3.3)$$

In the equations, L is the tunnel length, TGM is the AADT*10-4, D1 and D2 are dummy variables (it is 1 if the TGM exceeds 5000 or 13000 daily vehicles respectively for unidirectional and bidirectional tunnels, otherwise it is 0), VP is the HGV %, NC is a

dummy variable (which is 1 or 0 if the tunnel has 3 or 2 lanes), M is a dummy variable (that is 1 if there is a verge, otherwise 0).

3.1.3 Fires in road tunnels

Fires can occur as a result of a collision or other causes. Typical fire rates have grabbed the attention of researchers and some orders of magnitude are now available. However, the range of data is highly disperse and prediction is difficult due to the nature of rare event of the tunnel fire. In Table 3.1, the fire rate per km is reported over the observed period from 2006 to 2011 (all fires with no distinction for the causes are considered).

Table 3.1. Fires in tunnels in Italy (Commissione Permanente Gallerie, 2012)

Year	2006	2007	2008	2009	2010	2011
Reference tubes	416	416	416	418	652	652
Km	504.3	504.3	504.3	505.2	754.5	754.5
Number of fires	19	35	24	28	15	18
Fires/km	0.038	0.069	0.048	0.055	0.020	0.024

CETU (Table 3.2) provides typical fire rates by distinguishing light vehicles from HGV fires. Car fire rates do not depend on the type of road, while HGV fire rates have a maximum for motorways with high slopes, curves and national roadways. Nonstandard rates are related to tunnels with very difficult access (Mont Blanc and Frejus tunnels). PIARC (1995) provides typical fire rates (Table 3.3) for the categories of unidirectional from bidirectional tunnels. The Italian guidelines (ANAS, 2009), similarly, distinguish urban, motorways and nonurban bidirectional tunnels (Table3.4). Considering the causes, it is difficult to estimate the percentage of fires deriving from vehicle accidents or failures of the mechanical systems, because they are generally not reported. Failures seem to be more significant than accidents (CETU, 2003; Ahrens, 2010). However, statistical data on the ratio between failures resulting in fires and

overall failures in tunnels are in the range of 0.2-1% (NCHRP Synthesis 415, 2011) but they have not been confirmed by other studies.

On the other hand, the proportion of accidents resulting in fires compared to the overall number of accidents is within a range of 5-10% (ANAS, 2009). CETU adds a difference according to the type of burning vehicle: 7-20% for light vehicles and 5-15% for HGVs.

Table 3.2. Fires in tunnels per 10^8 veic km (CETU, 2003)

	Minimum	Maximum	Nonstandard
Car fires	2	2	2
HGV fires	1.5	4.5	13.5
Non controlled fires	0.5	1.5	4.5

Table 3.3. Fires in tunnels per 10^8 veic km (PIARC, 1995)

	Minimum	Maximum
Unidirectional	0	10
Bidirectional	0	15

Table 3.4. Fires in tunnels per 10^8 veic km (ANAS, 2009)

	Minimum	Maximum
Urban	0	10
Motorways	0	10
Bidirectional / non urban	0	15

3.1.4 Case history

In the last years, many accidents have happened in different typologies of existing tunnels (road tunnels, railway tunnels, underground – metro tunnels, etc.).

A brief description of some events that caused injuries and fatalities is reported.

- Channel Tunnel fire (51 km long, France – UK, 1996)

The fire was caused by the overheating of a train carrying goods. No people died, but there were several injured due to the high level of smoke and the evacuation was difficult. The safety systems did not work as they should have: moreover, the tunnel

design provided a window for a rescue train to reach a point adjacent to the fire train, but this did not happen.

- Mont Blanc Tunnel fire (11.6 km long, France – Italy, 1999)

It was a single – bore, bi – directional tunnel, connecting France and Italy. A HGV caused the fire at about 6 km from the French portal and the accident involved other vehicles: the traffic flow was of average intensity (4 – 5 vehicle / minute) and vehicles continued to enter the tunnel even if the road traffic signals were red. In all, 39 people died: most of them perished in their vehicles (Figure 3.2). In addition, firefighting teams tried to enter but found difficulties due to smoke and some of them perished inside the tunnel.

The tunnel had the usual safety systems, but they did not work as they were supposed to. For instance, the video recording system did not operate on the French side and the fire detection system on the Italian side had been disabled the day before the accident because of false alarms.

- Tauern Tunnel fire (6.4 km long, Austria, 1999)

The accident involved 2 HGVs and some vehicles: a severe fire developed. The safety systems included CCTV cameras, but they were immersed in dense smoke after some seconds from the ignition time. The traffic flow was high, drivers ignored the red traffic signals and 12 people died, some in their vehicles.

- Kitzsteinhorn Funicular Tunnel fire (3.3 km long, Austria, 2000)

It was a 2.2 km-long inclined tunnel and it was part of the first Alpine underground railway in the world. A fire developed in the ascending train: the inclined tunnel behaved like a chimney and it was rapidly filled by smoke. Only 12 people survived in the tunnel because they escaped downwards, going past the fire: 155 people died, trying to evacuate upwards.

- St Gotthard Tunnel fire (16.9 km long, Switzerland, 2001)

The accident was caused by a collision between two HGVs, which were travelling in opposite directions (the tunnel is single – bore bidirectional). The fire was severe and 11 people died: they all died from smoke inhalation, also from a large distance from the origin of the fire (up to 2 km).

Figure 3.2. Damage after the Mont Blanc tunnel fire

- Frejus Tunnel fire (12.9 km long, France – Italy, 2005)

Following the Mont Blanc tunnel fire in 1999, safety measures in the Frejus tunnel were improved at the beginning of 2000. A strict 70 km/h speed limit and a safe distance of 150 m between vehicles were imposed. The tunnel was equipped with the latest smoke and flame detectors and a system of video cameras in the tunnel to detect the speed of traffic, as well as fire and smoke; temperature sensors were installed at short distances throughout the tunnel, monitored from a central control room. Fire hydrants were installed every 130 m and there are 11 safety points along the tunnel, equipped with telephones and loud speakers connected to the control room, with a separate ventilation duct to supply fresh air. These were separated from the main tunnel by two fire doors. Finally there is a 'thermal gate' system at each entrance to identify any overheating

vehicles. Despite these measures, on 4 June 2005, a fire caused the death of two HGV drivers, several injured and the closure of the tunnel to traffic for several weeks.

3.2 In force-regulations and best practice

3.2.1 Overview

A first comprehensive study on the legislation on tunnel safety was conducted prior to 2004 by the European Thematic Network FIT "Fire in Tunnels", whose Technical Report n°2 (CETU, 2005) is an example of detailed comparisons of the specific requirements and restrictions for road tunnels among the European countries.

After the entry into force of the Directive 2004/54, the Committee on Operational Safety of Underground Facilities (COSUF) of the International Tunnelling and Underground Space Association (ITA) carried out two surveys, respectively in 2008 and in 2011, in order to update the list and include more recent data of existing regulations and recognised recommendations (ITA-COSUF, 2011). In addition, the list mentions several guidelines and best practice published by PIARC (World Road Association), ITA, NVF (Nordic Road Association): the majority of them are in English and still in use. The national legislations have often stricter requirements compared to those of the EU Directive, which are sometimes extended to the overall road network (non-TERN tunnel).

For instance, in Germany, the Directive has been transposed into national legislation (RABT) in 2011. The document approves two risk assessment methods. One method is used for the risk assessment of tunnels with special characteristics, for the assessment of compensatory measures in existing tunnels and for the decision of the ventilation system in bidirectional tunnels with a length from 600 m to 1200 m. This method also takes into account cost-benefits considerations. The second method is used for risk

assessment of dangerous transports through road tunnels and the categorisation of the tunnels according to ADR.

In Switzerland, the Guidelines released by the Government in 2010 are compulsory for motorway network and explains how the EU Directive will be applied.

In France, the EU Directive was incorporated in the national legislation in 2011. The law applies similar procedures to all tunnels longer than 300 m, regardless of their being concerned with the Directive or not. When risk analysis must be performed, this is supported by a constantly revised and updated database of tunnel accidents (available since 2001).

In the Netherlands, the EU Directive has been transposed in 2006 and, similarly to France, where stricter requirements are applied to all tunnels longer than 250 m, also if they are not part of the TERN. The Netherlands has a long tradition of risk assessment, originating from the study on floods and dams and, in fact, quantitative risk analysis and risk analysis based on scenarios have been developed.

This issue of stricter requirements occurred also in Italy. For example, the Ministerial Decree 2001 required shorter distance among the emergency exits (not exceeding 300 m) compared to the European requirement of 500 m. It was realised that this was a strong limitation, considering also the high number of existing tunnels in Italy. Therefore, this incoherence was solved through the Legislative Decree 2012/1 in which it is stated that it is not possible to apply parameters and requirements functionally and technically stricter than those asked by European legislation to new and existing road tunnels.

In the following paragraphs, some relevant points contained in the Directive 2004/54/EC and the NFPA 502 are described.

3.2.2 The Directive 2004/54/EC

The European Directive 2004/54 is the most important document in Europe for the tunnel safety standards. All the trans-European tunnels longer than 500 m are covered by the Directive. It contains standards for the construction of new tunnels and for the management and improvement of existing ones. The most important innovation of the Directive is the introduction of the concepts of risk and risk analysis as essential parameters in the tunnel design.

In order to guarantee a minimum level of safety for all the users of the European road network, the Directive integrates and improves the previous norms and imposes specific requirements depending on the tunnel length, the traffic volume and the number of tubes.

Some points contained in the Directive are reported in the following short list.

• The Directive decrees that Member States must designate an administrative authority that has responsibility of ensuring the whole safety requirements.

• The Member States must fix the methodology of risk analysis and the acceptability criteria.

• Some parameters are identified as risk factors and are subjected to requirements imposed by the Directive for new and existing tunnels. Some of these parameters are: tunnel length, number of lanes and tubes, cross-sectional geometry, alignments, type of construction, unidirectional or bidirectional traffic, traffic volume, risk of congestion etc. In case the parameters do not comply with the minimum requirements of the Directive, for existing tunnels a specific risk analysis is admitted in order to define additional and compensatory measures.

• The mechanical ventilation is required for tunnels longer than 1000 m and traffic higher than 2000 vehicles per lane per day.

• For unidirectional tunnels, longitudinal ventilation system is admitted up to a length of 3000 m. Over this value, transverse and semi transverse systems are required.

• For bidirectional tunnels or unidirectional with congested traffic, the longitudinal ventilation can be admitted up to 1500 m only if risk analysis is conducted or additional measures are used. In the other cases, transverse and semi transverse systems are required.

• Emergency exits must conduct always outside of the tunnel (no refuges without exits) and can be of different types: direct exit to the outside, transversal tunnel between tubes, exit towards an emergency tunnel, refuge with escape routes separated from the tube. Fire doors and pressurisation strategies are required in order to keep the escape route free from smoke and heat.

• For new tunnels with traffic volume > 2000 vehicles per lane per day, emergency exits must be placed at a distance of 500 m; for existing tunnels with the same conditions of traffic and L > 1000 m, assessment and feasibility analysis must be done, in order to assess if the emergency exits are necessary or can be compensated by other measures.

3.2.3 The NFPA 502

Another fundamental document in the road tunnel field is represented by the NFPA 502, which is the standard for road tunnels, bridges and other limited access highways. By looking at the minimum safety requirements similarities and differences with the European Directive are identified.

The NFPA is well known in tunnel fire safety because of the clear indications on the fire scenarios (Table 3.5), normally adopted as reference values by designers.

Considering the mechanical ventilation systems, like the Directive, the emergency ventilation is mandatory for tunnels longer than 1000 meters. In addition, recommendations on the air velocities in tunnels are provided: these should be within a

range of 0.76 m/s and 11.0 m/s, where the lower limit is to prevent backlayering, the higher one is for motorists comfort.

Considering the means of the egress system, the emergency exits must be designed for tunnels longer than 300 m, with an egress analysis supporting the relative spacing. However, spacing between exits for protection of tunnel occupants should not exceed 300 m (lower than the 500 meters prescribed by the Directive).

The maximum walking speed of the occupants evacuating the tunnel should be computed for reduced visibility due to a smoke-filled environment (0.5–1.5 m/s depending on visibility, luminance, design of exit signs and egress pathway). Furthermore, the evacuation path requires a height clear of smoke of at least 2.0 m. However, given that the current accuracy of modelling methods is within the 25 %, when advanced modelling is used a height of at least 2.5 m is recommended above any point along the surface of the evacuation pathway.

Table 3.5. Order of magnitude of fire growth (NFPA 502, 2011)

Vehicles	Peak Fire Heat Release Rate MW	Time to Peak HRR min
Passenger car	5-10	0-30
Multiple passenger cars (2-4 cars)	10-20	13-55
Bus	20-30	7-10
Heavy goods truck	70-200	10-18
Tanker	200-300	-

3.3 The case of Italy

3.3.1 A tunnel-country

Due to its morphology, Italy is the European country with the highest percentage of the Trans European Road Network (TERN) tunnels. It is estimated that the overall extension of TERN-tunnels is approximately 750 km, considering 654 road tunnels (each

tube is considered as a single tunnel). Furthermore, considering the local urban road network, there are other 250 road tunnels whose length exceeds 500 meters and an even larger number of shorter ones (estimated as 850 tubes).

The period of construction of most of these tunnels is ample, with a large variety of different techniques accomplishing the in-force regulations. Many of these tunnels have been refurbished during the last years, adding safety measures appropriate to the current standards. However, the upgrading process of the existing tunnels is often difficult and sometimes it is not possible to fulfil all the safety requirements due to geographical or geometrical constraints as well as exaggerated costs. It is not rare to find a long tunnel without emergency exits or ventilation due to impossibility of upgrading or delay in approving the refurbish project. The awareness of these aspects help to understand the importance of tunnel systems in the national road network and the impact of these elements on the safety of users.

As introduced, in Italy there are several hundreds of kilometres of road tunnels. Due to historical, geographical and morphological reasons, each tunnel is different from the other, not only for its geometry but also and mostly for its safety equipment.

A first step to classify the existing road tunnels is to divide them into categories of different length. With the aid of regional fire authorities (Report DCPST, 2016), it has been possible to obtain the results represented in Figure 3.3 using real data on the length of road tunnels (TERN and non-TERN). Figure 3.3 shows that more than 50 % is composed by tunnels whose length goes from 500 to 1000 meters, while the other half is composed by categories of longer tunnels.

The identification of the riskier length category is not possible, as tunnels with different characteristics (TERN and non-TERN) are part of each category. Moreover, length is not the only risk factor for tunnel safety and should be coupled with data of the safety system, traffic volume etc.

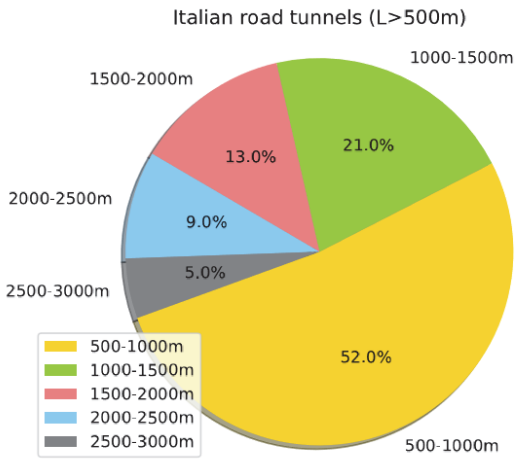

Figure 3.3. Percentage of road tunnels by length (Report DCPST, 2016)

Other information provided by the fire authorities concern the number of fatalities and injuries due to fire, explosions or accident. In Table 3.6 this data is calculated as the sum of regional data in the period 2011-2016. Considering that data related to 2016 is partial, on average there are approximately 8.2 fatalities per year in road tunnels and more than 50 injuries. It must be recognised that the number of fatalities is lower compared to that of the overall road network; nevertheless, ten fatalities per year is still an important number.

During the period going from 2011 to August 2016 Sicily was the region with the greatest number of fatalities (13), followed by Lombardia (11) and Liguria (6). However, Liguria is the region with the greatest number of tunnels with lengths larger than 500 meters (183 tunnels), followed by Lombardia (115 tunnels) while Sicily has only 36 tunnels with those characteristics. Considering the number of injuries, Lombardia, Piemonte and Liguria were the first of the list, each with 60-70 injuries in the period above mentioned. Again, the systematic individuation of the region or type of tunnel with the highest level of risk is not possible due to lack of basic data regarding, for example, ventilation strategies, escape routes, traffic.

If one normalises the accidents with the km, the length of the tunnel is certainly an intrinsic measure of risk (the longer the tunnel, the higher the probability of accident). Nevertheless, the minimum requirements increase for longer tunnels and this makes shorter tunnels less equipped, modern and sometimes safe.

Table 3.6. Statistics for road tunnels in Italy (Report DCPST, 2016)

Year	Injuries	Fatalities
2011	24	9
2012	57	5
2013	33	11
2014	25	10
2015	104	6
2016 (Jan-Aug)	97	8
AVERAGE	**56.7**	**8.2**
STANDARD DEVIATION	**36.0**	**2.3**

3.3.2 Firefighters rescue operations

According to the Presidential Decree 2011/151, road tunnels whose length exceeds 500 meters are premises subjected to fire prevention controls by Fire Brigades and Services Department. Apart from that, the Italian National Fire Brigades and Services have the task of emergency rescue in case of fire or any event involving public safety. With the aid of real data reported by firefighters teams involved in accidental events in road tunnels, it has been possible to focus on the main problems occurred from 2011 to August 2016.

Looking at Table 3.7 it appears that firefighter teams were involved in a large number of operations in road tunnels for fire, explosion or accidents (on average, slightly less than one operation per day). The total number of operations (on average, 528 per year) highlights that probably other types of problems such as maintenance and drainage are very common.

Table 3.7. FF operations in road tunnels in Italy (Report DCPST, 2016)

Year	N. of operations	N. of operations for fire or accidents
2011	481	236
2012	510	235
2013	521	288
2014	585	329
2015	629	404
2016 (Jan-Aug)	443	302
AVERAGE	**528.2**	**299**
STANDARD DEVIATION	**68.2**	**63.4**

3.3.3 Italian Legislative Decree 2006/264

In Italy the European Directive 2004/54 has been approved by the Legislative Decree 2006/264. The Decree covers all the TERN-tunnels whose lengths exceed 500 meters, new, existing or still under construction.

The most interesting news is the risk analysis (see Chapter 4), which is becoming the fundamental tool of assessment and decision-making for the design process of road tunnels. The aim of risk analysis is to measure the level of risk for a road tunnel in terms of safety indicators. The methodology consists in considering the probability of accidents in the tunnel, taking account of all its details (both geometrical, such as number of lanes, and performance, like ventilation system, emergency exits, lighting system), including the traffic conditions (percentage of HGVs per day).

Different scenarios have to be considered. Moreover, the procedure of risk analysis allows to specify the fault-tree, the critical-beginner event and the event tree: each event has its own probability of occurrence, conditioned by the reliability and efficiency of the safety facilities. The result of the risk analysis is an F (probability of variants) – N (number of fatalities) curve: the level of acceptability is fixed in a graph, according to the ALARP criterion (As Low As Reasonably Practicable). In Chapter 4 risk and risk analysis are widely described.

Chapter 4

Basic concepts of risk analysis

4.1 What is risk?

4.1.1 Terminology

There is no general agreement on a comprehensive definition of risk. Risk is the combination of the probability of an event and its consequence, when both are expressed numerically (API, 2016). Risk can be also defined as "the potential for realisation of unwanted, adverse consequences to human life, health, property, or the environment" (SRA, 2000). The concept of risk should not be confused with that of hazard, which is any condition potentially able to cause damage to people, property, or the environment (AIChE, 1989). Risk (4.1) is measured in terms of consequences (expected effects) and likelihood (a description of probability or frequency).

$$Risk = f\ (frequency\ or\ probability; consequence) \tag{4.1}$$

In the case of premises with a specific risk R_i far more relevant compared to the others, the risk is expressed as the probability P_i that this event will occur multiplied by the consequences C_i caused by the same event (4.2). The overall risk R_s (4.3) of a system is the sum of all the specific risks of all critical events of that system.

$$R_i = P_i * C_i \tag{4.2}$$

$$R_s = \sum_{i=1}^{N} R_i \tag{4.3}$$

4.1.2 Risk types

Life safety risks are normally presented from two different points of view: individual or societal risk (Figure 4.1).

Individual risk (IR) is defined as the probability that an average unprotected person, permanently present at a certain location, is killed due to an accident resulting from a hazardous activity (Bottelberghs, 2000). The IR is thus a property of the place, useful in spatial planning. Similar to the individual risk are some expressions available in literature (HSE, 1989; Bedford et al, 2001). For example, the measure of "activity specific hourly mortality rate" computes the probability per time unit while engaged in a specified activity (the risks of travel by car, train or airplane are often expressed as the number of fatalities per kilometre travelled).

The societal risk (SR), instead, is defined as the relationship between frequency and the number of people suffering from a specified level of harm in a given population from the realisation of specified hazards (Institute of Chemical Engineering, 1985). While the IR gives the probability of dying on a certain location, the SR gives a number for a whole area or infrastructure or engineering system, no matter precisely where the harm occurs within that area (Jonkman et al, 2003).

By integrating the individual risk levels and the population density, the expected value of the number of fatalities can be determined (Lanheij et al, 2000) as in (4.4).

$$E(N) = \iint IR(x,y) * m(x,y)\, dx\, dy \tag{4.4}$$

where $E(N)$ is the expected value of the number of fatalities per year and $m(x,y)$ is the population density on location (x,y).

Although IR and SR calculations are often based on the same data, no mathematical relation has been established yet between them. Both simultaneous IR and SR calculations are often carried out with numerical methods.

SR is often represented graphically in a FN-curve. This curve displays the probability of exceedance as a function of the number of fatalities, on a double logarithmic scale. The probability of exceedance $P(N > x)$ is expressed as in (4.5):

$$1 - F_N(x) = P(N > x) = \int_0^\infty f_N(x) \tag{4.5}$$

where $f_N(x)$ is the probability density function (pdf) of the number of fatalities per year and $F_N(x)$ the probability distribution function of the number of fatalities per year (representing also the probability of less than x fatalities per year).

A simple measure for the societal risk is the area under the FN-curve, labelled as Expected Value of the number of fatalities per year $EV(N)$, often proposed as the fundamental measure for the societal risk (Ale et al, 1996) in the decision-making process (4.6).

$$EV(N) = \int_0^\infty x\, f_N(x) dx \tag{4.6}$$

In several countries, a FN criterion line limits the risks of various hazardous activities. These standards can be described with the following general formula (4.7):

$$1 - F_N(x) < \frac{C}{x^n} \tag{4.7}$$

where n is the steepness of the limit line and C the constant that determines the position of the limit line. A standard with a steepness of n=1 or n=2 is called risk "neutral" or "averse" respectively (Vrijling et al, 1997). In the last case, larger accidents are weighted more heavily and are only accepted with a relatively lower probability. Commonly, as a part of the standard, an ALARP region has been determined below the limit line, in which the risk should be reduced to a level that is As Low As Reasonably Practicable.

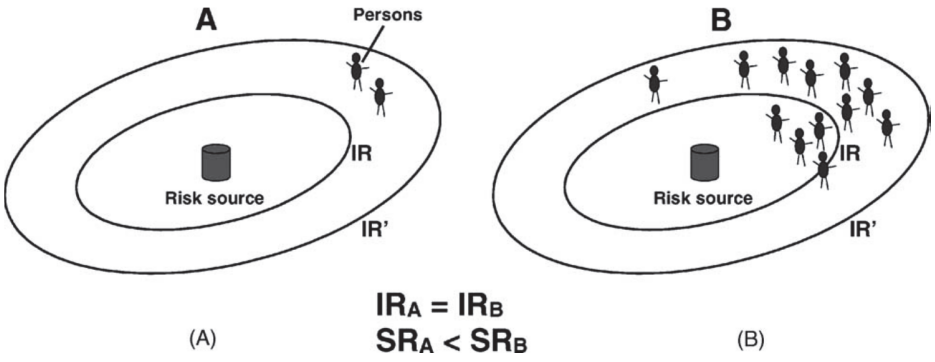

Figure 4.1. Individual (IR) and societal (SR) risk (Jonkman, 2003)

4.1.3 What is risk analysis?

Risk analysis is a structured, rigorous and systematic approach carried out when undesirable and potentially severe critical events need to be investigated, providing information and numerical quantification of the probabilities and expected consequences for the identified risks (API, 2016).

The main output of the risk analysis is the risk estimation. The risk estimation implies the measurements of the consequence (fatalities, injuries, structural damage, etc.) of the given event and should be made as quantitative as possible. That estimation, considered inside the more general risk assessment procedure, must be interpreted and evaluated in terms of judgements and tolerability thresholds. Zero risk does not exist, but residual risk might be excessive and in that case, alternative measures and risk management strategies must be adopted, in order to reduce the risk to an acceptable level.

Risk analysis is particularly useful for significantly complex and highly technological systems, such as chemical plants, nuclear plants or, more recently, infrastructures. For these systems, in fact, a large number of uncertainties are present and any decision taken by the stakeholders (risk mitigation measures, refurbishment interventions, etc.) may put forward a large amount of money, bringing up serious concerns and debates.

In fire safety engineering, risk analysis is generally used to evaluate fire protection strategies for a particular application or for a class of facility (Watts et al, 2016). Although it has been used for several years, there is currently neither a unique measure for fire risk nor an acceptable level and criteria. The only established concept is that zero risk is not achievable, because uncertainty is widely spread and technology is not entirely reliable against accidental events. However, risk analysis, supported by sensitivity analysis, is becoming the tool for decision-making processes under uncertainty.

4.2 The fire risk assessment procedure

Fire risk assessment is a comprehensive approach that permits examination of all types of fires that can challenge a premise, including the likelihood and consequences associated with each fire scenario. In Figure 4.2, a scheme of the main steps of the risk assessment procedure is reported (the steps are then described in dedicated sections), while Table 4.1 summarises the wide array of methods that can be followed when a fire risk assessment procedure is needed for a given premise.

Table 4.1. Approaches to risk assessment

HAZARD IDENTIFICATION Checklists/Index methods, Structured methods, Logical diagrams		
QUALITATIVE RISK ANALYSIS - Unstructured - Structured	**SEMI-QUANTITATIVE RISK ANALYSIS** - Point schemes - Matrix methods	**QUANTITATIVE RISK ANALYSIS** - Probabilistic analysis - Full quantitative analysis
RISK ESTIMATION (-)	**RISK ESTIMATION** (Score, Risk magnitude, etc.)	**RISK ESTIMATION** (FN diagram, EVs, etc.)
ACCEPTANCE CRITERIA Absolute, Comparative, Financial		

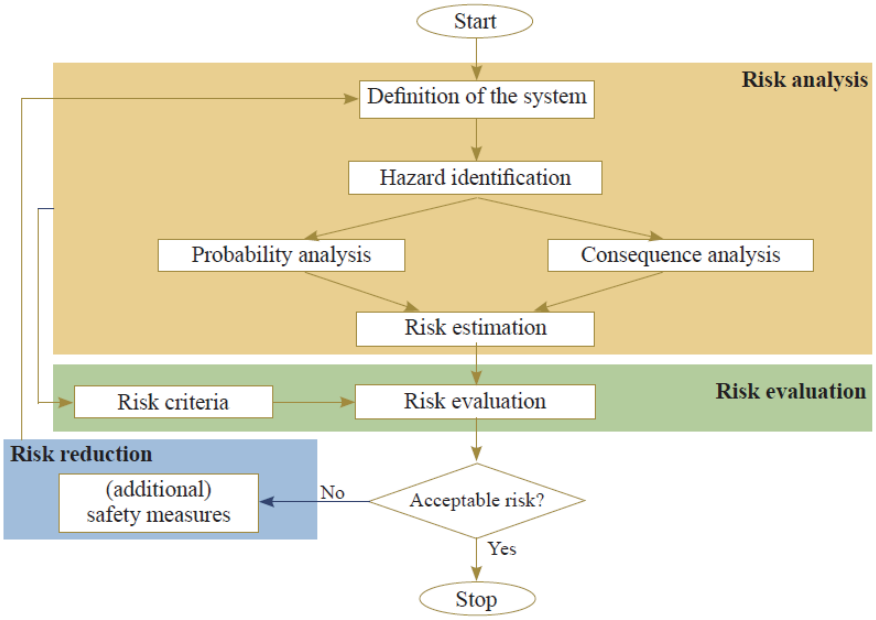

Figure 4.2. Risk assessment procedure (PIARC, 2008)

4.3 Methods for hazard identification

The first step of the risk assessment procedure is represented by the identification of the hazards for the given environment (fire, explosions and toxic releases, for example, are typical hazard for road tunnels). The same type of hazards (for example, a fire) can start from a different system, like the overheating of HGV brakes or the failure of the electrical cables of the tunnel. In order to do this procedure, the system must be broken down into a number of components and subsystems, which can possibly be interested by a state of failure, resulting in the occurrence of a hazard.

Several methods can be used to identify the weakest point of a given system, which will result in the "initiating event". In this sense, a key role is maintained by the experience: historical database of accidents and expert judgments. However, this is not enough when, for example, new technologies and operations must be considered which do not provide a very thorough statistical database. Prediction elements can prove to be very

useful with more structured approaches. Three categories can be identified: checklists and index methods, structured methods and logical diagrams.

4.3.1 Checklists and index methods

This first category is strongly based on the previous experience and consists of tools like Checklists, Safety Review, Index Methods.

A traditional fire safety Checklist or Worksheet is a list of specific items used to identify known types of hazards, design deficiencies and potential fires associated with specific buildings, equipment and operations. Documentation usually consists of a summary of noted deficiencies and specific recommendations for fire safety improvements with appropriate explanations.

4.3.2 Structured methods

Some examples of structured methods are described below.

What-if analysis is a safety study by which investigative questions are asked by an experienced team promoting a brainstorming approach. Risks are normally expressed in a qualitative numerical series (e.g. 1 to 5).

The HAZOP (HAZard and Operability analysis) analysis is systemic (considering all the components in their logical dependency), repeatable in time (well-established structure) and uses conversational approaches, involving the largest number of personnel. The HAZOP analysis is intended as a critical safety study according to which failures are only associated to deviations from the normal serviceability state.

The Failure Modes and Effects Analysis is a systematic, tabular method of evaluating the causes and effects of known types of component failures. It applies to electrical, mechanical and flow systems only when very high reliability factors are needed (such as fire-fighting water supply systems). Both HAZOP and FMEA are often preparatory for mathematical and quantitative analysis (such as FTA and ETA).

The Preliminary Hazard Analysis (PHA) is derived from the U.S. Military Standard System Safety Program Requirements and is often used to evaluate hazards early in the life of a process. This technique is generally applied during the conceptual design of a process plant or as a design review tool before implementing new protective measures.

4.3.3 Logical diagrams

Fault Tree Analysis (FTA) is a graphical representation showing the logical and temporal sequences that can trigger the failure in a system. Event Tree Analysis (ETA) is analogous but is related to the possible outcome deriving from a "top event". Specifically, the top event is an undesired event or incident at the "top" of a fault tree that is traced downward to more basic failures using Boolean logic gates to determine the possible causes of the event.

4.4 Methods for risk estimation

4.4.1 Qualitative methods

Qualitative methods rely on the identification of factors that affect the risk. These factors may be those that affect the level of the specific hazard or the level of the fire precautions intended to mitigate those hazards. These methods can be structured or unstructured, but in both cases, nonstandard situations cannot be addressed. The methods do not provide for a numerical estimation of the risk and most of the times are limited to a hazard and operability analysis, accompanied by means of precautions and indications.

4.4.2 Semi-quantitative methods

Semi-quantitative fire risk assessment methods place some numerical values on the level of risk, but those numerical values do not represent a precise estimation of risk (they can be index or codified expressions like high-medium-low risk).

4.4.2.1 Point schemes

Point schemes are similar to qualitative methods, but assign some numerical values to the risk. This is realised by assigning a score to each fire safety aspect (from geometrical conditions to preventive or protective measures) and finally an overall score for the given premise is determined. Point schemes have the advantages of being relatively easy and quick to use although providing a degree of resolution of the level of risk by producing a number. Their disadvantages include the relatively arbitrary values given to the weightings, the implicit fire safety strategy (not clear) that they represent and the freedom to develop high scoring fire safety solutions that are not applicable in practice.

4.4.2.2 Matrix methods

Matrix methods (Figure 4.3) are often used as a preparatory study for quantitative risk assessment. They consist in broad categories of risk, where frequency and consequences are considered as "order of magnitude" and the judgments can largely be evidence-based, auditable and mathematically robust. The disadvantages are that the risk categories are broad and judgments are often subjective.

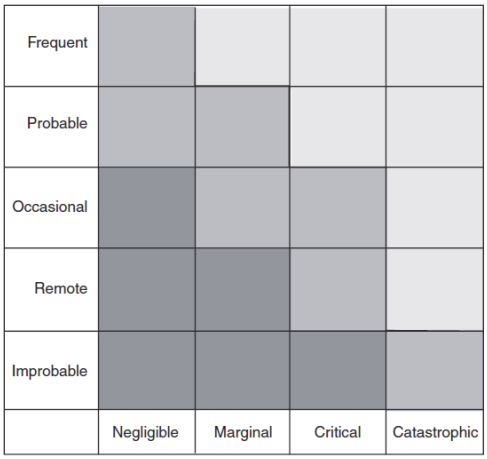

Figure 4.3. Risk matrix (NFPA 551, 2012)

4.4.3 Quantitative methods

Quantitative risk assessment methods predict a discrete level of risk. They tend to use a combination of probabilistic and/or physical modelling to predict the frequency of certain events and their likely consequences.

4.4.3.1 Probabilistic risk assessment

Probabilistic methods simply use statistical analysis to predict the frequency or probability of an unwanted event. The consequences of the unwanted event are taken directly from the statistical information, e.g. probability of fire spread beyond the item first ignited or probability of area damaged being greater than x. The advantage is the affordable theoretical basis of this approach, but the numerical prediction of risk still depends strongly on the available fire statistics.

4.4.3.2 Full quantitative risk assessment

Full quantitative fire risk assessment predicts the level of consequences from unwanted events as well as their frequency. Consequences can be estimated through fire and evacuation modelling; more difficult proved to be the estimation of the frequency of the event. In fact, fires, when not controlled in the initial phase, are severe events whose frequency is luckily low: however, the rarity of these events implies difficulties in making predictions simply based on historical data. This is the reason why the "fire scenario" must be decomposed into a chain of temporally and logically dependent sub-events, which are instead more frequent and easier to be characterised in terms of frequency, considering the database available from the nuclear industry (Franzitch, 1998). This is the explanation of the need for Fault Tree Analysis and Event Tree Analysis for quantitative risk estimation (Figure 4.4).

4.4.3.3 Fault trees (FT)

A fault tree is a method for representing the logical combinations of various system states that lead to a particular outcome, by logical dependency. It portrays the combination of failures that can lead to a specific main failure or accident, expressed generally in annual estimation. This logic model graphically portrays the combinations of failures that can lead to a specific main failure or incident of interest (Top event). This method uses the Boolean Logic (And & Or logic gates) and assigns statistical values to each end point of a branch.

The fault tree analysis (FTA) is the tool to describe the series of failure which lead to the top event (the most dangerous event as identified by the hazard analysis), characterizing its frequency and the minimum cut set (shortest way of failure of a system).

4.4.3.4 Event trees (ET)

The initiating events are identified through the HAZOP and are the starting point for the ETA (event tree analysis). The objective of the ETA is the determination of the frequency of occurrence of the system's weakest branch through decomposition in a logical series of events. The event tree is a graphical logic model that identifies and quantifies possible outcomes following an initiating event by temporal sequence. Probabilities are calculated on each branch of the tree while consequence must be estimated at the outcomes. It assigns statistical values to each end branch point (failure or condition) and allows the calculation of composite risk starting from an initiating event.

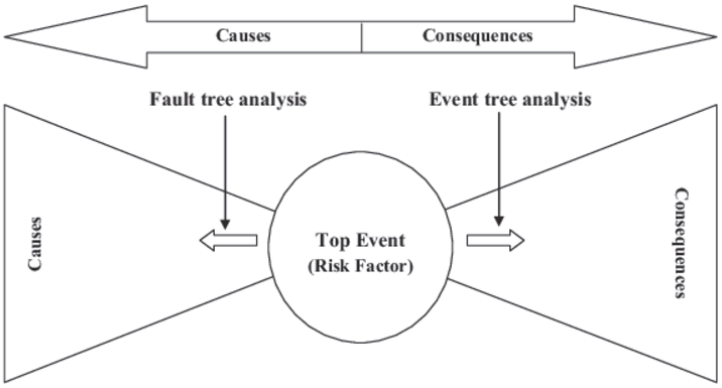

Figure 4.4. Bow-tie model (Mokhtari et al, 2011)

4.5 Acceptance criteria

4.5.1 Risk perception

The concepts of risk perception and aversion against a specific incident are strictly dependent on the characteristics of the society where risk is evaluated: culture, wellness, average level of education are some of the factors that influence people's perception of a risk, determining, therefore, the tolerability or intolerability of the specific risk. For qualitative and semi-quantitative risk assessment, the risk is considered acceptable by comparison with an accepted standard or if a certain score is reached (point schemes and matrix methods). For quantitative risk assessment, instead, a different approach is required.

In mathematical terms (4.8), the risk aversion α is represented by the gradient of the curve in the FN bilogarithmic plane.

$$\propto = \frac{d\ logF}{d\ logN} \tag{4.8}$$

As shown in the Figure 4.5, the higher the inclination of the curve, the higher the aversion of the society against the specific risk. In other words, the same event with F* frequency will be responsible for N2 fatalities greater than N1 fatalities when the

aversion factor is $\alpha 2 > \alpha 1$. For road tunnels, typical aversion factors are one ("risk neutral") or two ("risk averse"). See paragraph 4.5.3 for more information.

In the same plane, the increasing level of risk is instead obtained by going form bottom-top (Figure 4.6). The number of fatalities N* is obtained for a more frequent event (F2 > F1) when risk is higher (R2 > R1).

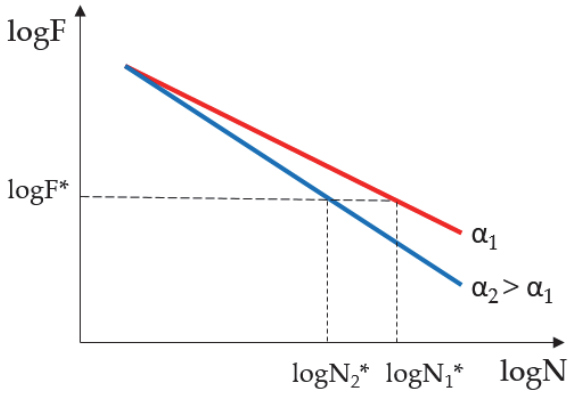

Figure 4.5. Risk by varying the aversion factor α on the FN diagram

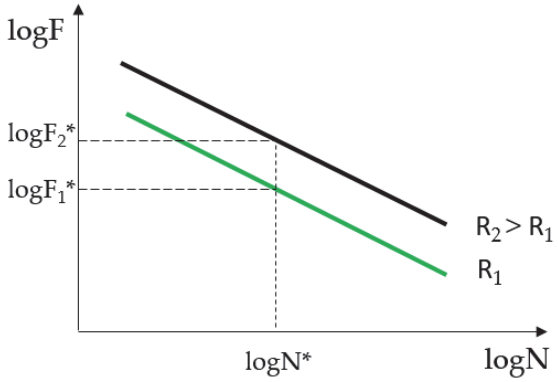

Figure 4.6. Risk magnitude R on the FN diagram

Generally, risk is more accepted by society if it is caused by a voluntary action. For example, radiations from mobile phones are much more accepted compared to those coming from electrical towers. Similarly, considering tunnels, in Italy the risk related to roadways is more accepted compared to railway transport system (Figure 4.7A-B): the

aversion factor fixed by Decree is, in fact, 1 and 1.5 respectively for the first and the second case. Furthermore, the ALARP band (comprised between the upper and the lower limit) is larger for road tunnels (three decades instead of two of railway tunnels) and this implies greater tolerability against fire risk for such systems (see paragraph 4.5.2 for ALARP description).

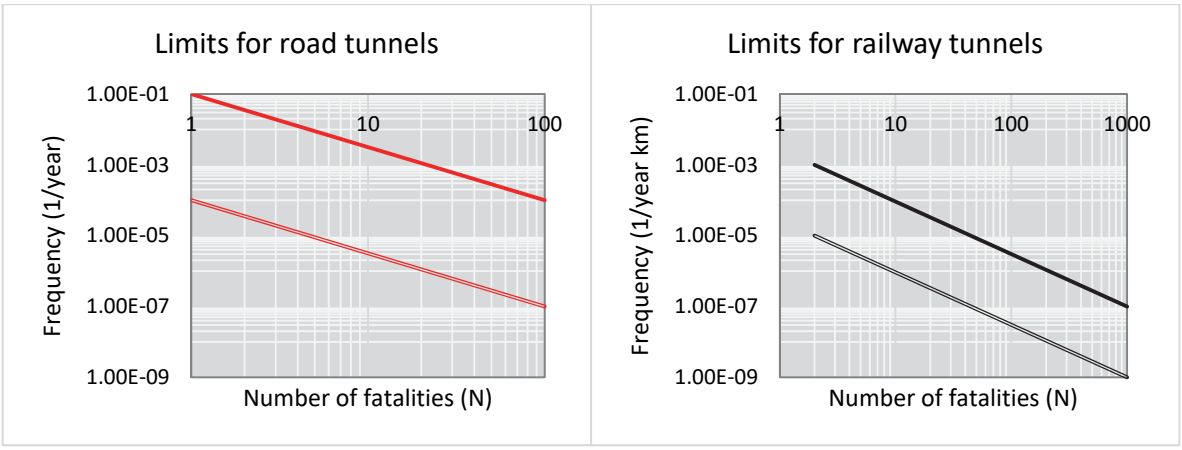

Figure 4.7A-B. Roadway and Railway tunnel ALARP band in Italy

4.5.2 Types of criteria

The acceptance criteria have been implemented through some general principles, among which the most known are the following three:

- ALARP (As Low As Reasonably Practicable);
- MEM (Minimum Endogenous Mortality);
- GAMAB (Globalement Au Moins Aussi Bon) or GALE (Globally at least as good).

The ALARP principle was established by the UK Health and Safety Executive (HSE) in 1974 and aims to minimise the societal risk, assessing what is technically feasible from an economic point of view. This principle is naturally used for systems where comparative criteria has to be used and, in fact, accounts for three regions labelled as non-acceptable, tolerable and negligible risk (Figure 4.8). If the risk is unacceptably

high, significant improvements must be provided for the system. On the other hand, if the risk is in the negligible region, no further measures are required. Finally, when the risk falls into the tolerable region (briefly called "ALARP zone" in the FN plane), a cost-benefit analysis is generally required to assess if additional measures must be implemented, because the improvement in terms of risk reduction should be greater than the cost, which, anyway, cannot be disproportionate. In this sense, the state of the art technology can fix the limit of the feasible risk reduction. Therefore, an FN curve (initial state of the tunnel), which lies only partially in the ALARP region, may be considered as acceptable if the cost for reducing the residual risk is non sustainable according to authorities and stakeholders.

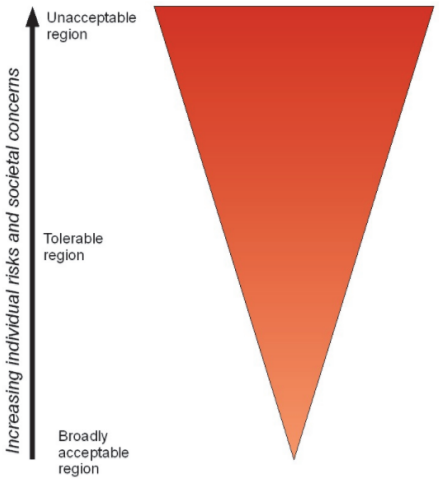

Figure 4.8. ALARP principle (source Wikipedia)

Considering road tunnels and the Italian Legislation (Legislative Decree 2006/264), two quantitative indicators of risk must be calculated when performing a quantitative risk analysis. The first risk indicator is the FN curve itself, which must be compared in absolute (and prescriptive) terms with the thresholds imposed by the law, graphically represented in the FN diagram as three zones (acceptable, ALARP and unacceptable). The second risk indicator is the Expected Value of fatalities (EV) that is particularly

useful for existing tunnels or every time the quantitative risk analysis is aimed to determine alternative measures to mitigate the residual risk. Contrary to the FN curve, the Expected Value must be interpreted in terms of comparison with a reference tunnel (whose definition will be discussed later). The EV should be, therefore, considered as the fundamental indicator for a risk-based approach, which acts as a standardised and harmonised tool for supporting the stakeholders' decision-making.

However, the limitation of the risk-based approach are inherently linked to the definition of the reference tunnel. The reference tunnel is normally a tunnel similar to the original tunnel but complies with all requirements and fulfils all conditions defined in the regulations (PIARC, 2012). In practice, it is sometimes unclear how to exactly define this reference tunnel. .

Moreover, it must be highlighted that even if a tunnel fulfils all regulative requirements, it has a residual risk which is not obvious and not specifically addressed (PIARC, 2012). This is the reason why the comparison between the redesigned and the reference tunnels is not done in terms of the FN curve, which makes sense as an absolute risk indicator, but in terms of the EVs, that is the area below the curve. From the practical point of view, this implies that when performing the QRA the risk analyst will:

- trace the FN curve of the as-designed or as-built tunnel;
- depending on the position of the curve in the FN diagram, alternative and mitigating measures may be proposed;
- in that case, the EV of the redesigned tunnel must be lower or at least equal to the EV of the reference tunnel;
- finally, the FN curve of the redesigned tunnel should be traced in the FN diagram, to verify in absolute terms the residual risk of the system.

It is worth noting that the FN curve of the reference tunnel is not asked to be represented in the diagram and nobody says that, in case it was, it would lie

continuously in the lower acceptable risk zone. Nevertheless, the risk associated to it should be assumed (D.Lgs. 2006) or demonstrated (FSV, 2010) to be acceptable, because the corresponding value of the EV is considered the target level by the stakeholders or authorities and used for the comparative analysis (compatible with GAMAB). The interpretation of the result using the comparative criterion is clear and the effect of the uncertainties is less evident because the same numerical method is used to estimate the EV for all states of the tunnel.

In Table 4.2 the thresholds of the absolute criteria adopted by some Member States are listed and in Table 4.3 the relative risk criteria are briefly described. The equations representing the upper and lower limits in Table 4.2 are defined for a certain range of fatalities (for example, 1<N<1000) while others are indefinite (N>1).

Table 4.2. Absolute risk criteria (N fatalities, F fire, E explosion, T toxicity) (PIARC, 2012)

	Absolute risk criteria					
FN curve	**Netherlands**	$F = 0.1\ N^{-2}$ per km per year, for N>10				
	Austria	$F = 0.1\ N^{-2}$ per year, for N>10 (L=1km) $F = 0.1\ N^{-2}\ L^{0.5}$ per year, for N>10 (other length)				
	Italy	Upper Limit $F = 0.1\ N^{-1}$ per year, for N>1 Lower Limit $F = 0.1\ N^{-3}$ per year, for N>1				
	Czech Republic (L=1km)	Upper Limit $F = 0.01\ N^{-1}$ per year, for 1<N<1000 Lower Limit $F = 10^{-4}\ N^{-1}$ per year, for 1<N<1000				
	Switzerland	ALARP (see Figure 4.9), for 100 m				
	Germany	(see Figure 4.10), for 1 km				
Expected Value (EV)		**Overall F+E+T EV**	**Specific F EV**	**Specific F+E EV**	**Specific E EV**	**Specific T EV**
[fatalities/year] [fatalities/year] [fatalities/km year] [fatalities/year]	**Austria** **France** **Germany** **Greece**	10^{-3} 10^{-3} $6.2 * 10^{-3}$ 10^{-3}	- - $5.0*10^{-3}$ -	- - $2.2*10^{-3}$	- - $1.0*10^{-6}$ -	- - $4.0*10^{-4}$ -

Table 4.3. Relative risk criteria (PIARC, 2012)

	Relative risk criteria		
FN curve	The most common applications among European countries are: - choice of alternative measures (basic vs alternative configurations); - transport of DG (forbid HGVs for a period etc.). Rarely for a comparison of the given vs reference tunnel (ambiguous).		
Expected Value (EV)		**Hazards**	**Reference tunnel**
[fatalities/year] [fatalities/year] [fatalities/km year] [fatalities/year]	**Austria**	Car fires Accidents	Compliance with the minimum safety requirements of the EU Directive; same length, type and traffic characteristics.
	Italy	Fires Acc.+fires Etc.	Compliance with the minimum safety requirements of the EU Directive; predefined performance of the safety systems; no indication for length and traffic.

The MEM criterion (Minimum Endogenous Mortality) is based on the individual risk. The idea behind this method is that new transport systems should not be the cause of the increasing level of endogenous mortality, historically linked to "technology" (work, entertainment, sport, etc.).

Finally, the GAMAB or GALE criterion (Globally at least as good) requires the existence of a reference system with accepted residual risks: the new systems, perhaps with the most innovative solutions, must not result in higher risks. The specificity of GAMAB is in the acceptance of the degradation of one residual risk provided that the overall risk is compensated by the enhancement of another risk feature.

4.5.3 European thresholds

Among the European countries, risk criteria differ for:

- the adopted aversion factor;
- the scope (including light vehicles or only dangerous goods);
- the nature (mandatory or suggested);
- the normalisation of the length of the tunnel in the calculation of the frequency.

Considering risk aversion, in Italy, Austria (FSV, 2010), UK and Czech Republic (2006) a unitary aversion factor is adopted for road tunnels, whereas in The Netherlands, Germany and Switzerland a value of 2 is preferred.

Regarding the scope of risk analysis for road tunnels, in Germany (RABT, 2006; BMVBS, 2009), Switzerland (2001) and Austria the acceptance criteria are referred only to dangerous goods. In addition, for these countries and Italy the risk assessment procedure has a mandatory nature (imposed by Decree) while in other countries such as The Netherlands and Czech Republic it is only a technical reference document.

Regarding the tunnel length, in Italy the risk of the tunnel is intended as a measure of the risk of the "tunnel's infrastructure" considered as a whole; therefore, there is no normalisation. Differently, for many other countries (Austria, Norway, Czech Republic, Germany, Switzerland) the risk is normalised for the overall extension of the tunnel. This type of difference is well shown in the two graphs in Figure 4.7A-B: the frequency for railway tunnels is expressed in annual events per kilometres, which is an implicit way of considering the length of the tunnel as a risk factor. On the contrary, road tunnels are approached like punctual infrastructure, for which the risk is related to the whole tunnel and does not depend on the length.

The following graphs (Figures 4.9- 4.11) summarise the previous information, reporting risk criteria for few countries with or without ALARP zone on the FN diagram.

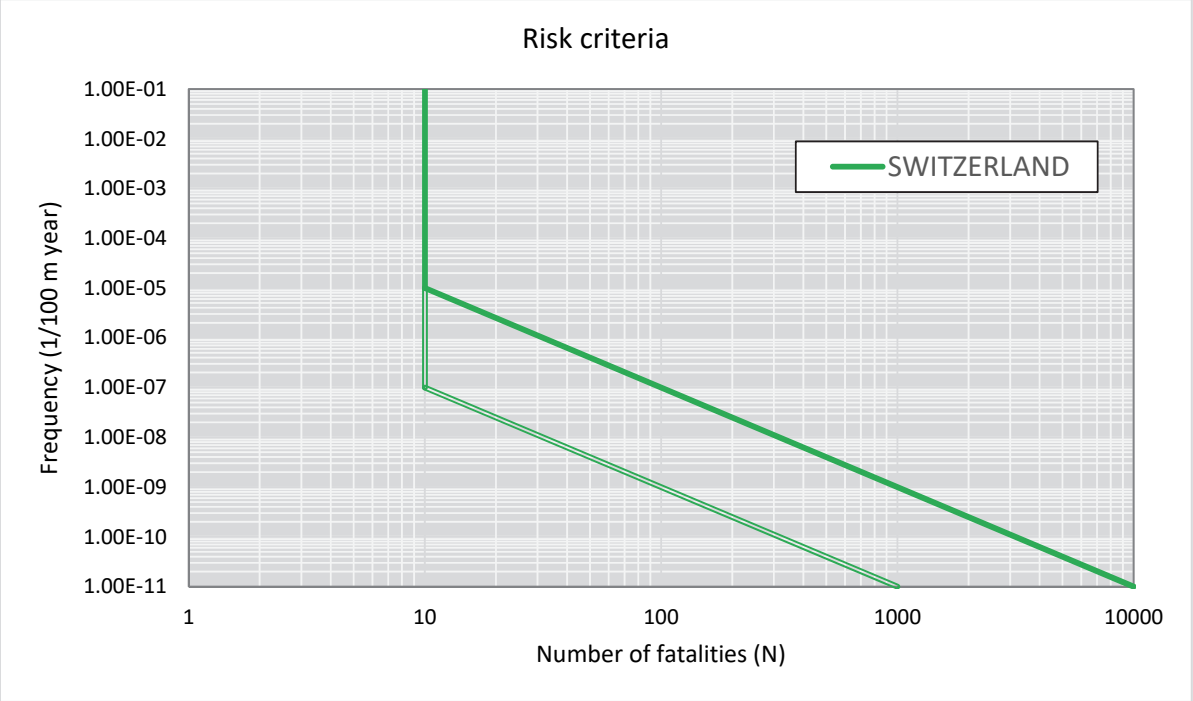

Figure 4.9. Swiss criteria

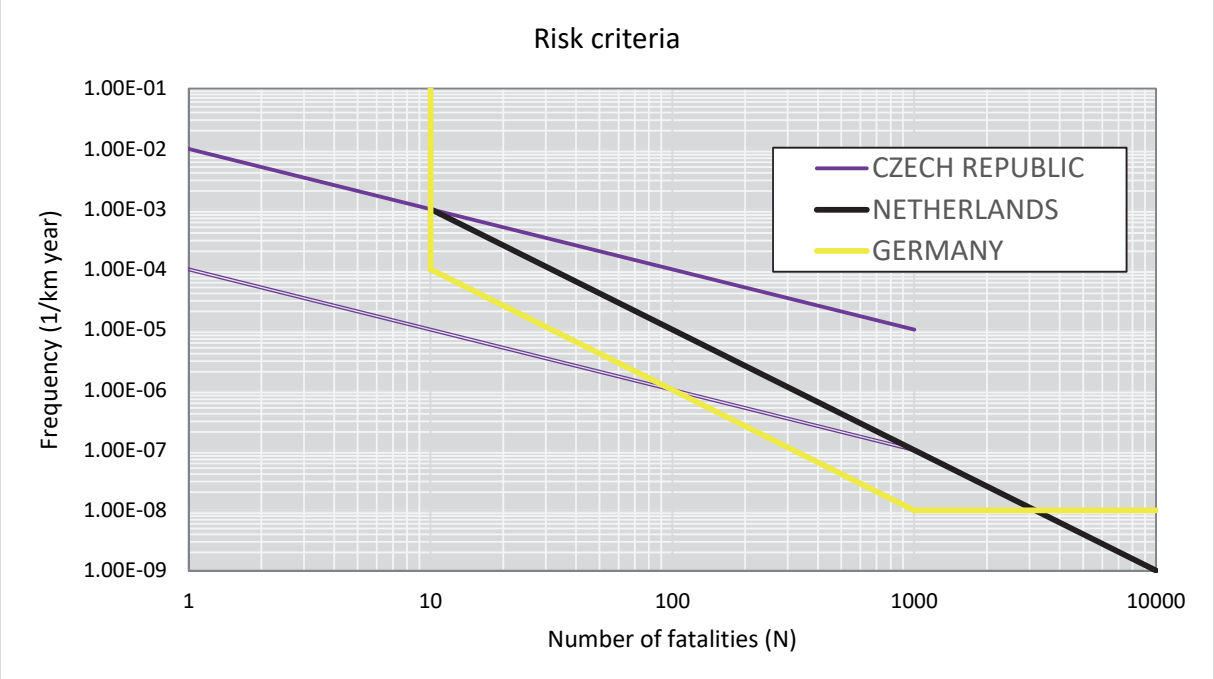

Figure 4.10. Czech, German and Dutch criteria

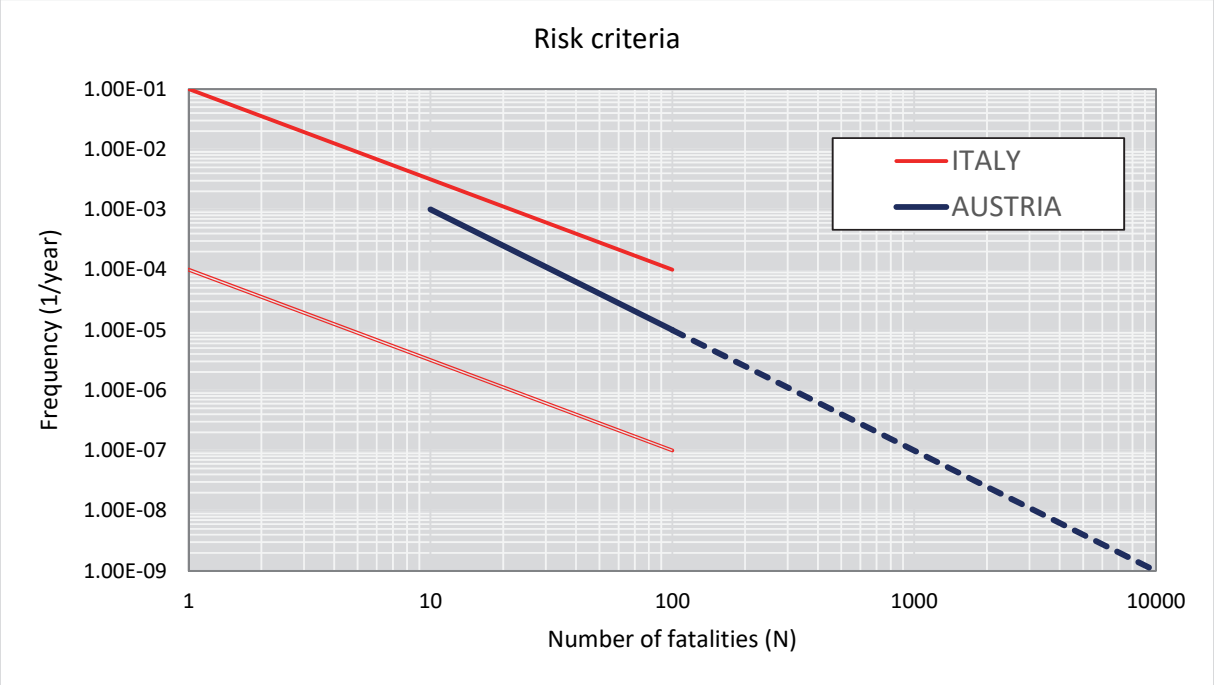

Figure 4.11. Italian and Austrian criteria

SECTION 2: BACKGROUND ASPECTS FOR TUNNEL FIRE SAFETY

5. FIRE ACTION

6. MATERIALS AND STRUCTURAL BEHAVIOUR

7. EVACUATION

Chapter 5

Fire action

5.1 Overview of full-scale tests

A thorough characterisation of a fire implies thermo-chemical and physical aspects, fluid dynamics notions and varying distribution of forces on the surrounding structure. Considering that fire is an accidental and rare action, this characterisation has required along the years a significant effort in conducting full-scale experimental tests.

The simplest way to represent a fire is a distribution of temperature over time at a given, and significant, point (e.g. up to the fire source). By representing a fire through an evolving trend of temperature, the effect of the fire can be easily transferred to the surrounding structure by studying heat transfer and then structural behaviour. However, in the fire compartment, temperature is spatially and temporally variable and only a very schematic approach can interpret a fire as a single trend of temperature. More interesting parameters are the heat release rate (HRR), expressed in MW, and the fire load, expressed in MJ. Roughly, the first is typical of the combustible materials whereas the second depends also on the quantity that can actively participate to the combustion.

Fire experimental tests involving HGV vehicles or other types of combustible materials have been conducted in order to establish a typical rate of heat release, a fire design curve for tunnel structures, a critical velocity preventing backlayering as well as a maximum temperature achievable on the ceiling and across the section. Below, an overview of the most significant fire tests is reported, including the main findings obtained.

- Tunnel fire tests at VTT, 1985

The fire tests were conducted in a short tunnel (approximately 183 m x 5.5 m x 5 m) in Lappeenranta, southeastern Finland, equipped with two fans and two pilot fire sources of wooden cribs. Test 1 represented a subway train and showed a brief ignition phase and a steady rate of fire spread (1.8 MW/s) while Test 2 involved several stacks of wooden cribs representing vehicles with a spacing of 1.6 m but no spread occurred. Spalling phenomena were observed during both tests.

- EUREKA – FIRETUN, 1990-1992 (Fires in Transport Tunnels)

21 tests were carried out in Norway (vehicles, train carriages, cribs, heptane pools, fully-loaded HGV), Germany (wooden cribs), VTT (wooden cribs) and INERIS (heptane pools). During these tests, the maximum temperatures reached for burning vehicles were 800-900 °C for vehicles and 1300 °C for HGV near the fire source, while much lower values were recorded upwind or within a short distance. Regarding the HRR, all vehicles showed a fast development in the first 15 minutes, with a growing phase from medium to ultra-fast depending on the ventilation conditions, and a HRR of 100 MW for HGVs.

- MTFVTP, 1993-1995 (Memorial Tunnel Fire Ventilation Test Program)

Pool fires were considered in the test series, with heat release rates ranging from 10 MW to about 100 MW in a 850 m long tunnel in the USA. The tunnel was equipped in order to check the reliability of different ventilation systems in extracting smoke.

The tests involving longitudinal ventilation systems showed that jet fans are effective for fires up to 100 MW and that airflow velocities of 2.5-3 m/s were sufficient to prevent backlayering. In addition, it was observed that the longitudinal air velocity depended on the number of the active fans and their thrust but not on the configuration.

The tests involving transverse ventilation systems showed that the extraction of smoke is beneficial and oversized exhaust ports as well as single-point openings for extraction improved significantly the smoke controlling capacities of a tunnel. Longitudinal air

velocity was still the most important parameter affecting smoke control, which defines the most restrictive conditions in terms of visibility instead of heat.

- FIT, 2001-2005 (Fire in Transport Tunnel)

The FIT project involved 33 partners from 12 European Countries in gathering information on fires in tunnels. The result of the work were three technical reports on the state of the art of the design fires, guidelines on fire safety design and best practice for fire management.

- DARTS, 2001-2004 (Durable and Reliable Tunnel Structures)

DARTS project regarded the development of tools for the choice of cost-optimal tunnel type, layout and construction procedures. Even if the project was mainly referred to new tunnels, the decisional procedures defined in the work are considered to be applicable also to upgrade existing tunnels.

- Safe Tunnel, 2001-2004

Safe Tunnel project was coordinated by the Centro Ricerche FIAT and aimed to reduce the number of road tunnel accidents by introducing preventive safety measures. Two strategies were investigated: the first was to deny access into the tunnel to vehicles with on-board anomalies and the second was to introduce measures help control the speed of vehicles in the tunnels.

- SIRTAKI, 2001-2004 (Safety Improvement in Road and rail Tunnels using advanced information, technologies and Knowledge Intensive decision support models)

The goal of SIRTAKI was to develop an advanced tunnel management system, fully integrated in the overall network management. Specifically, four aspects of tunnels management were considered in providing innovative technologies and installations: the prevention of conflicting situations and emergencies; support to tunnel managers; integrated management within the transport network; improvements to sensor and surveillance. The main component of SIRTAKI project is the Decision Support System, or

DSS, that provides an aid to the "crisis manager" in terms of real time information (to get the point of the emergency).

- Virtual Fires, 2001-2005

The scope of the project, coordinated by Austria (Institute for the Structural Analysis) was to develop a simulator to help firefighters in emergencies management training through the simulation of a virtual environment instead of field exercises.

- UPTUN, 2002-2006 (Upgrading Methods for Fire Safety in Tunnels)

UPTUN project involved 41 partners from 13 different Member States of the European Union, coordinated by the Dutch TNO and the Italian ENEA. The main objectives were to develop innovative and sustainable measures to limit the probability and consequences of tunnel fires and, secondly, a holistic approach to evaluate and upgrade the existing tunnels. The results are contained in seven technical work-packages.

- Safe-T 2003-2006 (Safety in Tunnels)

Safe-T was coordinated by TNO with the objective to draft harmonised guidelines for tunnel safety in Europe, based on the contributions of local authorities, fire brigades and emergency organisations.

- The Runehamar Tunnel fire test series, 2003

The test series consisted of four tests, carried out in a road tunnel (length 1.6 km and area 50 m^2, ad hoc reduced when necessary) in Norway. The tunnel was equipped with two fans and the fire sources were chosen so as to represent HGV fire load made of plastic and wooden pallets (in a proportion 0.2 and 0.8), reproducing peaks of heat release rate of 203, 158, 125 and 70 MW respectively as reported in Figure 5.1. Like during the Memorial Tunnel tests, temperatures around 1300 °C were registered near the fire source. Regarding the ventilation conditions, when the jet fan airflow was reduced to 2 m/s during the fully developed phase the backlayering of smoke started.

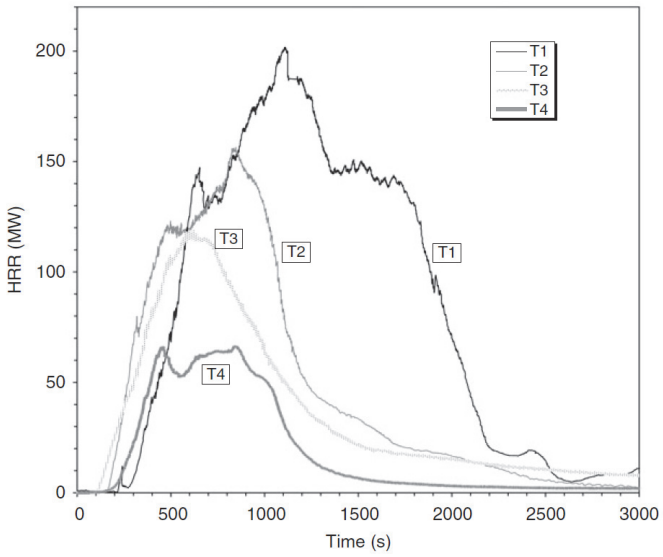

Figure 5.1. Heat release rate during the tests (SFPE, 2016).

During the Runemahar campaign tests the backlayering phenomenon was for the first time studied and, partially, addressed. The data collected were used to establish experience-based relationships (5.1) and (5.2) which allow to do simple calculations as those reported in Figures 5.2 and 5.3. Those graphs show that the flame length grows rapidly by increasing the heat release rate and, less evidently, by diminishing the height of the tunnel. The relationships, where Q* is the dimensionless HRR, consider the flame length both upwind ($L_{f,us}$) and downwind ($L_{f,ds}$) the fire source in case of low ventilation (LV) flow (good smoke stratification). Otherwise, in case of a high ventilation (HV) flow only the downwind direction is considered.

From Figure 5.2 it can be noticed that in case of low (or insufficient) longitudinal ventilation, for 120 MW fire the backlayering ($L_{f,us}=L_{f,tot}-L_{f,ds}$) does not exceed 100 m.

$$L_{f,tot_{LV}} = H * 10.2 * Q^* \quad (5.1)$$

$$L_{f,tot_{HV}} = H * 5.5 * Q^* \quad (5.2)$$

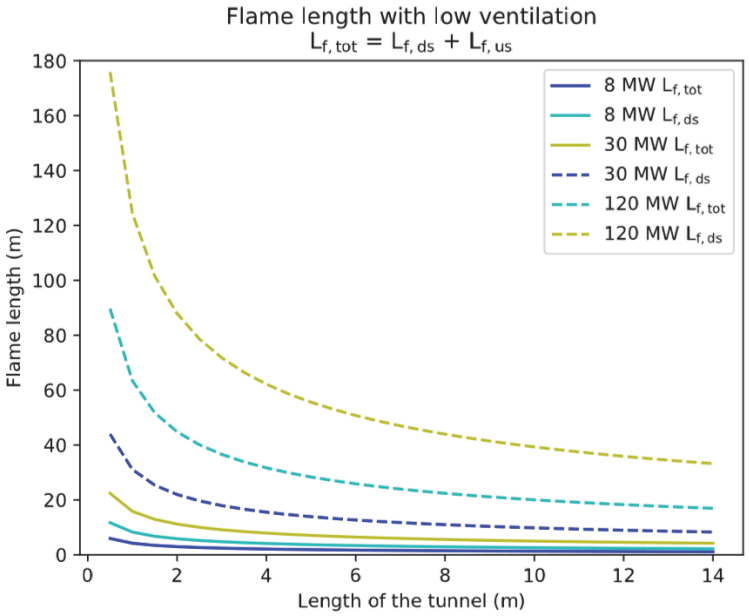

Figure 5.2. Flame length under low ventilation conditions

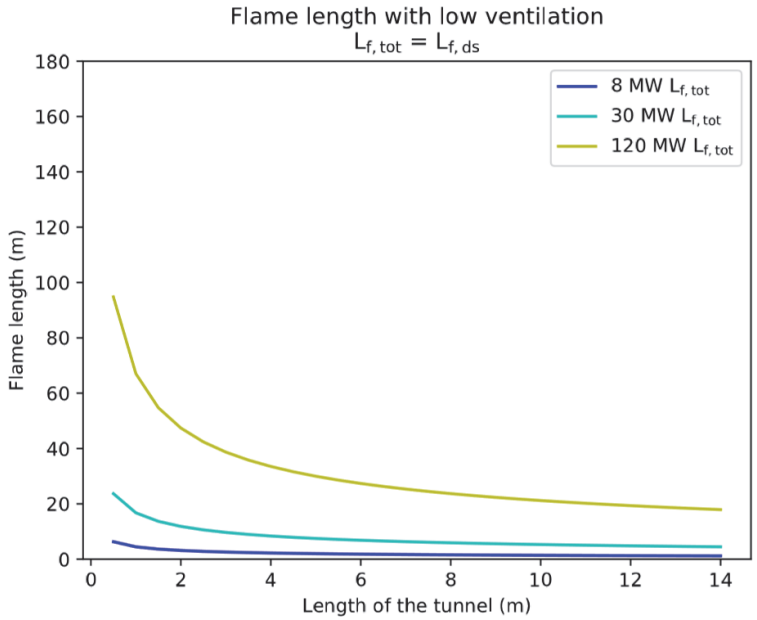

Figure 5.3. Flame length under high ventilation conditions

5.2 Fire scenarios for road tunnels

The definition of a fire scenario is crucial for the reliability of the results that will be obtained from the numerical analysis. In this section, the current state of the art is commented on and some recommendations are added. The difference between unidirectional and bidirectional tunnels will be considered when necessary.

5.2.1 Position of the fire

The positioning of the fire source is particularly significant when a single worst case scenario is analysed. In that case, it is crucial to understand which conditions are the most dangerous for life safety in order to be contemporarily on the safe side without contradicting the statistics. Therefore, a balance needs to be established considering the most frequent positions of accidents, queue formations and smoke dynamics.

Statistical data for road tunnels confirm that the variation of the visibility conditions near the portals affect the frequency of the accidents, which are more concentrated in the first and last sections for both unidirectional and bidirectional tunnels. By positioning the fire near the portals there is a coherence with the statistics but this assumption doesn't necessarily seem to be on the safe side from a queue formation and smoke extraction point of view. In fact, the position of the fire indirectly defines a different queue formation, which determines the number of people involved in the evacuation process; the more people inside the tunnel, the higher the risk of a fire scenario. In this case, it is worth to distinguish between unidirectional and bidirectional road tunnel, whose smoke management strategies generally imply respectively longitudinal and transverse ventilation system.

Considering unidirectional tunnels, it is generally assumed that vehicles downwind the fire source are able to exit the tunnel safely, while vehicles upwind need to stop and start the evacuation process: in this case, a fire position near the exit portal of the tunnel is on

the safe side, because more people would be involved in the evacuation. A good balance might be to locate the fire between the middle and the end of the tunnel, e.g. at 2/3 of the length. For bidirectional tunnels, instead, it is generally assumed a fire position in the middle of the tunnel, so as not to facilitate any direction of travel.

Finally, if one only wants to focus on the smoke dynamics, a fire position in the middle of the tunnel is generally assumed to be on the safe side (apart from specific cases of transverse ventilation system with a single point extraction, where the most conservative fire position should be chosen depending on the position of the extractor along the tunnel).

5.2.2 Heat release rate

As previously reported, the definition of the expected heat release rate in road tunnels has been investigated during full-scale tests in large experimental campaigns. Recently, a comprehensive report on the design fires currently adopted in Europe has been published by the World Road Association (PIARC, 2017).

If there are no specific restrictions on the traffic volume, two or three different orders of magnitude of HRR should be considered for a correct fire risk assessment of road tunnels. The three level of HRR can be related to car, bus and HGV fires.

Car fires are easily controlled by ventilation systems, but need to be considered because light vehicles represent the most significant percentage in the traffic volume. Bus and HGV fires are more difficult to manage, resulting in high temperatures and are generally represented by fast growth phase and long duration, up to several hours. Collisions between vehicles might lead to major fires, resulting in higher and longer heat release rate curves compared to the previous ones (Carvel, 2015), but they are generally not considered in the design and refurbishment process. However, it is worth noticing that all major fires had at least more than one vehicle involved in the fire.

5.2.3 Duration of the fire

The duration of the fire that one wants to investigate changes depending on the objective of the analysis. In general, the fire load affects the duration, which for a HGV fire inside a tunnel can last several hours, because in spite of being a confined environment, tunnels provide enough oxygen for fully developed fires.

As usual in the fire prevention field, the duration of the fire analysis may be limited to the first 15-20 minutes if life safety is the primary goal (after that period, no survivors are reported to be found in tunnels) while the entire heat release rate curve needs to be considered if fire resistance analysis are being carried out (Schröder, 2016).

5.2.4 Official recommendations

ANAS Guidelines suggest a distribution of values for non-ADR fire scenarios. Buses and HGVs are recommended but no information is given for light vehicles, although it is specified to consider them in the risk assessment procedure. No information is given regarding the position of the fire in case of worst case scenarios nor the duration of the fire simulation. Data recommended for risk analysis considering buses and HGVs fires are reported in Table 5.1.

Table 5.1. ANAS recommendations for fire scenarios

	Bus fire	**HGV fire**
HRR [MW]	Triangular distribution 20, 30, 35	15-150 (time to peak: 13 min)
Fire growth rate [kW/s²]	Triangular distribution 0.08,0.1,0.13	0.025-0.215
Fire load [GJ]	Uniform distribution 50-55	60-90

Other works (Persson, 2002) focused on design fires specifically for evacuation analysis. Starting from international guidelines and studies (Joyeux, 1997; PIARC, 1999), Persson

recommends a car and two HGV fires as shown in Figures 5.4-5.6. In the same figures, the curves representing slow, medium, fast and ultra fast fire growth are reported, whose time to reach 1 MW is respectively 600, 300, 150 and 75 seconds (Eurocode 1, Appendix E.4). Different growth rates are associated to the selected scenarios: car fire has between a medium and slow fire growth rate, while HGV fires are near the trend of a fast fire.

The HGV fires are related to heavy vehicles and intended as scenarios in which the ventilation system is able or not to prevent the spread of fire among multiple vehicles. Specifically, HGV_1 is a scenario where ventilation is able to limit the propagation of fire, while HGV_2 represents a fire involving more vehicles. It is deduced from the work that the fire is positioned in the middle of tunnel, that is unidirectional.

These curves are the basis of the fire scenarios chosen and explained in Chapter 8, which introduce the case studies contained in Chapters 9-10 for which QRA is conducted.

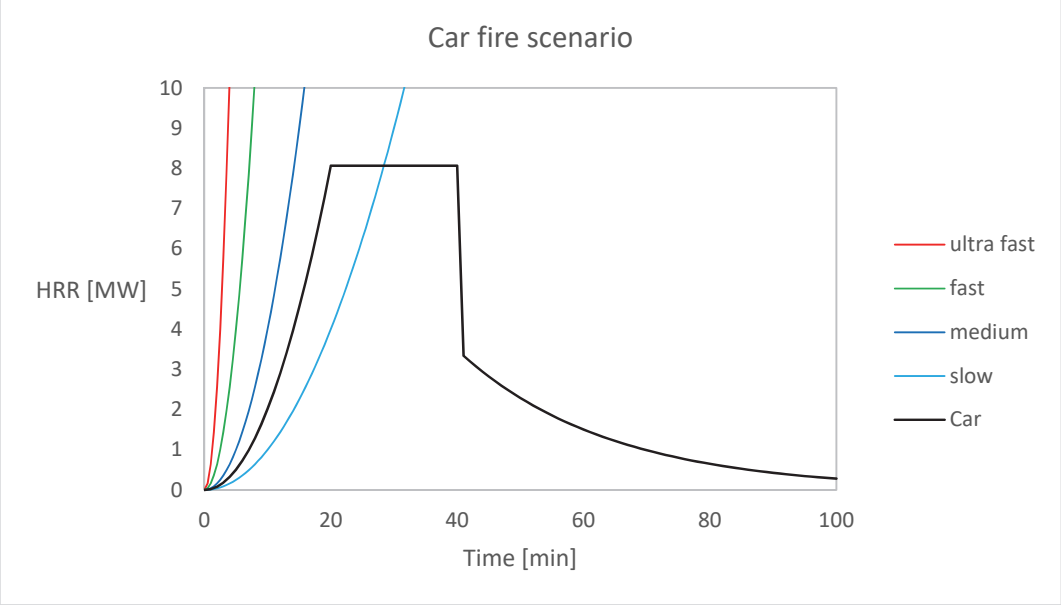

Figure 5.4. Car fire curve (Persson, 2002)

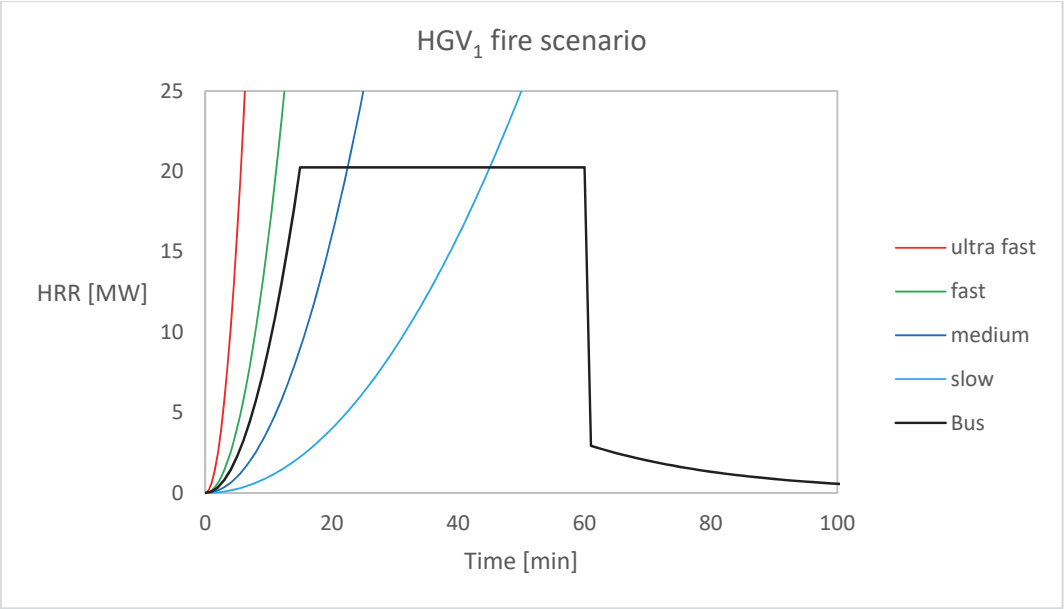

Figure 5.5. HGV$_1$ fire curve (Persson, 2002)

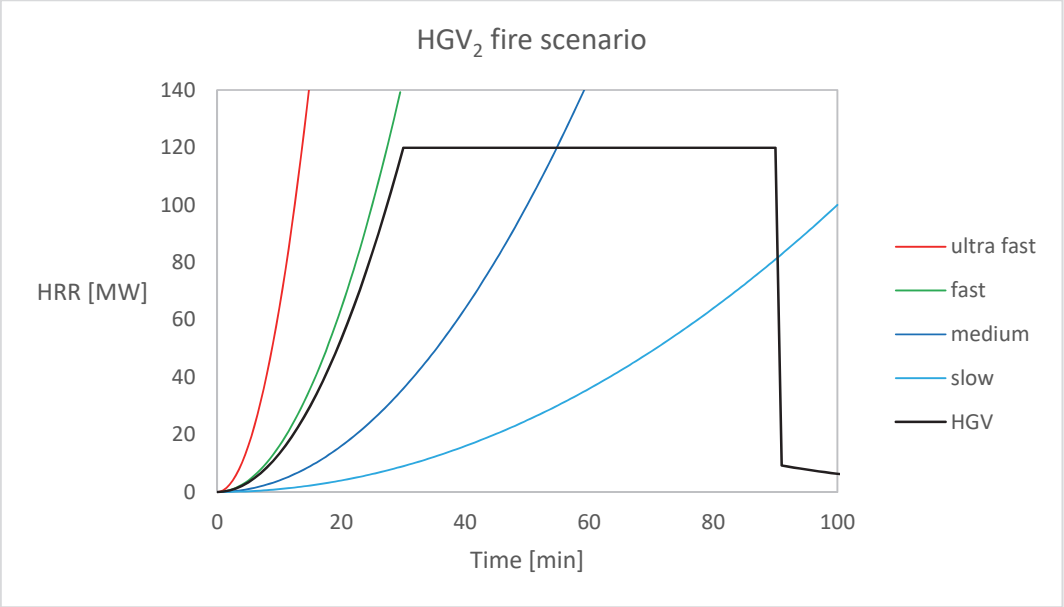

Figure 5.6. HGV$_2$ fire curve (Persson, 2002)

5.3 Fire modelling

5.3.1 Simplified models

Simplified models consist in a range of analytical relationships based on previous experimental campaigns and experiences. When it comes to simplified models, conventional fire curves are certainly the most known way to represent the effect of a fire event. Conventional fire curves represent gas temperatures in the fire compartment during the post-flashover phase, neglecting the ignition and propagation phases, which is typical of the initial part of the natural fire curve. Some conventional curves (ISO 834, Hydrocarbon) are monotonically increasing with no extinction phase, because they were developed to test fire resistance of structures.

Among the curves reported in Figure 5.7, the RWS fire curve represents tunnel fires for various combustibles, not necessarily hazardous materials or flammable liquids. This fire curve was initially developed during extensive testing conducted by the Dutch Ministry of Transport (Rijkswaterstaat, RWS) in cooperation with the Netherlands Organisation for Applied Scientific Research (TNO), later reproduced in the Runehamar tunnel tests. Compared with other conventional fire curves available in literature, the RWS is the highest: at 20 minutes it is respectively 400 °C and 200 °C higher than the standard ISO 834 and the Hydrocarbon curves.

The RABT curve (from German Guidelines) is also used to represent both road and railway tunnel fires: it is similar to the RWS in the first phase, but then it is the only one that provides an extinction phase.

Simplified models can be used also for other aspects of fire characterisation, such as the estimation of flashover in a fire compartment (Babrauskas, 1980; McCaffrey et al, 1981; Thomas, 1981) or the calculation of gas temperature at a given distance from the fire source (Hasemi et al, 1984; Heskestad, 1995). They can provide insights and good evaluations for simple cases and preliminary analysis. However, their use has strong

limitations, because they have been validated under well-defined geometrical conditions (area of the compartment, ceiling height, position of the openings) and fires of limited heat release rate.

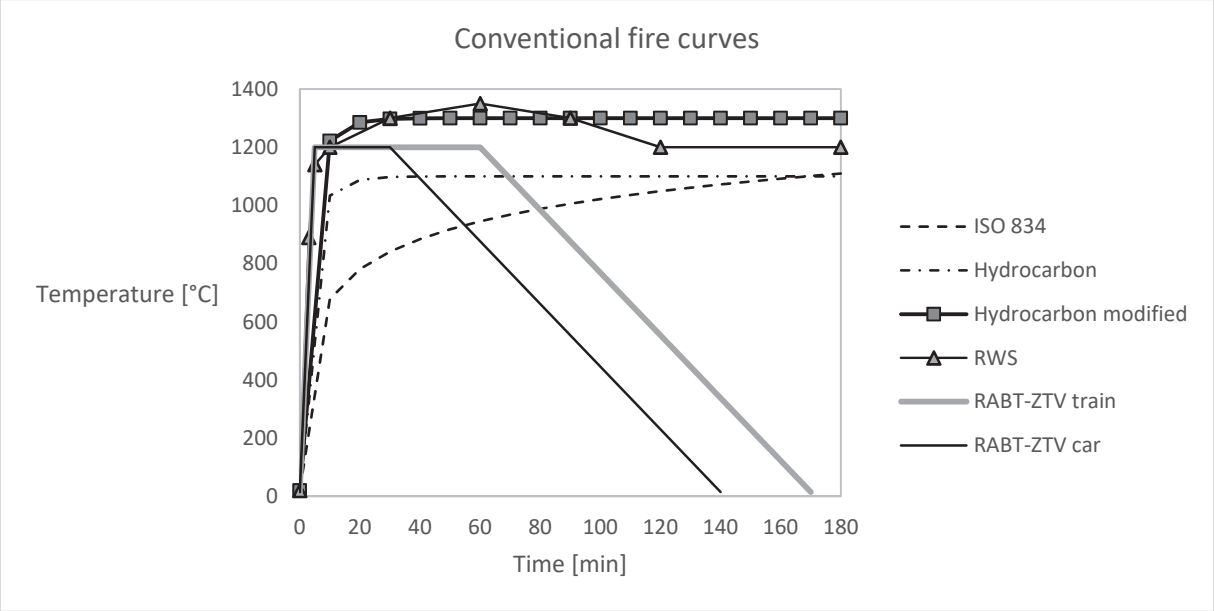

Figure 5.7. Conventional fire curves

5.3.2 Zone models

Zone models are a step further compared to simplified models. They solve the equations of mass and energy conservation in two controlled volumes, called "zones", where the macroscopic quantity (temperature, velocity, pressure) are spatially uniform but temporally variable. These models work well under the hypothesis of the formation of an upper layer of hot smoke and lower layer of fresh air at the steady state (Figure 5.8) and can be useful for predictions in regular geometries. The layer height defines the horizontal boundary between the two zones and its position can temporally vary depending on the evolution of the heat release rate and obviously geometrical characteristics. In order to describe slightly more complex geometries (more volumes connected with each other) more zones can be defined in the input file, provided that

they share one lateral surface. The output of the zone models are trends in time of the upper and lower layer temperature as well as layer height for each zone.

The most known zone models are CFAST and Ozone which slightly differ, for instance, for the maximum number of zones that can be defined, the plume correlation (Heskestad model in CFAST, McCaffrey and Thomas models in Ozone) and the orientation of the openings (vertical or horizontal at the ceiling). The use of zone models is also limited to a relatively low heat release rate (approximately 4 MW or 1 MW/m^3) and fixed geometrical characteristics (area and height of the fire compartment). By exceeding these values the stratification into two zones is not guaranteed nor confirmed by experimental tests. In addition, zone models do not directly model combustion and turbulence phenomena, which can strongly affect fire and smoke propagation inside the compartment and the fluid dynamics interaction with the lateral walls.

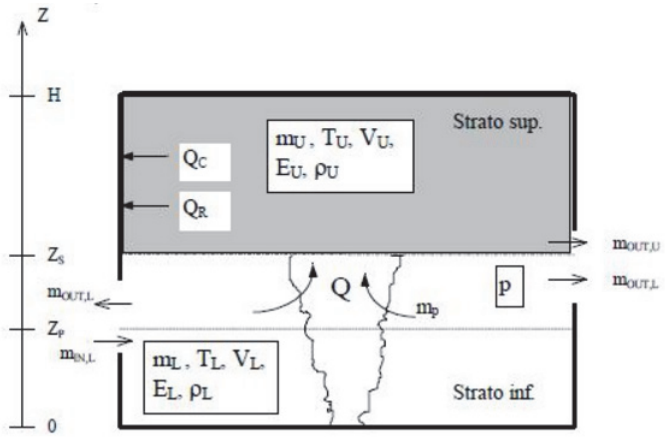

Figure 5.8. Two-zones model scheme

5.3.3 Field models

Field models are the most advanced tools to describe the fire phenomenon and smoke dynamics. Mass, energy and momentum equations take the form of the Navier-Stokes (NS) equations, a set of nonlinear partial differential equations that, together with transport, combustion and radiation equations, wholly describe the behaviour of a fluid

during a fire. The computational fluid dynamics (CFD) is the branch that deals with NS equations, whose solution in closed form is still not available and constitutes one of the unsolved problems of mathematics. Different schemes of discretisation (finite differences, finite volume, finite element) have been developed and are used in commercial softwares together with turbulence models (also known as "closure models") whose choice depends on the characteristics of the problem. Field models can be also combined with simplified 1D models for reduced computational effort but maintaining reasonably good accuracy in sections interested by complex flows (Colella, 2012; Cosentino, 2017).

DNS (Direct Numerical Simulation), LES (Large Eddy Simulation) and RANS (Reynolds Average Navier Stokes) are the three numerical formulations used by CFD software to predict pressure, velocity and temperature fields in the area (Figure 5.9).

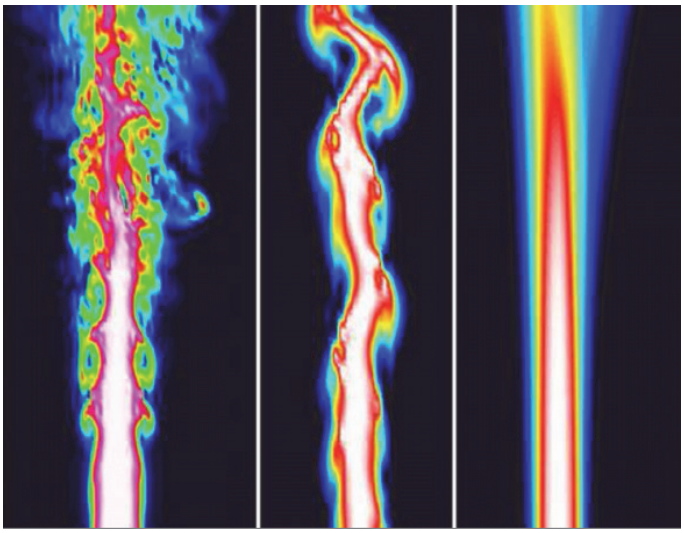

Figure 5.9. RANS, LES and DNS predictions of a turbulent jet (Maries et al, 2012)

DNS is the most accurate formulation and its level is comparable to experimental tests. Very fine grids (mm or less) are used and the computational effort is extremely high (weeks or more for few seconds in small areas), therefore its use is restricted to non-civil applications (micro flame studies, droplets, reaction of species, etc.).

LES provides a good level of accuracy because it directly models large and medium size eddies (whose dimension is related to the grid size) by filtering lower scale eddies and accounting for the energy dissipation with a closure model (Smagorinsky or Deardoff model). To have an idea of the quality of the simulation, one should assure that the ratio between the subgrid kinetic energy (k_{SGS}) and the total kinetic energy ($k_{SGS}+k_{LES}$) does not exceed 0.2. Keeping this ratio, also called "measure of turbulence resolution", below 0.2 guarantees that only a small part of the total energy is cut and modelled through a closure equation whereas the remaining part is directly solved (Pope, 2004).

The RANS formulation solves an average field of variables. Additional equations are needed to close the problems and several models are available (k-ε, k-ω, etc.). The results are less accurate but in some cases can be sufficient to make predictions on gas temperature.

The solver of the CFD software can use explicit or implicit schemes for the time integration to solve the time-dependent equations and, additionally, other conditions may be imposed for stability and convergence.

The quality of the results can be highly affected by the choice of the computational grid. This should be defined in relation to the characteristic fire diameter D^* expressed by the following equation (5.1), where $\dot{Q}$ is the HRR, ρ_∞ is the density, c_p is the specific heat and T_∞ the gas temperature (∞ is related to ambient conditions). The accuracy of the simulation is given by the ratio D*/δ, from which is δ derived.

$$D^* = \left(\frac{\dot{Q}}{\rho_\infty c_p T_\infty \sqrt{g}}\right)^{2/5} \tag{5.1}$$

In the following paragraphs, the equations governing the motion of the fluid are reported whereas the fire model FDS is commented in Appendix B.

5.3.3.1 The governing equations

The fluid is considered continuous, even if in reality its structure is molecular, composed by particles, but this is meaningless for the length of the problem of fluid flows. In this context, the fluid is described by means of macroscopic quantities as velocity, pressure, density, temperature, spatially and temporally variable.

The governing equations of the fluid motion represent mathematical statements of the conservation laws of the physics:

- the mass of a fluid is conserved;
- the variation of the momentum equals the sum of the acting forces on the fluid;
- the variation of the energy equals the sum of addition of heat and of the work done on the fluid.

Mass conservation in three dimensions

The rate of increase of the mass in a fluid element is equal to the net rate of flow of mass into the fluid element. The resulting equation is called continuity equation (5.2):

$$\frac{\partial \rho}{\partial t} + div(\rho \underline{u}) = 0 \tag{5.2}$$

where ϱ is the density and $\underline{u}$ is the vectorial velocity (the term $\rho \underline{u}$ is the convective term). If the fluid is incompressible (i.e. liquid, with constant density) the equation can be written as in (5.3):

$$div\, \underline{u} = 0 \tag{5.3}$$

Momentum equation in three dimensions

The rate of increase of the momentum of the fluid particle is equal to the sum of forces acting on the fluid particle (5.4-5.6):

$$\rho \frac{Du}{Dt} = \frac{\partial(-p + \tau_{xx})}{\partial x} + \frac{\partial \tau_{yx}}{\partial y} + \frac{\partial \tau_{zx}}{\partial z} + S_{Mx} \tag{5.4}$$

$$\rho \frac{Dv}{Dt} = \frac{\partial(-p + \tau_{yy})}{\partial y} + \frac{\partial \tau_{xy}}{\partial x} + \frac{\partial \tau_{zy}}{\partial z} + S_{My} \tag{5.5}$$

$$\rho \frac{Dw}{Dt} = \frac{\partial(-p + \tau_{zz})}{\partial z} + \frac{\partial \tau_{xz}}{\partial x} + \frac{\partial \tau_{zy}}{\partial y} + S_{Mz} \tag{5.6}$$

where p is the pressure (normal direction), τ are the viscous stresses (tangential direction) and S_M are the volume forces.

Energy equation in three dimensions

The rate of increase of the energy of the fluid particle is equal to the sum of the net rate of head added to the fluid particle and the net rate of work done on the fluid particle.

$$\rho \frac{DE}{Dt} = -div(\rho \underline{u}) + \left[\frac{\partial(u\tau_{xx})}{\partial x} + \frac{\partial(u\tau_{yx})}{\partial y} + \frac{\partial(u\tau_{zx})}{\partial z} + \frac{\partial(v\tau_{xy})}{\partial x} + \frac{\partial(v\tau_{yy})}{\partial y} + \frac{\partial(v\tau_{zy})}{\partial z} + \frac{\partial(w\tau_{xz})}{\partial x} + \frac{\partial(w\tau_{yz})}{\partial y} + \frac{\partial(w\tau_{zz})}{\partial z}\right] + div(k\ grad\ T) + S_E \tag{5.7}$$

where the term $div(k\ grad\ T)$ represents the energy flux due to heat conduction, the term $div(\rho \underline{u}) + [\dots]$ is the work done by surface forces (p and τ), the term S_E is the energy source.

Navier – Stokes equations for a Newtonian fluid

The NS equations are the fundamental partial differential equations that describe completely the flow of any fluid, turbulent or laminar. The set of NS equations has to be completed by boundary and initial conditions. Their solution is the velocity field of the fluid (5.8-5.10).

$$\rho \frac{Du}{Dt} = -\frac{\partial p}{\partial x} + div(\mu\ grad\ u) + S_{Mx} \tag{5.8}$$

$$\rho \frac{Dv}{Dt} = -\frac{\partial p}{\partial y} + div(\mu\ grad\ v) + S_{My} \tag{5.9}$$

$$\rho \frac{Dw}{Dt} = -\frac{\partial p}{\partial z} + div(\mu\ grad\ w) + S_{Mz} \tag{5.10}$$

The term S_{Mx} includes the momentum source and other small contributions of the viscous terms, due to the volumetric deformations. This derivation is possible because, for a Newtonian fluid, the viscous stresses are proportional to the rate of deformation. Specifically, the coefficient μ and λ are the dynamic viscosity (relating stresses to linear deformations) and the second viscosity (relating stresses and volumetric deformations).

A turbulent flow is characterised by nonstationarity and randomness: it has an apparently chaotic and irregular 3D movement, without ordered paths of the particles that compose the fluid and there is a great presence of vorticity and mixing. The Reynolds number, which represents the ratio between inertial and viscous forces (5.11), is high for turbulent flows.

$$Re = \frac{uL}{\nu} \tag{5.11}$$

where u is the characteristic fluid velocity, L is the characteristic length of the problem and ν is the kinematic viscosity (equal to the ratio between dynamic viscosity μ and density ϱ).

Kolmogorov studied the phenomena of formation and breaking up of eddies, known also as Kolmogorov's theory. In the initial phase, large eddies are produced by taking energy from the fluid motion: they develop and grow to the dimension L, called macroscale, or integral scale and coincides with the characteristic length of the system. At that time, eddies start to break down into smaller eddies: this is a gradual process with transfer of energy from large to smaller structures (Figure 5.10). This process continues until reaching very small eddies called microscale or Kolmogorov's scale: at this dimension, the energy is dissipated into heat by viscosity, because it is impossible to continue with the transfer of energy. This process is known as cascade energy and it regulates the formation and destruction of eddies.

If Re is low, the NS Equations can be solved easily; otherwise, if Re is high statistical considerations must be done to simplify the resolution of the problem.

The Mach number represents the ratio between inertial and pressure force and accounts for the effects of compressibility of the fluid (5.12).

$$\mathrm{Ma} = \frac{\mathrm{v}}{\sqrt{\gamma \mathrm{RT}}} < 0.3 \tag{5.12}$$

where R is the universal gas constant, T is the absolute temperature and γ is the adiabatic coefficient.

Another important simplification can be done if the Mach number is low: in this case, the fluid is treated as incompressible and the solution is easily obtained. FDS for example, works under the hypothesis of Low Mach Number (see Appendix B).

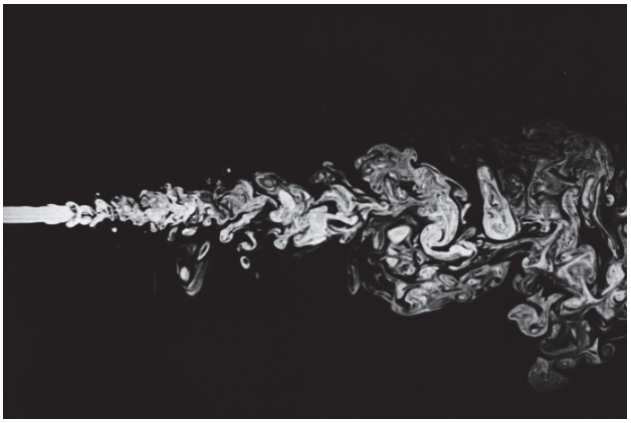

Figure 5.10. Small and large vortex structures (Source: Van Dyke, 1982)

5.4 Parametric study using FDS

A simple cut-and-covered tunnel is modeled with FDS. It has a central burner at x = 50 m and its dimensions are 100 m x 10 m x 5 m in the x, y and z axis.

A parametric study is carried out to understand how some parameters characteristics of tunnel fires affect the quantities of temperature, radiative heat flux gas, visibility and FED. These quantities are monitored in the centerline of six cross sections placed at x = 0, 10, 20, 30, 40, 50 m (Figure 5.11) and comparisons are made for steady-state conditions (HRR is constant for each simulation and the tunnel has only natural ventilation).

The study addresses 10 features that must generally be defined in the input file for tunnel fire modelling. These parameters are: grid resolution, HRR, fire source area, fire source dimensions, soot yield, material of the surrounding structure, presence of vehicles as

obstructions, length of the external boundary, longitudinal inclination and initial temperature. Each parameter P_i (i=1,…,10) is associated to three conditions (Run 1,2,3).

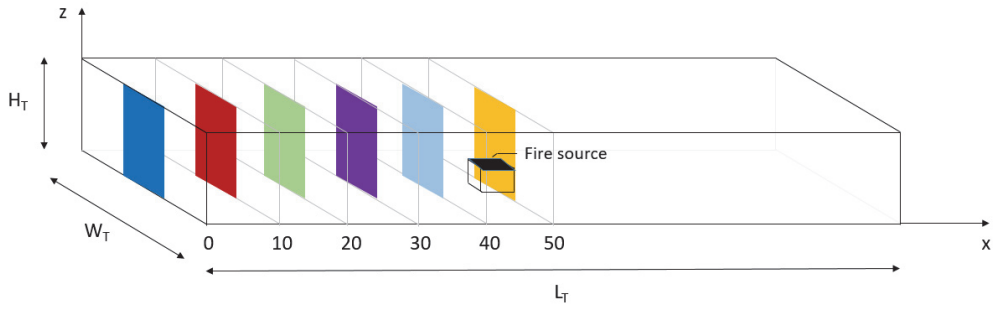

Figure 5.11. Scheme of the case study

For the complete results in terms of % differences, slice and graphs see the content of Appendix C.

It is worth highlighting that the following considerations can be generalised to tunnels or case studies similar in terms of geometry and boundary conditions to the one used for the analysis (single fire source, steady state conditions, measurements at the centerline of the cross sections every 10 meters).

The general findings are listed below:

- The four output quantities show very high differences along the entire length of the tunnel when some parameters are modified; these parameters are: HRR, material behaviour and longitudinal inclination. This highlights, on the one hand, that the FDS model is able to evaluate different hazards (HRR) and boundary conditions (longitudinal inclination). On the other hand, attention must be given to the choice of some parameters (material behaviour for temperature predictions).

- The four output quantities show very low differences along the entire length when some parameters are varied; these parameters are: fire source area, fire source B/W, initial temperature.

Table 5.2. Description of the parametric study

i	Parameter		Unit	Run 1	Run 2	Run 3
1	Grid resolution		cm	Coarse	Medium	Fine
2	Heat release rate	Coarse Medium Fine	MW	5	30	100
3	Fire source. Area		m^2	1	2	4
4	Fire source. B/W		-	1/1	2/1	4/1
5	Soot yield		g/g	0.05	0.10	0.20
6	Material behaviour		-	Inert	Concrete	Adiabatic
7	Presence of vehicles		-	No vehicles	Low traffic	Queue
8	External boundary. L_{ext}		m	3/5 Ht	Ht	2Ht
9	Longitudinal inclination		%	- 5 %	0 %	+ 5 %
10	Initial temperature		°C	10	20	30

- Some parameters affect only some of the four output quantities along the entire length: soot yield, for example, strongly affects the visibility but the other quantities are not influenced.

- Some parameters affect the quantities only near the fire source. This is in the case of the grid resolution.

- Among all the measured quantities, the temperature seems the most robust and reliable for most of the cases.

- Predictions on the first section X = 0 m, connected with an open boundary, are sometimes affected by large differences.

- Limited to the analysed cases, the lower layer is generally more sensitive to the variation of the parameters compared to the upper layer.

Considering the specific cases, the following considerations can be done:

- The grid resolution strongly affects the temperature only in the proximity of the fire source, whereas the other quantities are affected along the entire length of the tunnel. The temperature, in fact, drops quickly by going far from the ignition source, therefore its

values are not largely influenced (Figure 5.12). For most of the cases (5, 30 and 100 MW) the differences are below the 20 %.

- By increasing the HRR, the difference related to the grid resolution are more disperse across the whole section and for 100 MW important difficulties in predictions of the lower layer are identified. See Figures 5.12 for temperature comparisons for the 30 MW case.

- The HRR is confirmed to be the key parameter for fire models: its magnitude has reasonably a strong influence on the maximum temperature achieved and this is in agreement with the common sense of fire hazard and consequence analysis.

- The fire source area and ratio between the horizontal dimensions (B/W) do not affect significantly the output quantities. This is an encouraging result, because it implies that no matter what the dimensions of the fire source are (which is sometimes an open issue for CFD users), the overall behaviour is caught.

- The soot yield, which represents the chemical reaction occurring during the burning of the vehicle, has a considerable effect only on the visibility. On the other hand, according to the simulations the gas temperature is not significantly dependent on this parameter. See Tables 5.3 and 5.4 for the variation of the quantities with the soot yield.

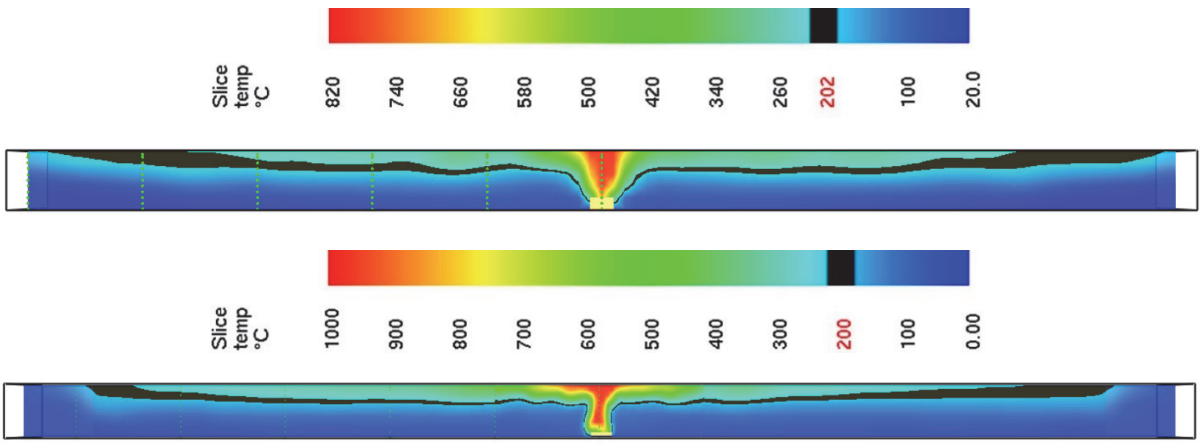

Figure 5.12. 30 MW fire scenario for coarse and centered-medium grid resolution

Table 5.3. Difference (%) by varying the soot yield, Upper layer (z=4m).

UPPER LAYER – SOOT VARIATION (0.05-0.2 g/g)	
TEMPERATURE	RADIATIVE HEAT FLUX GAS
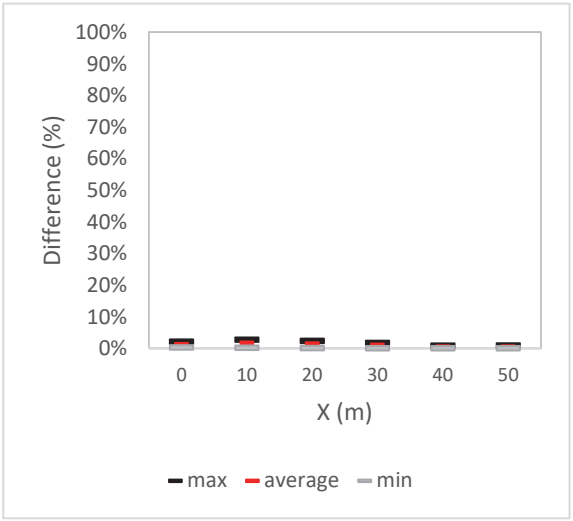	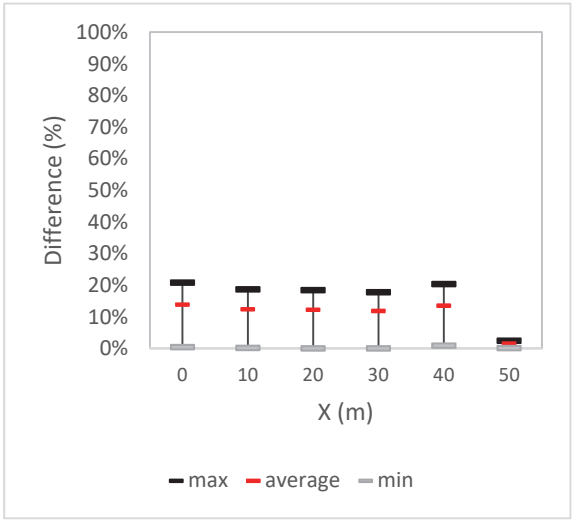
VISIBILITY	FED
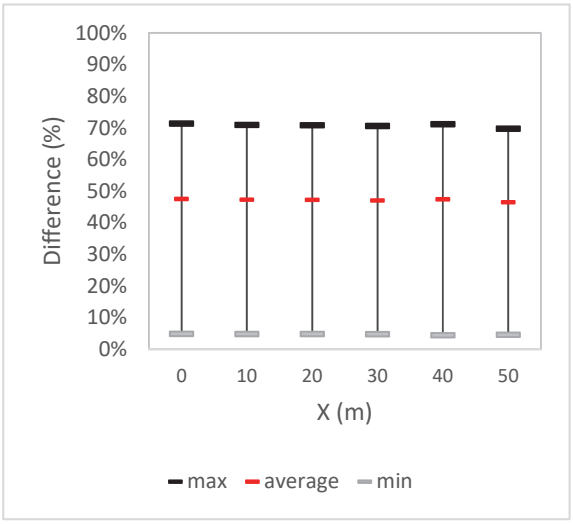	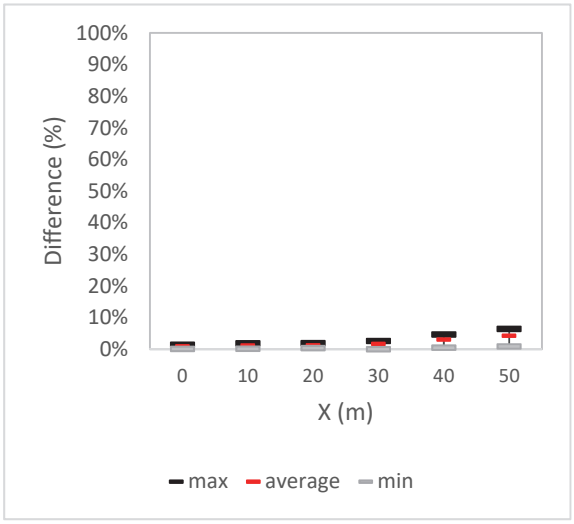

Table 5.4. Difference (%) by varying the soot yield, Lower layer (z=2m).

LOWER LAYER – SOOT VARIATION (0.05-0.2 g/g)

TEMPERATURE

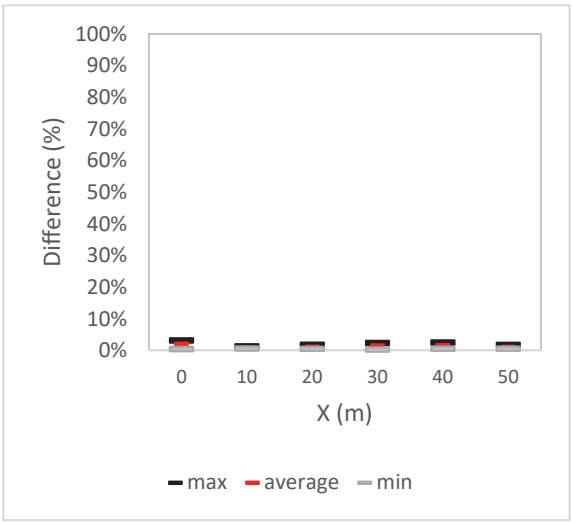

RADIATIVE HEAT FLUX GAS

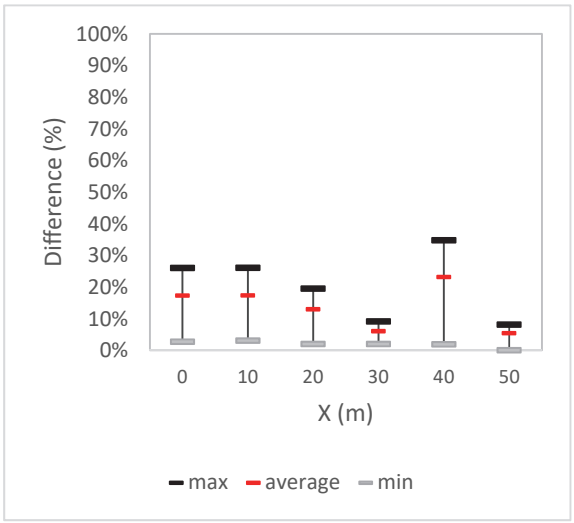

VISIBILITY

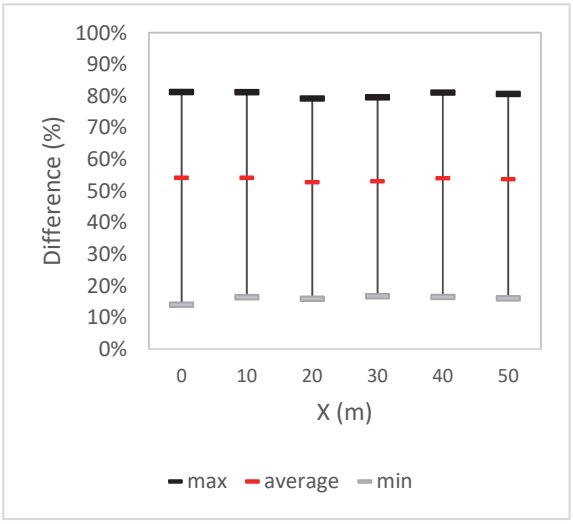

FED

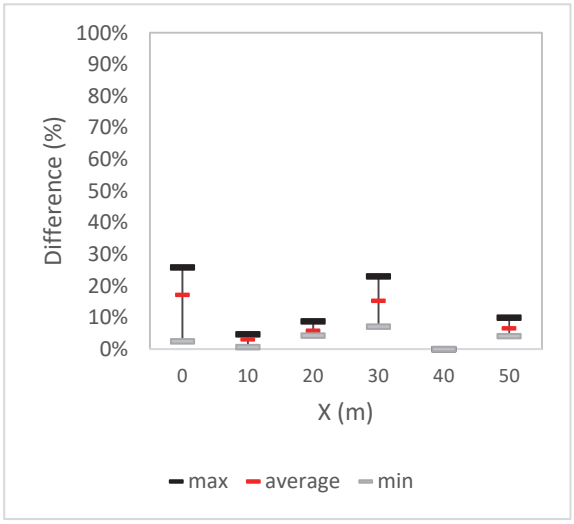

- Regarding the material, the adiabatic conditions are extremely different from those of inert or concrete materials (Figure 5.13 and Appendix C-Tables C.18-19). Therefore, the choice of the characteristics of the material of the surrounding structure is to be made with accuracy.

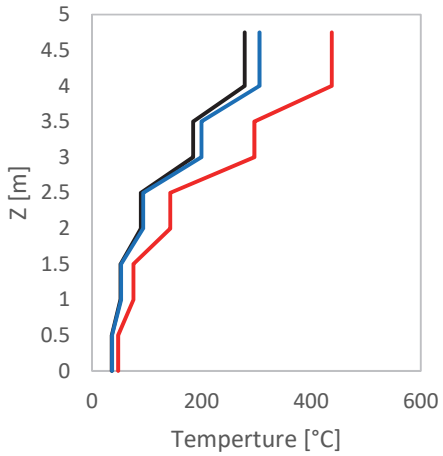

Figure 5.13. Temperature for inert, concrete and adiabatic materials at x= 30 m (30 MW fire)

- The presence of vehicles as geometrical obstructions affects all output quantities on the lower layer (20-30% difference) while on the upper layer no differences are recorded except for the fire source section.

- The length of the external area does not affect the result apart from the interface section X = 0 m. A small length is enough for making predictions inside the a.

- The longitudinal inclination of the tunnel dramatically affects the smoke dynamics and consequently the temperatures reached along the tunnel. This is a positive feature of FDS, because it means that inclined tunnel and chimney effect can indirectly be modeled by modifying the gravity vector (Figures 5.14, 5.15 and 5.16).

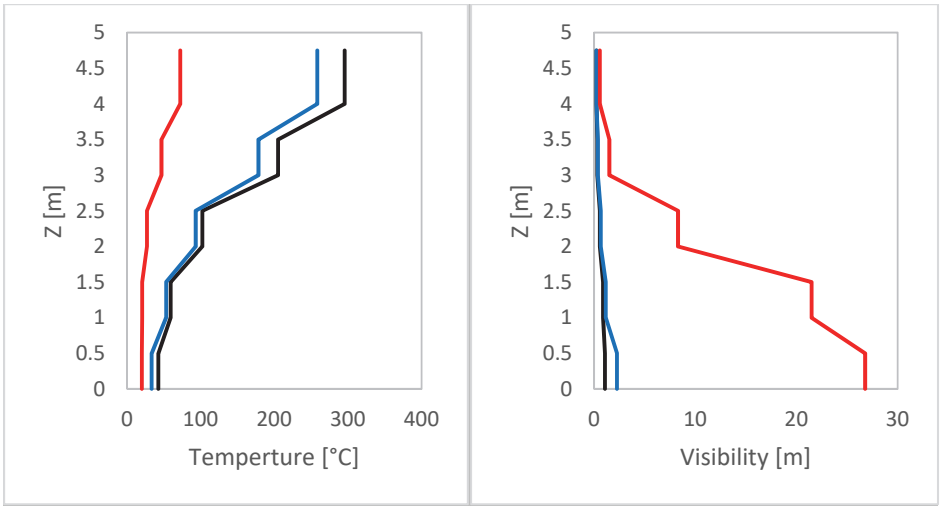

Figure 5.14. Temperature and visbility for upwards, plane and downwards tunnel at x= 20 m (30 MW fire)

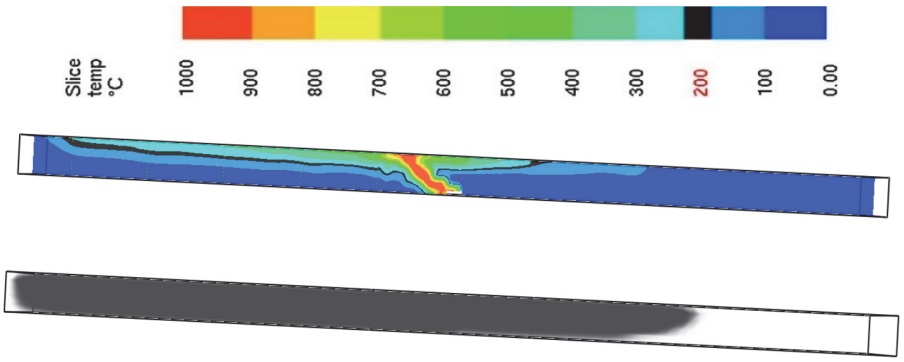

Figure 5.15. Temperature and smoke distribution for downwards tunnel

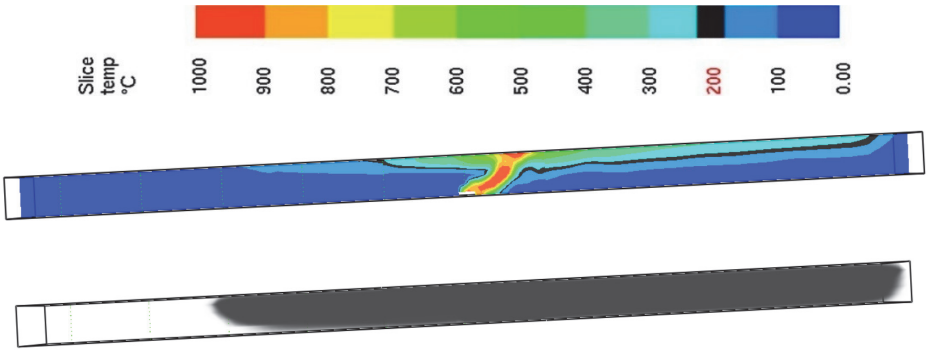

Figure 5.16. Temperature and smoke distribution for upwards tunnel

- The initial temperature appears to slightly affect the results only in the lower layer of the tunnel: this implies that the temperature reached inside the hot superior layer depends much more on the combustion process rather than the initial temperature (Figure 5.17).

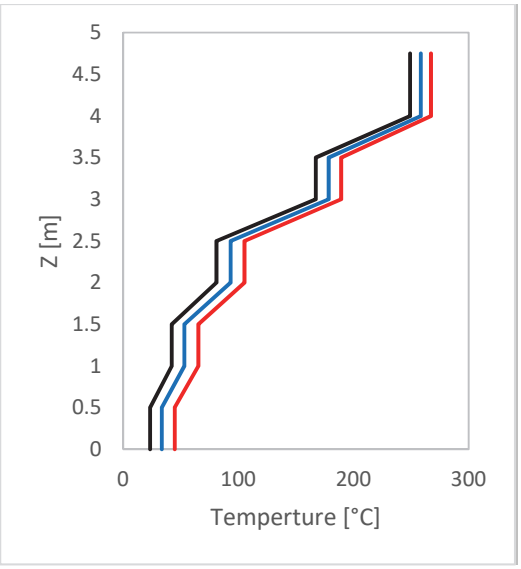

Figure 5.17. Profile of temperature for varying initial temperature

Chapter 6

Materials and structural behaviour

6.1 Materials and passive fire protection

Tunnel safety comprehends fire rating and fire resistance of all materials that can be found in a tunnel: from the concrete structure to the technical installations, systems, cables and signage.

Considering the tunnel equipment, the European Directive 2004/54 EC states that a sufficient level of fire resistance must be provided depending on the technological possibilities, aimed to maintain the original functionality in case of a fire. The tunnel equipment is ample and, in general, includes ventilation, lighting, water supply and monitoring systems.

Considering the structure, the European Directive 2004/54 EC affirms that a sufficient level of fire resistance of a tunnel structure must be guaranteed where a local collapse could have catastrophic consequences, like for immersed tunnels or in case of neighboring built-up areas. Specifically, in Italy the Legislative Decree 264/2006 states that the fire resistance must be at least 120 minutes for a nominal hydrocarbon fire curve for both new and existing tunnels.

In Italy, the standard for the performance levels and the resulting fire resistance classes is the Ministerial Decree 14/10/2008 that states the "Approval of new technical standards for construction".

6.2 Nonstructural tunnel components

Tunnels comprehend a large array of non-structural elements, which contribute to the fire safety of the whole tunnel system according to the performance that they can guarantee during an accidental event.

For instance, cables must comply with CEI requirements and wall coatings and coating panels must be made of non-toxic materials with Class 0 reaction.

The ventilation system (most often, jet fan-based) is one of the key nonstructural elements for road tunnels. Generally, they can resist against increasing temperatures up to 400°C: after that threshold, the supporting parts crack (Table 6.1).

Table 6.1. Failure temperature for fan systems

	Temperature	Time
Jet fans	400 °C	90 min
Exhaust fans	400 °C	90 min
Dampers	400 °C	90 min
Supports	400 °C	90 min

6.3 Reinforced concrete material

Among the structural material, concrete undoubtedly shows by a good behaviour when submitted to fire action. Its massive section, together with low conductivity, result in high thermal inertia and, consequently, structural members generally show a quite satisfactory behaviour, assuring also a natural protection for reinforcing bars. Anyhow, as the National Institute of Standard and Technology admits (Beitel et al, 2008), hyperstatic concrete structures experienced some partial or global collapses (Fig. 6.1), including casualties and economic damages, thus highlighting the need for a better understanding of structural behaviour during fire.

The behaviour of concrete structures is complex, firstly because of the complexity of the material: concrete is indeed a composite material. Water, cement paste and aggregate

contribute to its thermal and mechanical properties, which vary according to their rates and nature.

Since the seventies, experimental tests have been carried out in different countries and institutions. These tests aim to investigate both the structural behaviour of single members as well as the degradation of thermal and mechanical properties of concrete with increasing temperature. Unluckily, the complexity of concrete behaviour makes it difficult to reproduce well-standardised testing conditions and the resulting in a wide scatter in the data, that is sometimes conflicting. An attempt towards the harmonisation of these results has been done through the development of Eurocodes for the Design of Concrete Structures in Fires (EN 1992-1-2: 2004), in which reference constitutive equations are given.

Figure 6.1A-B. Apartment in St. Petersburg (Russia, 2002); CESP 2 Core collapse in Sao Paulo (Brazil, 1987)

The FIB (International Federation for Structural Concrete) in 2007 published the Bulletin n°38, where the major causes for the dispersion of the data regarding concrete parameters are summarised as follows.

• Concrete type. The nature of concrete was often not fully specified, leading to apparently different behaviour.

• Testing conditions. Size of the specimen, steady state or transient heating, moisture content and load conditions have strong impact on material behaviour and test results.

• Testing equipment. The first equipment were very complicated and the evolution of the machinery allows us today to look into more specific aspects of the structural behaviour.

Regarding the structural behaviour, concrete structures have been studied for a long time considering the behaviour of single members under a fire load. Depending on the external restraints, verification procedures could vary from single-section to less immediate formulas. Nevertheless, the behaviour of concrete structures is deeply connected to their inherent level of hyperstaticity, whose neglect might lead in some cases to unsafe estimations of fire resistance. The only way to take into account secondary effects such as coaction forces and inhibited thermal expansion is considering the global structure in the verification procedure as a whole instead of a sum of parts.

Indirect actions are those effects arising from restrained thermal expansion. Restraint to axial expansion induces axial compression forces in beams which, depending on the application point of the resultant component, have positive or negative effect. Generally, the former occurs when the restraint is in the low level of the section, providing a reaction that counteracts the imposed load, whereas the latter occurs when the restraint is in the upper level, thereby creating an additional bending moment. While a beam impeded to expand longitudinally will experience an increase in the axial force, which occurs when concrete slabs exhibit large deflections out of the plane, a membrane tension effect might develop providing stability. Additionally, in columns an increasing compressive force appears but considering the structure as a whole this effect cannot be detrimental like for continuous beams. The problem of providing detailed calculations is that the vertical position of the resultant force accounting for all indirect actions changes over time, because the stress state evolves according to the

development of the fire and the degradation of the material. Furthermore, thermal stresses are linked to the incompatibility of thermal strains (that is a material property, depending on temperature rise and thermal coefficient for expansion) and compatibility requirements (that is, boundary conditions and kinematic equations), conditions that makes mechanical strains develop and stresses occur, with strength and stiffness reduced from fire temperatures. Thermal stresses can be calculated accurately by considering the non-linear behaviour including cracking, transient creep and plasticity but this is not a simple issue.

Nowadays the possibility of numerical modelling of fire behaviour is increasing and more widely accepted because computer analysis are less time-consuming and expensive compared to experimental tests. Several detailed studies are available (Riva, 2004; FIB, 2008).

6.3.1 Degradation of thermal properties

The thermal analysis of a structural member subjected to fire exposure is the first step to understand and predict a plausible mechanical behaviour. Considering a cross section, the spread of heat from the external layer to the internal core is influenced by the evolution of thermal conductivity (W/mK), density (kg/m^3) and specific heat (J/kgK). These parameters are normally measured under steady-state temperature conditions, not reflexing the real fire exposure and adding effects linked to the physico-chemical decomposition of the microstructure of concrete material. In addition, different procedures and equipment used during test series in many countries led to relationships that can differ even by a factor of two. The assumption of some data instead of others must be driven by a careful judgment, looking for experimental tests or literature values obtained during the same tests conditions (concrete type, boundary

conditions, etc.). Many authors (Hertz, 1981) report collections of data available from a wide range of tests.

Thermal conductivity is a measure of the ease of the extending incoming heat flux and it is often estimated indirectly. The thermal conductivity of concrete depends on that of its constituents, but aggregation is the most influencing component together with moisture content. By increasing the temperature, this parameter decreases and, even if cooled, the greatest part of the process is irreversible, restoring a low percentage of the initial value. On average, the thermal conductivity of conventional normal strength concrete, at room temperature, is in a range between 1.4 and 3.6 W/m°C (Fig. 6.2A).

Specific heat is the amount of heat per mass unit required to change the temperature of a material by one degree and is often expressed in terms of thermal (heat) capacity, which is the product of specific heat and density. Specific heat is highly influenced by moisture content, aggregate type, and density of concrete (Fig. 6.2B).

The density, in an oven-dry condition, is the mass of a unit volume of the material, consisting in the solid itself and the air filled pores. With increasing temperatures, materials such as concrete, that have a high amount of moisture from their initial state, experience a loss of mass resulting in the evaporation of moisture due to chemical reactions. Assuming that the material is isotropic compared to its dilatometric behaviour, its density (or mass) at any temperature can be calculated from thermogravimetric and dilatometric curves.

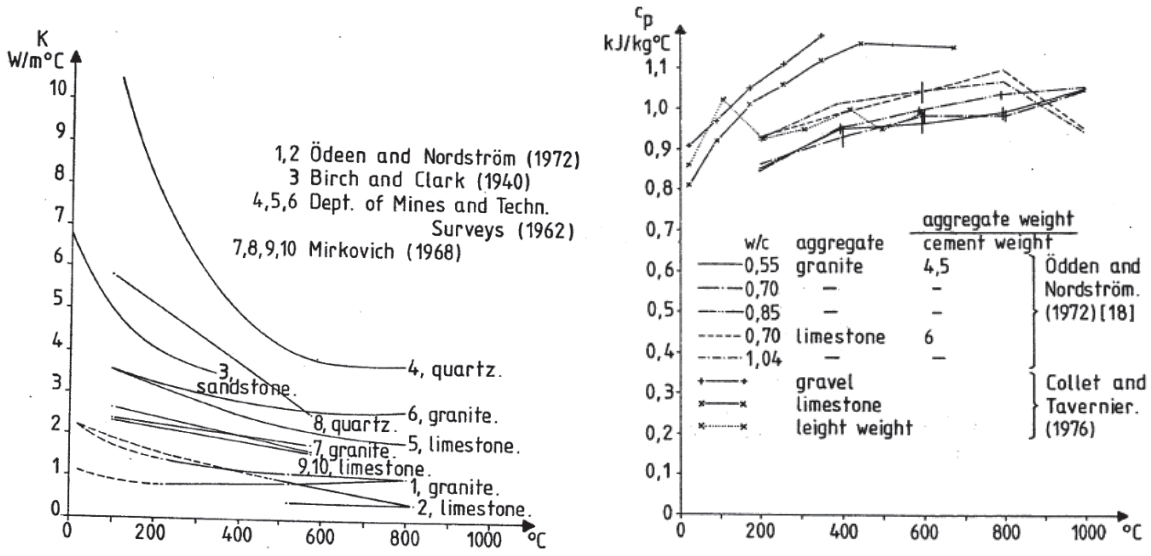

Figure 6.2A-B. Thermal conductivity; Specific heat (Hertz, 1981)

6.3.2 Degradation of mechanical properties

Mechanical properties of concrete at elevated temperatures have been studied extensively in literature as opposed to thermal properties. High temperature mechanical property tests have been generally carried out on concrete specimens that are typically cylinders or cubes of different sizes. Kodur (2014) reports a very detailed description of the most important properties of concrete.

Figure 6.3A shows the evolution of the ratio between the compressive strength at a target temperature and normal strength, including the uncertainties in the reported test data. The variation is large but uniform throughout a 20-800 °C temperature range can be attributed to the use of different heating or loading rates, specimen size and curing, condition at testing (moisture content, age of specimen) and the use of admixtures.

The modulus of elasticity of various concretes at room temperature varies over a wide range and is dependent mainly on the water-cement ratio in the mixture, the age of concrete, the method of conditioning and the amount and nature of the aggregates. The modulus of elasticity decreases rapidly with the rise of temperature, and the fractional

decline does not depend significantly on the type of aggregate. Figure 6.3B illustrates a variation of ratio of the elastic modulus at a target temperature to that at room temperature. It can be seen that there is a significant variation in the reported test data. The degradation of the modulus in both normal strength concrete and high strength concrete can be attributed to excessive thermal stresses and physical and chemical changes in the concrete microstructure.

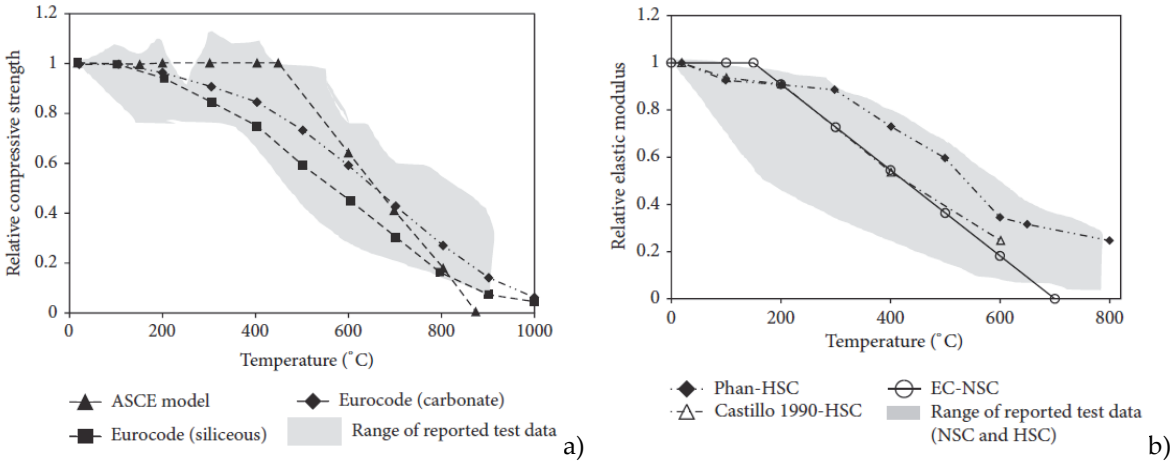

Figure 6.3A-B. Relative compressive strength; Relative elastic modulus (Kodur, 2014)

The reduction of the modulus of elasticity E has direct consequences on the correct understanding of the global behaviour of the structure. Thinking back to the historically used single-section verification, the precautionary reduction of E has been considered on the safe side, implying high deformability and thereby cracking. This is true unless the global behaviour is taken into account. In fact, in case indirect actions develop, their effect is dramatically underestimated for low modulus of elasticity and sometimes unpredicted collapse mechanisms might occur, with a substantially lower fire resistance.

Following the logic of the single-section verification, the constitutive equations of the Eurocode show an initial "hot" value of the modulus smaller by approximately twice compared to the reference "cold" value (the ratio depends on the type of concrete). The

justification regards the accidental nature of the fire action, which is likely to occur when the structure has been in service for several years preciously, and most probably lacking the preservation of the original characteristics. However, this reduction, consisting in several aspects including age of the structure, presence of cracks, etc., might be too high for global verification. Moreover, fires are short-term phenomena compared to the life of the structures; therefore the material will react to high temperatures with the instantaneous mechanical properties instead of the decreased ones.

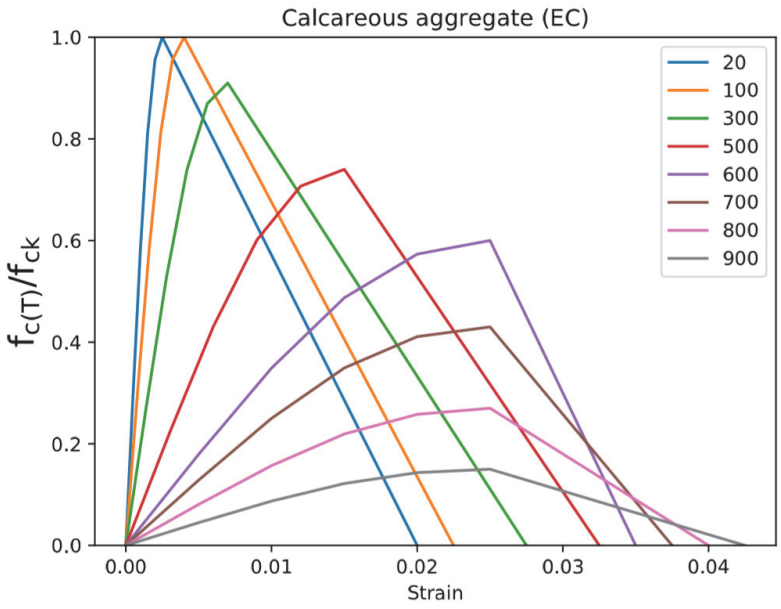

Figure 6.4. Stress-strain curve with increasing temperature

6.3.3 Creep phenomena at high temperature

Apart from the thermal strain (load free), the Load Induced Thermal Strain (LITS) is a nonlinear component of the strains developing during heating, predominant up to about 450°C and dependent on the applied load as well as the aggregate volume as shown in Fig. 6.5 (Hertz, 1981; FIB 2007; Kodur, 2014). LITS consists in transitional thermal creep (related to non-drying concrete), drying creep (or transient creep), time-

dependent creep and changes in the elastic strain during heating under load. Transient creep (assumed to be temperature-dependent and not time-dependent) is the largest component of LITS, it is irrecoverable and develops rapidly above 100°C. The process of creep is caused and accelerated mainly by moisture movement and dehydration of concrete due to high temperatures and acceleration in the process of breakage of bond.

For concrete reactor vessels (Dwaikat et al, 2009), steady state creep is important for service conditions, that is for long-term temperatures lower than 150 °C. When a fire occurs, the creep rates observed under transient conditions are much more important. For loaded specimens, throughout the temperature range 20-400°C, LITS constitutes in excess of 65% of the total contraction during first heating.

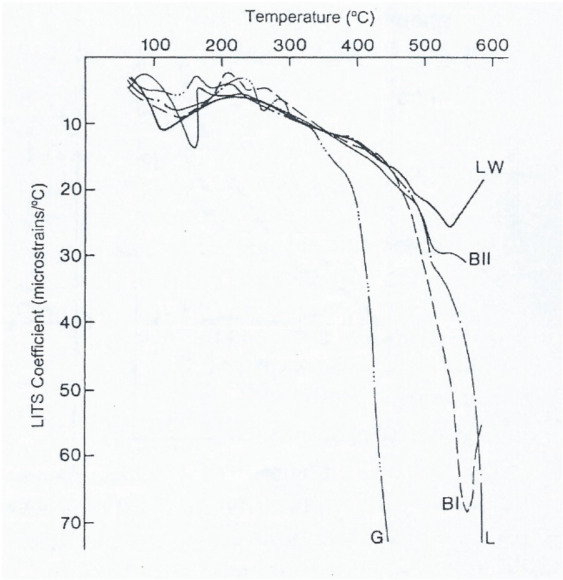

Figure 6.5. LITS development up to 600°C (FIB 2007)

Equations for creep (6.1) and transient (6.2) strains are suggested by Anderberg et al (1976), where ε_{cr} = creep strain, ε_{tr} = transient strain, $\beta_1 = 6.28*10^{-6}$ $s^{-0.5}$, $d = 2.658*10^{-3}$ K^{-1}, T = concrete temperature (K) at time t(s), $f_{c,T}$ = concrete strength at temperature T, σ = stress in the concrete at the current temperature, k_2 = a constant ranges between 1.8 and 2.35, ε_{th} = thermal strain, and $f_{c,20}$ = concrete strength at room temperature.

$$\varepsilon_{cr} = \beta_1 \frac{\sigma}{f_{cT}} \sqrt{t} e^{d(T-293)} \tag{6.1}$$

$$\varepsilon_{tr} = k_2 \frac{\sigma}{f_{c,20}} \varepsilon_{th} \tag{6.2}$$

Instead of this direct approach, in order to provide more immediate formulas, the constitutive equations contained in the Eurocode implicitly take into account the transient creep, but in which measure is a questionable issue.

6.3.4 Considerations about spalling

ling is a long studied phenomenon (Gross, 1975; Khoury, 1983; Khoury et al, 1985), defined as the breaking of layers of concrete from the surface of the concrete elements when those are exposed to high and rapidly rising temperatures. Spalling can occur soon after the exposure to heat and can be accompanied by violent explosions ("explosive spalling") or it may happen when concrete has become so weak after heating that, when cracking develops, pieces fall off the surface. The consequences may be limited as long as the extent of the damage is small, but extensive spalling may lead to early loss of stability and integrity due to exposed reinforcement.

Spalling is believed to be caused by the increasing of pore pressure during heating. The extremely high water vapor pressure, generated during exposure to fire, cannot escape due to the high density (and low permeability) and grows. When the pressure exceeds the tensile strength, spalling occurs. Generally, the lower the permeability, the higher the spalling. Apart from permeability, the high compression stress level is a key factor influencing the occurrence of spalling, like shown in Figure. 6.6. The influence of the compression forces (whose origin is linked to the inhibited thermal expansion) is particularly evident in Figure 6.7 where most of the spalling occurred in the central part

of the concrete element (where the deformation cannot occur) while near the junctions there is no presence of spalling.

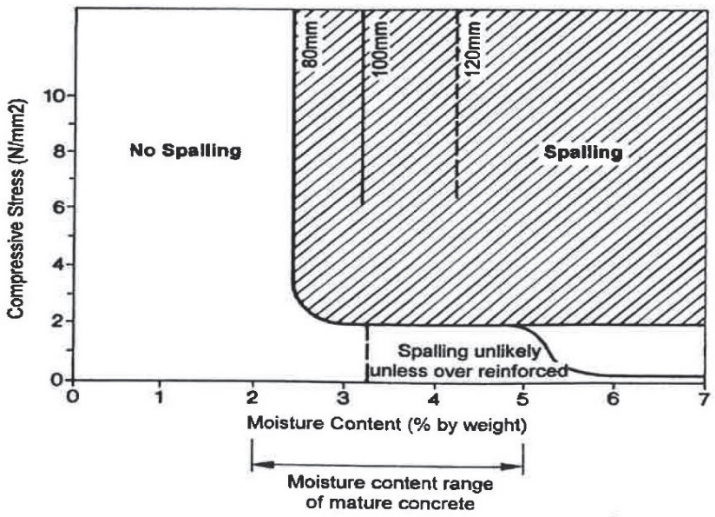

Figure 6.6. Spalling as a function of compressive stress and moisture content (Meyer-Ottens, 1972)

Figure 6.7. Zoom near fire source during tests in the Channel tunnel

6.3.5 Steel

Concrete sections are a natural protection for steel bars, which do not experience significant increase of temperature until spalling phenomena occurs. In fact, the partial loss of a section might be followed by fast exposition of steel bars to high gradient of temperature, causing rapid loss of resistance (Nigro, 2009).

In Figures 6.8 and 6.9, the reduction of steel strength and Young modulus by increasing temperature is reported.

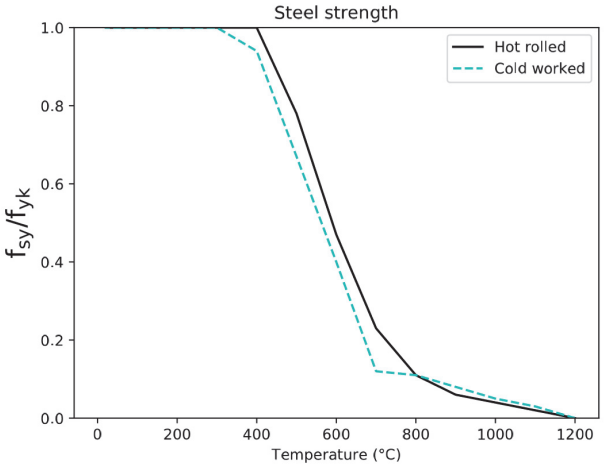

Figure 6.8. Steel strength by increasing temperature

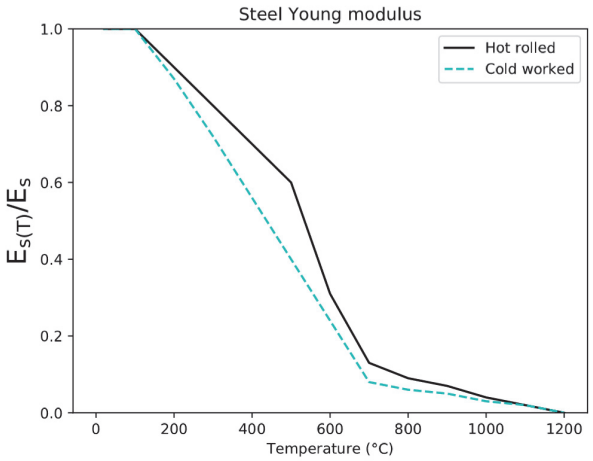

Figure 6.9. Steel Young modulus by increasing

6.4 Conclusions

From the point of view of the structural safety, tunnels with circular or polycentric cross sections have always demonstrated good performance in case of a fire. In fact, during the previously described major fires (Chapter 3), there have been no collapses but significant structural damages, mainly due to spalling phenomena near the fire source.

Similarly, cut and cover sections show high fire resistance when continuity is guaranteed between the ceiling and the lateral walls ("frame" behaviour in the section). Otherwise, when the continuity is not guaranteed and the ceiling is simply supported by the lateral walls of the tunnel, the collapse is possible for typical design fires, especially in those tunnels that have been built before fire resistance was a standard requirement.

However, the collapse of a structure is always associated to a time interval much larger than those related to self-evacuation. Therefore, even for a tunnel with the worst initial conditions considering the structural resistance, the exit time for people is certainly much lower than the time for the structure to crack and eventually collapse.

For this reason and considering that the work is focused on the QRA for life safety in road tunnels, the structural analysis is not conducted. Moreover, this choice is also in agreement with the very limited interaction of spalling phenomena with the occupants, which are very unlikely to be hit by parts of the concrete material because spalling phenomena is generally localised near the fire source, where high temperature gradients occur.

If structural analysis for tunnels is conducted, it is recommended to take into account the secondary effects, because they are particularly important for concrete structures, especially for those hyperstatic structures with predominantly impeded expansive behaviour.

Chapter 7

Evacuation

7.1 Literature review on evacuation from tunnels

7.1.1 Peculiarity of human behaviour in road tunnels

Depending on the position and relevance in the road network, large traffic volumes may daily transit in road tunnels, determining a potentially large number of people exposed to fire hazard. Life safety is, therefore, a priority for the fire design of this type of environment, confined and significantly extended in the longitudinal direction, which consequently is affected by specific issues of smoke management and evacuation.

In normal situations, people report feelings of claustrophobia, boredom and perceive the area as alien, even if they have driven through it several times. The position of the means of egress, SOS stations and the presence of jet fans is normally not noticed, differently from what happens for regular users of building facilities such as office.

In case of an accident or a fire, the stress of the occupants (already higher than in usual situations) may cause irrational and difficultly predictable behaviour. For example, people are reported to prefer the entrance portal, that is a well known escape route, rather than an emergency exit: they do not feel safe using the last one, because they do not know where it leads to. This could also encourage drivers to behave badly by making U-turns even when it is forbidden. Other recurrent features in the evacuation from tunnel fires are the reluctance in the abandonment of objects and people and the tendency to form groups. For instance, families tend not to divide themselves (even at the cost of dying) in

case of emergency whereas independent travellers may act as conformists, choosing the same decision taken by a group of unknown people, who have already validated that decision, so that it appears reliable by the other occupants. A substantial amount of research available in literature illustrates that the egress behaviour is a collective behaviour around a situational leader (it can be a police officer or a person who naturally takes leadership, with experience of such events).

However, during tunnel fires, the main causes of death are the incapacitation induced by the inhalation of toxic gas and the exposure to high level of radiative heat or temperature, exceeding the capabilities possible for a human body. The loss of visibility is not directly a cause of death, but is linked to one's orientation in space. The lower the visibility, the more the behaviour is confused and uncertain. In addition, the longer the time to reach the exit, the higher the probability is of getting intoxicated.

The condition of zero risk is never achievable, but the presence of fatalities and injuries must be investigated from the point of view of a failure of the evacuation system.

In this sense, some reasons are identified at the origin of the occurrence of fatalities:

1. inappropriate decisions of people (e.g. remaining closed inside the vehicle);
2. inappropriate means of egress system (emergency exits not properly positioned);
3. inappropriate smoke control and management system (lethality, loss of visibility).

The first point is the most difficult to quantify. In order to understand the process of decision – making of people during road tunnel fires, many studies and research are available and represent a base of knowledge, even if there is still a lot to understand about the psychological process that occurs during such situations (Ronchi, 2016).

Certainly, the layout of a tunnel can potentially facilitate the evacuation process, inducing people to act rationally. A good tunnel design should be the one whose safety measures are perceived and understood by drivers and passengers, as if they have been thought and designed in function of the users. Recently, experimental tests involving people have

been done, with the aim of investigating how the individual velocity decreases in presence of smoke, irritant or not (Xie et al, 2012). Exit choice and efficiency of lighting emergency signage have also been widely studied in Northern Europe (Galea et al, 2014). The second point is immediate to understand: if the exits are placed too far, the evacuation time prolongs, the walking speed can decrease due to physical effort and thus occupants are more exposed to toxic gas. The eventuality of emergency exits whose distance exceeds the recommended 500 metres is common and, in the following chapters, the possibility for reducing the risk of these cases will be detailed.

The third point is related to, on the one hand, the choice of the ventilation system (longitudinal or transverse) and, on the other hand, the reliability of the process that activate the ventilation system. For unidirectional tunnels, for instance, a longitudinal ventilation system should be able to prevent backlayering (Figure 7.1). If baklayering occurs, the consequences are the increment of the toxic gas and a probable loss of visibility at a certain time upwind the fire source (when the hot smoke decreases its temperature it moves from the ceiling towards the floor). A bad smoke management could be responsible for the impossibility of using an emergency exit, due to low visibility.

Figure 7.1. Baklayering effect (METRO Project,2012)

7.1.2 Behavioural scenarios in road tunnels

7.1.2.1 Occupant characteristics

The occupants' characteristics define the evacuation dynamics and determine the overall evacuation time. They can be divided into two categories, which are physical and psychological characteristics. Both categories are influential on the pre-evacuation time and the movement time.

Physical characteristics of the occupants depend mainly on gender, age, state of health (permanent or temporary disabilities). For instance, the walking speed, the resistance to the fire effects (smoke, radiative heat, etc.) and capabilities like good sight and hearing are strongly dependent on gender and age.

Psychological characteristics instead depend mainly on personal previous experiences and natural instincts where their dependence is far less simple to identify. The choice of the escape routes (e.g. between portals or emergency by-pass for a road tunnel) and the reaction time are both typically psychological features, for which generalisation is complicated and debated.

In the fire prevention regulations, the occupant's characteristics are often related to the type of building where people are located (NFPA 101, 2015). This implies, for example, that people inside a shopping centre will behave differently from people inside an office or a hospital, because the average characteristics of the people and their state of mind are not the same as well as their knowledge of the layout of the building.

For road tunnels, it is hardly possible to predict the occupancy type, because the traffic volume is generally very ample. One could make predictions considering the geographical position of the route and its importance (as part of strategical or local traffic network), but a large distribution of people, with mixed gender, age and physical capabilities is the wisest choice.

Considering the walking speed, ANAS Guidelines recommends the set of values contained in Table 7.1 where the initial walking speed depends on qualitative levels of visibility. This correlation is in line with the negative interaction between walking speed and smoke density (responsible for the drop of the visibility) explained in 7.2.1.4.
In general, the assumption of 1 m/s of walking speed (good visibility) is not conservative if one thinks of the evacuation of the elderly, children and impaired people, whose initial walking speed is below 0.8 m/s. However, the recommended value is on the safe side if the exposed group of people is composed mainly by adult evacuees with full physical capabilities (their speed can arise value of 1.5 m/s) (ISO/TR 16738).

Table 7.1. Walking speed vs visibility correlation (ANAS, 2009)

Visibility	Walking speed
Good	1 m/s
Scarce	0.5 m/s
None	0.3 m/s

7.1.2.2 Pre-evacuation time

The pre-evacuation time is a synthetic parameter which aims to quantify the amount of time taken by each occupant from the occurrence of an accident to their initial movement towards an exit.
This parameter is affected by large uncertainties, most of them linked to the unpredictable character of the human behaviour, both in normal and emergency conditions. However, lots of research have been carried out as an attempt to decompose the complexity of the human behaviour into several features and address them independently (ISO/TR 16738). The awareness of the surrounding where the evacuation takes place has been confirmed to be one of the most important aspect for a safe evacuation. Being familiar with the escape routes of a building implies spending less time to find the nearest exit and therefore a higher possibility of reaching a safe place in a short time. For a road tunnel,

the familiarity with the structure and its escape routes is rarely present among the evacuees, even for frequent users of the tunnel. In addition, the underground environment is often perceived as alien due to confinement and lack of visibility, which could worsen people's feelings during the evacuation.

The geometry of the building and its means of egress system also affect people's evacuation. For road tunnels, this is not very influential because the evacuation process occurs on a two-dimensional surface represented by the sidewalk or the verge. However, the interaction with the vehicles across the carriageway may cause a significant psychological constraint.

The level of alertness is generally variable along the tunnel, because perception is not as obvious as it would be inside a building compartment, especially for very long tunnels. In fact, by approaching the fire or the accident the perception is generally high, as people see first-hand the presence of the anomaly, whereas at a given distance people may be unaware of the situation, especially if there is some deficiency in the alarm system. The emergency management inside a road tunnel may be addressed by CCTV, control center and fire service teams deputed to firefighting operations in case of emergency can provide a significant support.

For the evacuation design, international standards generally consider pre-evacuation time as a function of the above commented occupancy type, alarm system, building complexity and fire safety management. However, for a road tunnel it is not entirely applicable for now, due to the features described above.

During the Mont Blanc accident, 30 seconds are reported as the exit time required from most of the vehicles (Purser, 2009). Similarly, 35 seconds are reported as a result of experimental tests (Frantzich and Nilsson, 2009). Later, the importance of considering several scenarios was highlighted (Ronchi, 2010), including probability distribution (normal and uniform) varying between 30 and 210 seconds as well as a gradual

decreasing of the pre-evacuation time by approaching the burning vehicle. To be on the safe side, Italian Guidelines (Direzione Progettazione ANAS, 2009) suggest a constant value of 300 and 90 seconds respectively for vehicles and HGVs' drivers. Regarding the use of fixed or distributed values, the opinion of the academic community is not generally in accordance and fixed values are sometimes preferred to varying distribution (Sargant, 2014).

7.1.2.3 Queue formation models

Queue formation models are needed for quantitative risk analysis of fire events because they determine the amount of vehicles and, therefore, the amount of drivers and passengers, who have to evacuate the tunnel in case of an accident.

Two models (Figures 7.2 and 7.3) are described below: they are very simple and affected by aleatory uncertainties that are not taken into account in the research.

The ANAS model has the following hypothesis on the traffic volume:

- eulerian representation of the traffic;
- steady and homogeneous traffic.

Considering I as the distance among the vehicles and I* the safety distance (depending on speed and length of the vehicles), when $I < I^*$ the traffic is congested upwind the fire event. Consequently, the delay τ of stopping approaching vehicles can be expressed in terms of AADT, speed and I: if $\tau > \tau^*$ (time to close the tunnel) the entire length will be filled with vehicles, otherwise the vehicles will interest a shorter length.

In this way, the amount of people and their position can be calculated by knowing the traffic composition and the number of vehicles.

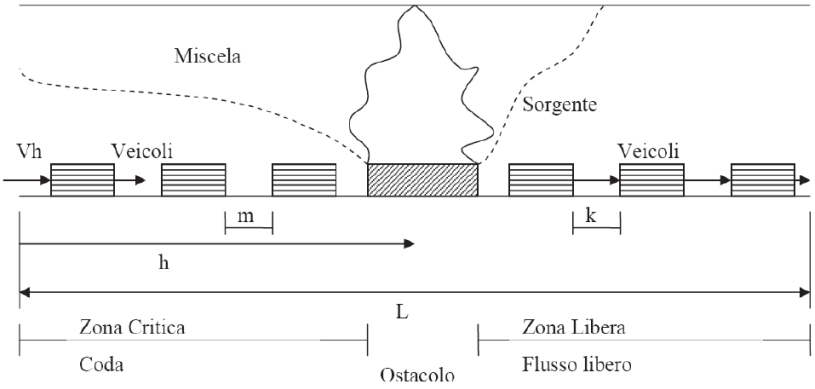

Figure 7.2. Queue model (ANAS, 2009)

In Persson's model a slightly different scheme is given. Similar to the ANAS model, it is assumed that the vehicles downwind the accident can exit safely the tunnel while upwind a queue develops. The presence of warning signs can be taken into account by representing a non-homogeneous queue along the tunnel, at various distances from the accident site. However, a delay (e.g. 1 minute) must be considered because the behaviour of drivers is uncertain, as they might not stop at the red light. The vehicles that initially do not stop at the warning signs will thus join the end of the next queue. Then, by using information on the traffic composition and on an average number of people per type of vehicles, the number of evacuees can be estimated. Other hypothesis of the model adopted in Persson's work are that the distances between the vehicles in the queues are negligible and all vehicles travel at the speed limit of 80 km/h.

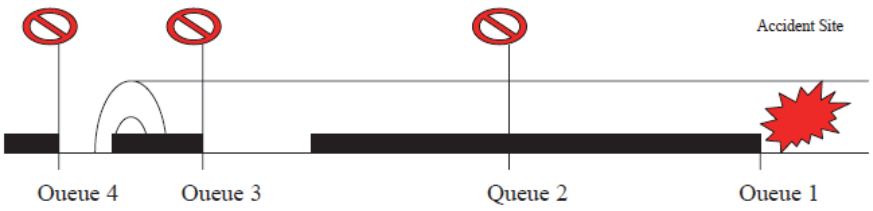

Figure 7.3. Queue model (Persson, 2002)

7.1.2.4 Incapacitation

Road tunnel evacuation is peculiar because people can be forced to cover long distances to reach a place of relative safety, much longer compared to typical travel distances of building compartments. Considering the most unfavourable position of an occupant, when the tunnel does not lack emergency egress routes, the order of magnitude is 100-300 metres. However, this value dramatically increases if an exit is not available (for bad smoke stratification or just absence of the requested provision). The physical effort (i.e. fatigue) is unavoidable and temporary disabilities can affect people. In agreement with this aspect, studies (Ronchi, 2016) confirm the need to take into account a decrease in the speed after some hundreds metres are walked to reach a safe place. It must be noted that this decrement of the speed is due to the physical effort and overlaps to the negative interaction of speed with smoke gases (Figure 7.4).

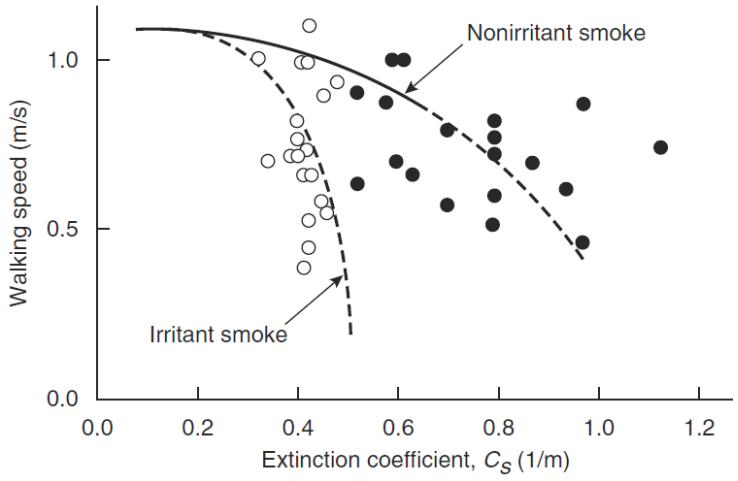

Figure 7.4. Negative interaction of walking speed and smoke (Purser, 1980)

7.2 Tenability criteria and thresholds

During the evacuation in case of a fire, the occupants of the enclosures are exposed to hazardous conditions, which are represented, for instance, by smoke effluents, toxic gas and high temperatures. These conditions spatially and temporally vary inside the enclosure and in order to guarantee life safety conditions one should verify that the quantities do not exceed certain thresholds along the escape routes, where the occupants are expected to walk and evacuate.

The quantities that are generally considered are visibility, gas temperature, radiative heat, carbon monoxide, FED (Fractional Effective Dose). They should be measured at a conventional human height, normally fixed at 1.8-2 m from the floor (the latter choice is on the safe side because a higher tenable zone is admitted). The tenability has been largely studied (Purser, 1986; Jin, 1997) and its evaluation aims to compare the ASET (Available Safe Egress Time) with the RSET (Required Safe Egress Time) as reported in Figure 7.5.

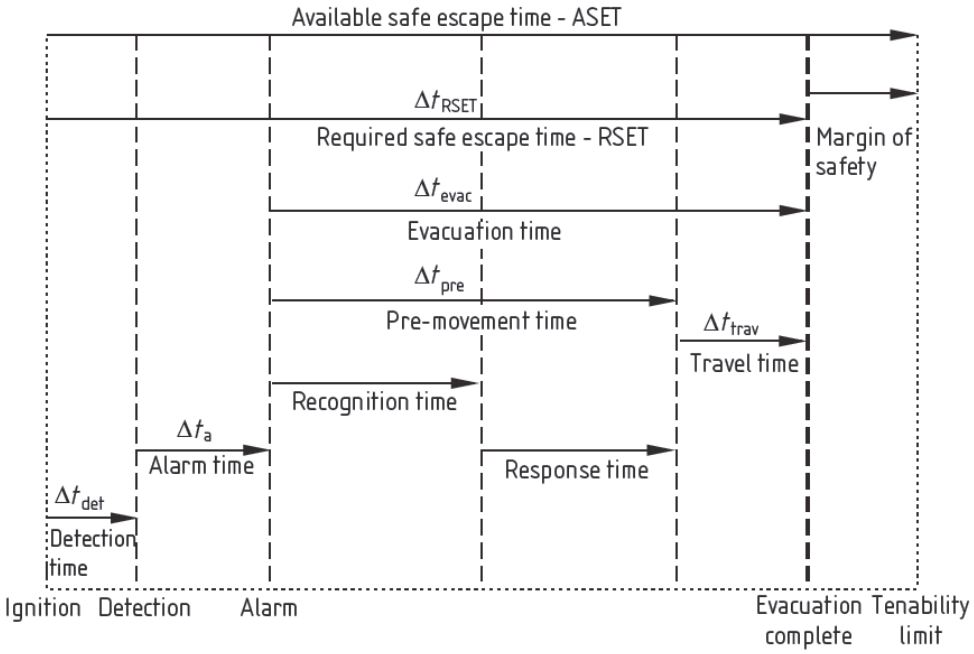

Figure 7.5. Processes involved in RSET compared to ASET (PD 7974-6)

The ASET, therefore, determines the time to reach the tenability limit and the global ASET is defined as the minimum of the ASET evaluated according to four models: toxic gas model, irritant gas model, heat model and visibility model. The RSET, instead, is the time the last occupant exits the building and can be decomposed in detection time, alarm time, pre-movement time (sum of recognition and response time) and the proper travel time. Often, the RSET is simply decomposed into pre-evacuation time and evacuation time, where the former is the sum of all the four components previously mentioned and the latter is the travel time (or movement time). The RSET should be sufficiently lower than the ASET and the difference ASET-RSET is the safety margin.

In Table 7.2, an example of tenability thresholds is reported (each model will be discussed in the following sections). Less restrictive tenability thresholds can be admitted if the life safety conditions for rescuers want to be assessed: they, in fact, wear protective clothes and devices and can afford higher level of stress and fatigue.

Table 7.2. Examples of tenability thresholds (ISO 13571)

Model	**Performance**	**Threshold for occupants**		**Threshold for rescuers**
Visibility	Minimum visibility	10 m		5 m
Toxic gas	Maximum FED	0.1 (1.1% of incapacitated people)		No evaluation
Irritant gas	Maximum FEC	F_{HCl} F_{HBr} F_{HF} F_{SO2} F_{NO2} $F_{acrolein}$ $F_{formaldehyde}$	1000 µl/l 1000 µl/l 500 µl/l 150 µl/l 250 µl/l 30 µl/l 250 µl/l	No evaluation
Heat	Maximum temperature	60 °C occupants		80 °C rescuers
Heat	Maximum radiative heat	2.5 kW/m^2		3.0 kW/m^2

7.2.1 Toxic gas model

The toxic gas model uses the concept of exposure dose and lethal dose, whose ratio is called FED (Fractional Effective Dose). The exposure dose is defined as the inhaled dose of a toxic species (CO, HCN, etc.) present in the air integrated during the exposure time (it is a cumulated measure). The lethal dose is the dose that determines the incapacitation of an exposed person, on average, and, in fact, when FED is 1, the person is assumed to die. The designer can choose a lower level of FED as the target threshold in order to limit the negative effects on less physically capable categories (elderly, children and impaired people).

In the formula below (7.1), φ is the average concentration of the species (carbon monoxide and hydrogen cyanide) in Δt (the dose is a concentration multiplied for Δt).

$$X_{FED} = \sum_{t_1}^{t_2} \frac{\varphi_{CO}}{35000}\, \Delta t + \sum_{t_1}^{t_2} \frac{\exp(\varphi_{HCN}/43)}{220}\, \Delta t \qquad (7.1)$$

The reduction of oxygen under 13% is able to cause asphyxiation. The narcotic effect of CO_2 is not significant during fire conditions, but if over 2% it can cause hyperventilation, amplifying the velocity of inhalation of toxic gas. Therefore, a corrective factor can be added to the previous formula (7.2).

$$\nu_{CO_2} = \exp[\varphi_{CO_2}/5] \qquad (7.2)$$

The lethal doses have been studied mainly through animal experiments and fix the value at which a given percentage of a sample of people would die in case of exposure to that quantity for a certain period of time. Therefore, there is a non-negligible uncertainty linked to the FED concept (±35% according to ISO 13571).

For example, for fire evacuation it is considered that a person, on average, would die after being exposed to 3500 ppm of carbon monoxide for 10 minutes. In that case, the FED is 1 and the ASET for carbon monoxide is 10 minutes.

7.2.2 Irritant gas model

The irritant gas model uses the concept of FEC (Fractional Effective Concentration). Similar to the FED, the FEC is defined as the ratio between the concentrations of the inhaled species and their lethal concentrations for an average person. In this case, the concentration is taken into account instead of the dose, because irritant gas are able to affect people immediately after the contact.

In the formula below (7.3), φ is the average concentration and F is the lethal concentration of the irritant species. The effect of the species is considered instantaneous and summed.

$$X_{FEC} = \frac{\varphi_{HCl}}{F_{HCl}} + \frac{\varphi_{HBr}}{F_{HBr}} + \frac{\varphi_{HF}}{F_{HF}} + \frac{\varphi_{SO_2}}{F_{SO_2}} + \frac{\varphi_{NO_2}}{F_{NO_2}} + \frac{\varphi_{acrolein}}{F_{acrolein}} + \frac{\varphi_{formaldehyde}}{F_{formaldehyde}} + \sum \frac{\varphi_{irritant}}{F_{C_i}} \qquad (7.3)$$

The uncertainty linked to the model is ±50% according to ISO 13571. This verification is generally omitted unless the combustible materials are expected to release irritant gas.

7.2.3 Heat model

The exposition to heat can damage the human body causing hyperthermia, burns on the skin and inside the breathing apparatus.

The model proposed by ISO 13571 for the radiative and convective heat is similar to that of FED (7.4), where t_{Irad} and t_{Iconv} are the period for a person to be incapacitated (they depend on clothes as reported in ISO 13571).

$$X_{FED} = \sum_{t_1}^{t_2} \left(\frac{1}{t_{Irad}} + \frac{1}{t_{Iconv}}\right) \Delta t \qquad (7.4)$$

However, the same relation can be verified (ASET always larger than 30 minutes) by guaranteeing that the temperature and the radiative heat do not exceed respectively 60 °C and 2.5 kW/m^2, with any clothes. The uncertainty linked to the model is ±25% according to ISO 13571.

7.2.4 Visibility model

The first research project focusing on the visibility through smoke was made in Japan (Jin, 1965) after it was recognised that many people died due to intoxication in fire accidents. Experimental tests with different combustible materials during which people were involved in the evacuation from a tunnel filled with smoke are the basis of the development of the current visibility model. The visibility model is linked to the concept of smoke obscuration and minimum perceived contrast (or minimum difference of luminosity) between visible object and background (Figure 7.6). The following formula (7.5) where L is the visibility (m), σ is the specific extinction coefficient (10 m^2/g) and ϱ_{smoke} is the smoke aerosol mass concentration (g/m^3)

$$C = \sigma \rho_{smoke} L \tag{7.5}$$

C is the dimensionless constant assumed equal to 3 or 8 depending on the type of signage (non illuminated/reflecting and illuminated/emitting light signage).

The soot density, the dimensions of the soot particles, their distribution, the optical property of the smoke and the intensity of the light affect the visibility in presence of smoke. This concept is summed in the Brouger'law reported below (7.6), where I and I_0 are the intensity of the light over a certain distance L with and without smoke and K is the extinction coefficient (m^{-1}).

$$\frac{I}{I_0} = e^{-KL} \tag{7.6}$$

Specifically, K can be obtained by multiplying σ and ϱ_{smoke} (characteristics of the burning species). The visibility is, therefore, evaluated as C/K.

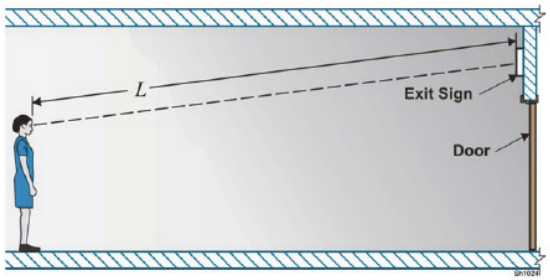

Figure 7.6. Scheme of the visibility model

7.3 Evacuation models

7.3.1 Generalities

Evacuation models are today an advanced tool internationally recognised, whose validation is still object of studies and understanding by the academic community (Ronchi, 2016). The quality of the results is, in fact, strongly dependent on the input data defined by the user and indeed only expert users should use such advanced tools.

Evacuation models deal with emergency conditions, during which social behaviour appears as group formation and leader-followers features. These models are sometimes confused with pedestrian models, which instead aim to reproduce human behaviour in normal conditions, and are useful to analyse large and overlapping flows of people (hubs, train stations, large-scale events) and to optimise the layout design (Fruin, 1971). Some models can be used in both modalities (emergency evacuation and pedestrian dynamics).

For a long time, evacuation models have been limited to movement models, in which relationships among walking speed, flow (persons/sec) and density (persons/m^2) are used to simulate the egress of people from a compartment, considering also the influence of stairs, ramps and corridors on the parameters previously mentioned (Figure 7.7). The concept of effective design width is also considered, highlighting the fact that people move maintaining a certain distance by lateral obstructions (walls, objects).

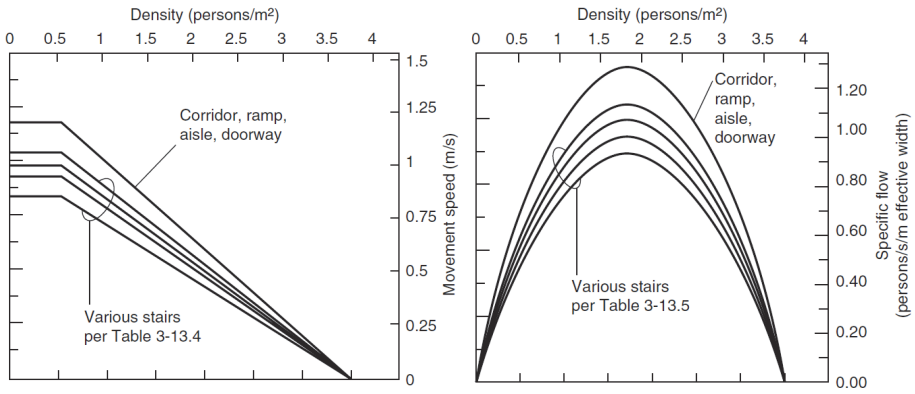

Figure 7.7. Movement speed and specific flow over density (Gwynne & Rosenbaum, 2015)

However, trials and drills carried out by varying density and boundary conditions in simple geometries like corridors showed significant differences from the well-known trends previously commented. For example, results reported in Figure 7.8 showed that for 4 people/m² there is necessarily no congestion of the evacuation, but only a significant reduction in the specific flow and eventually other peaks in this parameter can be recorded by increasing the density (Figure 7.9). In addition, initial walking speed higher than 1-1.2 m/s has been recorded, even in case of counter flows.

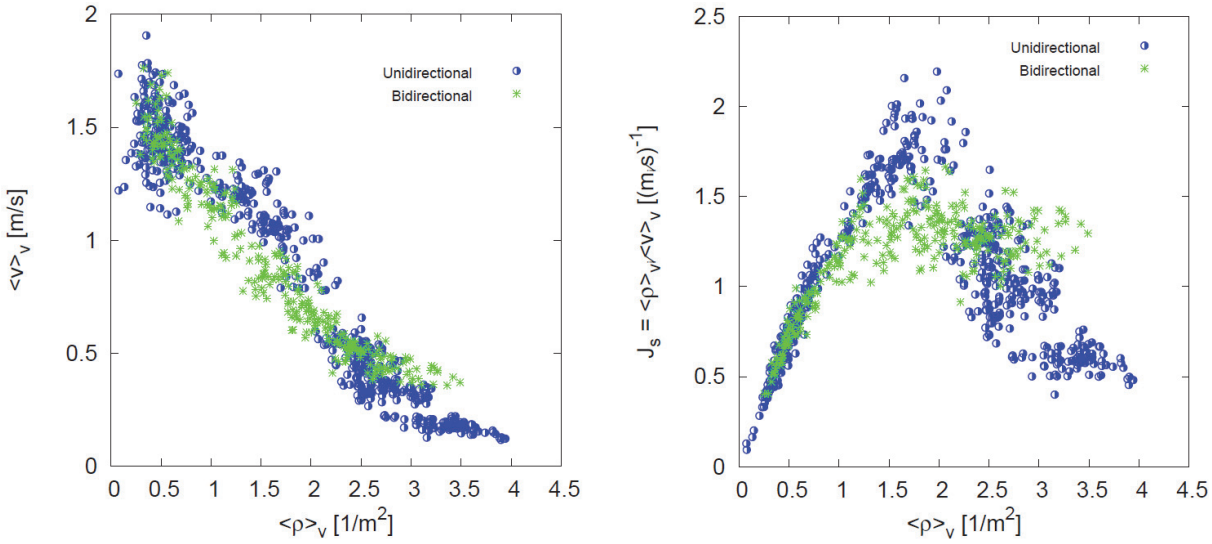

Figure 7.8. Results from drills in a corridor (Zhang and Seyfried, 2012)

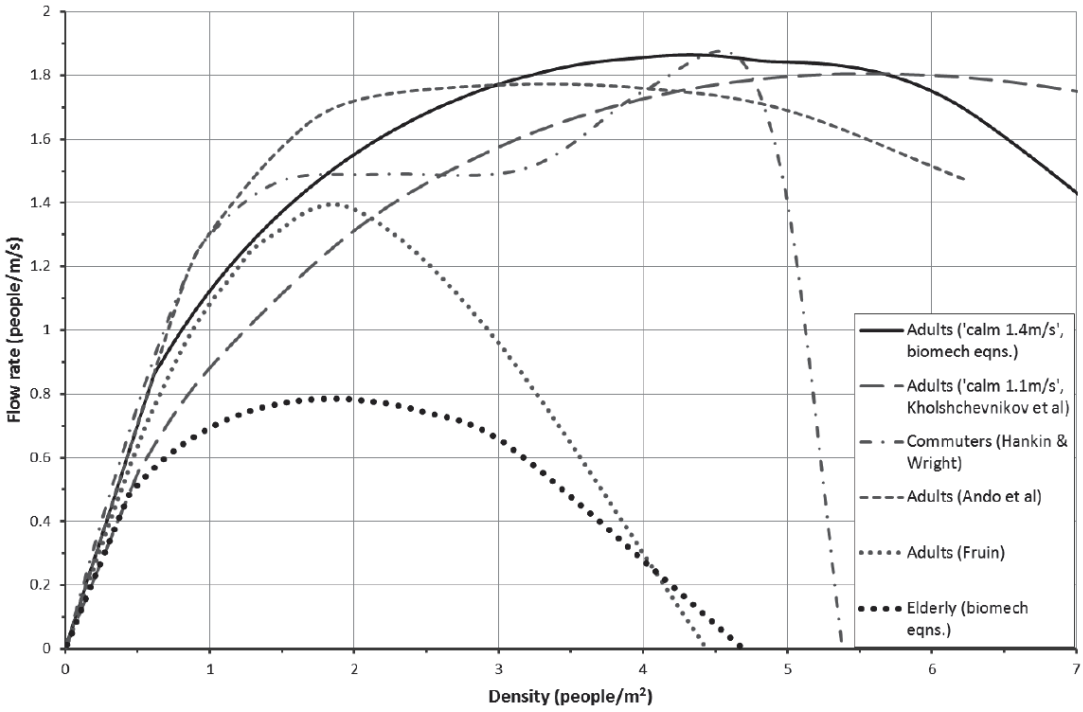

Figure 7.9. Specific flow vs density (Thompson et al, 2015)

7.3.2 Classification by movement algorithm

The simplest classification of the evacuation models is done according to the algorithms used for driving human motion. The categories identified in literature (Kuligowski, 2015) are movement, semi-behavioural and behavioural models.

In movement models the motion of the occupants is defined essentially by the hydraulic models, according to the laws reported in the SFPE Handbook of Fire Protection Engineering. They are very simple models, useful when pre-evacuation time is not significant nor the choice or the path for the exit; they have been progressively replaced by the following categories.

Semi-behavioural models are quite more advanced compared to movement models, because a more accurate description of the evacuation process can be inserted. This is done through the definition by the user of probability functions for the reaction times, alarm times, familiarity with the escape routes and so on. These models still rely on the

input defined by the user. FDS+Evac, Pathfinder, buildingExodus are considered semi-behavioural models.

Behavioural models are more complex in the definition of the algorithms that drive human movement. Specifically, they offer a wide range of "behaviour" that can be taken into account in the evacuation simulation: patience level, specific tasks, etc. MassMotion, for instance, is considered a behavioural model.

The reason for the selection of one model instead of another lies in the needs of the user: some models are very complicated because no user interface is available, while others do not allow an accurate definition of the space (only 2-dimensional space). Other reasons can lie in the opportunity of coupling evacuation simulations with fire simulations, which are sometimes possible thanks to the share of the same mesh (the 2-dimensional plane used for the evacuation is a slice of the 3-dimensional volume used for the fire calculations).

7.3.3 Classification by space discretisation

In addition to the movement algorithm, the existing evacuation models differ from each other also for the discretisation of the space where the occupants move.

In coarse network models, the user is required to artificially segment the structure into compartments in order to produce that will appear in the network. Each compartment is represented as a point (Figure 7.10) connected to the other volumes (such as corridors and stairways) that lead to the exit. The main output is the overall evacuation time, but no information is given regarding the movement inside the area. The buildingExodus software can be performed using coarse and fine network, depending on the needs.

In fine network models (such as FDS+Evac, Pathfinder, buildingExodus) the space is discretised into an appropriate mesh, whose size is set by the user. The mesh can be uniform and rectangular (Figure 7.11) or triangular and variable (which is useful when

curved geometries must be drawn). The logic behind the approach is similar to a cellular automata with the difference that more occupants can occupy a single cell (a limit is generally set, often 4 persons/m^2). This approach is useful when one wants to directly simulate the movement of people in the area.

Continuous models (such as MassMotion) represent the building floor as a continuous plane that simulates the movement of the occupants on a coordinate-based system over all walkable space (Figure 7.12). Similar to the fine network model, in this case the movement of the occupants is directly simulated.

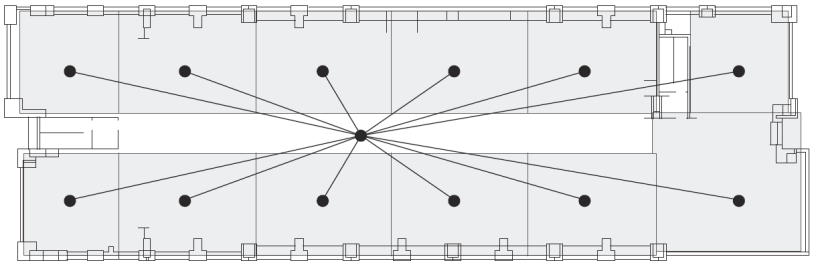

Figure 7.10. Corse network discretisation (Kuligowski, 2015)

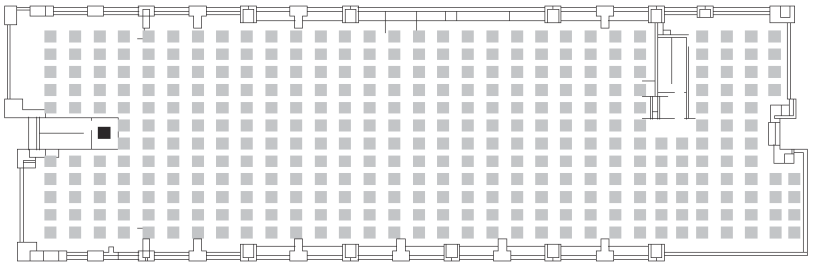

Figure 7.11. Fine network discretisation (Kuligowski, 2015)

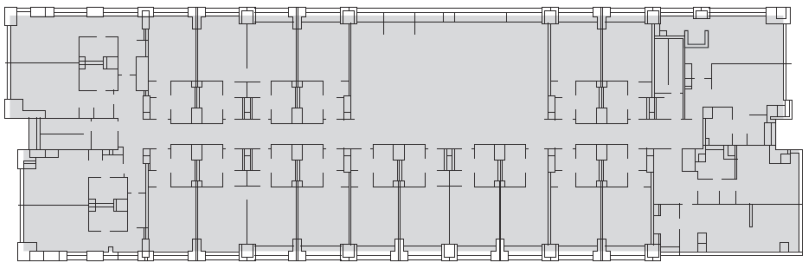

Figure 7.12. Continuous discretisation (Kuligowski, 2015)

7.3.4 Potentialities and limitations

Evacuation models are certainly able to reproduce basic qualitative behaviour as those shown in Table 7.3. In this table some pictures obtained during drills conducted in the Directorate of Technical Safety and Fire Prevention are reported. Over 200 firefighters participated in the drills and several geometrical configurations were analysed.

Specifically, the left column shows the clogging of the exit, where the crowd forms a typical arching shape: this behaviour is similarly reproduced by FDS+Evac and Pathfinder. The right column, instead, shows an asymmetric use of the exit doors, typical of real situations, which naturally emerge with FDS+Evac, which is based on the concept of social force (Helbing, 1995), whereas Pathfinder shows a symmetric use of the exit.

Table 7.3. Qualitative comparison between drills (DCPST, 2017) and evacuation models

	Single exit (1.2 m width)	Two exits (each 1.2 m width)
Drills		
FDS+Evac	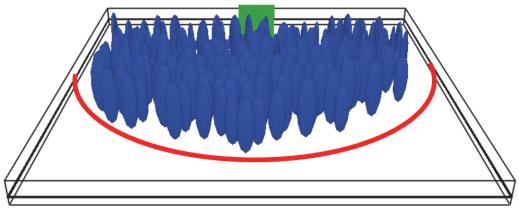	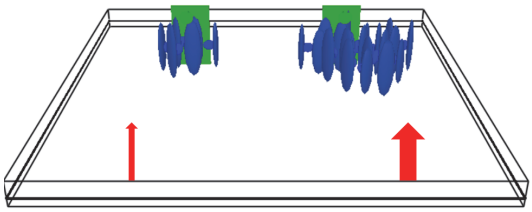
Pathfinder	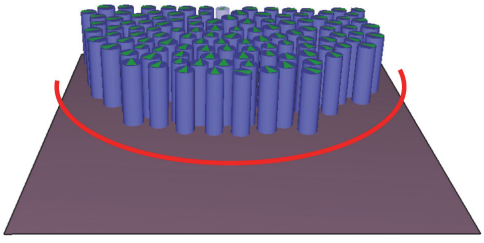	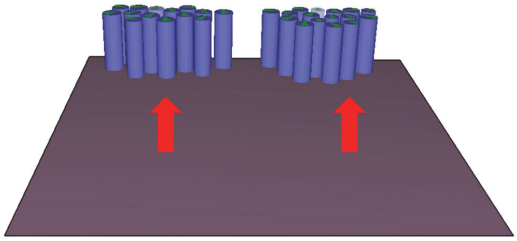

In this case, only qualitative behaviour is compared and the results are satisfactory.
The quantitative comparisons of drills and models can be found in literature for a large number of buildings and many cases are satisfactory, because by calibrating the input data of walking speed, pre-evacuation time and exit choice a high level of agreement can be obtained (Rinne et al, 2010; McConnel et al, 2016; Hostikka et al, 2007).
Nevertheless, the use of evacuation models for making predictions with few information of people's characteristics is still a matter of discussion. In fact, the evacuation models have necessarily intrinsic limitations, linked to the unpredictable character of the human behaviour. This type of limitation can be overcome only by improving the understanding of the psychological and social phenomena emerging during evacuation, whereas the physiological effect of fire products on people is quite well understood.
Besides this aspect, another type of limitation is linked to the structure of the code and its algorithms: for instance, some codes cannot exceed a certain number of people for each simulation or have geometrical constraints (2D instead of 3D geometries, etc.). This aspect can be certainly enhanced and is, in fact, a growing field of research.
Currently, there is no international standard for verification and validation of evacuation models. It is worth to highlight that verification is related to the capability of the model to reproduce what one expects according to the mathematical calculation, while validation is instead linked to the accuracy of the model in representing the phenomena typical of the real world.
Recently a great effort has been spent in recommending a set of examples for testing the capabilities of the models regarding the features of pre-evacuation time, movement and navigation, exit usage, route availability and flow constraints (Ronchi et al. 2013). In addition, it is recognised that tests are often used out of their original context: this is the case of the IMO (International Maritime Organisation) series of 11 tests, which were developed for maritime applications and are instead used for building evacuation

models. Nevertheless, they can be a starting point to develop new tests based on real drills.

For example, simple geometries can be used to reproduce the ability of evacuation models to qualitatively reproduce results reflecting the current knowledge on human behaviour in fire (Figure 7.13). Besides these simulations, analytical verifications with hand calculations should also be done, to check the predicted results with evidence.

Sensitivity analysis and validation with real data are a guaranty of reliability of the software and should be used to understand if the given cases is within the scope of the code or not.

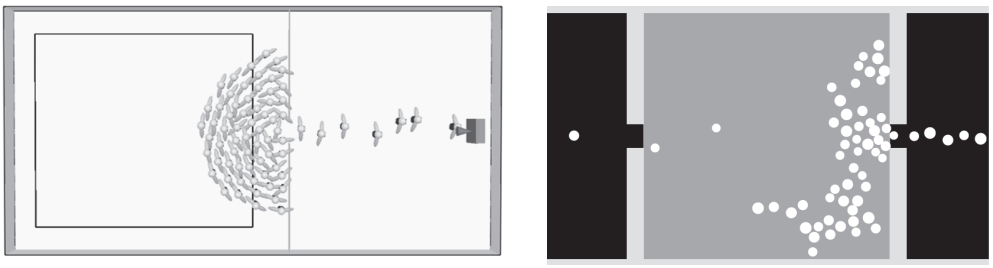

Figure 7.13. Clogging and arching towards a door; active vs herding behaviour (Helbing, 2000)

7.4 Sensitivity analysis of FDS+Evac and Pathfinder

7.4.1 Generalities

As it has been highlighted previously, evacuation models are the most detailed tool for life safety verifications in the fire safety field. Their strength is in the possibility of modelling directly the movement of the single occupant, including its attitude to the most probable pattern and basic behavioural features (e.g. nearest vs fastest way to reach the exit). However, the reliability of such models is still a matter of discussion (Purser, 2008). Reliability implies affordance in making predictions, but this might be very difficult when dealing with human behaviour, especially in fire emergencies.

In the thesis, only agent-based model (ABM) are considered and specifically FDS+Evac (Korhonen et al, 2009) and Pathfinder (Thunderhead Engineering, 2016) are selected.

A sensitivity analysis is conducted for both FDS+Evac and Pathfinder, with the aim of assessing the reliability of the results by varying the size of the mesh and the characteristics of the occupants as reported in the Tables 7.4 and 7.5. No behavioural features are implemented. The geometry of the area is a square room (10 m edge) with a single central exit of 1.2 m (similar to the model shown in Table 7.3). Two levels of initial density are considered: 2 and 0.8 occupants per square metres.

For FDS+Evac, regular squared meshes are considered. Otherwise, as Pathfinder uses a triangular mesh, two parameters are taken into account: the maximum length of the single triangle and the minimum angle between the edges. Regarding the characteristics of the occupants, three sets of pre-evacuation time distribution and three categories of occupant types are considered (the properties of the occupant types are chosen as the default in FDS+Evac). In this way, the aspect of reproducing the basic features of the human movement (when for human movement is intended the physical attitude of the spectrum of people) is the objective, together with the capability of the model to correctly implement different levels of speed and radius of the occupants.

Table 7.4. Parameters used for the analysis

	Case 1	**Case 2**	**Case 3**
Mesh size **- FDS+Evac** **- Pathfinder**	 0.2 m No constraint 0°	 0.4 m 2.5 m 10°	 0.6 m 1 m 20 °
Pre-evacuation time	0 s	30 s	0 - 30 s (av. 15 s, st. dev. 5 s)
Occupant type	Adult	Child	Elderly

Table 7.5. Description of the categories for the occupant types

Type	Shoulder width (cm)	Walking speed (m/s)
Adult	44-58	0.95-1.55
Child	39-45	0.60-1.20
Elderly	46-54	0.50-1.10

The softwares are recommended to be used in Monte Carlo mode and, in line with this, each scenario is performed 10 times. The sources of randomness are not the same for the softwares. Both FDS+Evac and Pathfinder assign different values for radius, speed and pre-evacuation time to each occupant for each scenario according to the distribution given as input, but the former also uses random forces (different from run to run) in the algorithm that solves the movement of the occupants.

Average, minimum and maximum values among all runs for each case are shown in the following figures, where different time steps are reported and are associated to the time spent by the 25 %, 50 %, 75 % and 100 % of the total number of occupants to exit from the area. This is done to emphasize the agreement between the two softwares along the entire simulation time (not only the last occupant exits at the same time but also the intermediate ones). In addition, the maximum dispersion among the 10 runs is reported, by calculating the dispersion of the maximum and minimum RSET compared to the average RSET for all parameters (mesh, pre-evacuation time, agent type). Finally, the maximum difference among the average values for all parameters at different time steps is reported.

7.4.2 Results with FDS+Evac (2 p/m²)

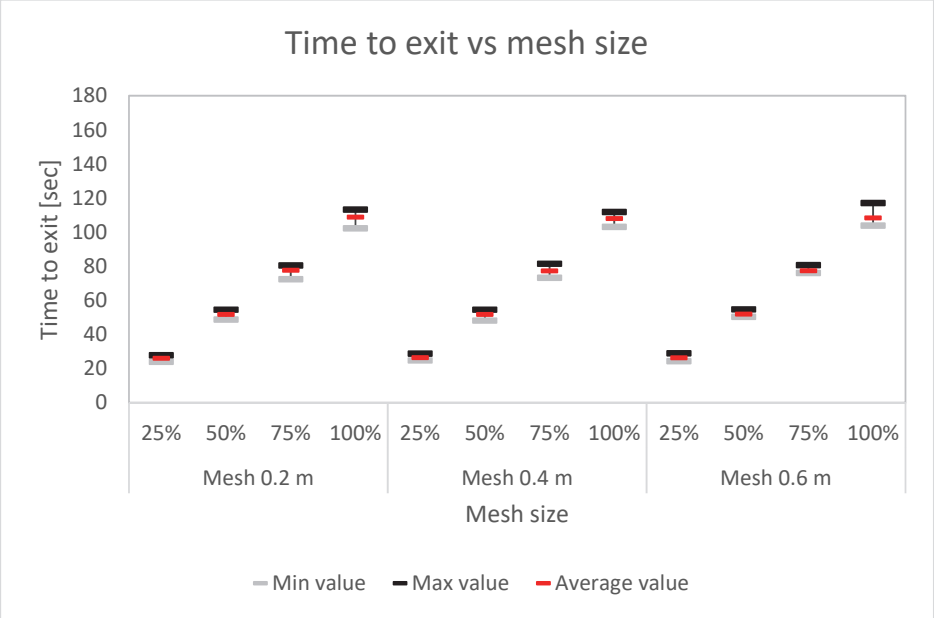

Figure 7.14. Time to exit vs mesh size for 2 p/m² using FDS+Evac

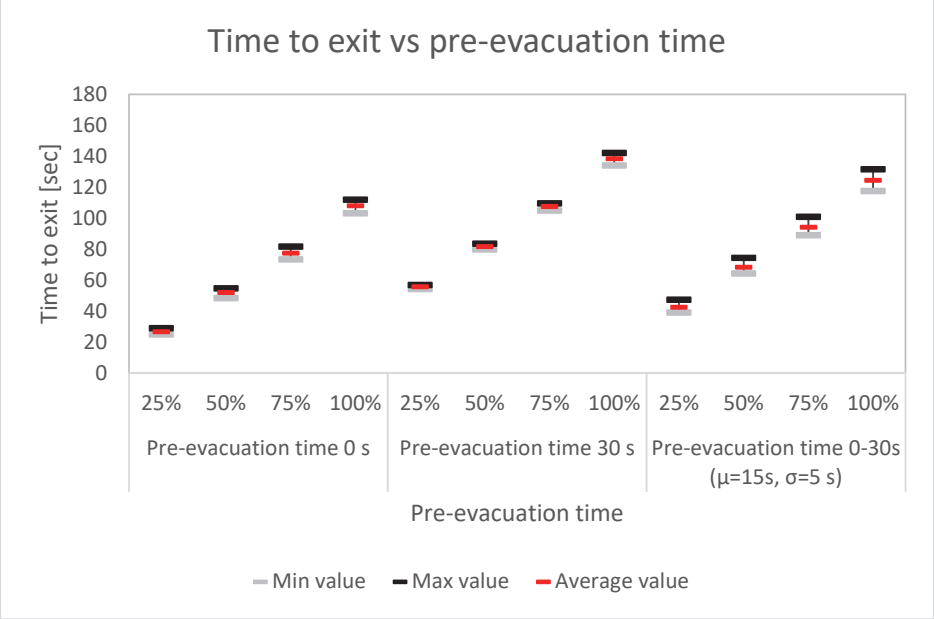

Figure 7.15. Time to exit vs pre-evacuation time for 2 p/m² using FDS+Evac

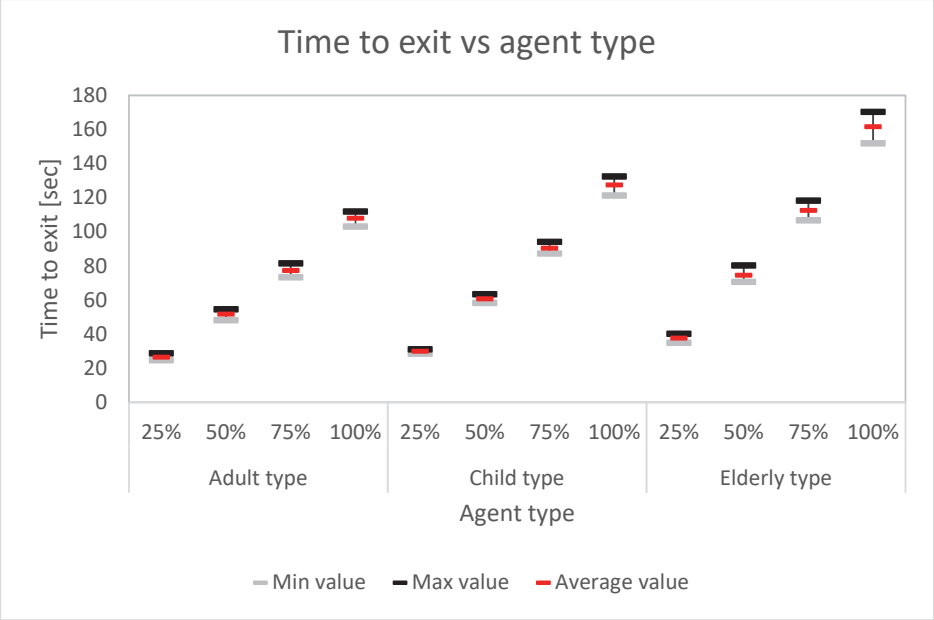

Figure 7.16. Time to exit vs agent type for 2 p/m² using FDS+Evac

Table 7.6. Maximum dispersion (%) among the runs (FDS+Evac, 2p/m²)

	Max difference (%)		
	Mesh	Pre-evacuation time	Agent type
Min-Av.	9%	8%	7%
Max-Av	10%	11%	8%

Table 7.7. Maximum difference (%)among the average values (FDS+Evac, 2p/m²)

	Max difference (%) among average value		
Evacuated occupants	Mesh	Pre-evacuation time	Agent type
25%	1.29%	70.96%	16.60%
50%	0.84%	46.14%	34.96%
75%	0.39%	32.62%	36.06%
100%	0.79%	24.64%	37.08%

7.4.3 Results with Pathfinder (2 p/m²)

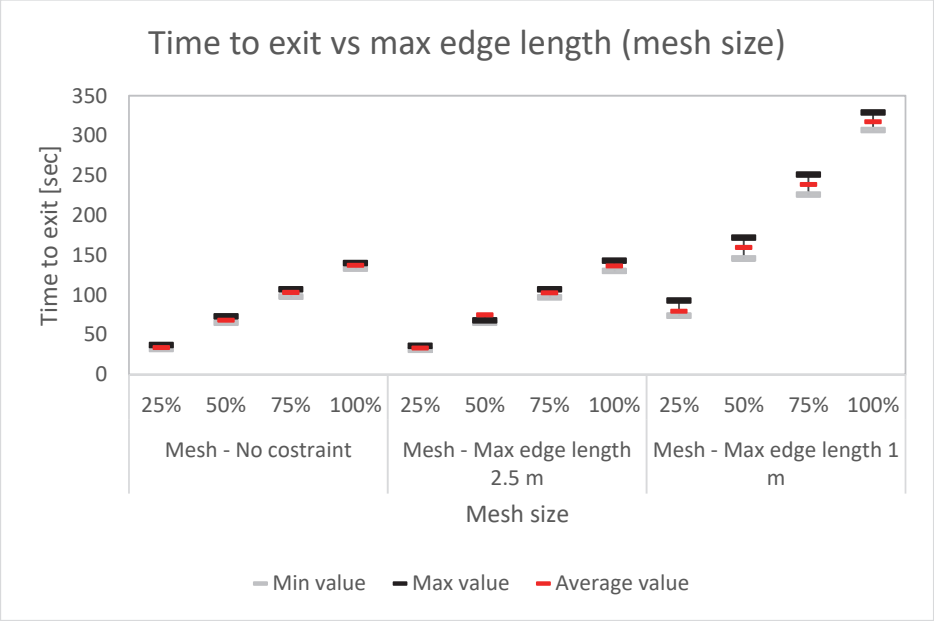

Figure 7.17. Time to exit vs max edge length for 2 p/m² using Pathfinder

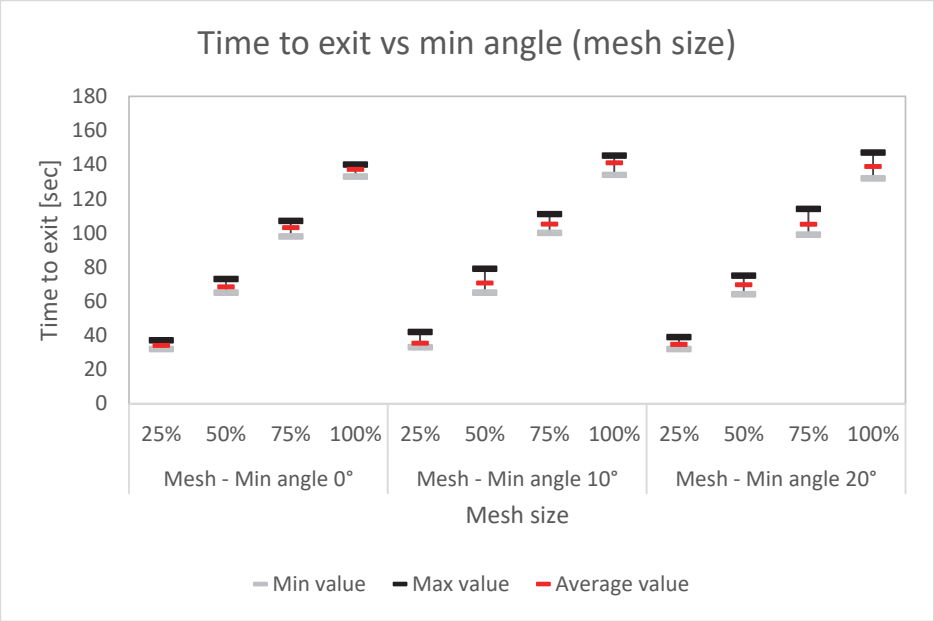

Figure 7.18. Time to exit vs min angle for 2 p/m² using Pathfinder

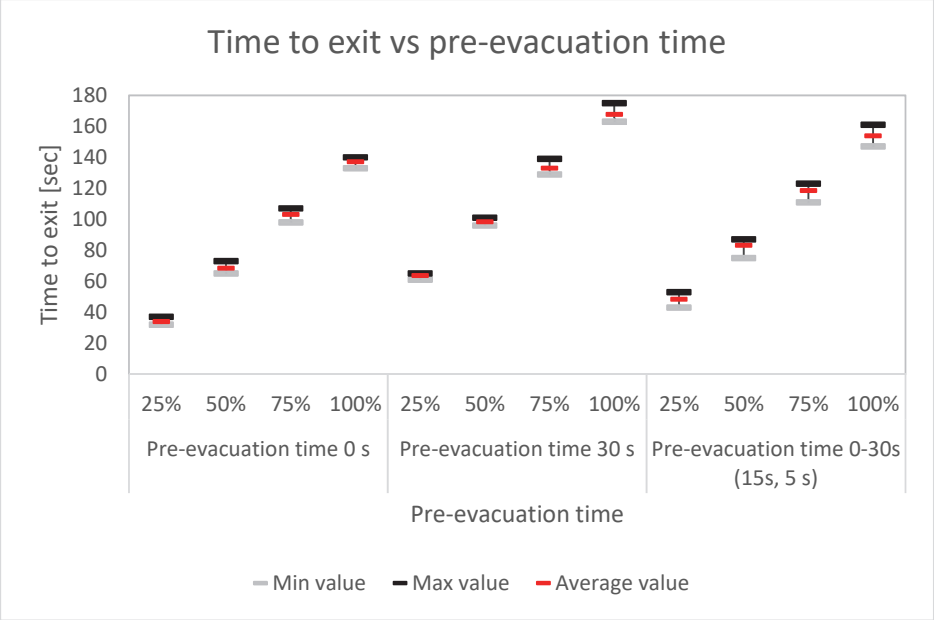

Figure 7.19. Time to exit vs pre-evacuation time for 2 p/m² using Pathfinder

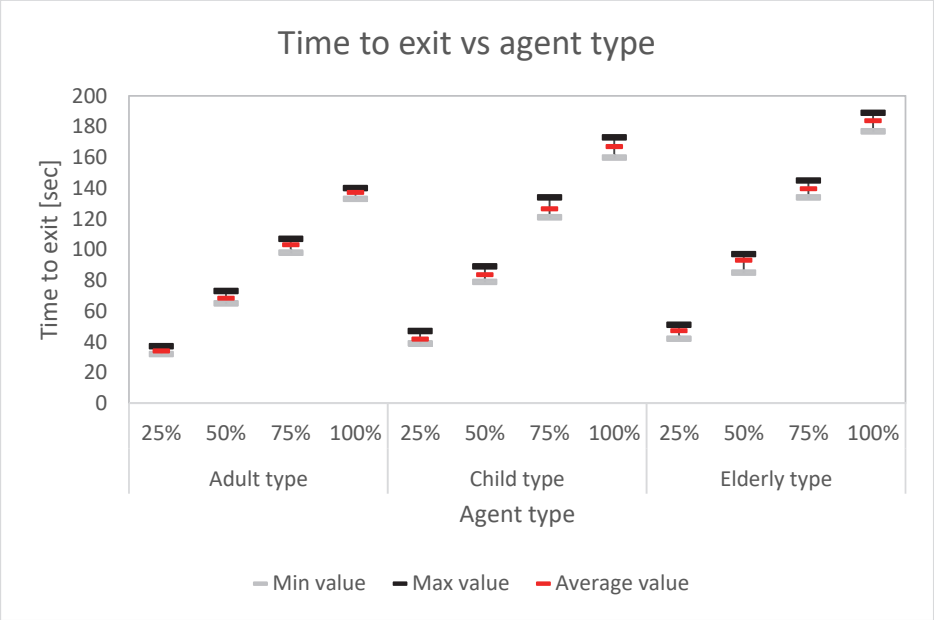

Figure 7.20. Time to exit vs agent type for 2 p/m² using Pathfinder

Table 7.8. Maximum dispersion (%) among the runs (Pathfinder, 2p/m²)

	Max difference (%)			
	Mesh edge	Mesh angle	Pre-evacuation time	Agent type
Min-Av.	14%	8%	12%	12%
Max-Av	16%	17%	9%	12%

Table 7.9. Maximum difference (%) among the average values (Pathfinder, 2p/m²)

	Max difference (%) among average value			
Evacuated occupants	Mesh edge	Mesh angle	Pre-evacuation time	Agent type
25%	1.78%	4.03%	60.80%	20.34%
50%	80.07%	3.17%	35.97%	32.51%
75%	80.00%	2.02%	25.40%	30.59%
100%	79.38%	2.82%	20.07%	30.08%

7.4.4 Results with FDS+Evac (0.8 p/m²)

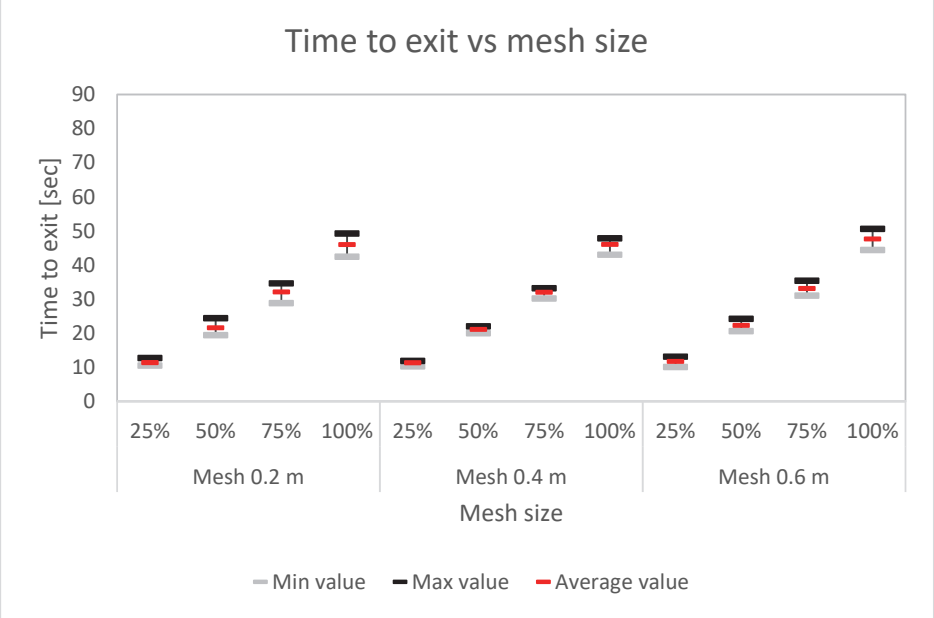

Figure 7.21. Time to exit vs mesh size for 0.8 p/m² using FDS+Evac

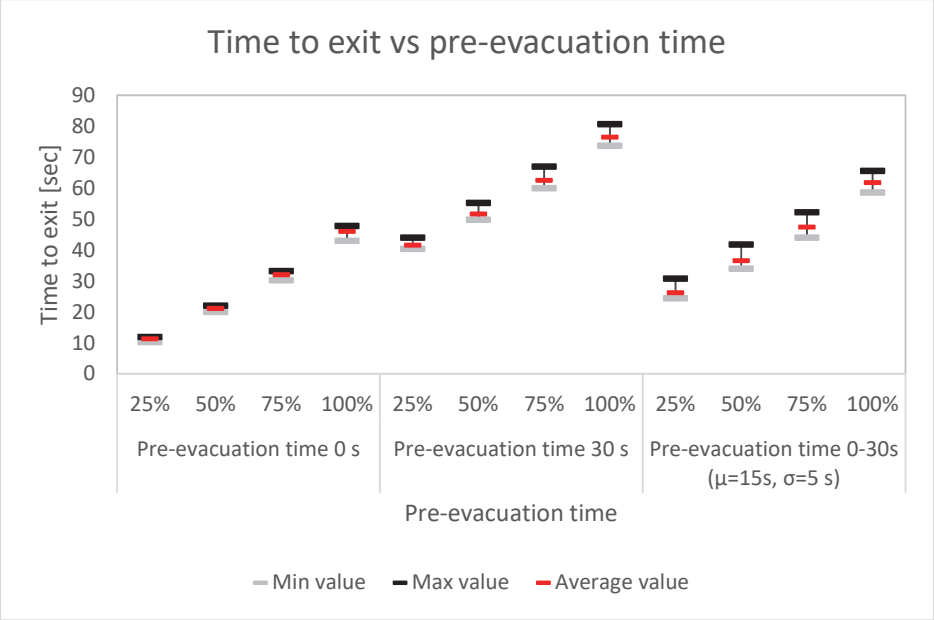

Figure 7.22. Time to exit vs pre-evacuation time for 0.8 p/m² using FDS+Evac

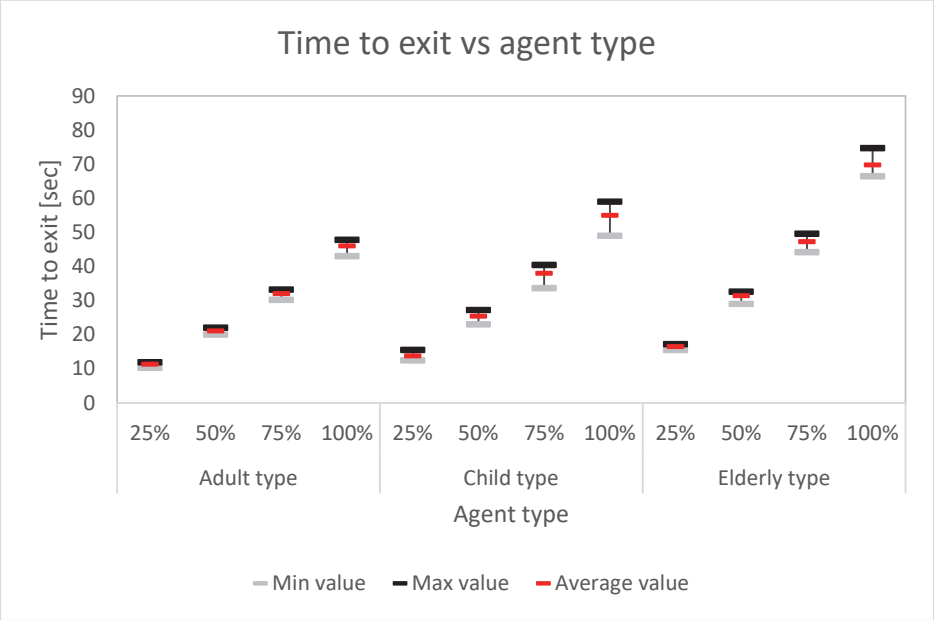

Figure 7.23. Time to exit vs agent type for 0.8 p/m² using FDS+Evac

Table 7.10. Maximum dispersion (%) among the runs (FDS+Evac, 0.8 p/m²)

	Max difference (%)		
	Mesh	Pre-evacuation time	Agent type
Min-Av.	15%	9%	12%
Max-Av	12%	16%	12%

Table 7.11. Maximum difference (%)among the average values (FDS+Evac, 0.8 p/m²)

	Max difference (%) among average value		
Evacuated occupants	Mesh	Pre-evacuation time	Agent type
25%	0.53%	114.44%	19.60%
50%	3.11%	83.89%	37.24%
75%	3.01%	64.52%	39.27%
100%	3.07%	49.78%	38.41%

7.4.5 Results with Pathfinder (0.8 p/m²)

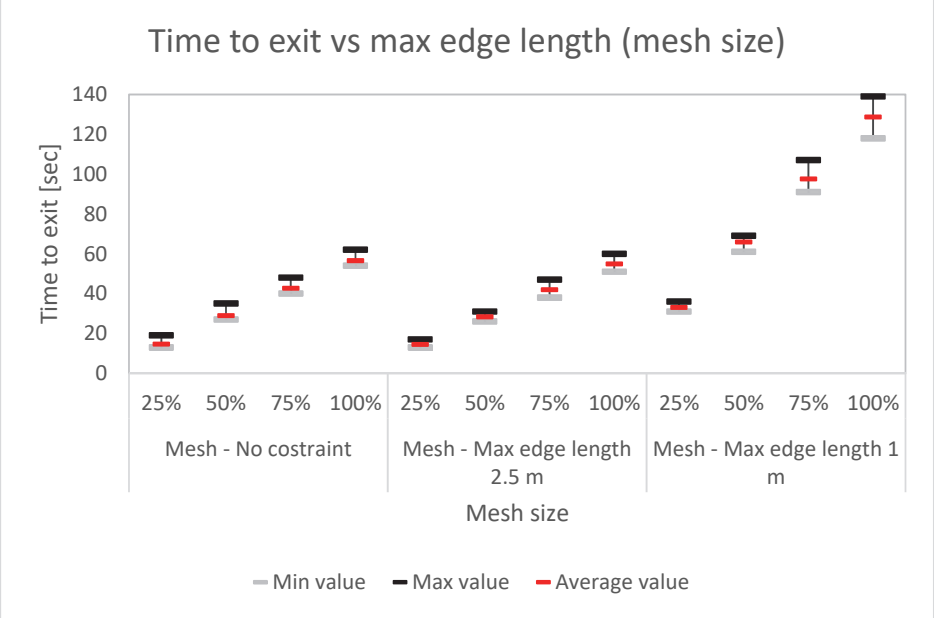

Figure 7.24. Time to exit vs max edge length for 0.8 p/m² using Pathfinder

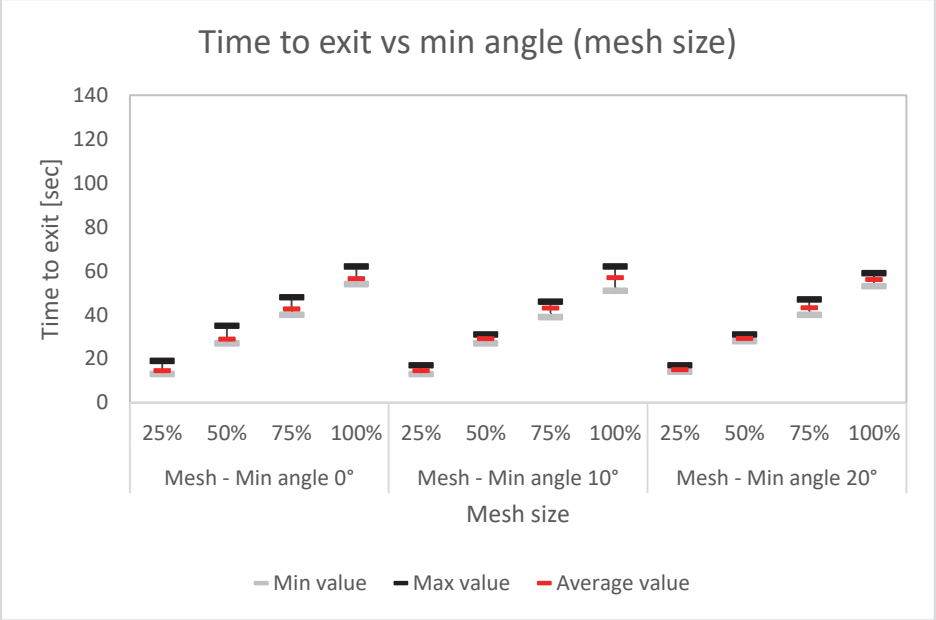

Figure 7.25. Time to exit vs min angle for 0.8 p/m² using Pathfinder

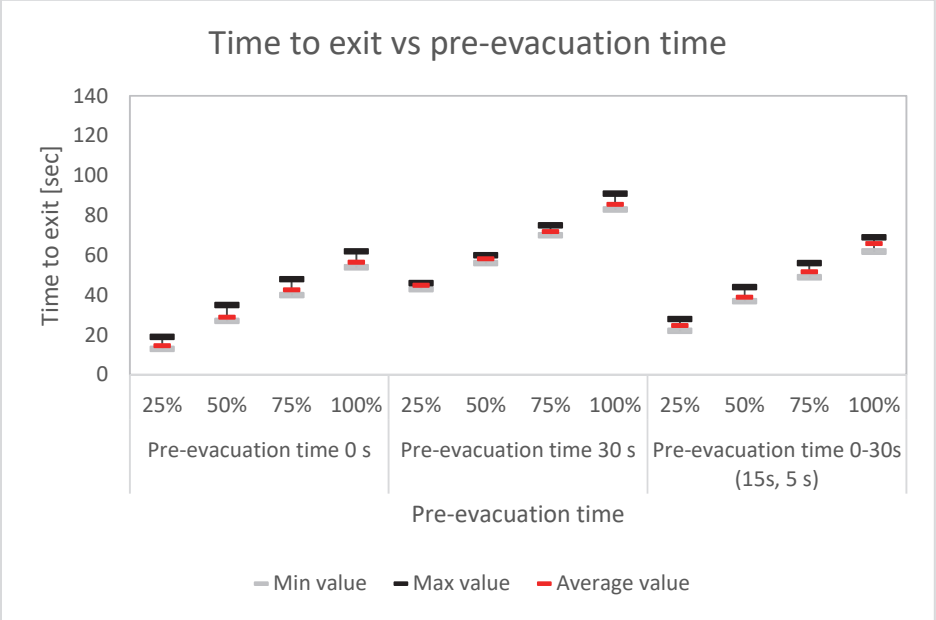

Figure 7.26. Time to exit vs pre-evacuation time for 0.8 p/m² using Pathfinder

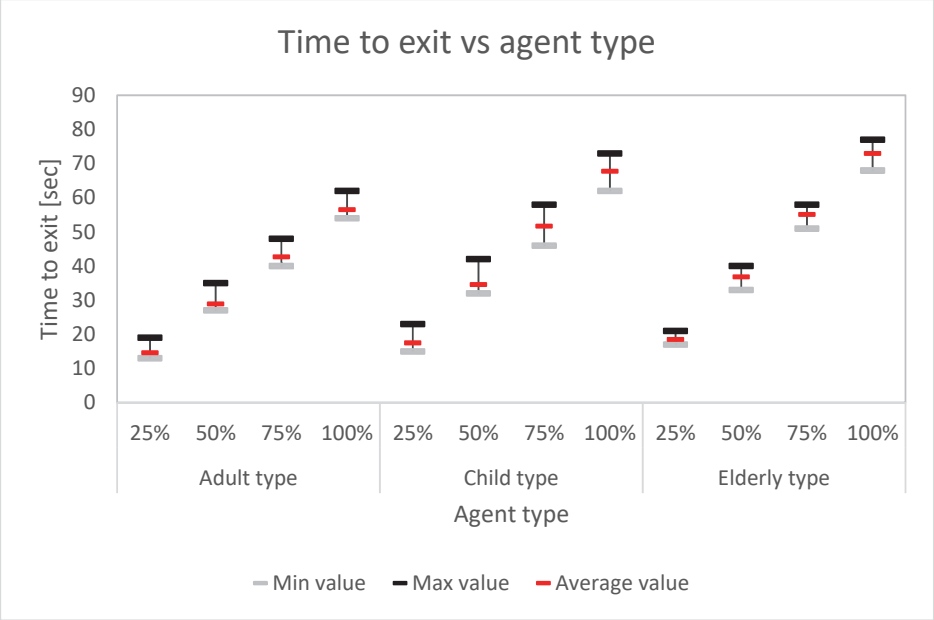

Figure 7.27. Time to exit vs agent type for 0.8 p/m² using Pathfinder

Table 7.12. Maximum dispersion (%) among the runs (Pathfinder, 0.8 p/m²)

	Max difference (%)			
	Mesh edge	Mesh angle	Pre-evacuation time	Agent type
Min-Av.	12%	12%	12%	15%
Max-Av	26%	26%	26%	27%

Table 7.13. Maximum difference (%) among the average values (Pathfinder, 0.8 p/m²)

	Max difference (%) among average value			
	Mesh edge	Mesh angle	Pre-evacuation time	Agent type
25%	2.87%	0.71%	101.85%	18.18%
50%	77.31%	2.70%	67.28%	23.56%
75%	78.06%	1.03%	50.96%	24.05%
100%	78.26%	1.16%	40.96%	25.36%

7.4.6 Conclusions

The sensitivity analysis allows to draw some conclusions concerning the reliability of the selected models. The main findings are reported below:

- Regarding FDS+Evac, the software seems to be extremely robust regarding the mesh size. In fact, the same results are obtained for 0.2 m, 0.4 m and 0.6 m. The user should only pay attention to the size of the mesh because it snaps the obstructions and the width of the exits (for example, to model an exit of 1.2 m the user cannot use a mesh of 0.5 m, while 0.2 m, 0.4 m and 0.6 m are correct).

- Pathfinder is sensitive to the variation of the size of the triangle when the maximum length of the edge is decreased. The variation of the minimum angle instead does not affect the exit time. It is noticed that the results obtained with the default value of the mesh ("No constraint" case) are in agreement with those of FDS+Evac.

- Both using FDS+Evac and Pathfinder the difference among adult, child and elderly occupants is reproduced according to the common sense and experience: the elderly occupants are the slowest, the child occupants are slightly faster than the former and the adult occupants are the fastest among all the groups.

- The same trends are obtained for the cases of 2 and 0.8 p/m^2, with the only difference of the maximum value reached. Generally, it can be concluded that the exit times calculated by Pathfinder are slightly larger than those obtained by FDS+Evac (approximately the magnitude is the 15 %).

- Considering the maximum dispersion among the runs (Tables 7.6, 7.8, 7.10, 7.12), the results show that the dispersion is higher for the lower density (16% for FDS+Evac and 26% for Pathfinder) compared to the higher density (11% for FDS+Evac and 17% for Pathfinder).

- Considering the difference among the average values, larger differences are noticed for the lower density.

- Specifically, the pre-evacuation time largely affects the first time step (25% of the occupants exited) over the 100% in the worst case and decreases to 20-50% when the last time step is considered.
- The influence of the agent type is higher on the time to exit of the last occupant compared to other time steps.
- The dispersion of the data between the minimum and maximum values of the exit time of the selected time steps (25, 50, 75, 100 % of the total number of occupants) is very limited. For geometry and input values similar to the analysed cases 10 runs for each scenarios can be considered as acceptable.

The analysis of the tunnels contained in Chapter 9 and 10 will be carried out using Pathfinder, which on average provides for higher value of the evacuation time thus is on the safe side from the life safety point of view.

SECTION 3: PROPOSED PROCEDURE AND APPLICATIONS

Chapter 8

Proposed procedure of risk assessment

8.1 Scheme of the procedure

The procedure adopted for the quantitative fire risk assessment is illustrated in Figure 8.1. The structure of the procedure follows the one developed by the World Road Association (PIARC, 2008) and is detailed in the chapter in order to encourage the use of direct modelling of fire and evacuation, providing recommendations on the scenarios to be taken into consideration, necessary and sufficient to assess the fire risk of a given road tunnel.

A preliminary step for the use of advanced models is to conduct an independent sensitivity analysis which can provide information on the capabilities of the models. Verification and validation studies are generally available for commercial software; however, apart for few researchers (Ronchi, 2013) these models have not been put into practice necessarily in the context of road tunnels, basically because they require a large amount of time due to the longitudinal extension of the area. For this reason, the previous numerical analysis (Chapters 5 and 7) are considered essential for the reliability of the results of the following chapters.

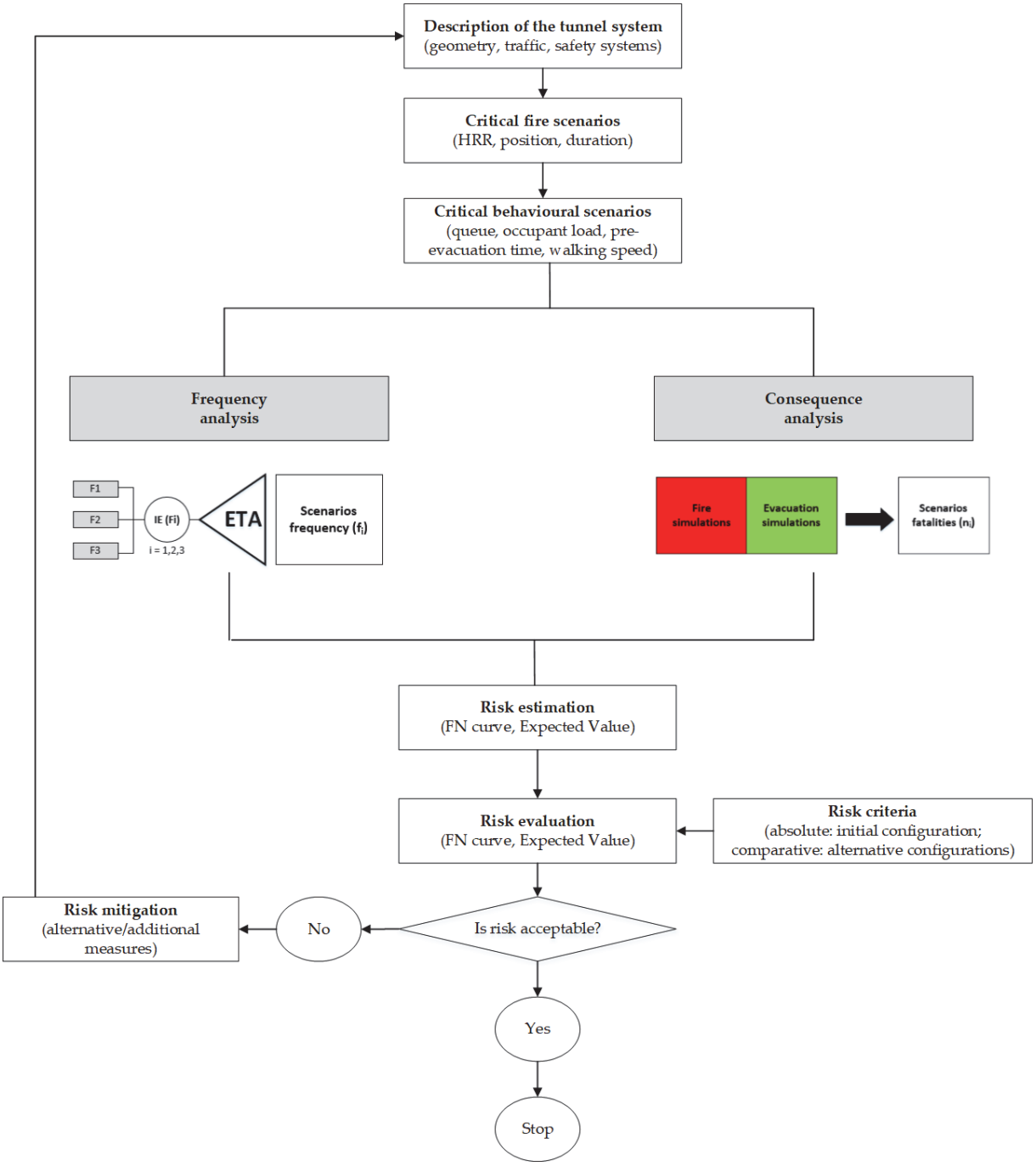

Figure 8.1. Procedure for the fire risk assessment of road tunnels

8.1.1 Fire scenarios

Several fire scenarios have to be analysed, considering the following aspects: position of the fire inside the tunnel, magnitude of the fire and activation of the longitudinal ventilation system. Specifically, three positions of the fire have been studied: X1 ($X_{entrance\ portal}$ + 200 m), X2 ($X_{L/2}$ at the middle of the tunnel), X3 ($X_{exit\ portal}$ - 200m). For each position of the fire, in agreement with the literature (Persson, 2002), three levels of fire hazard have been considered: a car fire (F1, 8 MW), a bus fire (F2, 20 MW) and a HGV fire (F3, 120 MW). Finally, for every case the success or the failure in the activation of the ventilation system has been inserted in the model. The design fire curves are represented in Figures 8.2, 8.3 and 8.4. The results were restricted to the first 20 minutes of the simulation time, because the objective of the QRA is to determine the number of fatalities which depend on the possibility of a safe evacuation. These indications are not contradictory with the design fires recommended in Italy (ANAS, 2009), which leave large choice to the designer (i.e. HGV fire comprised between 15 and 150 MW). On the contrary, they appear to be more specific because the worst positions of the fire are also provided.

In line with the event tree analysis (see point 8.2.2) the only system taken into account in the fire modelling is the ventilation system. When activated, the jet fans blow air at a maximum power (a delay of 300 seconds is inserted in the model as a ramp to reach the steady capacity). Otherwise, for those scenarios in which the ventilation system is supposed to fail, a minimum flow is kept; in this way, a flow of air naturally induced by the different meteorological conditions at boundaries is guaranteed. Alternatively, this could represent the failure conditions for only a few of the jet fans while the others, far from the fire, are considered to work and establish a soft flow).

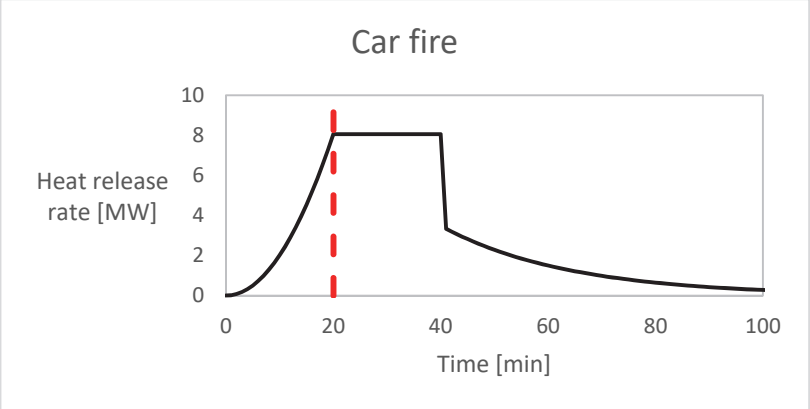

Figure 8.2. Car fire curve.

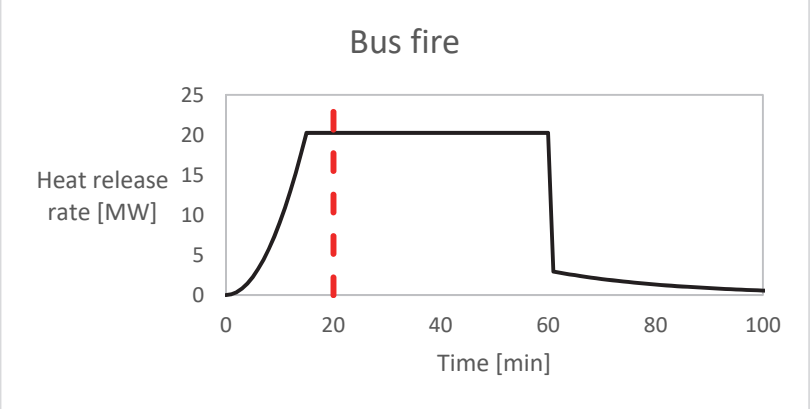

Figure 8.3. Bus fire curve.

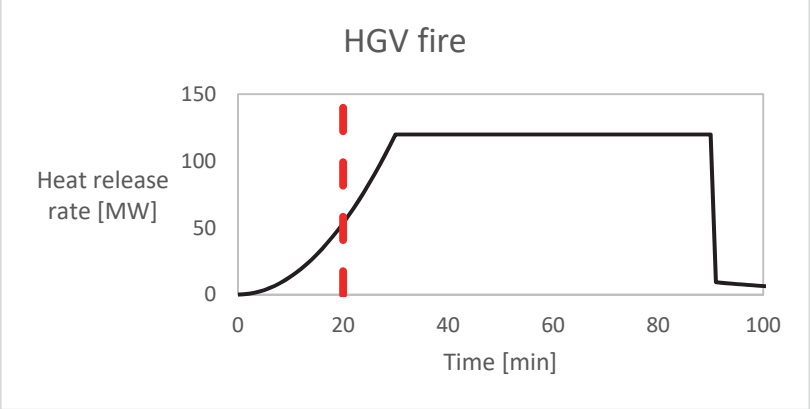

Figure 8.4. HGV fire curve.

8.1.1.1 Choice of the length of the model

Tunnels can be majorly extended in the longitudinal direction and the possibility of modelling their entire length is determined by the computational effort put in during the simulation. Several techniques are available for reducing the computational effort: OpenMPI or MPI can be helpful to speed-up the simulation by dividing the model into sub-models (multiple-meshes) which are solved contemporarily depending on the type of analysis. However, considering that several scenarios must be modelled for a comprehensive quantitative risk assessment of the tunnel and for life safety analysis an overall simulation time of 20 minutes is necessary to make appropriate considerations, the issue of reducing the length of the tunnel for modelling purpose is critical.

Scale modelling is not considered a solution, because despite a smaller extension of the model, a much finer grid resolution would be required, thus increasing again the computation effort. According to the FDS User's Guide, although it is not the best choice, a non-cubic grid resolution is allowed: for instance, the longitudinal direction might be extended up to 4 times as much as the other two directions. Nevertheless, the accuracy is not guaranteed when large dimensions of the grid (few metres) are reached and still the model might be quite expensive in terms of computational time.

Cutting the model to a shorter length might be suitable as long as the difference in the smoke dynamics and the macroscopic quantities (specifically, the gas temperature) with the much longer model fall within a certain range of acceptability (typically, 20 % for FDS simulations). Reducing the longitudinal dimension of the model is beneficial because the grid resolution can be restrained to a finer resolution, with sustainable computational effort, but far from the grid size typical of the scale modelling.

Two models are considered for the 8 MW fire.

- Model 1: cubic grid (50x50x50 cm), L_{tot}=400m, longitudinal ventilations with 2 jet fans placed at x = 150 m;

- Model 2: L_1=400m: cubic grid (50x50x50 cm) + L_2=400m: rectangular grid (100x50x50 cm), L_{tot}=800m, longitudinal ventilations with 2 jet fans;

In the following tables 8.1-8.4 the quantities of temperature, radiative heat flux gas, visibility and FED at z = 2 m in the middle of the cross section (y = 6 m) are reported at 300, 600, 900 and 1200 seconds (only the first 400 metres are reported, because this is the domain where the analysis wants to be carried out).

Considering the highly reduced computational time related to Model 1, the difference between this and Model 2 seems reasonable. Most of the differences are located in the vicinity of the fire source, but the curves overlaps for most of the length of the tunnel and sometimes the Model 1 shows conservative results with respect to the other one.

Specifically, the temperature shows very similar trends upwind the fire source, while downwind some differences are obtained, but they are contained. The visibility, instead, show significant difference, especially at 600 sec.

The radiative heat flux is almost not influenced by the choice of the length apart from the section where the fire source is placed. The FED shows different trend downwind the fire but the differences are much lower than the threshold of tenability (FED=0.1).

However, the difference does not exceed the typical uncertainty in fire modelling calculations. Therefore, the Model 1(L=400 m and cubic grid of 50 cm) is accepted.

Table 8.1. Temperature comparisons (Model 1 is red, Model 2 is black)

Temperature (y=6m, z=2m)	
300 sec	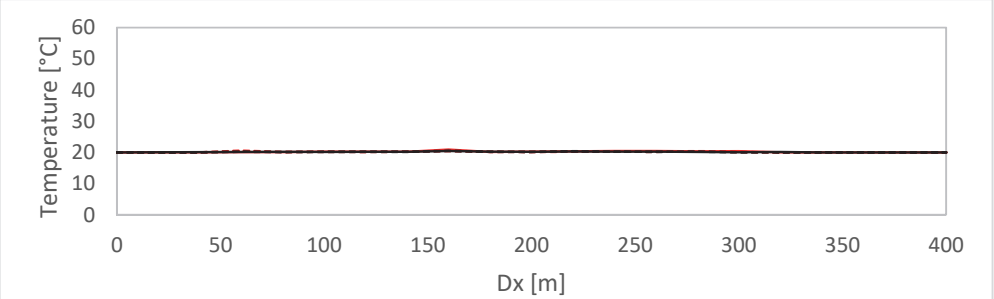
600 sec	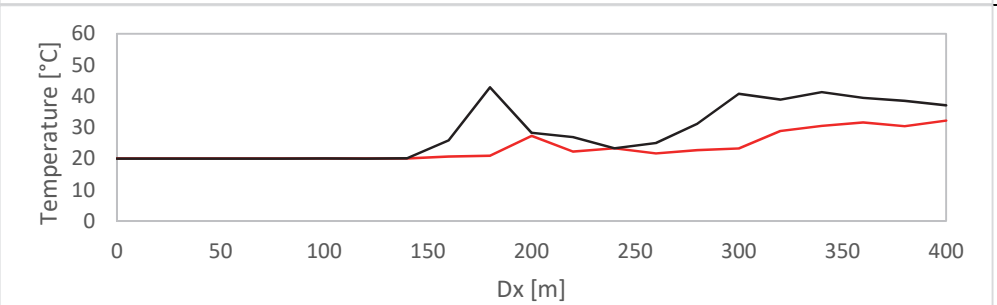
900 sec	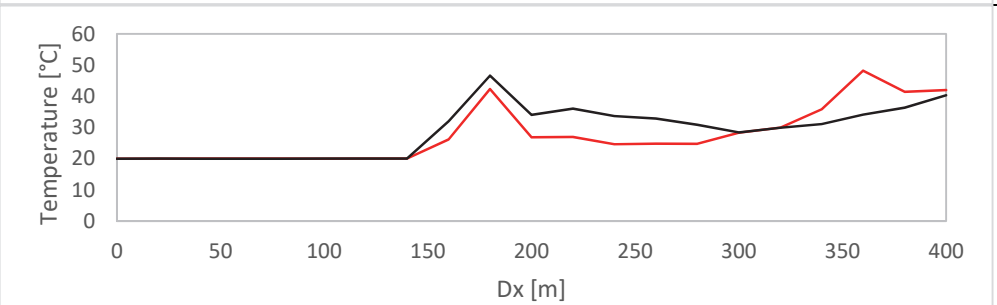
1200 sec	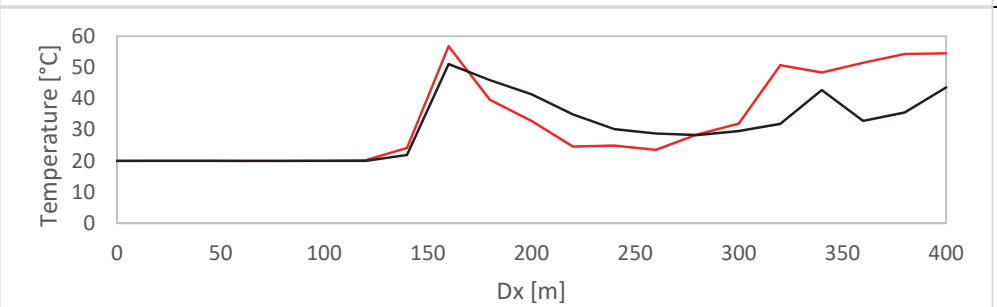

Table 8.2. Radiative hat flux gas comparisons (Model 1 is red, Model 2 is black)

Radiative heat flux gas (y=6m, z=2m)	
300 sec	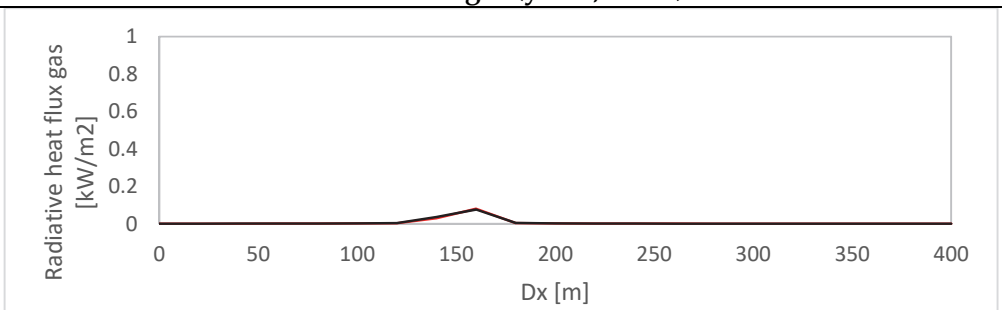
600 sec	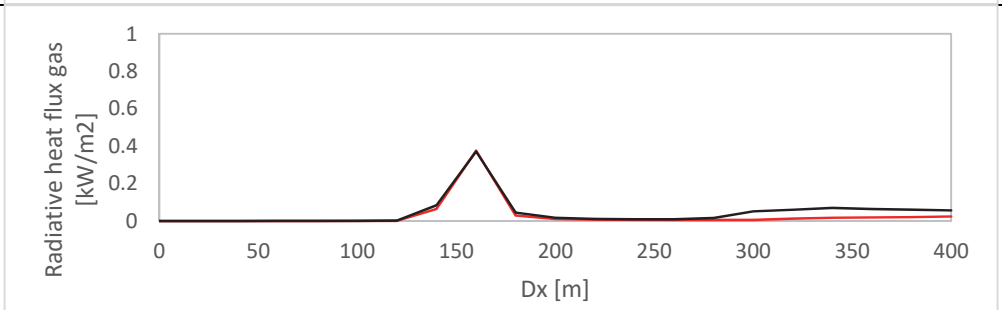
900 sec	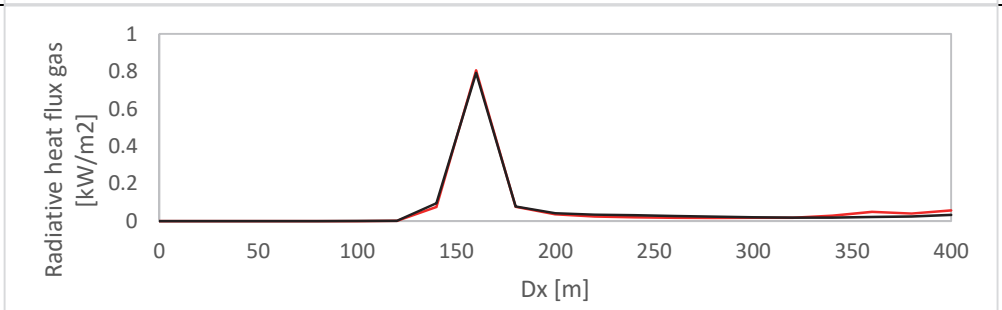
1200 sec	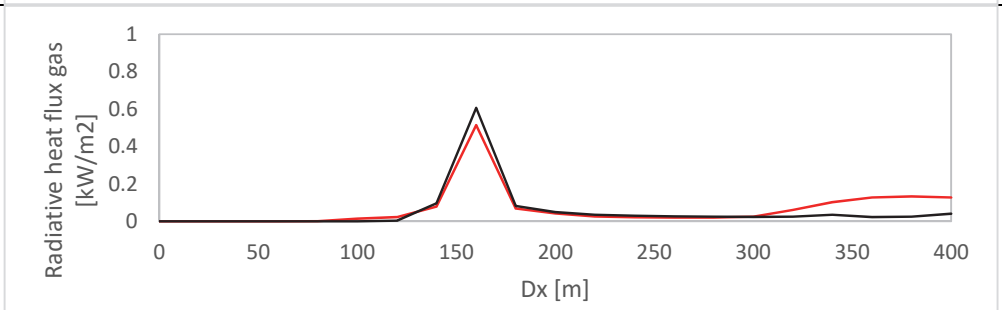

Table 8.3. Visibility comparisons (Model 1 is red, Model 2 is black)

Visibility (y=6m, z=2m)	
300 sec	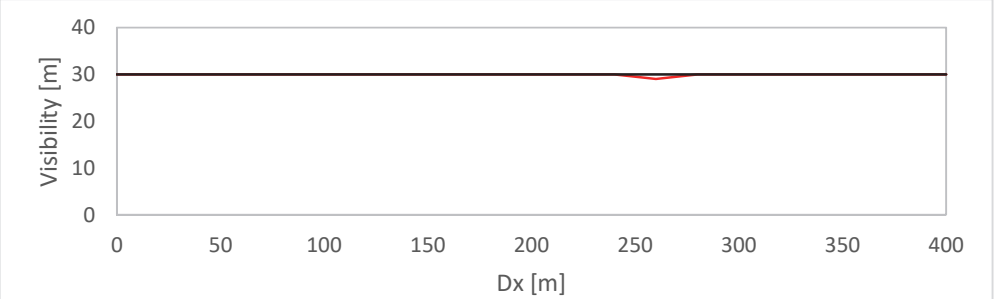
600 sec	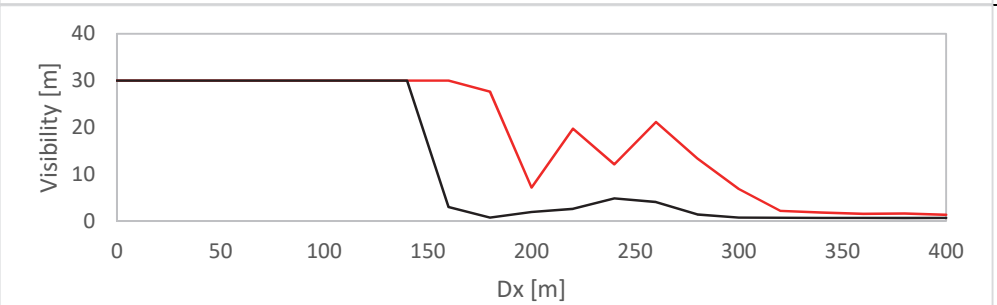
900 sec	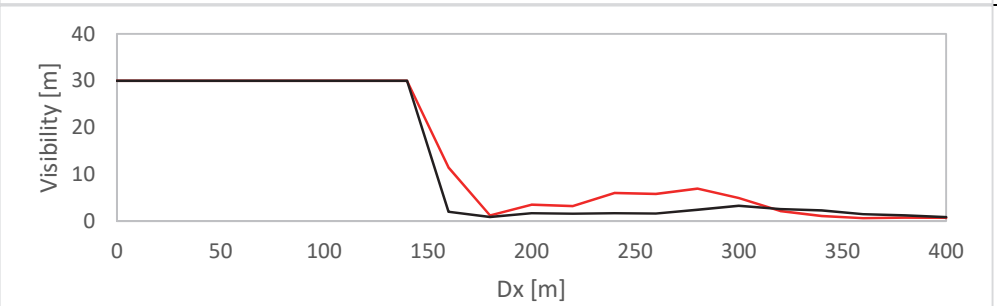
1200 sec	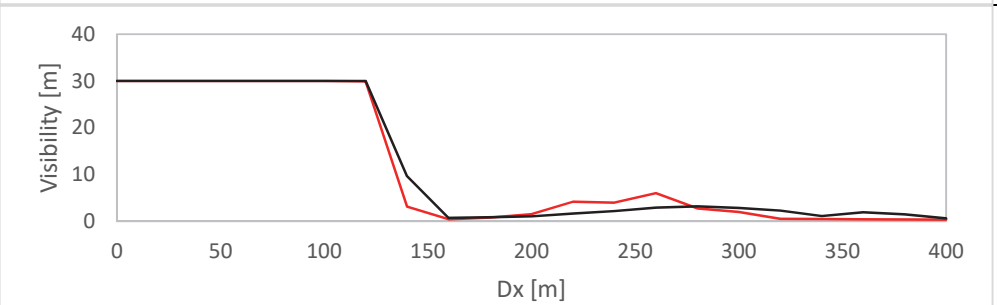

Table 8.4. FED comparisons (Model 1 is red, Model 2 is black)

FED (y=6m, z=2m)	
300 sec	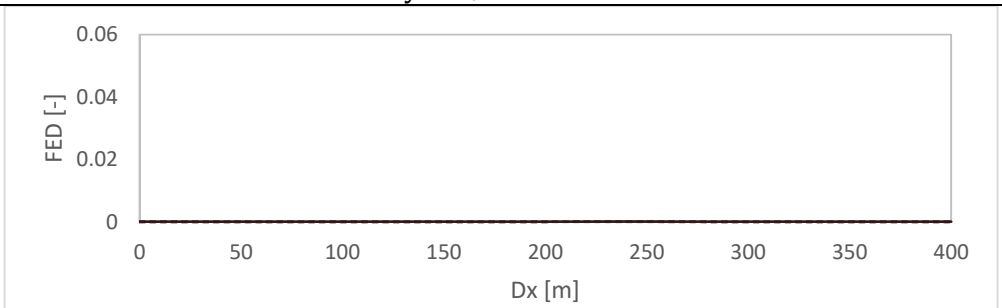
600 sec	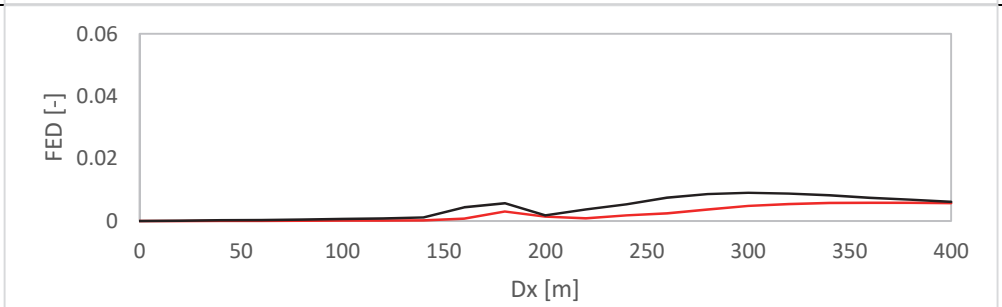
900 sec	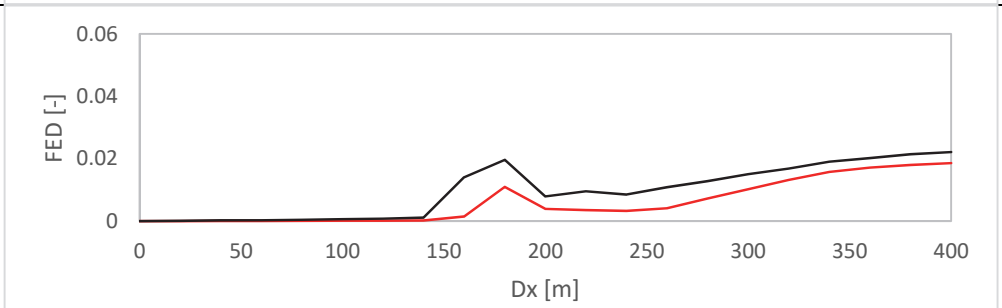
1200 sec	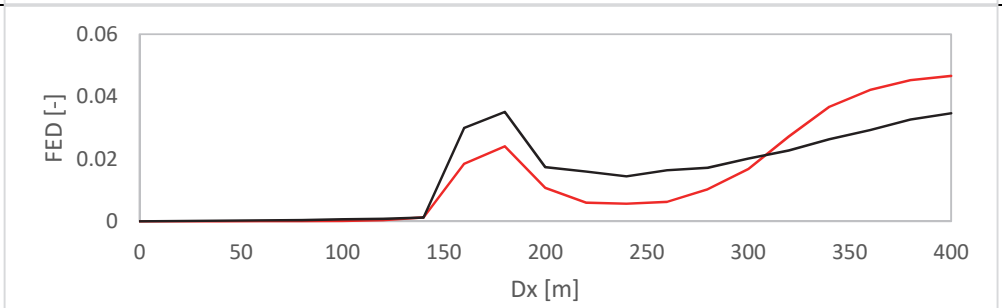

8.1.2 Evacuation scenarios

A simple queue model (ANAS, 2009) was used to calculate the number of people involved in the evacuation process, based on the traffic volume, vehicles speed and distance among vehicles. Then, the difference between the delay for stopping approaching traffic and the activation of an emergency traffic light (if present in the tunnel) determines the number of vehicles inside the tunnel, which can be distributed along its entire length or localised upwind the fire accident.

The average number of people per vehicles has been hypothesised as follows: 3 persons for light vehicles, 1 for HGVs and 40 for buses (Persson, 2002).

Evacuation scenarios correspond to fire scenarios. Given a tube with a single direction of travel, the queue is considered to be located upwind the fire source with vehicles stopping by approaching the fire, whereas vehicles downwind the fire are free to exit the tunnel through the opposite portal. For bidirectional tunnels instead, the queue is bound to develop on both sides of the burning vehicle and for this reason a double exposition of people is likely to take place.

The origin of the previous assumptions lies in the optimal ventilation strategies that should be theoretically adopted in road tunnels. For unidirectional tunnels the longitudinal ventilation should be coherent with the traffic flow and, if well designed, able to guarantee fresh air free of smoke upwind the fire source, exactly in the region where vehicles are supposed to stop and people evacuate. Differently, although its practical application is often more complicated due to higher cost and structural constraints, for bidirectional traffic flows the semi or fully transverse ventilation system should be adopted to facilitate the evacuation through both sides of the tunnel.

As motivated in Chapter 7, Pathfinder is the software chosen for the calculation and the following hypothesis are used to build the model.

1. Considered a queue of vehicles, the prevalent direction of evacuation of its occupants is opposite to the direction of travel;
2. The occupants will evacuate through the nearest available exit;
3. The initial walking speed is a uniform distribution between 0.5 and 1 m/s;
4. The pre-evacuation time is a normal distribution between 30 and 300 seconds;
5. The occupants are free to move across the carriageway (no vehicles are inserted in the model).

The first hypothesis is a consequence of the choice of ventilation system but derives also from the natural attitude of people to move towards a familiar environment (such as the entrance portal). The second hypothesis is made because although there is a growing attention of researchers on collective behaviour the process of decision making and choice of the escape routes are still a matter of discussion and no well-established standards have been developed in the context of road tunnels considering the choice between portal and emergency exits. The third hypothesis is based on the recommendations in the ANAS Guidelines, in which the walking speed is related to the level of visibility in the tunnel (see Chapter 7). The fourth hypothesis is made in order to connect the literature on the topic and the statistical reports of previous accidents with the recommendations contained in ANAS Guidelines (see Chapter 7).

The fifth hypothesis is made on the evidence of previous studies (e.g. Report in http://www.oasys-software.com/casestudies/casestudy/RomeUniRpaperMassM) in which it was observed that the presence of vehicles does not affect the evacuation time. In fact, the presence of obstructions can affect the path of a single occupant, but considering that the prevalent movement is along the longitudinal axis (instead of the transversal) this contribution can be neglected.

8.2 Frequency analysis

The frequency analysis is needed because, as widely explained in Chapter 4, it is very difficult to characterise in terms of frequency (or even more probability) the critical scenarios deriving from an initiating event for complex systems. In fact, when multiple systems and factors contribute to the overall risk it is much easier to decompose the critical scenarios in the chain of sub-events that lead to its occurrence, because the sub-events can be linked to the success and failure of sub-systems (smaller scale compared to the "tunnel system") which are more easily treated in statistical terms. The sub-events are certainly not arbitrary: they are chronological events and most of the time can be directly linked to the reliability of the safety systems available in the area.

As the thesis is limited to fire risk, the output of the frequency analysis will be the characterisation of the end-branch scenarios deriving from different initiating events in terms of yearly number of fires.

8.2.1 Initiating events

The initiating events (IE) are the starting point of the event tree analysis. The main characteristics of the initiating events are their mutual independency and incompatibility; in addition, they have to be chosen in order to define a finite, representative set of the much larger collection of events that can take place in the area. Normally, in fire risk analysis for tunnels the initiating event can be the frequency of fires or accidents per year and the characterisation of the initiating event can be performed by relying on statistics and literature or developing fault tree analysis.

However, as the thesis is more focused on the use of advanced fire and evacuation models for the consequence analysis, the range of values recommended by CETU is used for expressing the initiating event in terms of fires/year km 106 vehicles, where the maximum is assigned to bidirectional tunnels (Table 8.5). Three fire initiating events are

selected, which correspond to different levels of severity inside the tunnels: 8 MW corresponds to the ignition of a light vehicle, whereas 20 MW and 120 MW are both related to heavy vehicles (in fact, they are given the same frequency).

Another choice for the initiating event would have been to start from the number of accidents instead of fires. However, if the initiating event is the number of accident per year in the given tunnel and one aims to perform fire a risk assessment, the percentage of accidents that turn into a fire should be known but sadly data is very disperse and contradictory (Domenichini, 2016). It seems on the safe side to rely of CETU recommendations.

Table 8.5. Frequency of the initiating events

Initiating event (IE)			Frequency (fires/year km 10^6 vehicles)	
			Unidirectional tunnel	Bidirectional tunnel
F1	Light vehicle fire	8 MW	2	2
F2	Heavy vehicle fire	20 MW	2.5	4.5
F3	Heavy vehicle fire	120 MW	2.5	4.5

8.2.2 Event tree analysis

The event tree analysis (ETA) is performed by starting from all initiating events (F1, F2 and F3) and considering a sequence of three sub-events, which are suitable to describe chronologically the dynamics of fire and smoke propagation inside tunnel domains.

Research works listed below have been a valid source of information to choose the structure of the ETA and make hypothesis on the probability of the branches (Soons et al, 2006; Focaracci, 2010; Meng et al, 2010; Petelin et al, 2010; Qu et al, 2015).

In the Figure 8.5 the ETA is graphically represented. After the ignition of a vehicle (IE), the first sub-event "Fire development" represents the fact that the fire can develop into a large fire (Success) or be extinguished (Failure) naturally or artificially.

In case the fire is extinguished, the following sub-events are meaningless, whereas in the opposite case the fire can be detected or not (1st sub-event "Detection"). This has a direct influence on the queue of vehicles upwind the fire, because if the fire is detected (or the alarm is spread by some of the occupants) the traffic is supposed to be stopped at the entrance of the portal, therefore the queue of vehicles will be short and concentrated near the fire. Otherwise, if the detection system fails, or if the behaviour of drivers is not as rational as it is supposed to be, the queue will be extended along the entire length upwind the fire source.

The following and last sub-event is related to the activation of the ventilation system ("Ventilation" sub-event) and similarly to the previous branch the failure of the system can describe the missing activation of the ventilation or the local failure of the cluster of jet fans near the fire source.

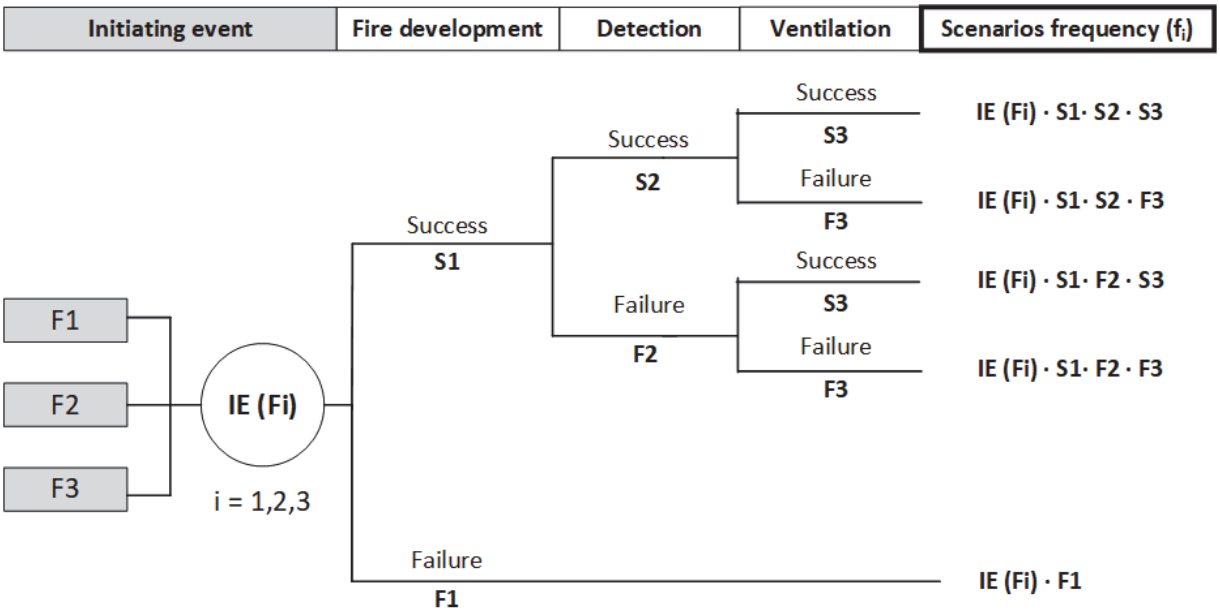

Figure 8.5. Event tree analysis for tunnels

In Table 8.6 the adopted probability of success and failure of each sub-events are considered. These values are normally obtained from considerations of the number of

failures per working hours or failures per year and can be selected according to statistical estimations, models of reliability of the systems, fault tree analysis or expert judgment.

Table 8.6. Success and failure probability for the system

Sub-events	Probability of success	Probability of failure
Fire development	0.6	0.4
Detection system	0.9	0.1
Ventilation system	0.9	0.1

Literature shows a large variability in the definition of the sub-events of the ETA. For example, ANAS recommends an additional last sub-event related to the lighting system, whose success and failure is linked to a different, but constant, walking speed of the occupants (respectively 1 and 0.5 m/s).

However, the walking speed is likely to decrease in case of low visibility conditions, but above all depends on the physical capabilities of the occupants from the initial conditions and can be widely different according to age and gender (see Chapter 7). Coherently, in the evacuation scenarios the walking speed is always assigned as a distribution of value between 0.5 and 1 m/s, thus indirectly taking into account both the variability of the population and the different visibility conditions inside the tunnel, without an additional explicit sub-event in the ETA.

Each branch can be obtained only through a different chain of sub-events starting from the IE: in other terms, the occurrence of each scenario is conditioned by the combination of the failure or the success of the systems present in the tunnel when the fire starts.

8.3 Consequence analysis

The consequence analysis is a parallel step to the frequency analysis and its objective is the numerical estimation of the "damage" n_i (in this case, the fatalities) related to each scenario, characterised in terms of end-branch frequency f_i.

This is done by running fire and evacuation simulations as if the problem was decoupling and the output are merged a posteriori in order to determine the fatalities. In the Figure 8.6 there is a sketch of the procedure that will be described from the practical point of view in the following section.

Three different fire locations and consequent evacuation scenarios are considered: there is no difference in the frequency of these events and this implicitly means that the fire events have the same probability for the three locations. This is in contradiction with the data reporting higher accidental rates near the portals, but the difference in the frequency can be taken into account only if the initiating event is the number of accidents per year, while in this approach the rate of fires is chosen as IE. As there is no unique set of data linking the number of fires and the location of the fire along the tunnel, the events are considered with the same level of probability.

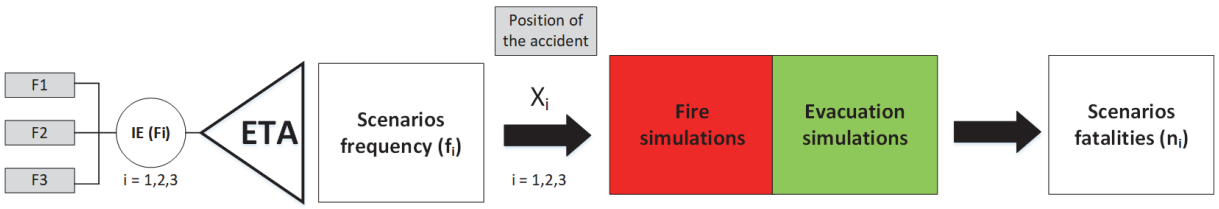

Figure 8.6. Scheme of the consequence analysis

8.3.1 Estimation of the fatalities

Using the results obtained from CFD and evacuation simulations the expected number of fatalities can be numerically estimated. This is done by monitoring the quantities of temperature, radiative heat flux gas, visibility and FED inside the tunnel area where actually the first phase of the evacuation process will take place (before people reach a safe place, outside or inside a means of egress). The superposition of the occupant's movement towards the exits and the smoke propagation inside the tunnel allows to calculate the number of people at a certain distance from the fire where the tenable conditions are not sustainable any longer.

In Figures 8.7-8.10 the schemes adopted for the calculation of the fatalities are drawn for unidirectional and bidirectional tunnels, in case of evacuation through the portals or the emergency exits (the reported number of fatalities is only illustrative). The evacuation dynamics is expressed in a time-space diagram, when the time is the y axis whereas the abscissa x represents the longitudinal position along the tunnel. A family of broken lines represents the movement of the occupants inside the tunnel: each line corresponds to a single occupant and two phases of the evacuation can be immediately recognised. In fact, the first phase is represented by a vertical segment, meaning that time is passing but the occupant is still in the original position (previously determined by the queue model): this is the pre-evacuation phase. The second phase is an inclined segment towards the nearest exit, where the inclination of the segment depends on the walking speed of the occupant (variable within the range of the distribution adopted in the evacuation model): this is the evacuation phase. The procedure is the same for unidirectional and bidirectional tunnels with the only difference in the queue model, which is double in the latter case and for this reason the number of fatalities is obtained by summing the fatalities calculated both upwind and downwind the fire.

This representation is considered very helpful for the purpose of the work, considering that the tunnel has a longitudinal prevalent direction where most of the evacuation and the fire dynamics develop and, therefore, the large amount of data coming from CFD and evacuation simulations can be merged in a single graphical representation.

The procedure is also suitable for an estimation of the expected number of injuries along the tunnel in case of a fire: this could be performed by setting different thresholds of the quantities governing the tenability criteria, lower than those associated to the death of the "average" occupant. However, in the thesis only fatalities will be calculated like in most of the risk assessment methodologies the damage in the FN diagram is expressed in terms of fatalities.

It is worth to notice that among the four quantities monitored along the tunnel, the visibility is always the most restrictive condition for the ASET, in line with the results of other research (Schröder, 2016). In other words, the ASET associated to the visibility thresholds (10 metres) is much lower than the ASET associated to temperature, radiative heat flux gas and FED thresholds. This is a recurrent aspect when FSE is applied not only in tunnels but also in building compartments and the scientific community is starting to wonder about the need of further research for the development of more recent database to improve the relationship between smoke obscuration and visibility. However, today there is no better approximation for modelling how people orientate inside an area during fire events and it is in line with the common sense that when people do not orientate themselves are likely to stop or behave irrationally. In addition, according to the regulations of fire prevention (including the recent DM 2015) the visibility verification is mandatory when FSE approach is performed. Therefore, the ASET related to the visibility is used to calculate the number of fatalities.

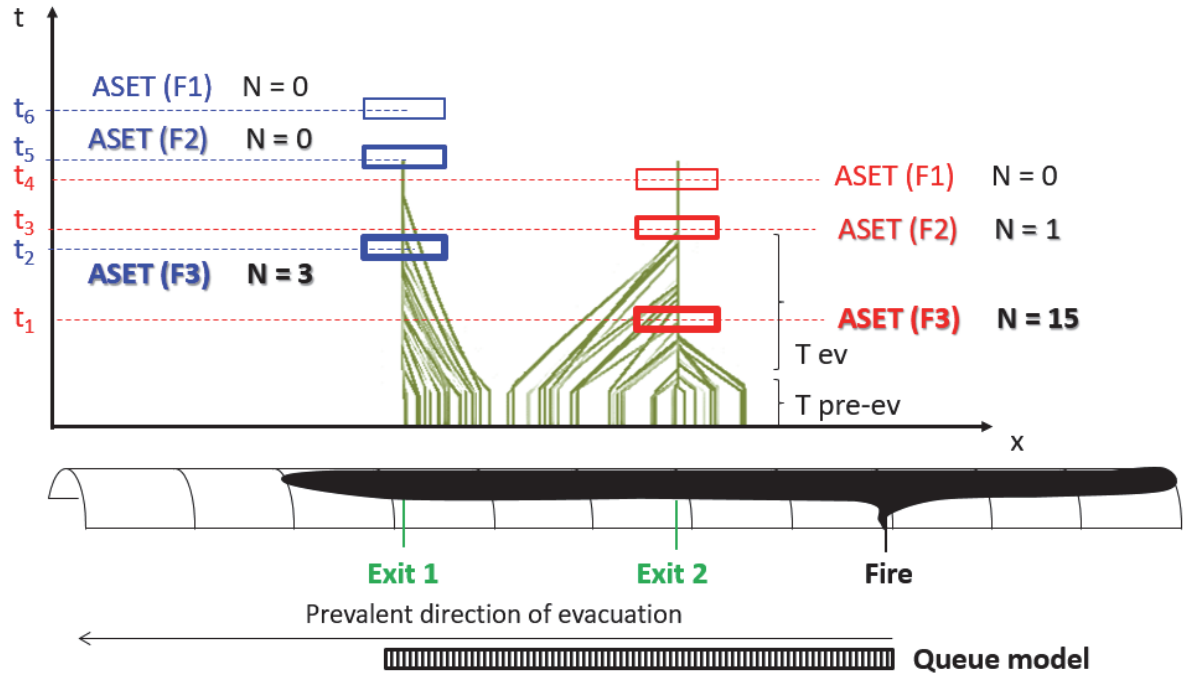

Figure 8.7. Scheme of the estimation of the fatalities for unidirectional tunnels (2 emergency exits)

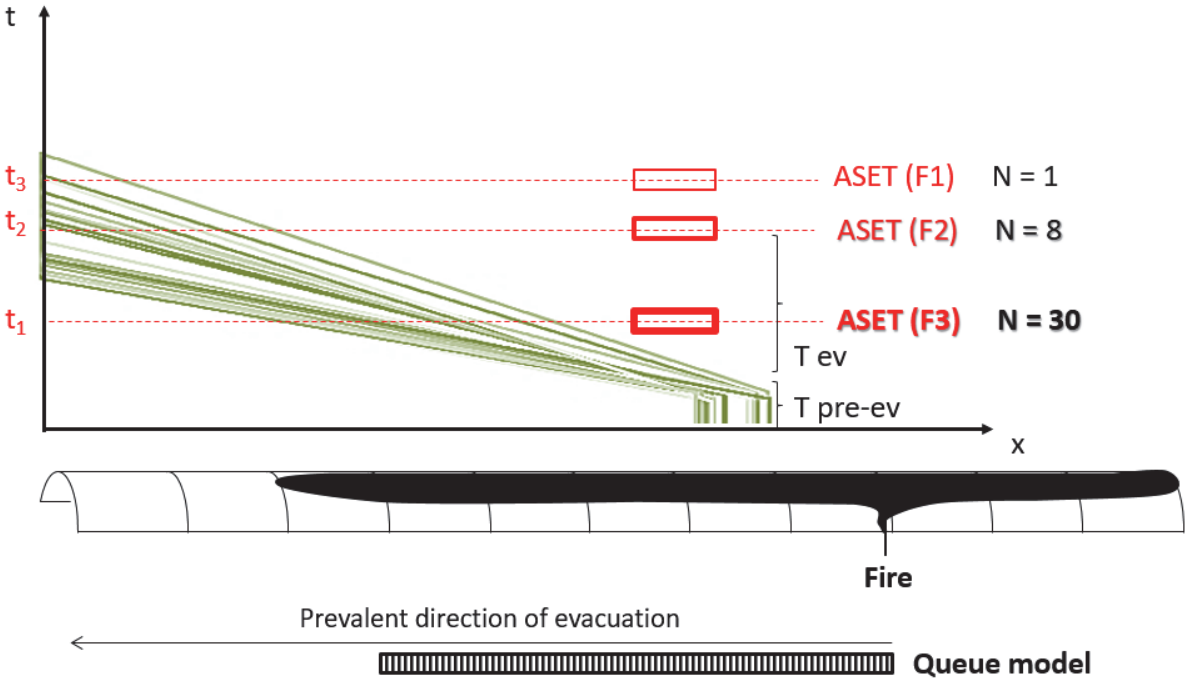

Figure 8.8. Scheme of the estimation of the fatalities for unidirectional tunnels (no emergency exits)

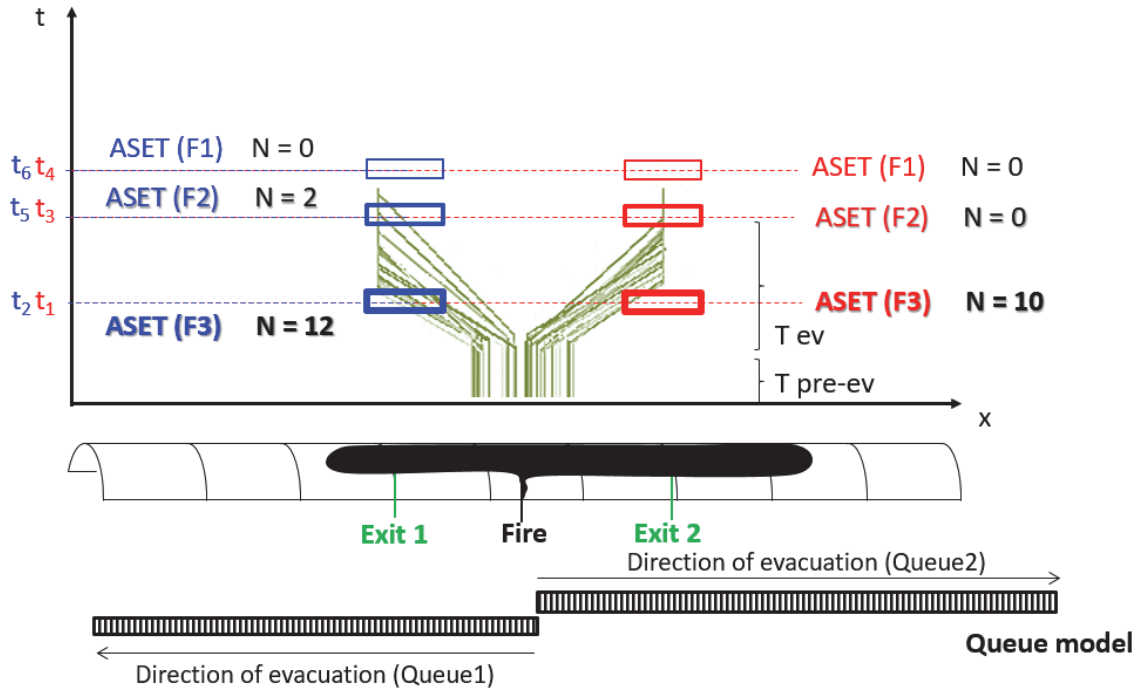

Figure 8.9. Scheme of the estimation of the fatalities for bidirectional tunnels (2 emergency exits)

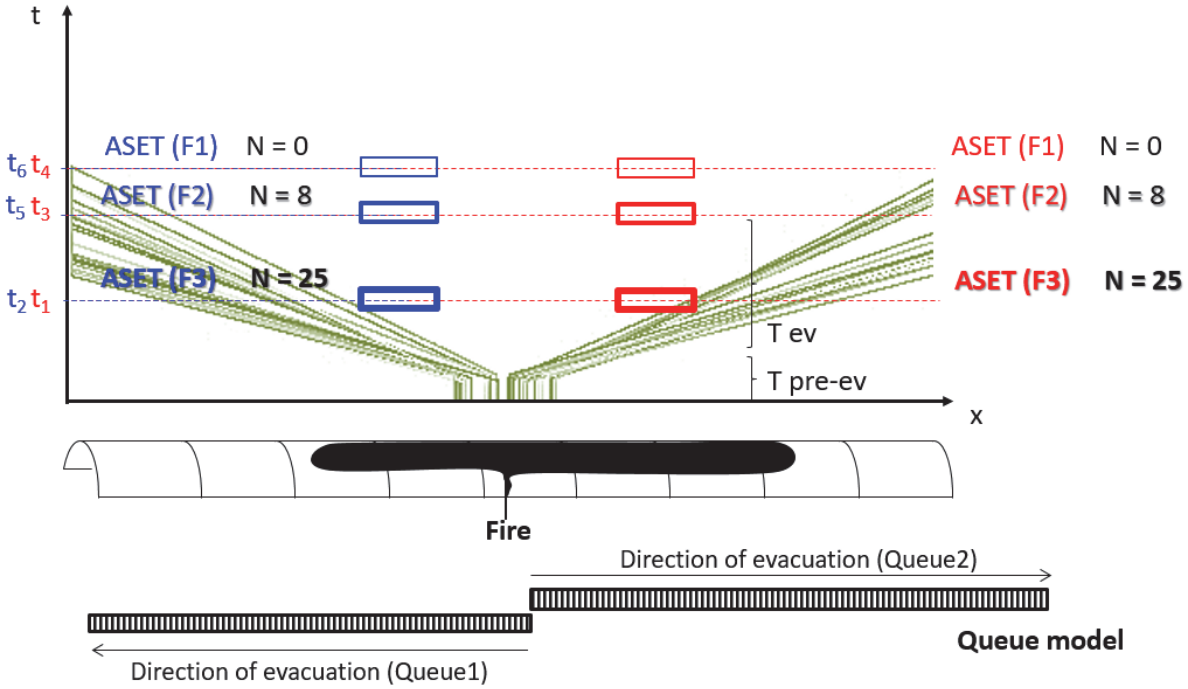

Figure 8.10. Scheme of the estimation of the fatalities for bidirectional tunnels (no emergency exits)

8.3.2 Calculation of the FN curve

Once all scenarios have been described in terms of frequency f_i and fatalities n_i, one can calculate the back-cumulated frequency Fi and draw the resulting FN trend in the bilogarithmic diagram as explained in the Table 8.7.

The curve, which is a risk indicator, is then reported in the FN diagram where the acceptability thresholds are represented by inclined lines. In the Figure 8.11, for example, the curve lies in the ALARP zone, therefore alternative configurations with additional measures need to be investigated.

Table 8.7. Example for the calculation of the FN curve

f_i	n_i		Fi	Ni
f_1	0		$f_2 + f_3 + f_4 + f_5$	1
f_2	2		$f_2 + f_4 + f_5$	2
f_3	1		f_5	5
f_4	2			
f_5	5			

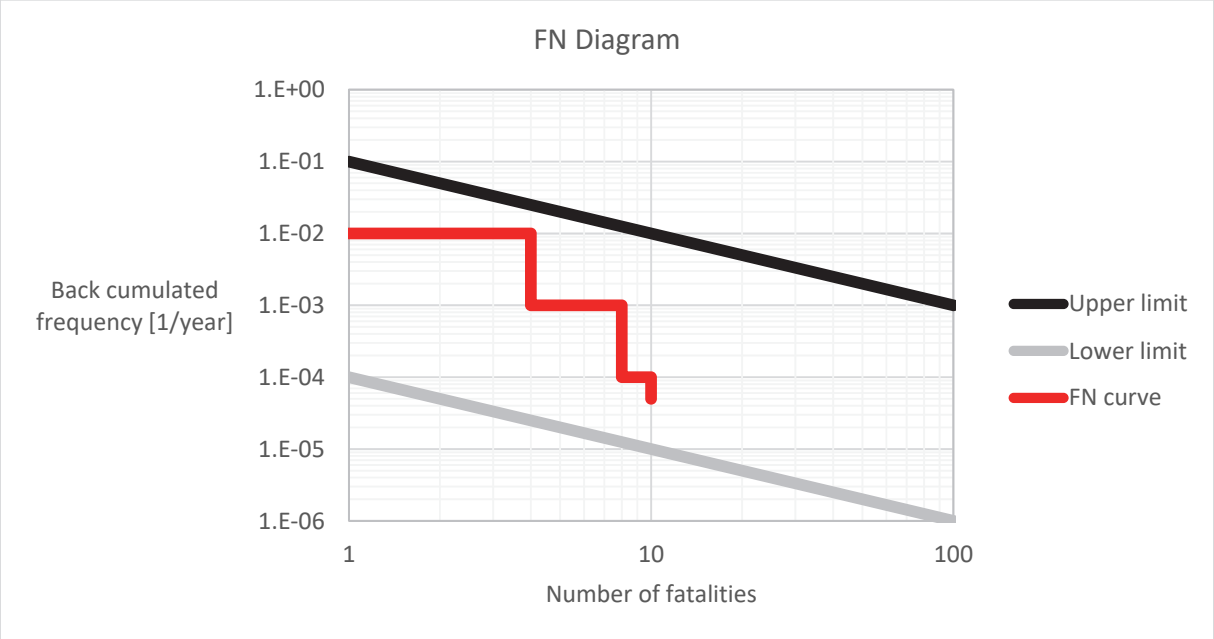

Figure 8.11. Example of FN curve

Another fundamental risk indicator is the Expected Value of fatalities, graphically represented by the area below the FN curve. This is particularly interesting when alternative solutions for the tunnel systems need to be evaluated in comparison with a reference tunnel which comply with the minimum requirements of the regulations. The EV of the reference tunnel is the target value when risk mitigation is needed: the risk is to be reduced until the EV of the new configurations meets the EV of the reference tunnel.

8.4 Advantages and disadvantages of the QRA

Some of the advantages of performing QRA through advanced models are listed below:

- The estimation of the fatalities is done according to the state of the art in the fire safety field and for all scenarios the analyst has an overall view of how the tenability conditions determined by temperature, radiative heat flux gas, visibility and FED evolve in the tunnel. Otherwise, QRA models would not allow to check precisely which conditions meets the tenability thresholds, for example if people are supposed to be incapacitated due to intoxication or to lack of visibility and orientation.
- At any given time the analyst can use CFD simulations of selected fire scenarios to support the design of additional measures (like jet fans) and verify the improvement of the tenability conditions. The design of the ventilation systems (longitudinal and transverse) through CFD simulations is increasingly used when complex HVAC systems need to be inserted.
- The use of the evacuation models can be helpful if different traffic conditions and occupant loads are to be analysed.

The disadvantages of the QRA can be synthesised in the following points:

- The process of exhaustively reducing a complex system like a road tunnel into a finite number of components and sub-systems is a difficult matter. In all likelihood, the analyst can miss one or more elements, but at the same time it is not certain that the procedure of QRA will be compromised (the measurement of the relative weight of a single sub-system is controversial).
- The identification of the initiating events is fundamental for assessing the residual risk of the tunnel.
- Considering the frequency analysis, it must be admitted that there is a general lack of reliable data regarding, mainly, the success and failure of the sub-systems.
- When using advanced fire and evacuation models for the consequence analysis, the computational burden is high and not necessarily sustainable with the available CPU. Approximations are essential in the process but might affect in some ways the results.

Chapter 9

Case study 1: unidirectional tunnel

9.1 Description of the tunnel

The first case study is represented by a motorway road tunnel whose length is 2700 metres, based on a real existing tunnel in the North of Italy and part of the TEN roadway. The tunnel has two separated unidirectional tubes, whose cross section is typical of the Italian motorways, with two lanes and a right verge. The track is not rectilinear, but present a curvature percentage of 5 %, and meteorological conditions at the entrance and exit portals can be different, causing a not negligible flow of air.

The tunnel is equipped with a mechanical ventilation system (longitudinal jet-fan based) parallel to the direction of the traffic flow and accounts for an overall number of 9 jet fans in the North tube and 6 jet fans in the South tube. The tunnel has a longitudinal slope (2.5 % as average) which automatically determines more dangerous conditions in case of fire of the South tube, where the chimney effect induced by the slope is opposed to the longitudinal ventilation flow.

The tunnel is located in a unstable bedrock, subjected to significant deformations, in which every structural intervention is extremely expensive in terms of direct and indirect costs. However, the tunnel would have the necessity to adapt the means of egress system to the EU Directive, which decrees a maximum safety distance among the exits of 500 m. Provided that the cost of this type of refurbishment is not sustainable, the Italian

jurisdictional authority accepted the design of alternative measures to mitigate the residual risk.

Along its overall length of 2700 m, apart from the entrance and exit portals, each tube has only three escape routes, represented by bypasses connecting the two tubes. In addition, the distance between the emergency exits is not homogeneous: considering the South tube and a curvilinear abscissa "s" starting from the entrance portal, the three emergency exits are located respectively at 1142 m, 1797 m and 2329 m (Figure 9.1). The average distance is 700 m, but the maximum is 1142 m.

Therefore, although the traffic load is relatively low for both tubes (15% lower than 2000 vehicles per day per lane), a long evacuation time may be expected in case of an accident. Furthermore, considering the traffic composition, there is no restriction for vehicles and the presence of HGVs is significant (30 % of the overall traffic volume according to data collection).

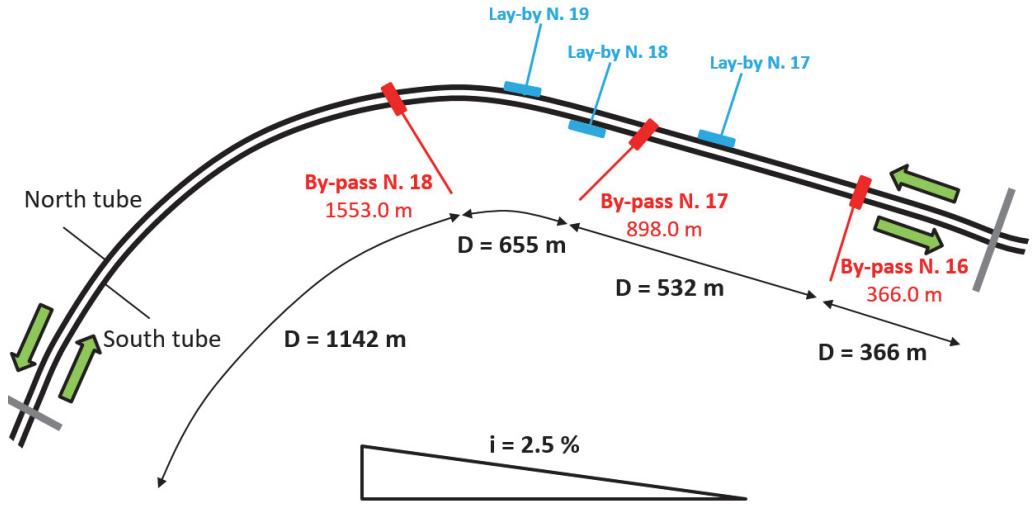

Figure 9.1. Sketch of the tunnel

According to statistical survey of the owner company of the motorway, there have been few accidents along that road network (reference period 2007-2014) with no fires in the selected tunnel. If only severe accidents are considered (with injuries and fatalities) a value of 1.97 accidents per 100 million vehicles km is obtained for the overall highway (8.20 per 100 million vehicles km is the reference value for the Italian national road network) and the half of them occurred in tunnels.

The quantitative risk analysis will be limited to the South tube, for the motivations previously explained. The configurations that will be examined are initial (as built), reference, first alternative, second alternative.

9.2 QRA for the initial configuration

The procedure of QRA is applied to the initial configuration. As previously explained, the fire and evacuation analysis are conducted independently and finally merged in order to draw the FN curve.

9.2.1 Fire scenarios

The results obtained by modellingg the initial configuration of the tunnel are reported in the Table 9.1. The CFD model is limited to 400 m of the length of the tunnel (validation is contained in Chapter 8), the grid size is cubic (50 cm edge) and was thoroughly described in Chapter 8. As explained in Chapter 8, F1, F2 and F3 scenarios are studied.

As one could expect, the ventilation system is not sufficient to prevent backlayering formation even for the case of relatively low HRR (F1 and F2), with limiting conditions reached by the visibility criterion before 600 seconds. The limiting conditions are reached near the fire source for the F1 scenario and are extended further in the other cases.

In the Tables 9.2 and 9.3 the smoke distribution along the tunnel and the visibility slice for the F1, F2 and F3 with activated ventilation system are reported.

Table 9.1. Results from fire modellingg for the initial configuration

Fire scenario		Ventilation system	Backlayering (t < 900 sec)	ASET t (sec) – x (m)		Criteria
F1	X1	Success	No	-	-	Visibility
F1	X1	Failure	Yes	534	60	Visibility
F2	X1	Success	No	986	60	Visibility
F2	X1	Failure	Yes	370	80	Visibility
F3	X1	Success	Yes	815	40	Visibility
F3	X1	Failure	Yes	347	40	Visibility
F1	X2	Success	No	-	-	Visibility
F1	X2	Failure	Yes	534	1210	Visibility
F2	X2	Success	No	986	1210	Visibility
F2	X2	Failure	Yes	370	1230	Visibility
F3	X2	Success	Yes	815	1190	Visibility
F3	X2	Failure	Yes	347	1190	Visibility
F1	X3	Success	No	-	-	Visibility
F1	X3	Failure	Yes	534	2360	Visibility
F2	X3	Success	No	986	2360	Visibility
F2	X3	Failure	Yes	370	2380	Visibility
F3	X3	Success	Yes	815	2340	Visibility
F3	X3	Failure	Yes	347	2340	Visibility

Table 9.2. Smoke distribution upwind and downwind the fire source for all scenarios (t=420 sec)

F1	
F2	
F3	

Table 9.3. Visibility slice at z = 2 m for all scenarios (t=420 sec) (red color is 30 m and blue is zero)

F1	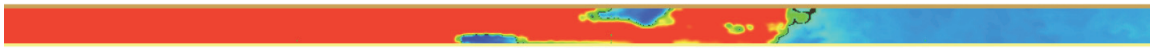
F2	
F3	

The Figures 9.2-9.5 report trends of temperature, radiative heat flux gas, visibility and FED for the three fire scenarios in the case of successful ventilation system at the human height assumed as z = 2 m to be conservative. Only visibility criterion is met.

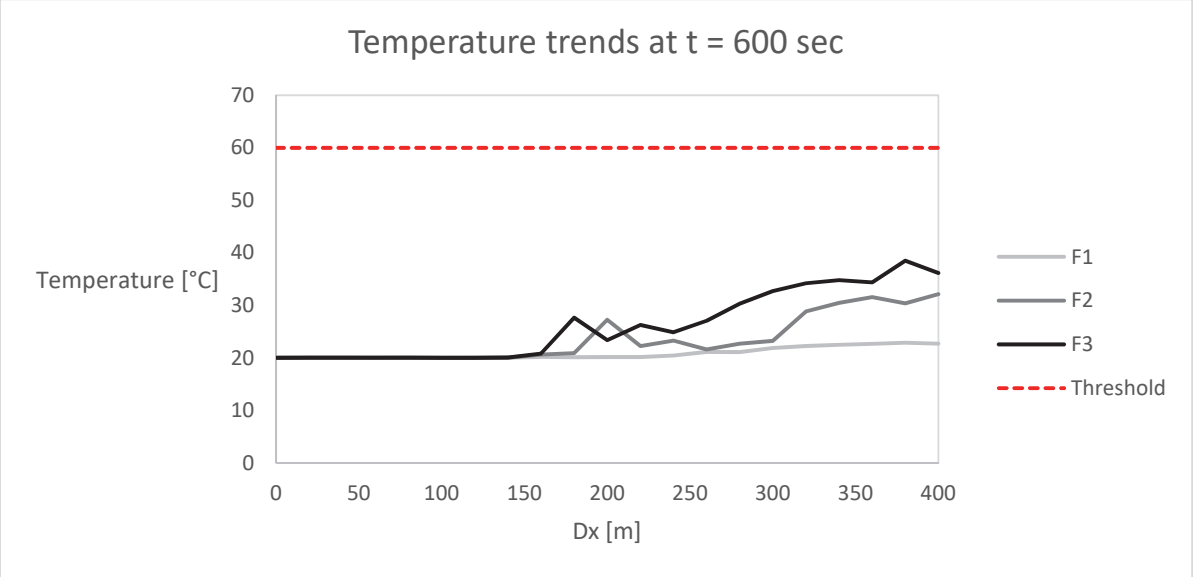

Figure 9.2. Temperature trends at z = 2 m for F1, F2 and F3 fire scenarios (successful ventilation)

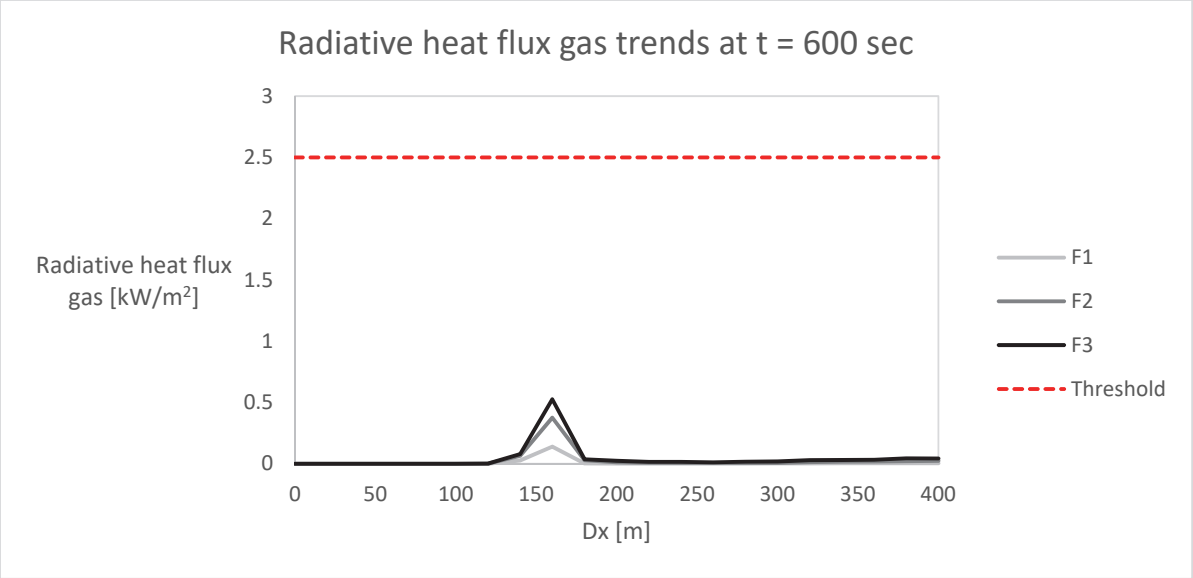

Figure 9.3. Radiative heat flux gas trends at z = 2 m for F1, F2 and F3 fire scenarios (successful ventilation)

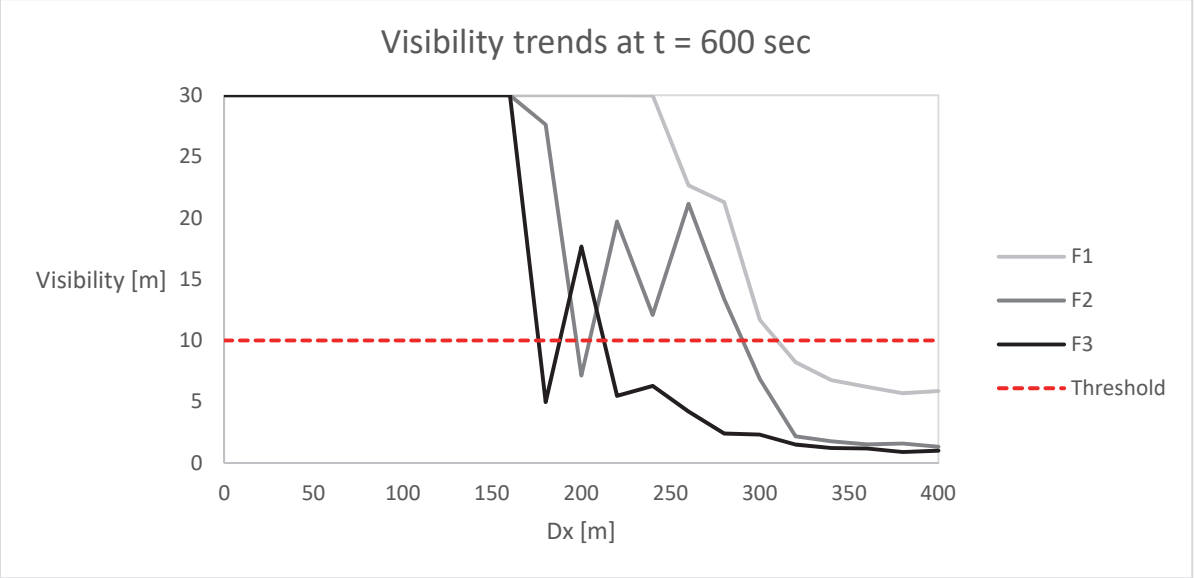

Figure 9.4. Visibility trends at z = 2 m for F1, F2 and F3 fire scenarios (successful ventilation)

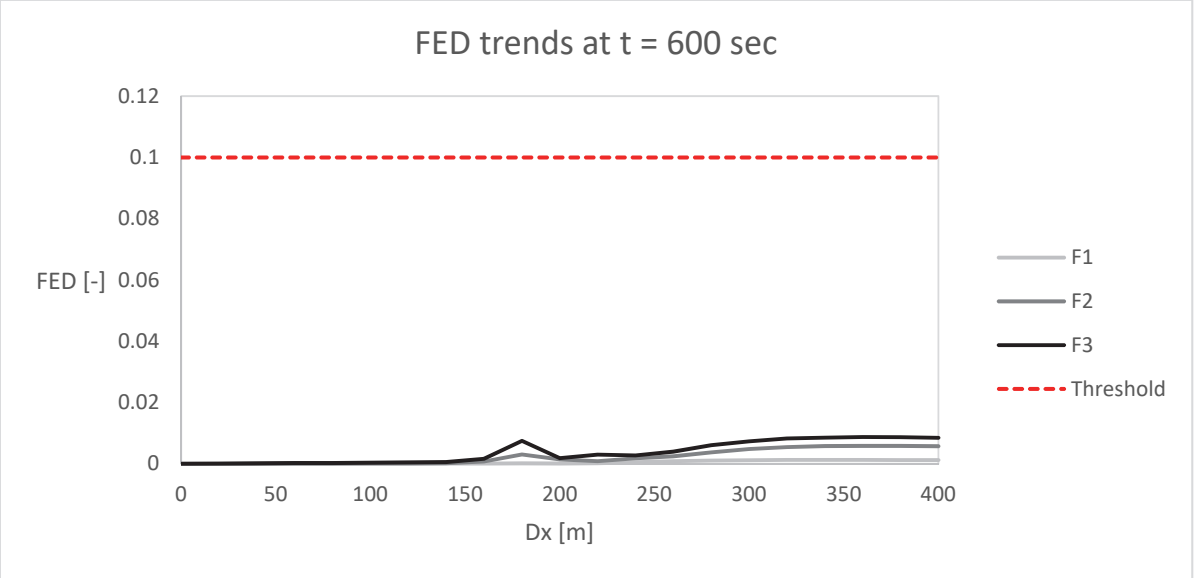

Figure 9.5. FED trends at z = 2 m for F1, F2 and F3 fire scenarios (successful ventilation)

9.2.2 Evacuation scenarios

Results from the evacuation analysis with Pathfinder are reported in the Table 9.4. As stated in the Chapter 8, the detection system has a direct influence on the formation of the queue upwind the fire (the tunnel is longer than 1000 m and equipped with traffic light able to stop the approaching vehicles in the hypothesis of "rational" behaviour of the occupants).

In case of success of the detection system, the queue (Q1) is assumed to be concentrated near the fire source while if the system fails or the drivers ignore the traffic light the queue (Q2) is extended along the entire length upwind the fire.

The big difference between the RSET related to Q2 and Q1 is due not only to the higher number of occupants inside the tunnel, but also by their distribution along the tunnel, whose emergency exits are significantly far from each other. Indeed, although all evacuation scenarios with Q1 (Success of detection system) are composed by few vehicles and people (only 8 occupants) their RSET is very different because the means of egress are not distributed homogeneously along the tunnel (the occupants of scenario X1-Q1 have to cover much shorter distance compared to those of scenario X2-Q1 and X3-Q1).

Table 9.4. Results from evacuation modellingg

Fire accident position		Detection system	Queue length (m)		Occupant load	RSET (sec)
X1	200 m	Success	Q1	27.9	8	383.5
X1	200 m	Failure	Q2	200	47	526.8
X2	1350 m	Success	Q1	27.9	8	855.8
X2	1350 m	Failure	Q2	1350	318	1243.7
X3	2500 m	Success	Q1	27.9	8	714.8
X3	2500 m	Failure	Q2	2500	588	1226.4

9.2.3 Risk estimation

Thanks to a graphical intersection between data coming from fire and evacuation simulations, it is possible to calculate the number of fatalities n_i associated to each scenario characterised by a frequency f_i.

As an example, in the Figures 9.6, 9.7 and 9.8 the family of broken lines representing the evacuees are reported in a time-space diagram (the abscissa is not the curvilinear abscissa of the tunnel but the real x obtained by Pathfinder, this is why the representation of the lines is sometimes stretched and narrowed).

Finally, the FN curve is calculated and drawn in the FN diagram (Figure 9.9). The curve is in the ALARP zone; therefore, a set of alternative measures should be prescribed to reduce the risk on a more sustainable level.

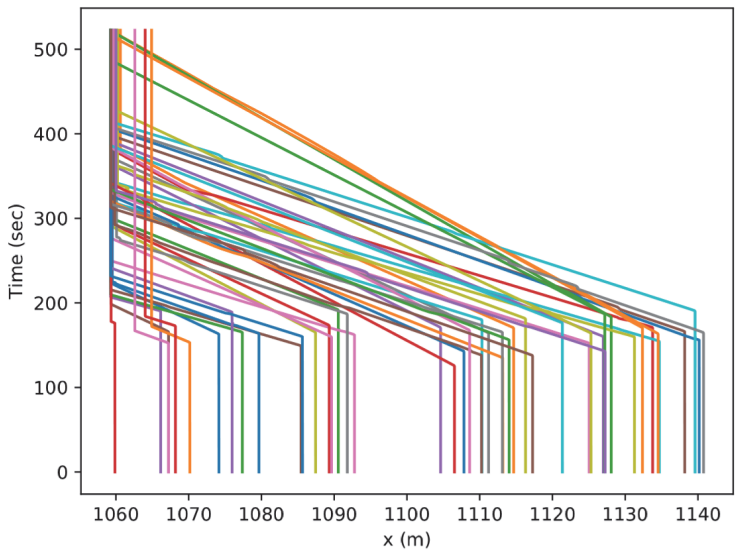

Figure 9.6. Time-space diagram for X1 Q2 evacuation scenarios

With the purpose of comparing different tools of QRA, the FN curve obtained with the QRAM software (OECD) is also drawn in the same diagram, highlighting that this last approach is not on the safe side when the attention of the risk analyst is restricted to fire hazard. Considering the QRAM curve, in fact, the number of fatalities is underestimated

because, on the one hand, the software is based on simplified equations for the fire propagation and the algorithms do not take into account the visibility conditions but only the toxicity level in the domain. On the other hand, frequencies are much lower because the software does not consider fires due to light vehicles.

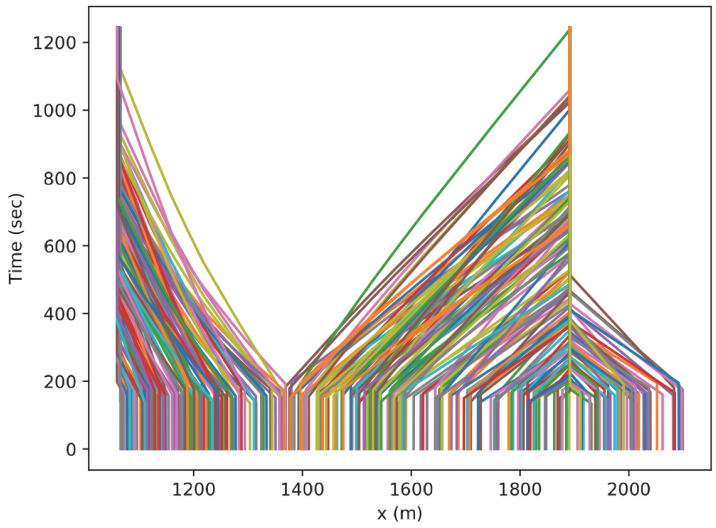

Figure 9.7. Time-space diagram for X2 Q2 evacuation scenarios

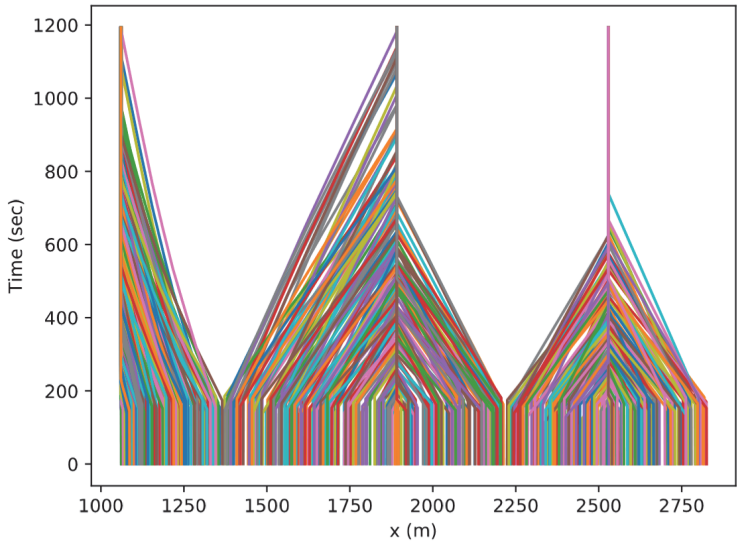

Figure 9.8. Time-space diagram for X3 Q2 evacuation scenarios

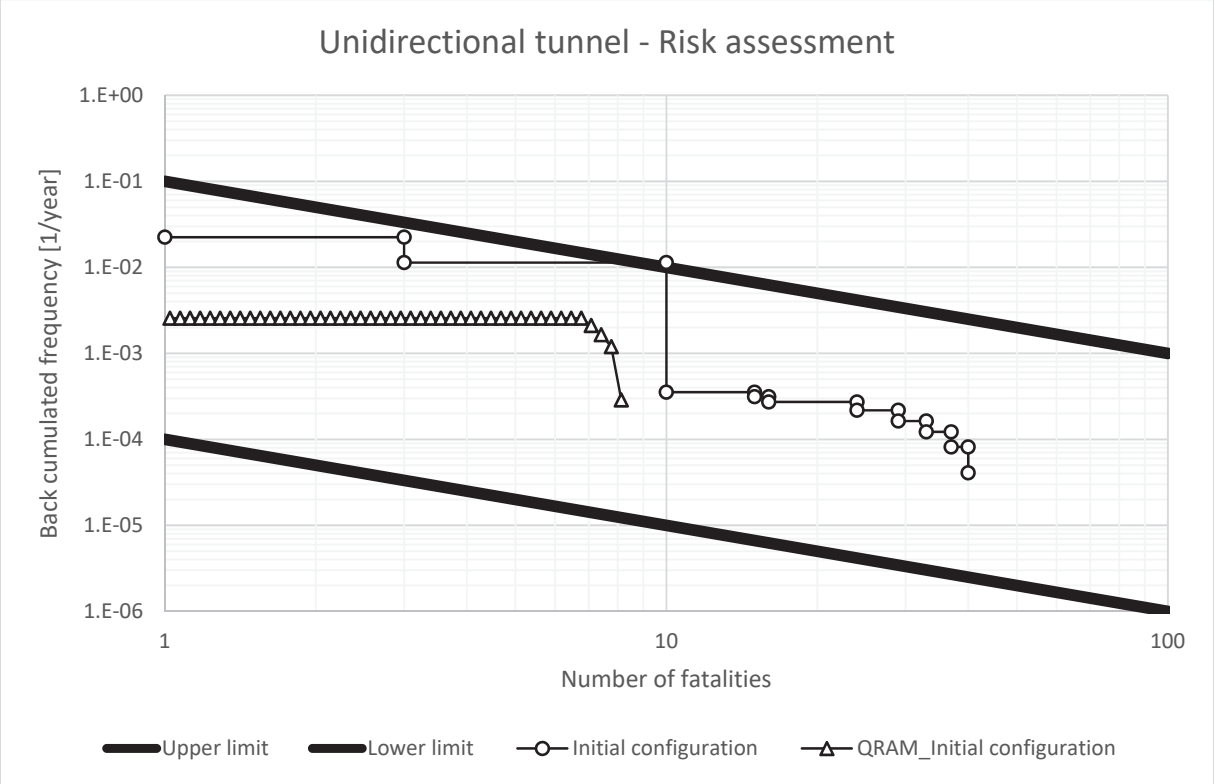

Figure 9.9. Risk related to the initial configuration

9.3 QRA for the first alternative configuration

The proposal of an alternative configuration for the given tunnel is implemented by doubling the number of jet fans along the tunnel. This is the easiest additional measure that can be proposed and is, in fact, the most common in the real projects. The procedure of QRA is now applied to the new configuration of tunnel.

9.3.1 Fire scenarios

The fire scenarios differ from those previously analysed because a new ventilation condition is established along the tunnel thanks to the introduction of new jet fans with the same characteristics of those already in the tunnel. The results are reported in the Table 9.5, while the slice are reported in the Tables 9.6 and 9.7, showing better results compared to the previous case in terms of backlayering.

Table 9.5. Results from fire modellingg for the first alternative configuration

Fire scenario		Ventilation system	Backlayering (t < 900 sec)	ASET t (sec) – x (m)		Criteria
F1	X1	Success	No	-	-	Visibility
F1	X1	Failure	Yes	534	60	Visibility
F2	X1	Success	No	-	-	Visibility
F2	X1	Failure	Yes	214	80	Visibility
F3	X1	Success	No	-	-	Visibility
F3	X1	Failure	Yes	124	40	Visibility
F1	X2	Success	No	-	-	Visibility
F1	X2	Failure	Yes	534	1210	Visibility
F2	X2	Success	No	-	-	Visibility
F2	X2	Failure	Yes	214	1230	Visibility
F3	X2	Success	No	-	-	Visibility
F3	X2	Failure	Yes	124	1190	Visibility
F1	X3	Success	No	-	-	Visibility
F1	X3	Failure	Yes	534	2360	Visibility
F2	X3	Success	No	-	-	Visibility
F2	X3	Failure	Yes	214	2340	Visibility
F3	X3	Success	No	-	-	Visibility
F3	X3	Failure	Yes	124	2380	Visibility

However, in the Table sometimes the ASET is reached before compared to the previous case and this is an effect due to destratification caused by more powerful ventilation flow. This happens strongly downwind the fire source, while upwind is more contained.

Table 9.6. Smoke distribution upwind and downwind the fire source for all scenarios (t=420 sec)

F1	
F2	
F3	

Table 9.7. Visibility slice at z = 2 m for all scenarios (t=420 sec) (red color is 30 m and blue is zero)

F1	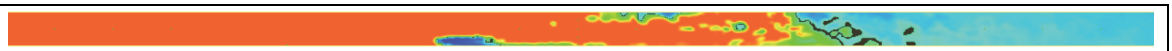
F2	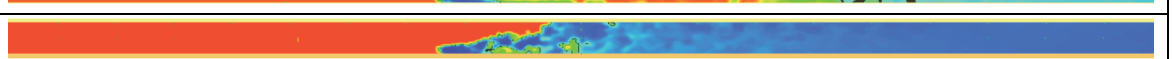
F3	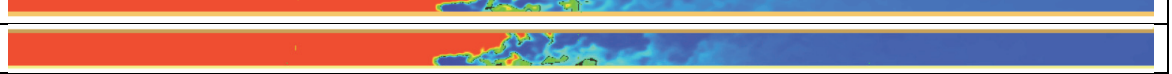

The Figures 9.10-9.13 report trends of temperature, radiative heat flux gas, visibility and FED for the three fire scenarios in case of successful ventilation system at the human height assumed as z = 2 m to be conservative. Only the visibility criterion is met.

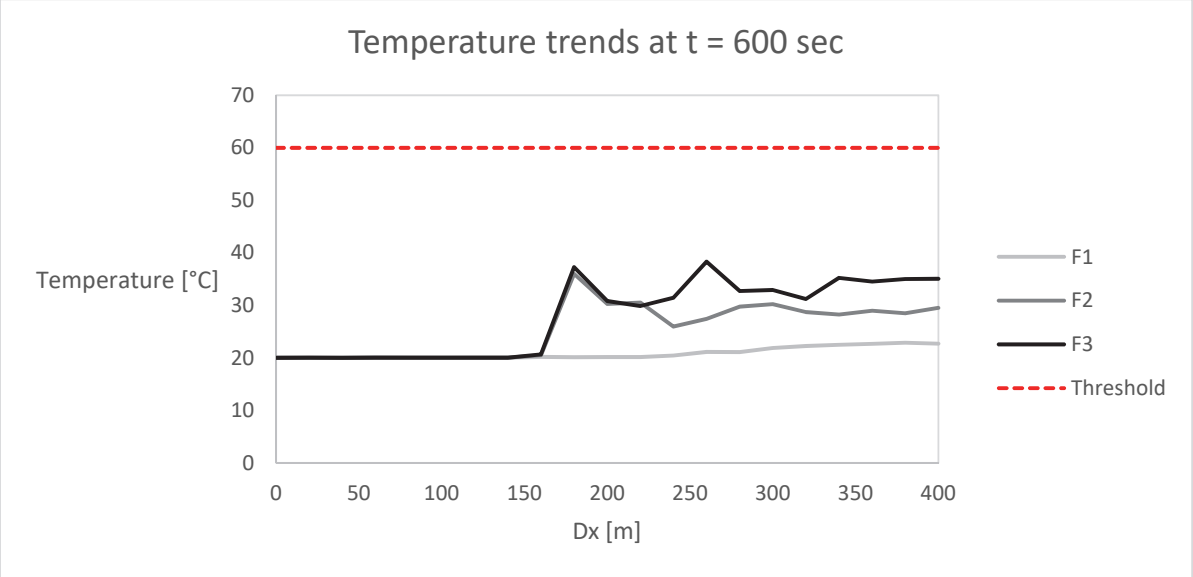

Figure 9.10. Temperature trends at z = 2 m for F1, F2 and F3 fire scenarios (successful ventilation)

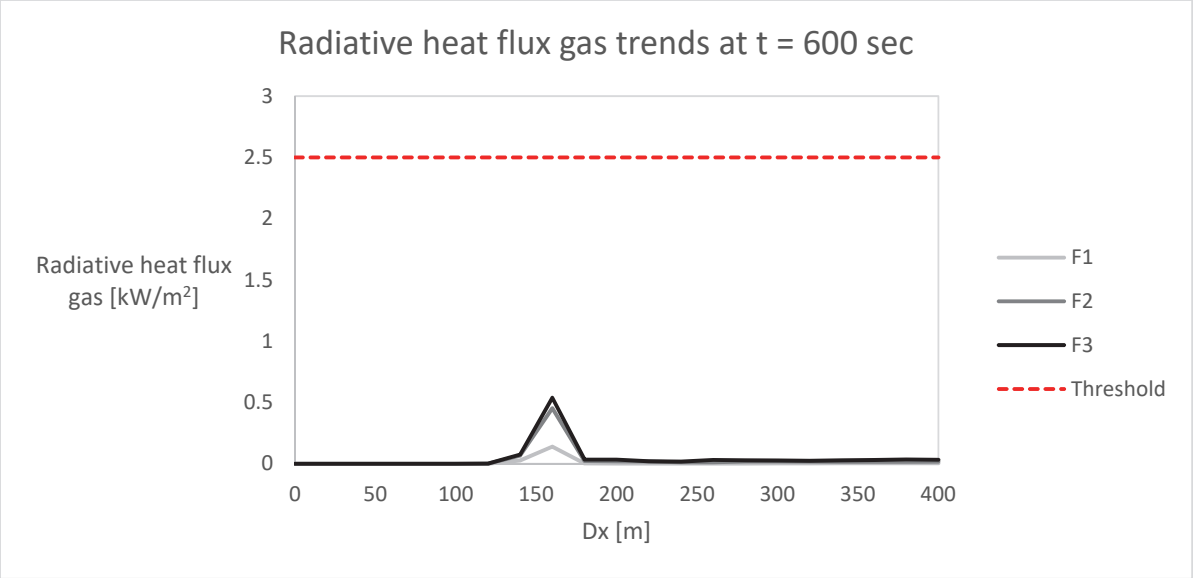

Figure 9.11. Radiative heat flux gas trends at z = 2 m for F1, F2 and F3 fire scenarios (successful ventilation)

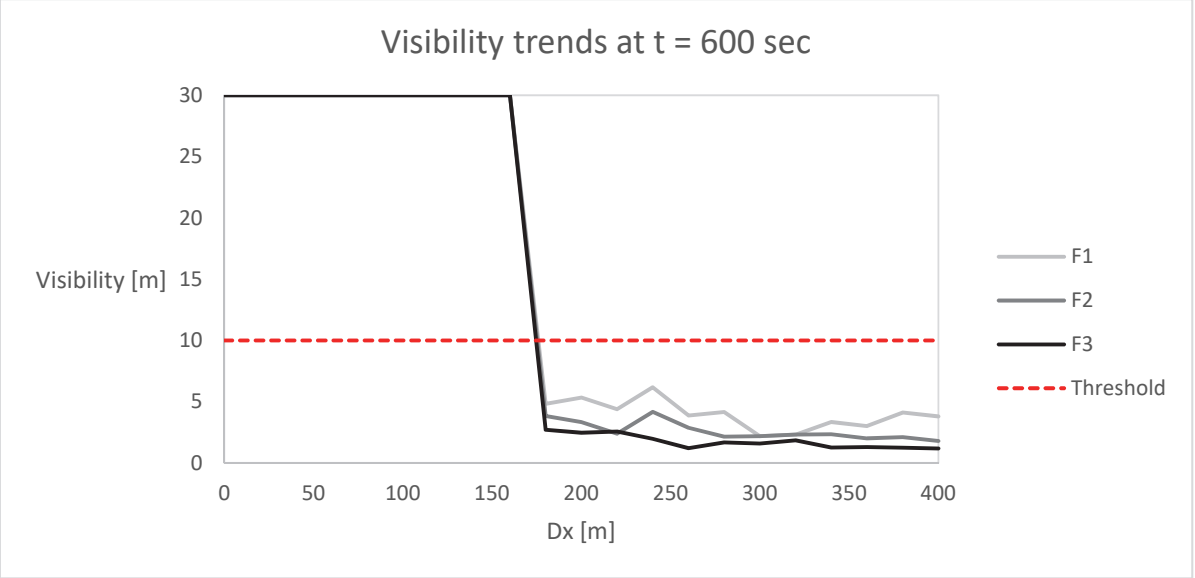

Figure 9.12. Visibility trends at z = 2 m for F1, F2 and F3 fire scenarios (successful ventilation)

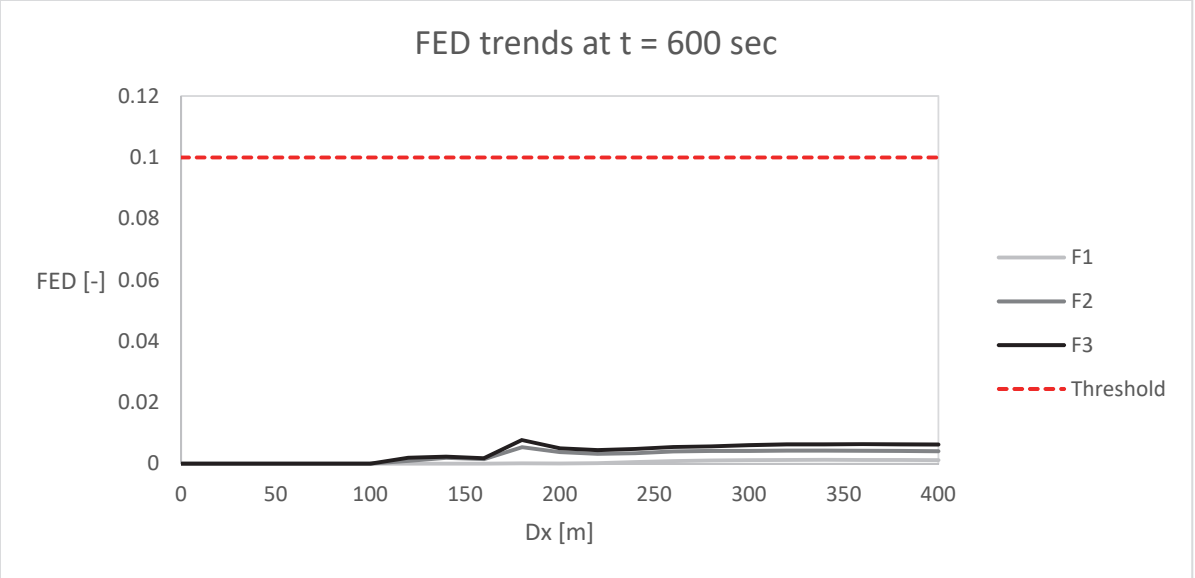

Figure 9.13. FED trends at z = 2 m for F1, F2 and F3 fire scenarios (successful ventilation)

9.3.2 Evacuation scenarios

As no additional emergency exits are added in the configuration, the evacuation scenarios do not differ from those of the previous configuration. Therefore, data are not reported again.

9.3.3 Risk estimation

Also in this case, the intersection between fire and evacuation models allows to calculate the number of fatalities for all scenarios and represent the risk in terms of FN curve (Figure 9.14).

The configuration is also analysed with the QRAM software, but the result is not satisfactory because it gives a curve identical to that of the initial configuration. The increasing number of jet fans is not accompanied by an improvement (or at least a modification) of the tenability conditions, which is something not realistic nor reliable because the initial ventilation was not very powerful considered the number of jet fans usually adopted in tunnels.

On the contrary, the FN curve calculated with advanced models results in a decrement in the Expected Value: however, this is not enough to be acceptable because, although there is a decrement compared to the initial configuration, the risk associated with the reference tunnel is not matched yet (Table 9.8).

For this reason, another configuration will be investigated.

Table 9.8. Expected Value for the first alternative configuration

Tunnel configuration	Expected Value (fatalities/year)
Initial	0.100
Reference	0.035
First alternative	0.043

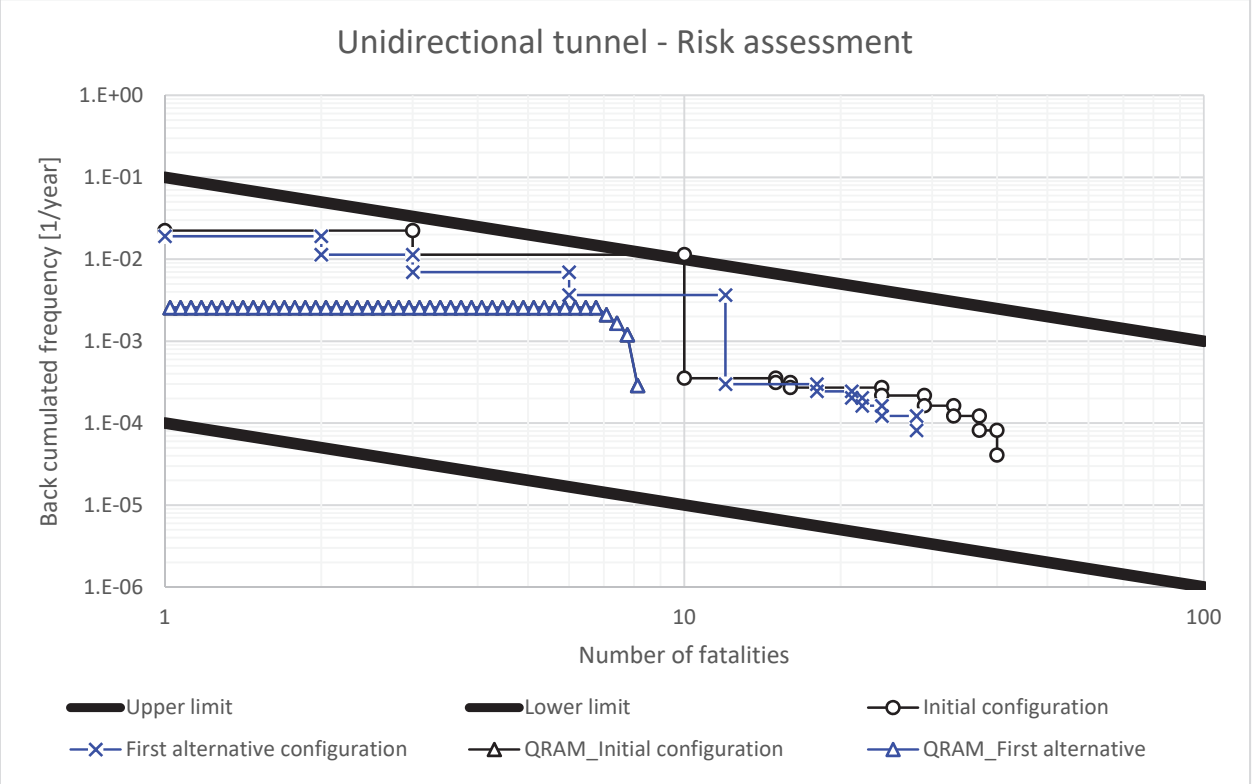

Figure 9.14. FN curve for the first alternative configuration

By looking at the Figure 9.14, it can be noticed that the decrement is not homogeneous along the entire curve. In fact, the improvement of the ventilation system provides very good results only for some scenarios (for instance, F1 and F2 scenarios) but it is not able to fully control the backlayering for F3 scenarios.

Moreover, the overlap of the blue and the black lines in the FN diagram is due to a locally different behaviour induced by the new ventilation system. As it is reported in the Figure 9.15, the new set of jet fans cause a more evident destratification near the fire source and can be able to decrease the visibility under the threshold before the previous case at some points. Nevertheless, they prevent the formation of the backlayering for other cases and therefore, globally, their effect is positive and advantageous.

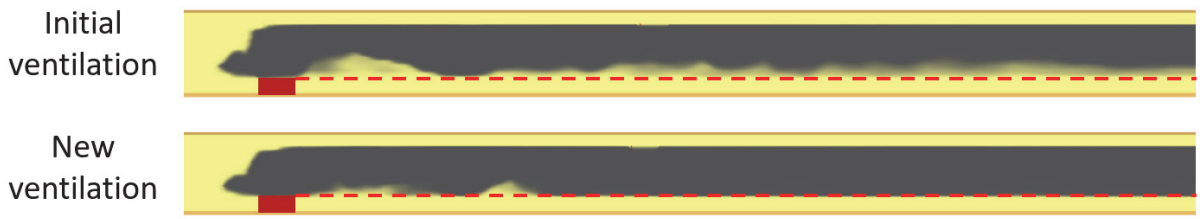

Figure 9.15. F2 scenario, smoke distribution for the initial and first alternative configuration at t = 600 sec

9.4 QRA for the second alternative configuration

A second alternative configuration is proposed in order to reduce the risk under the limit set by the reference configuration. In this case, the ventilation system is still empowered according to the first alternative configuration, but new management strategies are inserted. Specifically, it is assumed that the tunnel is monitored by a control center available 24/7 and, at the same time, CCTV circuit, loudspeakers and lighting panels are added into the tunnel.

These additional measures can be taken into account neither through fire nor evacuation models. Although this is not orthodox, it is preferred to modify the probability of success and failure of both detection and ventilation systems, which are now assigned as 0.95 and 0.05 respectively.

9.4.1 Fire scenarios

The Table is not reported because the fire simulation are the same of those contained in section 9.3.1.

9.4.2 Evacuation scenarios

In this case, the evacuation scenarios are those reported in 9.3.2.

9.4.3 Risk estimation

The FN curve is similar to the one of the previous case but shifted in the frequency axis (Figure 9.16). In this case, the QRAM curve is not drawn because it is not possible to add this type of management measures in the software.

This configuration shows a lower level of Expected Value compared to both the initial and reference configurations and, for this reason, is considered acceptable (Table 9.9).

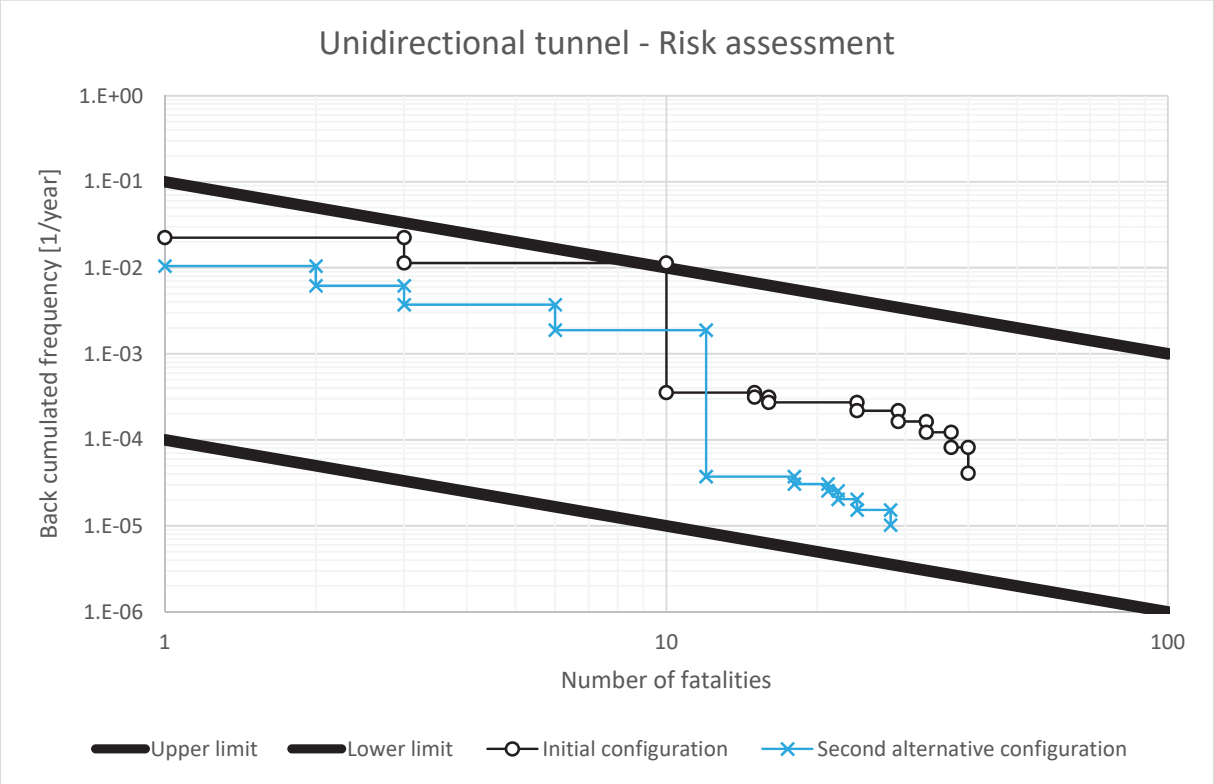

Figure 9.16. FN curve for the second alternative configuration

Table 9.9. Expected Value for the second alternative configuration

Tunnel configuration	Expected Value (fatalities/year)
Initial	0.100
Reference	0.035
Second alternative	0.023

9.5 Comparisons and comments

In the following Figures 9.17 and 9.18 the alternative configurations are compared in terms of FN curves and Expected Value EV.

Both alternative configurations provide a reduction of the risk from the initial level, measurable in terms of FN curve and EV. The reduction related to the second alternative configuration is below the threshold set by the reference configuration in terms of EV, while for the first alternative configuration the values are very similar and might be considered as acceptable in real cases.

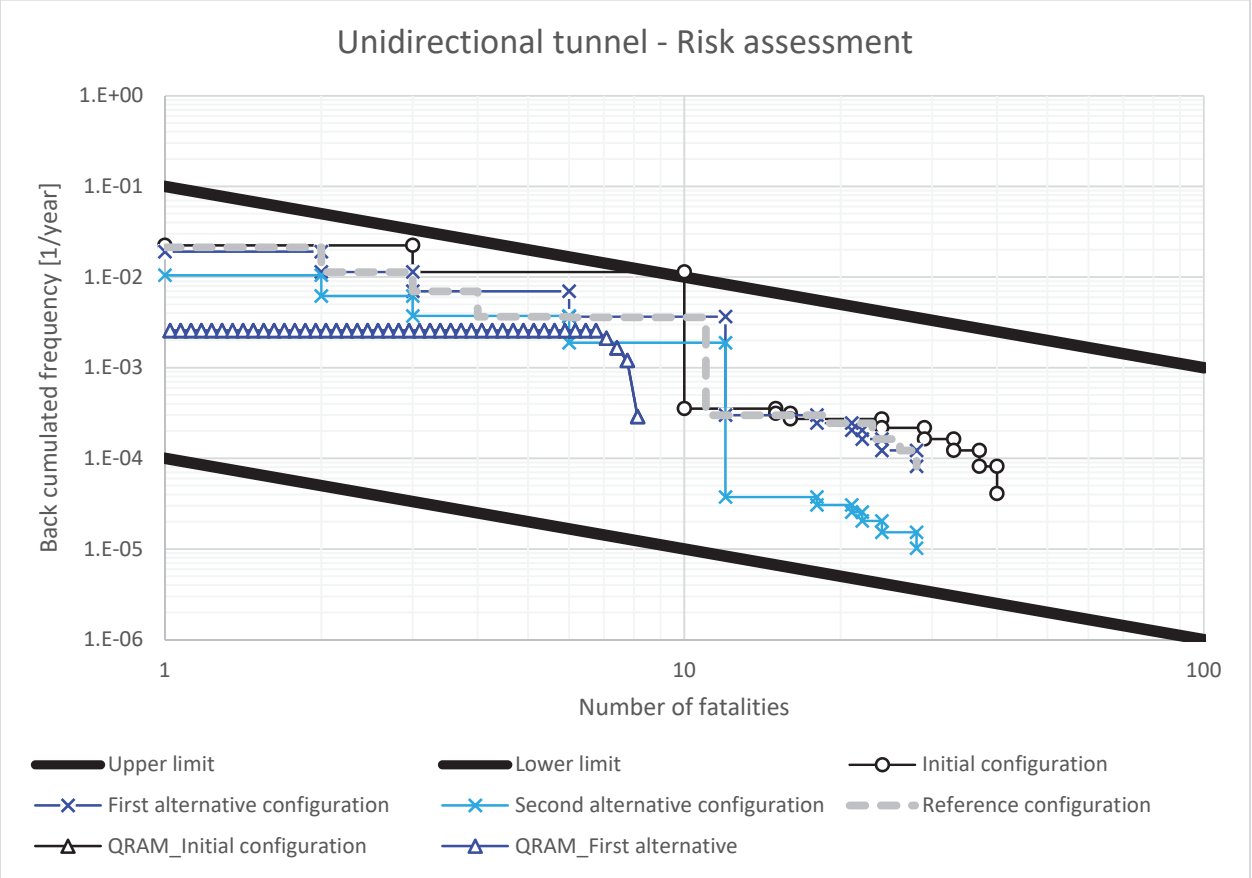

Figure 9.17. FN curves (all configurations)

The longitudinal ventilation system is confirmed to be a good strategy to compensate the risk related to the absence of emergency exits each 500 metres.

The threshold set by the regulations that admit longitudinal ventilation systems for unidirectional tunnels up to 3000 metres is confirmed to be consistent, because backlayering can be prevented and good smoke extraction from the exit portal is guaranteed if jet fans are correctly designed.

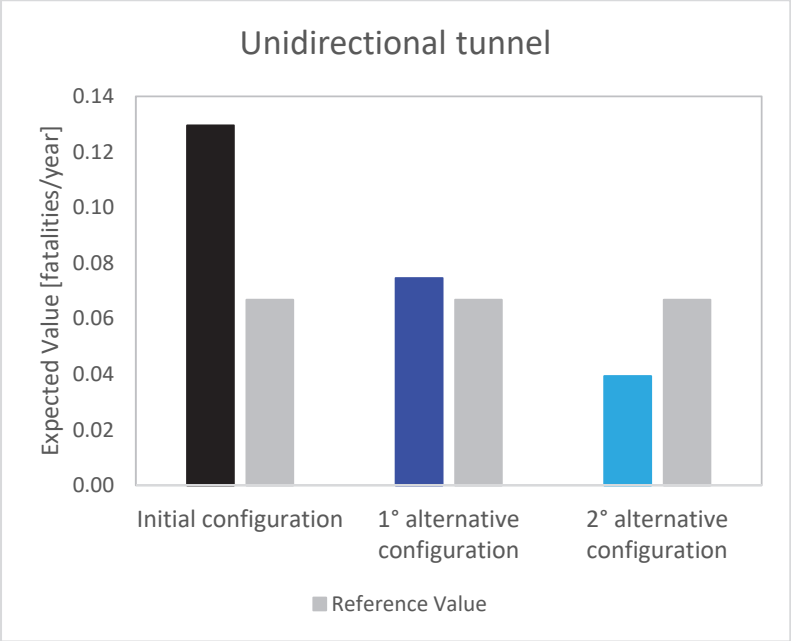

Figure 9.18. Expected Value (all configurations)

Finally, among all alternative strategies the effect due to the adoption of new emergency exits is not directly investigated in the Chapter as an alternative solution. This because, as stated in the introduction of the Chapter, the solution is not practicable in terms of excessive cost and safety of the work. However, some insights can be provided because the reference configuration has, apart from longitudinal ventilation, also the availability of the emergency exits at their theoretical positions, compliant with the regulations. The Figure 9.19 shows the evacuation paths for the reference tunnels (equipped with emergency exits placed homogenously so as to not exceed 500 metres). The maximum

evacuation time never exceeds 700 seconds, which is very low compared to those values (up to 1200 seconds) obtained in the initial configuration (see Figures 9.6-9.8). Therefore, the solution is certainly the safest in terms of time to exit the domain, but as it has been demonstrated in the Chapter, the adoption of alternative and correctly designed measures is able to mitigate the risk up to a tolerable level, as the regulations require.

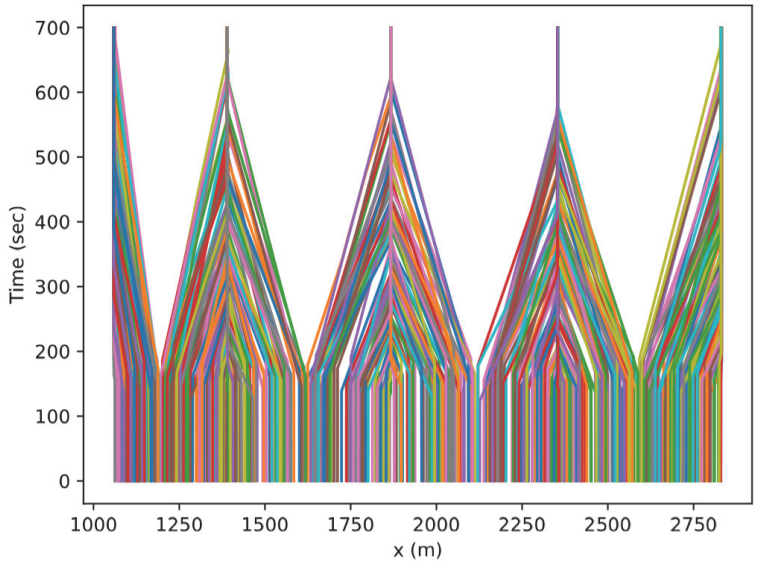

Figure 9.19. Time-space evacuation paths for the reference configuration (X3 position)

Chapter 10

Case study 2: bidirectional tunnel

10.1Description of the tunnel

The second case study is based on an existing bidirectional tunnel located in the North of Italy and part of the TEN roadway. The total traffic is 4630 vehicles per day, with a little presence of HGVs (1.3 % according to the data collection of the owner company). The track is not rectilinear and the overall length of the tunnel is 2410 metres, but two partially open sections interrupt its continuity. In fact, as it is reported in the sketch in Figure 10.1, the tunnel is composed by a sequence of five shorter tunnels, whose dimensional characteristics are reported in the Table 10.1. Specifically, the second and the fourth sections are rockfall galleries, with rectangular cross section and a series of openings along one of the lateral walls (see Figure 10.2). The two rockfall galleries are very similar in their structure and bounded along their extremities with the classical circular tunnel sections, whose length is 1367 m, 124 m and 605 m respectively for the T1, T3 and T5, and their cross section is typical of bidirectional carriageways. As it can be observed in the Figure 10.2, the ceiling of the rockfall galleries is more than 1 metres below the ceiling of the tunnels.

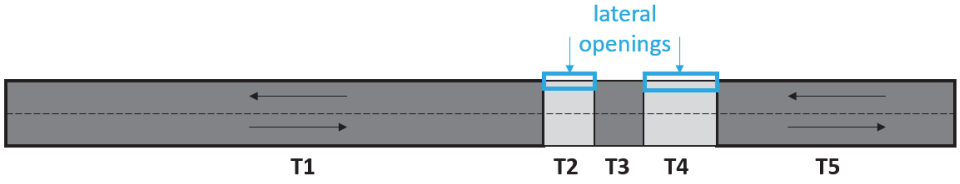

Figure 10.1. Sketch of the tunnel system

Considering the five sections as individual tunnels, only T1 and T5 are under the scope of the European Directive 2004/54/EC. In fact, the Directive is referred only to tunnels, where the definition of tunnel is a "section closed continuously along its four boundaries" (no rockfall sections T2 and T4) longer than 500 metres (T3 is excluded because shorter than the threshold).

The tunnels T1 and T5 bound with a portal and a rockfall gallery. However, before conducting a QRA for T1 and T5 as they were separated, one should consider that the tunnel has no means of egress along its length of 2410 metres. Therefore, T1 and T5 can be regarded as isolated tunnels provided that the ventilation conditions induced by the natural or mechanical ventilation are able to establish tenable conditions typical of a safe place at their extremities. CFD simulations will be used to support this aspect of the risk assessment.

Because the tunnel in its as-built configuration has neither emergency exits nor mechanical ventilation system, the jurisdictional authority has required a refurbishment aimed to restore the minimum safety level like the EU Directive requires. For this reason, mitigation strategies are investigated and the quantitative risk analysis is conducted for the initial, reference and alternative configurations of T1 and T5.

Table 10.1. Sub-sections of the tunnel

Section	Type	Length	Subjected to EU Directive?
T1	Tunnel	1367 m	Yes
T2	Rockfall (open)	127 m	No
T3	Tunnel	124 m	No
T4	Rockfall (open)	187 m	No
T5	Tunnel	605 m	Yes

Figure 10.2. Boundary between the tunnel and rockfall section

10.2QRA for the initial configuration

The procedure of QRA is applied independently to the initial configuration of T1 and T5. As for the analysis conducted for the unidirectional tunnel (Chapter 9) fire and evacuation simulations are merged a posteriori for the estimation of the risk.

10.2.1Fire scenarios

The tunnels have no mechanical ventilation in their initial configuration; therefore, the structure of the ETA will be less extended, because the sub-event linked to the "Ventilation" sub-system lack. As a consequence, the number of fire scenarios is halved (only natural ventilation is considered for F1, F2 and F3).

The results are contained in the Tables 10.2, 10.3 and 10.4 (the length of the model and the grid resolution are kept the same of those of the unidirectional tunnel studied in Chapter 9, because the dimensions of the cross section are similar).

In the Table 10.2 the smoke distribution along the tunnel is shown in the vertical plane (xz): smoke stratification is good, however at some points the visibility drops under the threshold of 10 m. In the Table 10.3 this effect can be easily read (black contour meets the 10 m value, while red and blue are respectively 30 m and 0 m).

In Table 10.4, instead, for all scenarios the minimum ASET of the tunnel is reported and characterised in terms of time and location along the tunnel). The governing criterion is not surprisingly again the visibility, while the criteria of temperature, radiative heat flux gas and FED are not met in reasonable time interval (1200 seconds) and therefore are not reported.

The fields and the ASET upwind and downwind are not perfectly symmetrical because a slight natural ventilation is inserted in the FDS model. Coherently with what one could expect, in case of no mechanical ventilation, the higher the HRR the shorter the time to reach the untenable conditions for people. Nevertheless, a low visibility level implies difficulties in the orientation but is not a quantity linked to lethality. Indeed, it is positive that the toxicity level (expressed by the FED) never exceeds the 0.1 level nor the temperature and the radiative heat flux gas their thresholds of 60°C and 2.5 kW/m^2 apart from the very proximity of the fire source.

For reason of completeness, the trends of the four quantities are reported for all fire scenarios in the Figures 10.3-10.6.

Table 10.2. Smoke distribution upwind and downwind the fire source for all scenarios (t=420 sec)

F1	
F2	
F3	

Table 10.3. Visibility slice at z = 2 m for all scenarios (t=420 sec)

F1	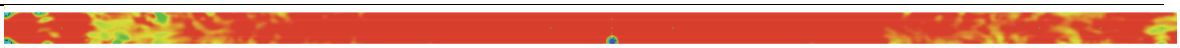
F2	
F3	

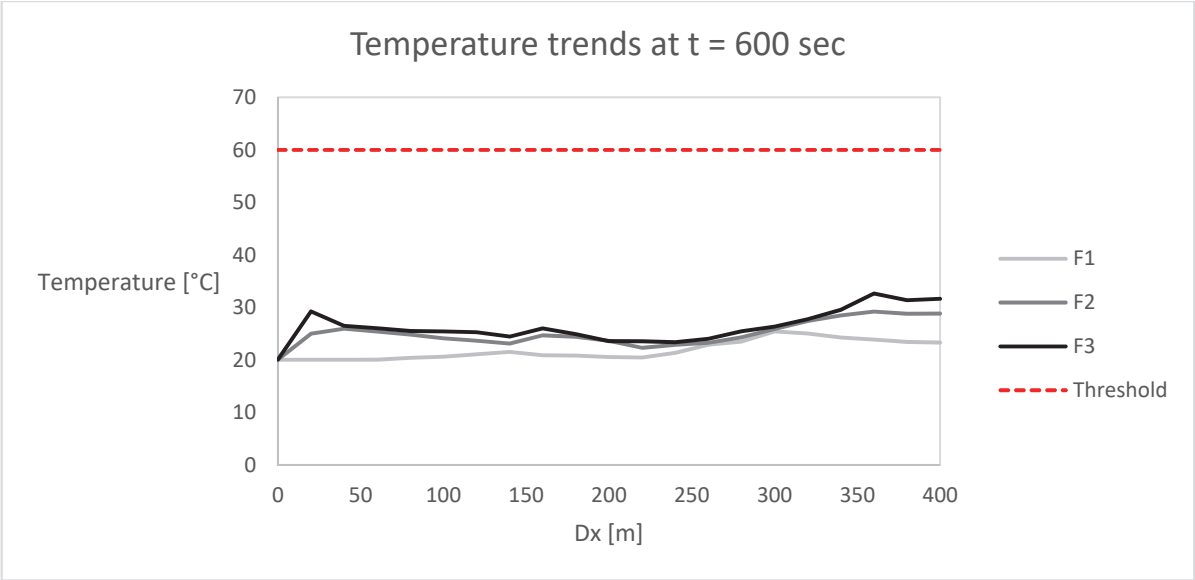

Figure 10.3. Temperature trends at z = 2 m for F1, F2 and F3 fire scenarios

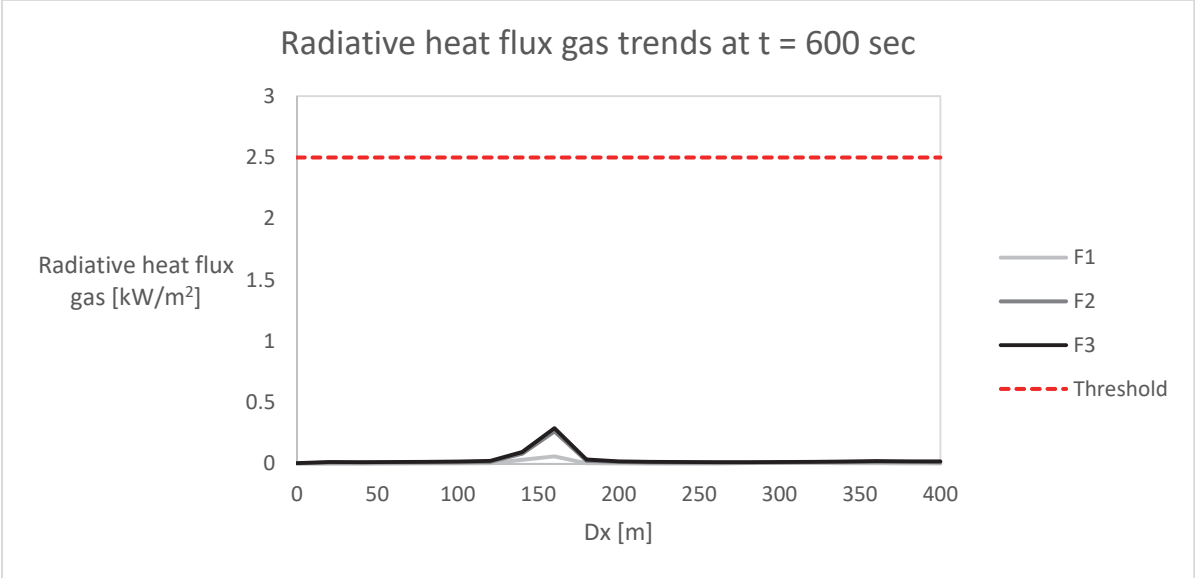

Figure 10.4. Radiative heat flux gas trends at z = 2 m for F1, F2 and F3 fire scenarios

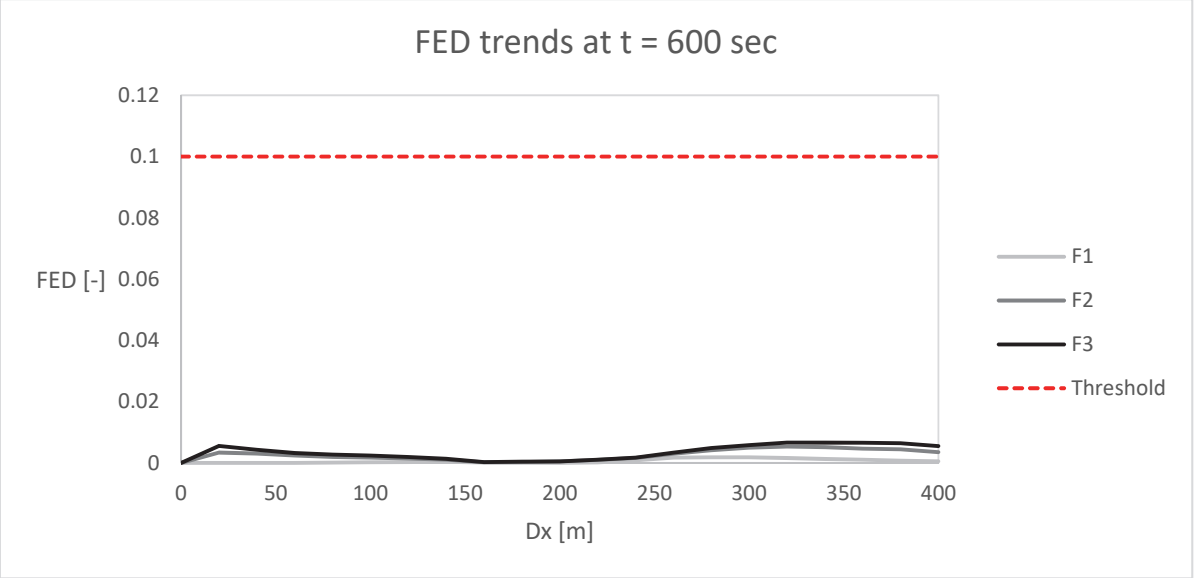

Figure 10.5. FED trends at z = 2 m for F1, F2 and F3 fire scenarios

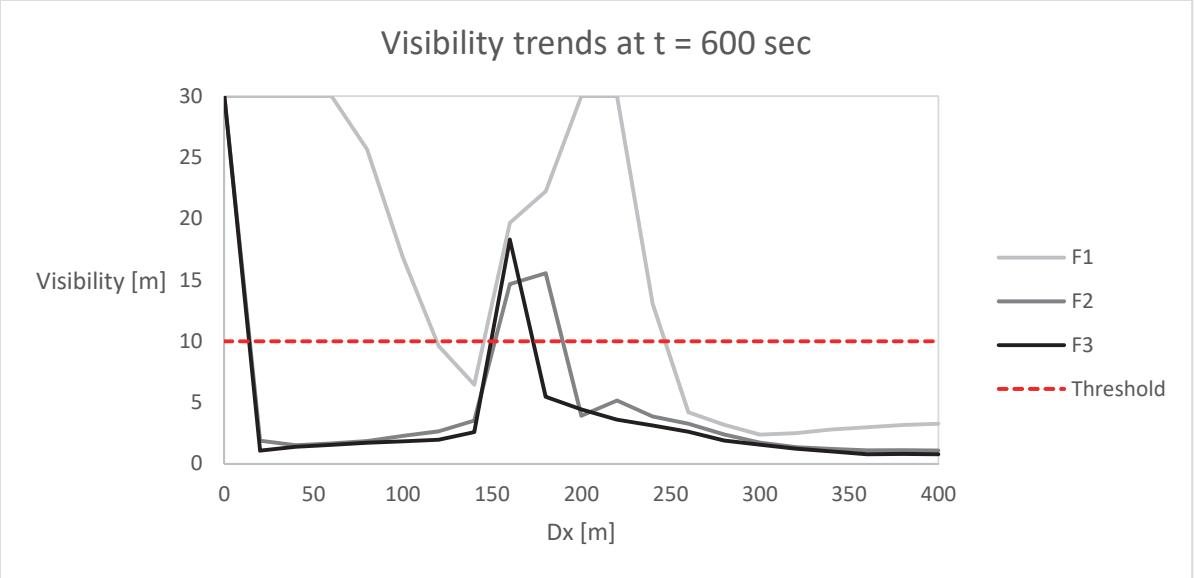

Figure 10.6. Visibility trends at z = 2 m for F1, F2 and F3 fire scenarios

Table 10.4. Results from fire modelling for the initial configuration of T1 and T5

Tunnel	Fire scenario		ASET upwind t (sec) – x (m)		ASET downwind t (sec) – x (m)		Governing criteria
T1 1367 m	F1	X1	503	40	448	1327	Visibility
	F2	X1	332	80	290	1287	Visibility
	F3	X1	230	100	202	1267	Visibility
	F1	X2	503	523.5	485	843.5	Visibility
	F2	X2	332	563.5	314	803.5	Visibility
	F3	X2	230	583.5	188	783.5	Visibility
	F1	X3	503	1007	459	360	Visibility
	F2	X3	332	1047	304	320	Visibility
	F3	X3	230	1067	212	300	Visibility
T5 605 m	F1	X1	503	1845	484	2087.5	Visibility
	F2	X1	332	1885	290	2067.5	Visibility
	F3	X1	230	1905	221	2057.5	Visibility
	F1	X2	503	1947.5	493	2036.25	Visibility
	F2	X2	332	1987.5	283	2016.25	Visibility
	F3	X2	230	2007.5	202	2006.25	Visibility
	F1	X3	503	2050	489	1985	Visibility
	F2	X3	332	2090	326	1965	Visibility
	F3	X3	230	2110	219	1955	Visibility

10.2.2 Evacuation scenarios

Results obtained with Pathfinder are reported in the Table 10.5 for both T1 and T5. As for the tunnel described in the previous Chapter 9, the success or failure of the detection system is associated to the formation of short or long queue, keeping in mind the operation of the traffic light at the entrance of the tunnel (mandatory because the tunnel exceeds 1000 m) or, alternatively, the behaviour of drivers ignoring the traffic light.

For bidirectional tunnels, the queue is double, because it develops upwind and downwind the fire accident. The evacuation paths of the occupants are reported in the Figures 10.7-10.12 in the time-space diagram. In the analysis it is considered that the occupants of each direction of travel will evacuate by going towards the portal used to enter the tunnel, based on the prevalent behaviour of people who do not approach the fire source in emergencies but go far from it.

The Figures 10.7-10.9 are related to tunnel T1 and highlight a much higher RSET compared to tunnel T5 (Figures 10.10-10.12). These Figures are related to the three positions of the accident (X1, X2, X3), with a Q2 queue type, associated to a tunnel filled with vehicles (no detection or drivers neglecting the stop of the traffic light). Similar curves are obtained for Q1 queue type, with a much smaller number of lines.

Table 10.5. Results from evacuation modelling for the initial configuration of T1 and T5

Tunnel	Evac scenario		Detec. system	Q. type	Queue length (m)		Occupant load		$RSET_{max}$ (sec)
					Upwind	Downwind	Upwind	Downwind	
T1 1367 m	X1	200 m	Success	Q1	65.6	65.6	21	21	2364
	X1	200 m	Failure	Q2	200	1167	59	343	2195
	X2	683.5m	Success	Q1	65.6	65.6	21	21	1450
	X2	683.5m	Failure	Q2	683.5	683.5	202	202	1494
	X3	1167 m	Success	Q1	65.6	65.6	21	21	2326
	X3	1167 m	Failure	Q2	1167	200	343	59	2365
T5 605 m	X1	200 m	Success	Q1	65.6	65.6	21	21	873
	X1	200 m	Failure	Q2	200	405	59	120	895
	X2	302.5m	Success	Q1	65.6	65.6	21	21	688
	X2	302.5m	Failure	Q2	302.5	302.5	91	91	739
	X3	405 m	Success	Q1	65.6	65.6	21	21	854
	X3	405 m	Failure	Q2	405	200	120	59	872

The Figures 10.8 and 10.11 represent a symmetrical evacuation through the extremities of the tunnels, while 10.7 and 10.10 are the "mirror" situation of the 10.9 and 10.12 (asymmetrical evacuation due to the asymmetrical position of the fire). The Figures represent a single run of the evacuation model, therefore they are not perfectly symmetrical as one could image due to randomness of the software and randomness linked to the probability functions assigned to radius, walking speed and pre-evacuation time of the occupants (see Chapter 7 for more comments).

The evacuation analysis is restricted to the length of the tunnels considered independently from the rest of the tunnel. This hypothesis will be commented a

posteriori with the results of CFD simulations, in which the lateral openings of the rockfall galleries at the internal boundary of the tunnel are inserted through the HOLE and OPEN VENT functions.

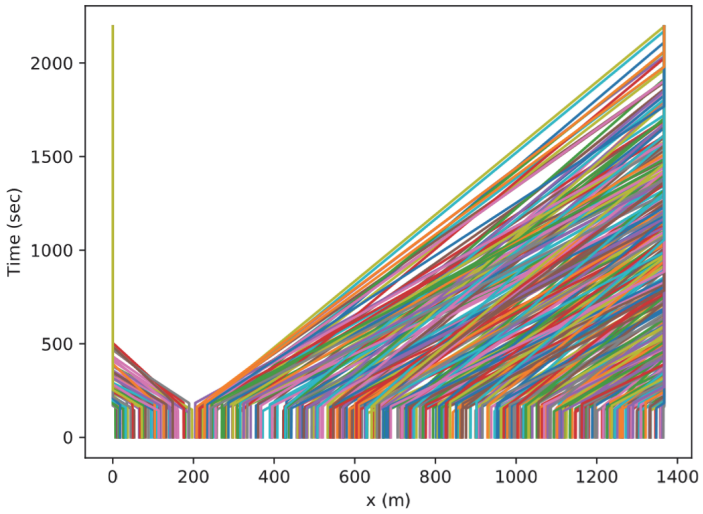

Figure 10.7. Tunnel T1, fire position X1, queue Q2

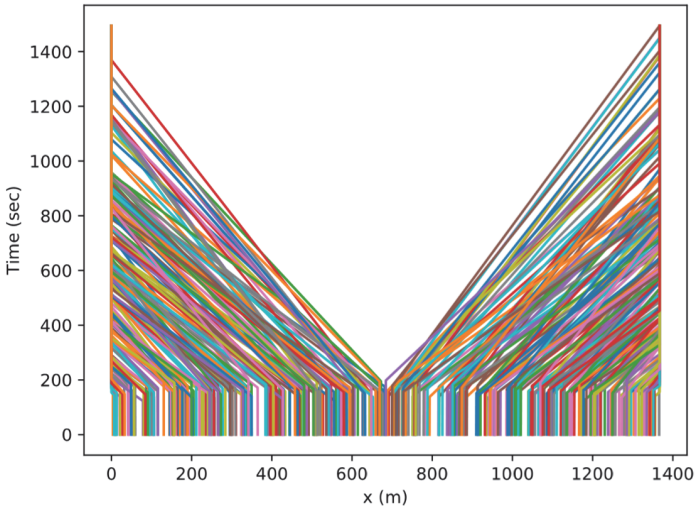

Figure 10.8. Tunnel T1, fire position X2, queue Q2

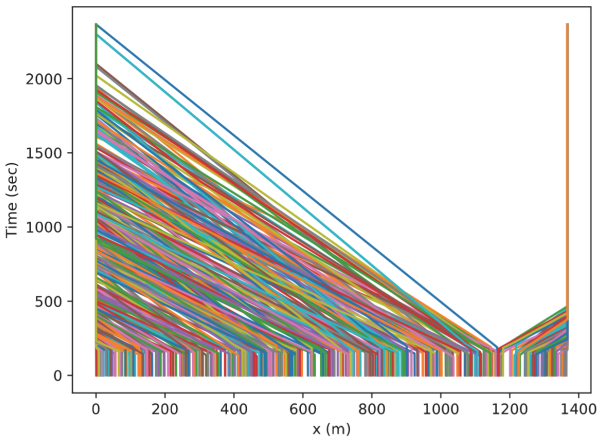

Figure 10.9. Tunnel T1, fire position X3, queue Q2

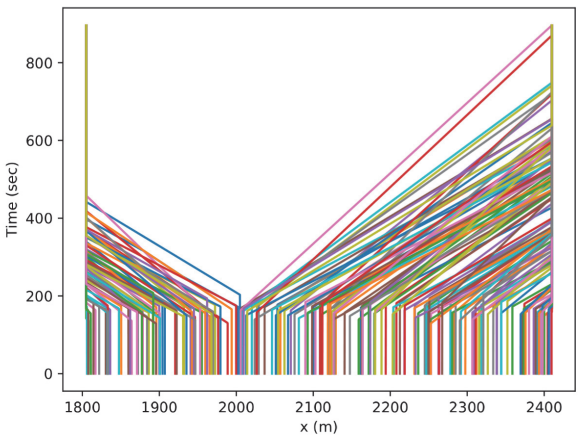

Figure 10.10. Tunnel T5, fire position X1, queue Q2

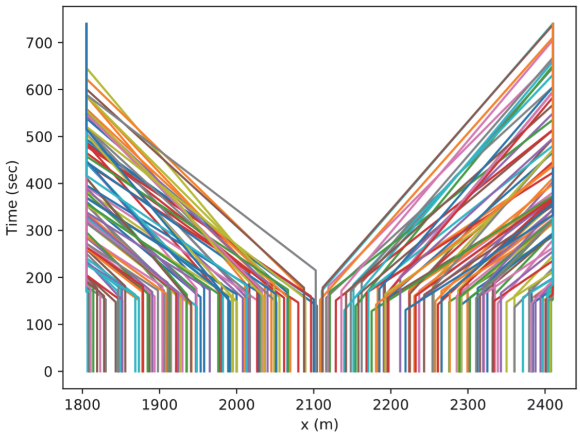

Figure 10.11. Tunnel T5, fire position X2, queue Q2

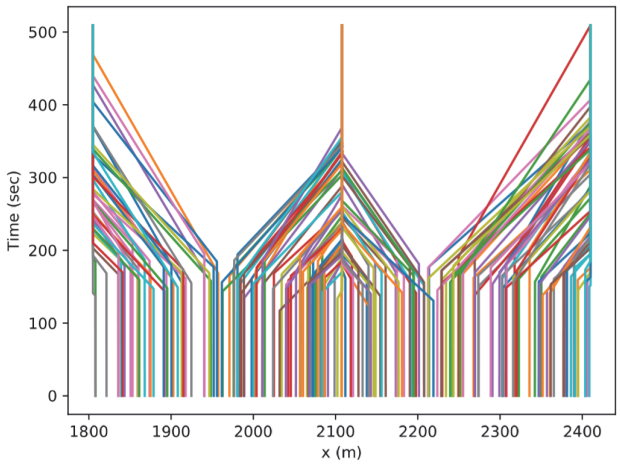

Figure 10.12. Tunnel T5, fire position X3, queue Q2

10.2.3 Risk estimation

In the following Figures 10.13 and 10.14, the risk related to the initial configuration of the tunnel T1 and T5 is drawn in the FN diagram.

The FN curve is the risk indicator considered in this first step and it is observed that both tunnels are in the non-acceptable zone, as their risk exceeds the upper limit of the ALARP zone almost along the entire length of the FN curves.

The FN curve of the tunnel T5 is less extended due basically to the shorter length of the tunnel, which contribute to the definition of the frequency of the initiating event (IE) as it has been explained in the Chapter 8.

The risk estimation is conducted also with QRAM software: the results for T1 and T5 show a slightly higher maximum number of fatalities, but the cumulated frequency is much lower. The curves lie in the ALARP zone for both case: however, as it was highlighted in the parametric study (Appendix A) the QRAM is insensitive to many parameters and these results, contradictory to those obtained through advanced models, are quite alarming. The ALARP zone, in fact, represent a zone of "conditional acceptability" and the configuration might be accepted from the jurisdictional authorities.

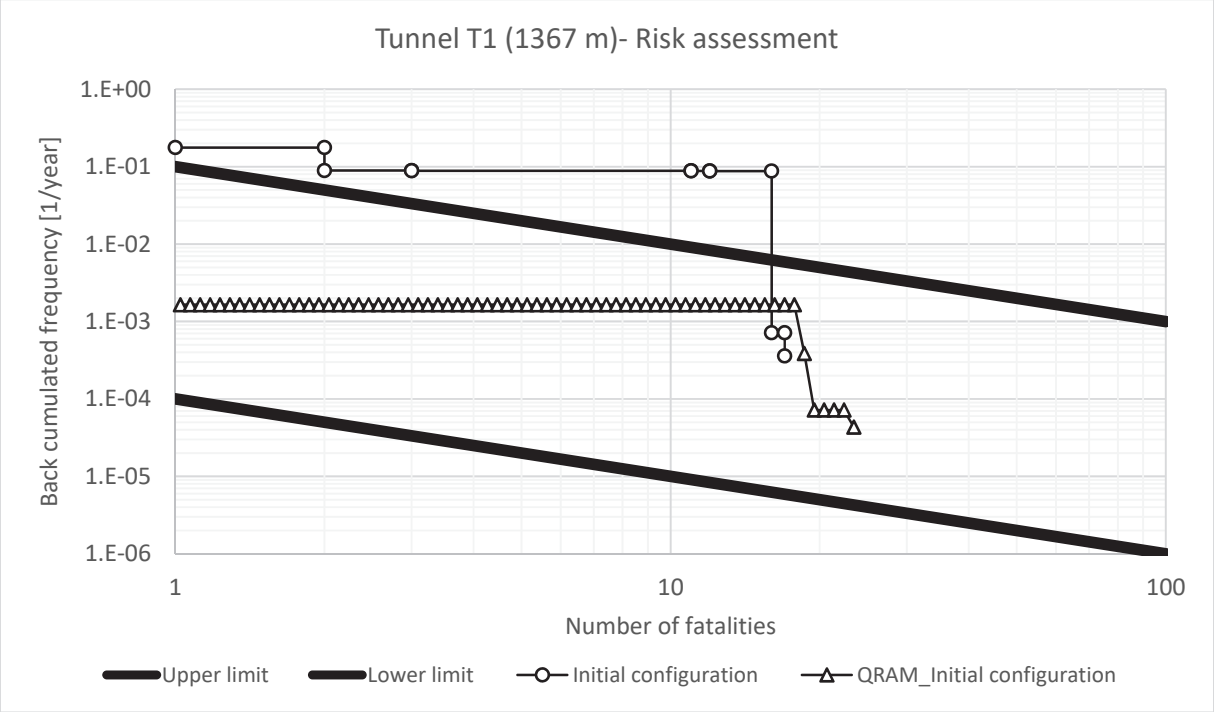

Figure 10.13. Tunnel T1, risk related to the initial configuration

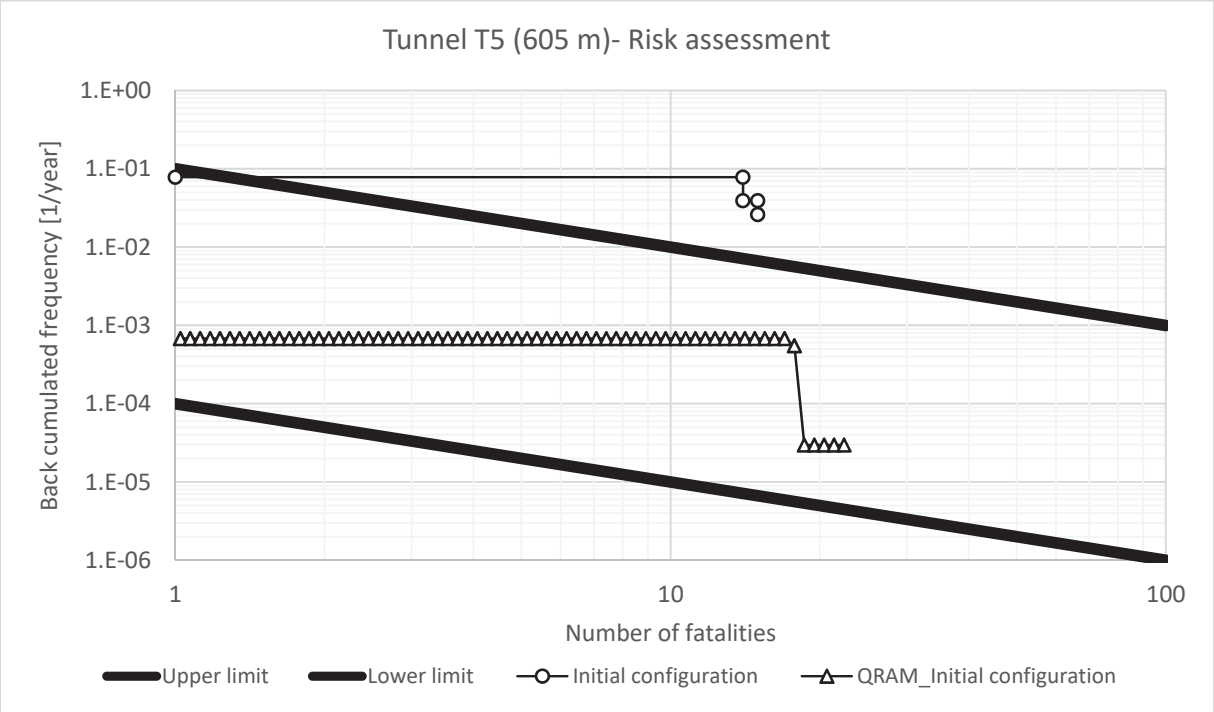

Figure 10.14. Tunnel T5, risk related to the initial configuration

The curve obtained with advanced models are assumed more reliable than those obtained through QRAM. Therefore, the initial configuration is considered non-acceptable.

Mitigation strategies are, therefore, investigated for both cases and QRA is conducted for some alternative configurations is conducted.

10.3 QRA for the first alternative configuration

The first proposal of risk mitigation for both T1 and T5 tunnels is represented by the introduction of a mechanical ventilation system composed by reversible jet fans whose characteristics are reported in Table 10.6.

The ventilation flow is parallel to the prevalent direction of traffic (T1 → T5) and the position of the jet fans is chosen as to facilitate the smoke extraction from the T1 tunnel through the lateral openings of the rockfall gallery T2. On the other hand, the extraction from the tunnel T5 is, for hypothesis, obtained by pushing the smoke towards the exit portal (the rockfall gallery T4 is located at the entrance portal of T5).

According to the EU Directive, the mechanical ventilation is not mandatory for the tunnel T5 (L<1000 m), but the solution is investigated in order to highlight the improvement or deterioration of the tenable conditions in the domain. In addition, two emergency exits are obtained at the boundaries between the tunnels and the rockfall galleries through the adjustment of these latter, which are regarded as a natural opening towards a safe place outside (where a local roadway is actually located).

Table 10.6. Characteristics of the jet fans in the first alternative configuration

Volume flow	24.3 m^3/s
Velocity	30.9 m/s
Diameter	1 m
Thrust	900 N
Power	27 kW

10.3.1 Fire scenarios

Fire scenarios are analysed in FDS model. As for the initial configuration, the results are reported in the Tables 10.7, 10.8, 10.9.

The smoke distribution along the tunnel and consequently the level of visibility at z=2m are very different from the case of natural ventilation. In fact, roughly the part of the tunnel where the ventilation flow is directed is much more penalised, while the other part of the tunnel (upwind the fire) is safer.

Backlayering phenomena occur and are significant especially in the case of F3 scenario (peak of 120 MW) while for F2 are more contained.

The criterion that governs the achievement of the tenability limit is again the visibility. However, the trends of the other quantities are reported in the Figures10.15-10.18.

Table 10.7. Smoke distribution upwind and downwind the fire source for all scenarios (t=420 sec)

F1	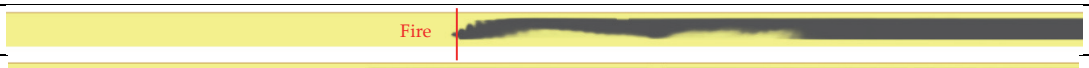
F2	
F3	

Table 10.8. Visibility slice at z = 2 m for all scenarios (t=420 sec)

F1	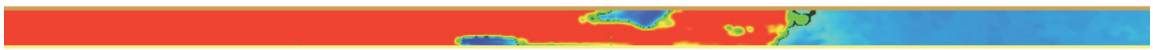
F2	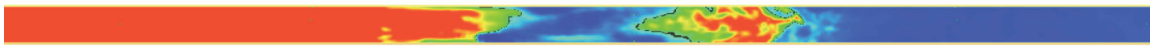
F3	

Table 10.9. Results from fire modelling for the first alternative configuration of T1 and T5

Tunnel	Fire scenario		Ventilation system	ASET upwind t (sec) – x (m)		ASET downwind t (sec) – x (m)		Criteria
T1 1367 m	F1	X1	Success	343	160	320	240	Visibility
	F1	X1	Failure	417	60	339	260	Visibility
	F2	X1	Success	257	60	312	300	Visibility
	F2	X1	Failure	257	80	312	300	Visibility
	F3	X1	Success	289	40	242	280	Visibility
	F3	X1	Failure	289	40	242	280	Visibility
	F1	X2	Success	343	643.5	320	723.5	Visibility
	F1	X2	Failure	417	543.5	339	743.5	Visibility
	F2	X2	Success	257	543.5	312	783.5	Visibility
	F2	X2	Failure	257	563.5	312	783.5	Visibility
	F3	X2	Success	289	523.5	242	763.5	Visibility
	F3	X2	Failure	289	523.5	242	763.5	Visibility
	F1	X3	Success	343	1127	320	1207	Visibility
	F1	X3	Failure	417	1027	339	1227	Visibility
	F2	X3	Success	257	1027	312	1267	Visibility
	F2	X3	Failure	257	1047	312	1267	Visibility
	F3	X3	Success	289	1007	242	1247	Visibility
	F3	X3	Failure	289	1007	242	1247	Visibility
T5 605 m	F1	X1	Success	343	1965	320	2045	Visibility
	F1	X1	Failure	417	1865	339	2065	Visibility
	F2	X1	Success	257	1865	312	2105	Visibility
	F2	X1	Failure	257	1885	312	2105	Visibility
	F3	X1	Success	289	1845	242	2085	Visibility
	F3	X1	Failure	289	1845	242	2085	Visibility
	F1	X2	Success	343	2067.5	320	2147.5	Visibility
	F1	X2	Failure	417	1967.5	339	2167.5	Visibility
	F2	X2	Success	257	1967.5	312	2207.5	Visibility
	F2	X2	Failure	257	1987.5	312	2207.5	Visibility
	F3	X2	Success	289	1947.5	242	2187.5	Visibility
	F3	X2	Failure	289	1947.5	242	2187.5	Visibility
	F1	X3	Success	343	2170	320	2250	Visibility
	F1	X3	Failure	417	2070	339	2270	Visibility
	F2	X3	Success	257	2070	312	2310	Visibility
	F2	X3	Failure	257	2090	312	2310	Visibility
	F3	X3	Success	289	2050	242	2290	Visibility
	F3	X3	Failure	289	2050	242	2290	Visibility

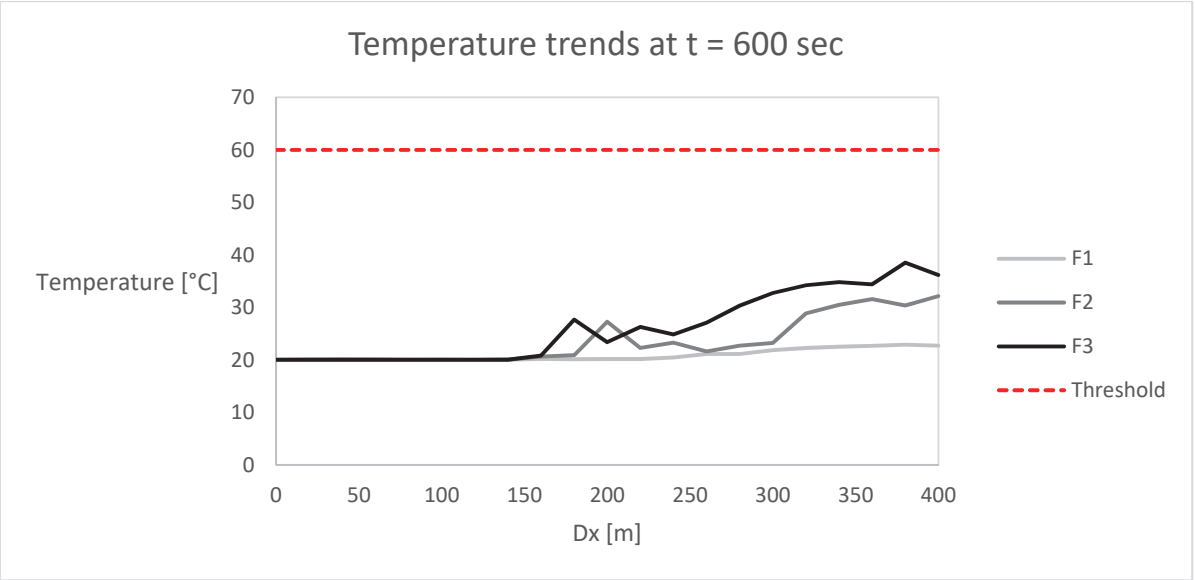

Figure 10.15. Temperature at z = 2m (600 sec) with longitudinal ventilation system

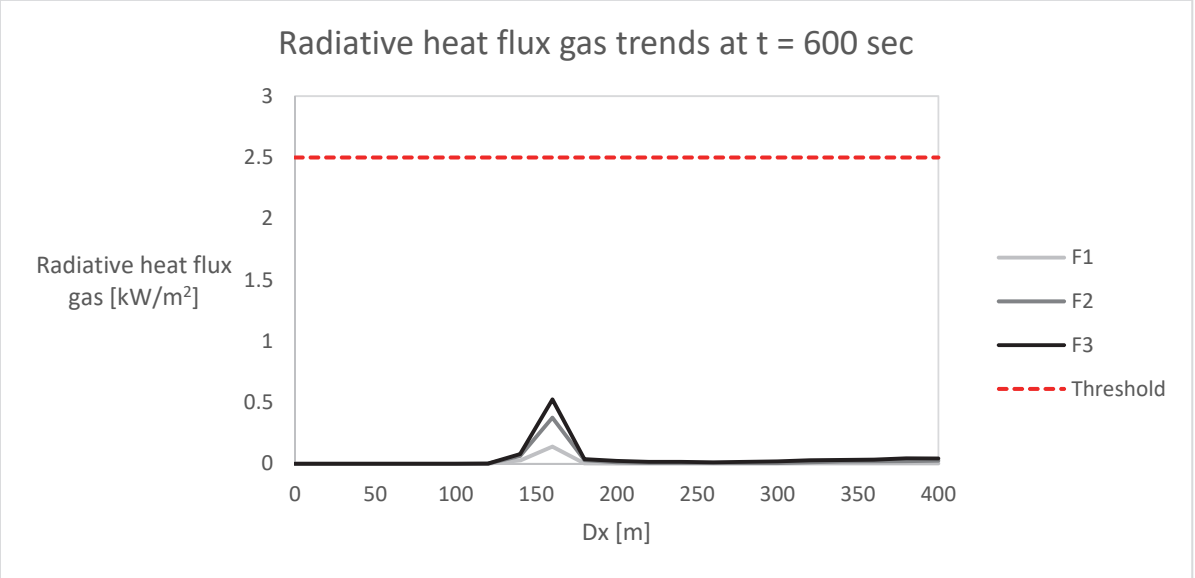

Figure 10.16. Radiative heat flux gas at z = 2m (600 sec) with longitudinal ventilation system

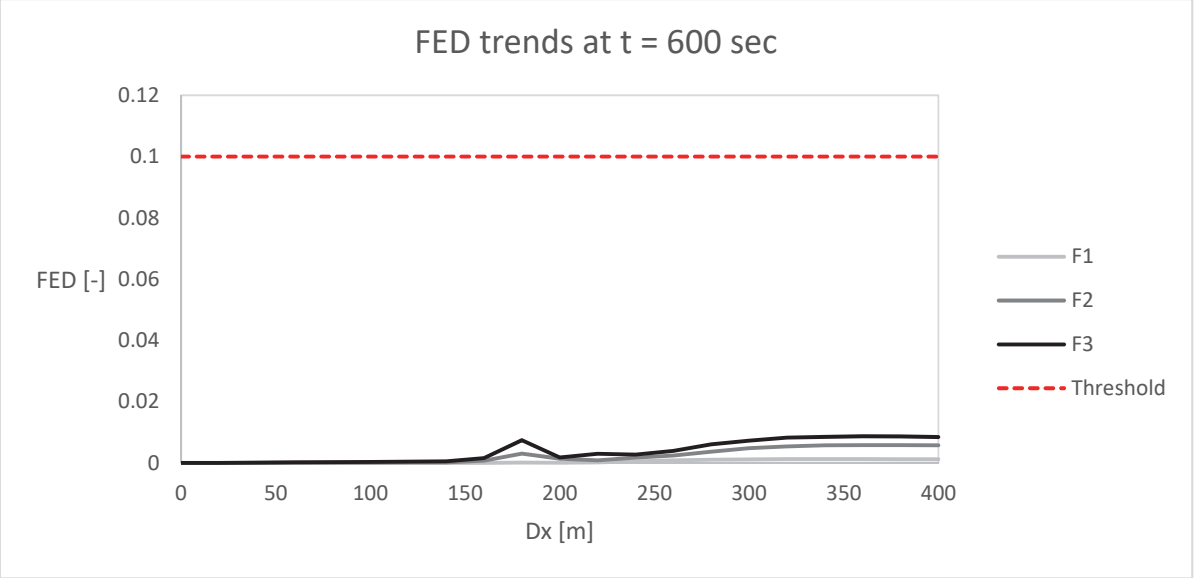

Figure 10.17. FED at z = 2m (600 sec) with longitudinal ventilation system

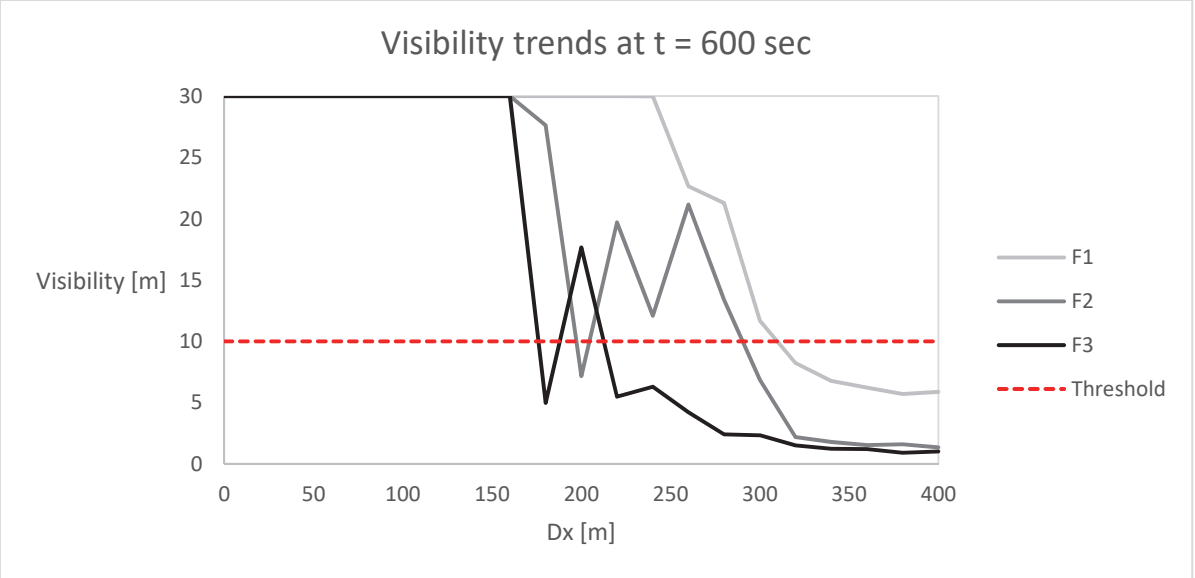

Figure 10.18. Visibility at z = 2m (600 sec) with longitudinal ventilation system

10.3.2 Evacuation scenarios

The evacuation scenarios are the same of the previous case. The traffic is considered symmetrical (4630 vehicles per day divided between the two directions of travel).

10.3.3 Risk estimation

The technical solution is not satisfactory because the resulting risk is increased with respect to the previous initial configuration both for T1 and T5 tunnels (Figures 10.19 and 10.20). The total number of fatalities is roughly double compared to the initial configuration and the back-cumulated frequency is also higher for tunnel T1.

The risk estimation is conducted also with QRAM software: for bidirectional tunnels the QRAM allows to model only semi-transverse ventilation, but the values have been changed ad hoc so as to indirectly model longitudinal ventilation. The shape of the FN curve is similar to that obtained with the adopted procedure and the maximum number of fatalities as well. However, the cumulated frequency is much lower and, therefore, the estimation is not on the safe side (the curve lie in the ALARP zone).

Considering the results obtained through the advanced consequence analysis, the configuration is not acceptable: this conclusion is also confirmed by the comparison among the Expected Value of the alternative configuration and the initial and reference value as well (Table 10.10).

Table 10.10. Expected Value for the configuration

Tunnel configuration	Expected Value (fatalities/year)	
	T1	T5
Initial	1.409	0.689
Reference	0.397	0.418
First alternative	3.191	2.034

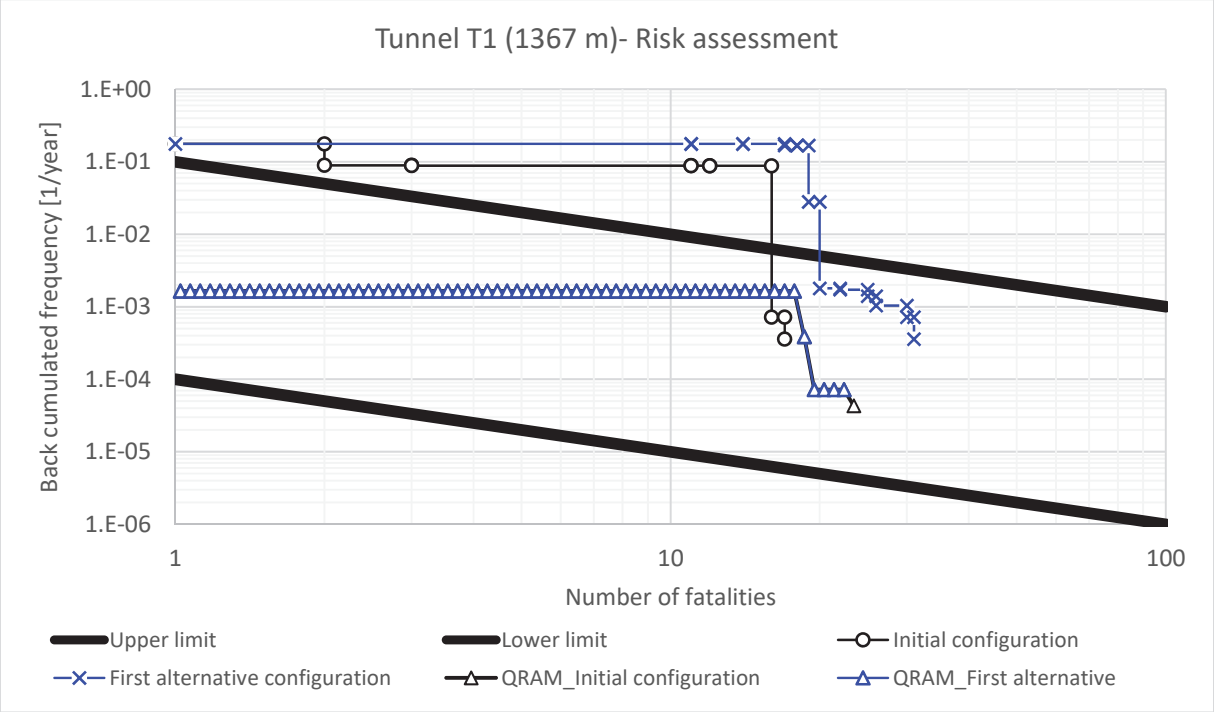

Figure 10.19. FN curve for T1 tunnel (1° alternative vs initial configuration)

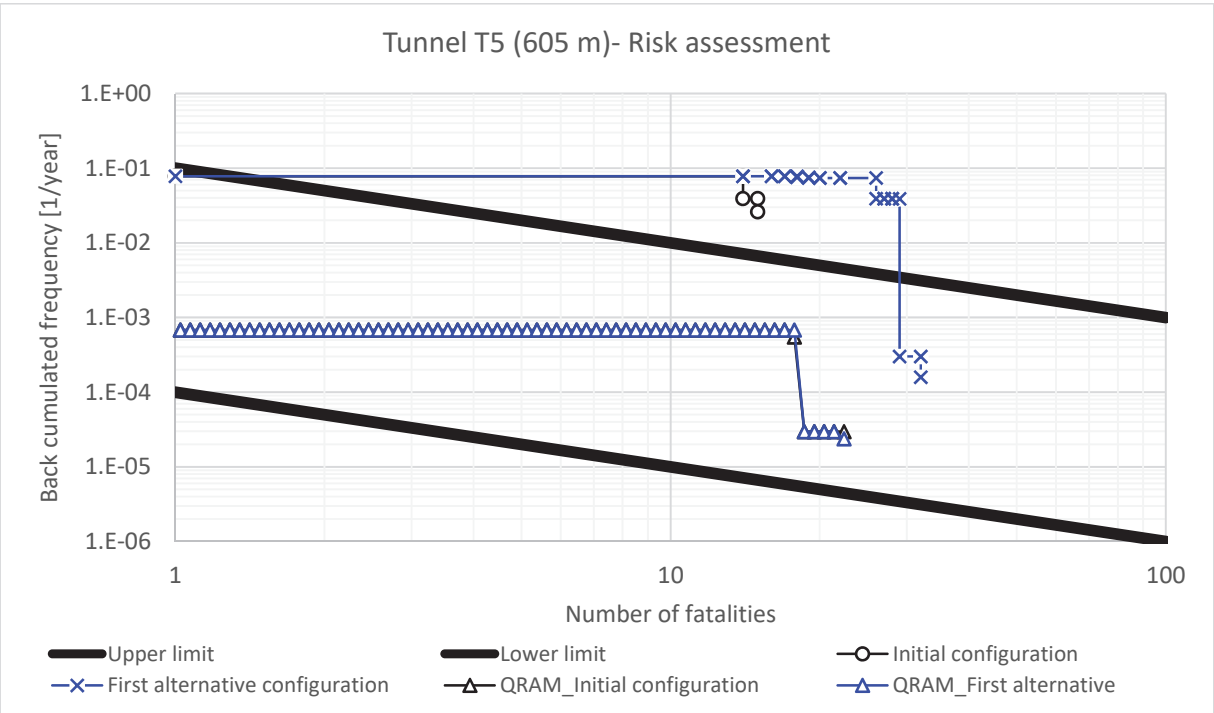

Figure 10.20. FN curve for T5 tunnel (1° alternative vs initial configuration)

The characteristics of the reference tunnel are in line with the minimum requirements contained in the EU Directive. The distance among the emergency exits does not exceed 500 m and the exits are placed homogeneously along the tunnel. The mechanical system is provided only for T1 (semi transverse ventilation system, with smoke extraction each 200 m) whereas T5 (L<1000 m) has no mechanical ventilation.

10.4 QRA for the second alternative configuration

A second alternative configuration is proposed in order to reduce the risk under the threshold set by the reference configuration. In this case, similarly to what is done in Chapter 9, new management strategies are inserted. Specifically, it is assumed that the tunnel is monitored by a control centre available 24/7 and, at the same time, CCTV circuit, loudspeakers and lighting panels are added inside the tunnel.

The safety systems are assumed more reliable and for this reason the probability of success and failure of both detection and ventilation systems are respectively modified as 0.95 and 0.05.

10.4.1 Fire scenarios

The fire simulations are the same of those contained in section 10.3.1.

10.4.2 Evacuation scenarios

The evacuation scenarios are those reported in 10.3.2.

10.4.3 Risk estimation

The FN curves (Figures 10.21 and 10.22) are very similar to those of the previous case. Differently from what obtained in the Chapter 9, the modification of the probability of success and failure of the safety systems does not affect significantly the back-cumulated frequency apart from the right portion of the FN curve.

The QRAM curve is not drawn because it is not possible to add this type of management measures in the input of the software.

The configuration is still non-acceptable: the Table 10.11 confirms that the risk is too high compared to the one of the reference tunnel.

This does not mean that the longitudinal ventilation system is always unacceptable for bidirectional tunnels. In the case of tunnel T1 and T5 the adoption of a longitudinal ventilation system is particularly disadvantageous because there are no emergency exits along the entire length and, therefore, the occupants (especially in case the fire accident is located at X3) are particularly penalised.

The configuration might be suitable for roadways with highly asymmetrical traffic flow, in which the jet fans might be able to blow air against the direction with less traffic, or for tunnels equipped with intermediate means of egress between the entrance and the exit portals so as to reduce the number of exposed people.

Table 10.11. Expected Value for the configuration

Tunnel configuration	Expected Value (fatalities/year)	
	T1	T5
Initial	1.409	0.689
Reference	0.397	0.418
Second alternative	3.528	2.661

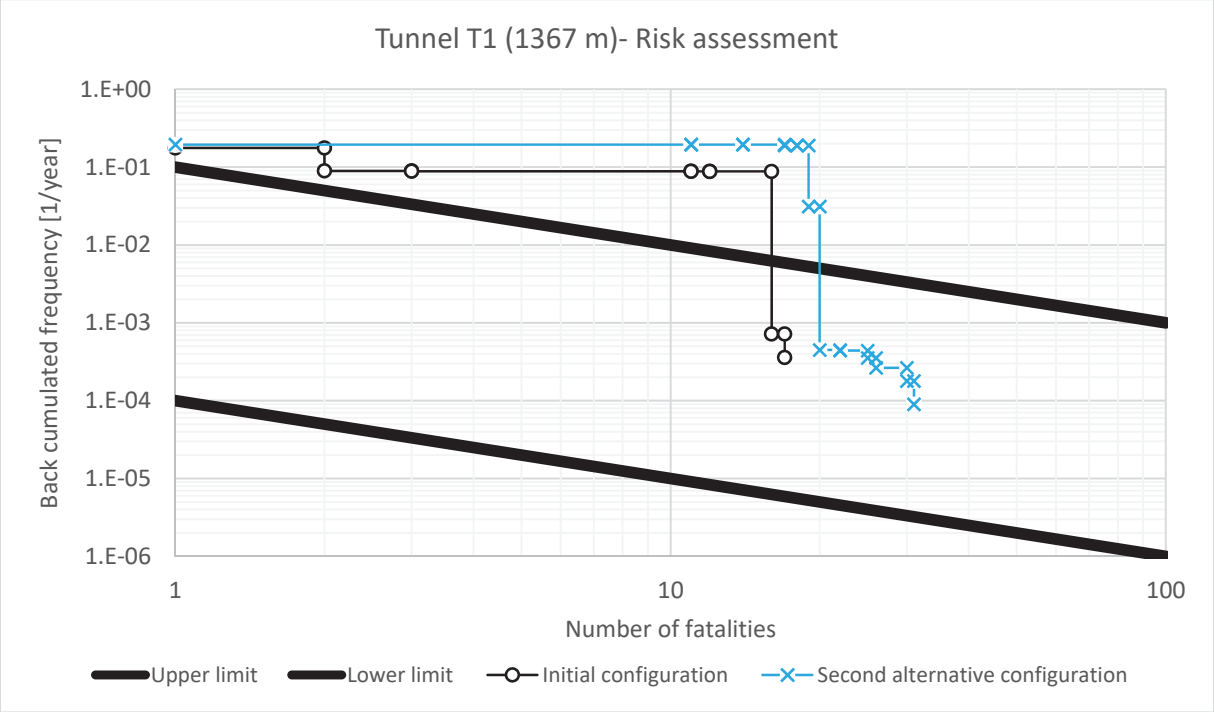

Figure 10.21. FN curve for T1 tunnel (2° alternative vs initial configuration)

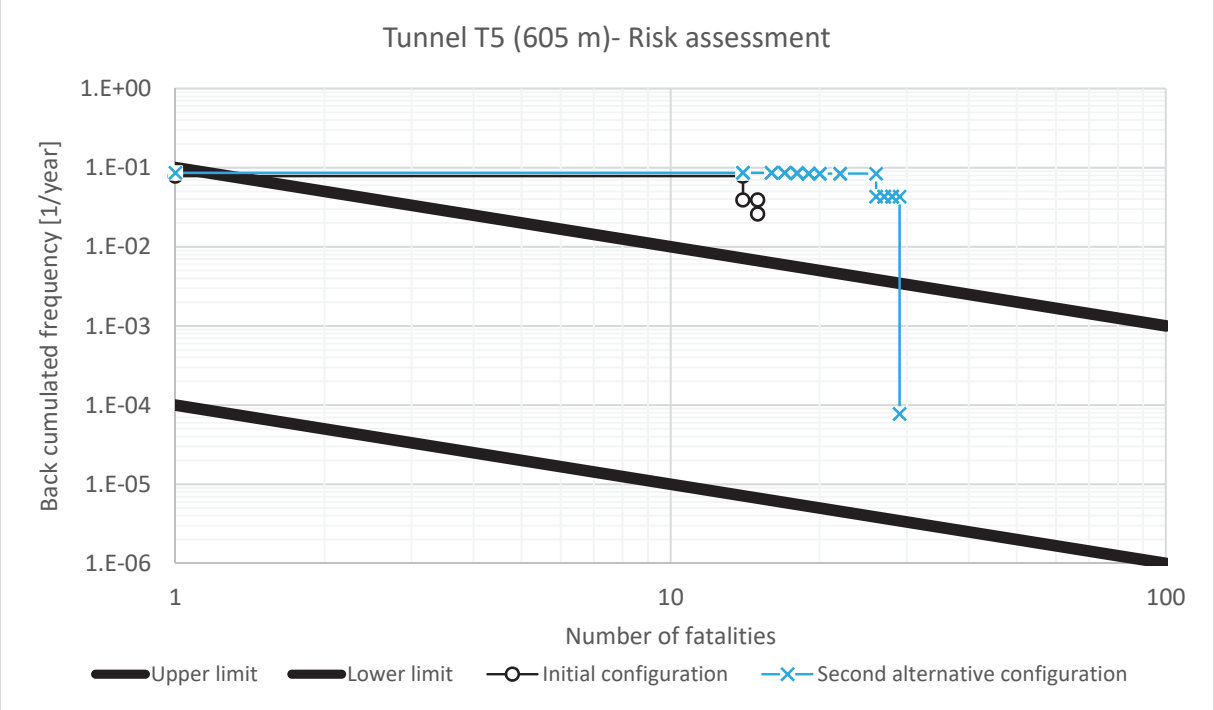

Figure 10.22. FN curve for T5 tunnel (2° alternative vs initial configuration)

10.5 QRA for the third alternative configuration

The third proposal of alternative measure is the introduction of a mechanical ventilation system composed by smoke extractors placed each 200 metres both for T1 and T5 tunnels.

The ventilation flow has two main directions: a horizontal flow along the tunnel induced by the vertical extraction at the ceiling level and the vertical flow which properly extract the mix of soot and air.

It is stated again that the mechanical ventilation is not mandatory for tunnel T5 but given the high initial risk of the tunnel it is necessary to investigate the solution which could be interesting from the engineering point of view.

As it was assumed for the other cases, two emergency exits are obtained at the boundaries between the tunnels and the rockfall galleries through the adjustment of these latter, which are regarded as a natural opening towards a safe place outside the tunnel (where a local roadway is actually located).

10.5.1 Fire scenarios

The smoke extractors in FDS are implemented by two vertical jet fans connected with the external air, at atmospheric pressure. The vertical ducts are not directly modelled but a length of 3 metres is taken into account through an HVAC function.

The results are shown in the Tables 10.12-10.16. The vertical extraction strongly affects the smoke distribution and the visibility field near the fire source: it creates a real barrier for the smoke propagation, as it was an aeraulic compartmentation. The performance of the smoke extractors differs among the three scenarios: the layer height of smoke is lower for F2 and even more for F3, creating zones with very low visibility. However, the system seems extremely advantageous outside the perimeter, determined by the position of the extractors.

Table 10.12. Smoke distribution upwind and downwind the fire source for all scenarios (t=420 sec)

F1	
F2	
F3	

Table 10.13. Visibility slice at z = 2 m for all scenarios (t=420 sec)

F1	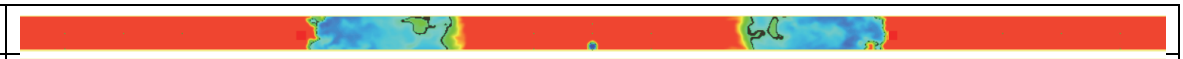
F2	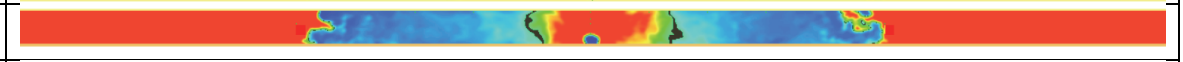
F3	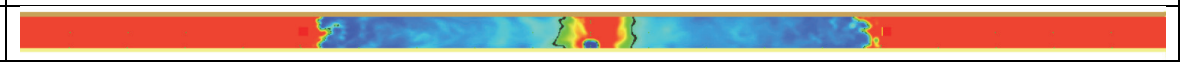

Table 10.14. Smoke distribution upwind and downwind the fire source for all scenarios (t=1200 sec)

F1	
F2	
F3	

Table 10.15. Visibility slice at z = 2 m for all scenarios (t=1200 sec)

F1	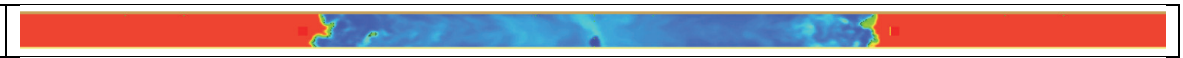
F2	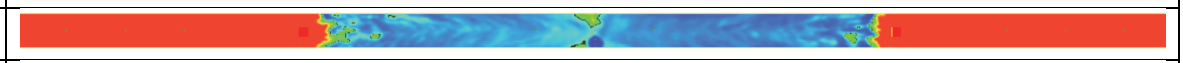
F3	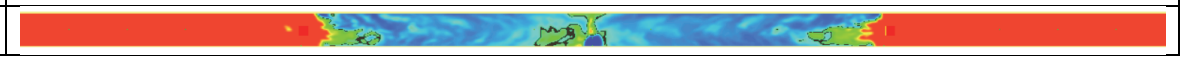

The Figures 10.23-10.26 show the trends of the temperature, radiative heat flux gas, FED and visibility at z = 2 m and y = 6 m at 600 seconds for the three fire scenarios. The temperature and the FED are under the acceptability threshold along the length of the model, whereas the radiative heat flux gas shows a peak exactly in the section where the fire source is located (which is obvious and not significant). The trends of visibility are in agreement with the slice previously commented.

10.5.2 Evacuation scenarios

The results are not reported as they are the same of the previous cases.

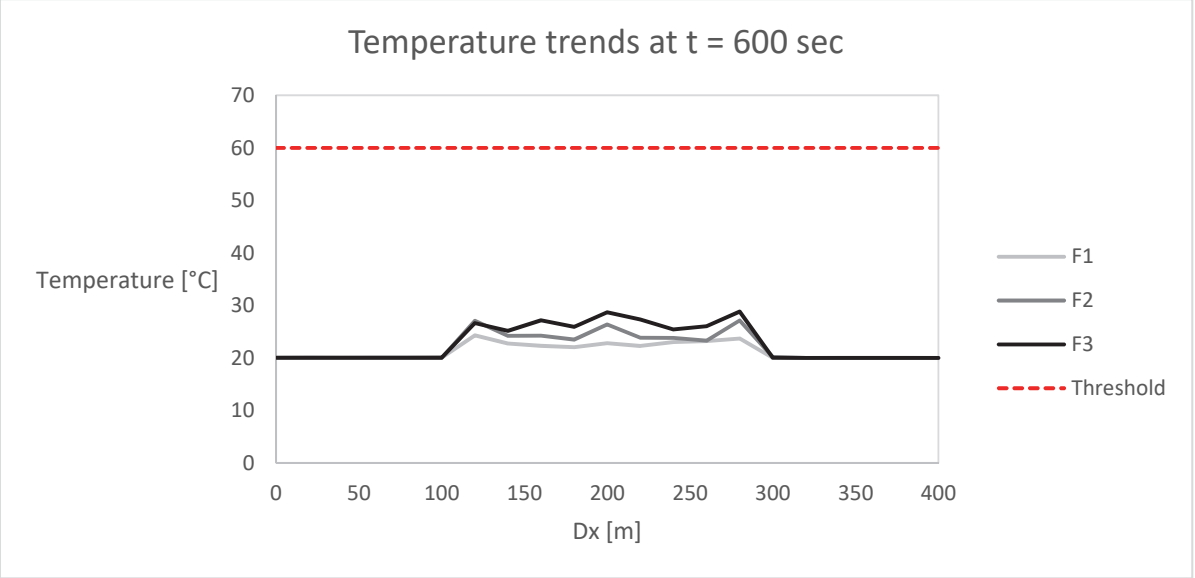

Figure 10.23. Temperature trends at z = 2 m for F1, F2 and F3 fire scenarios

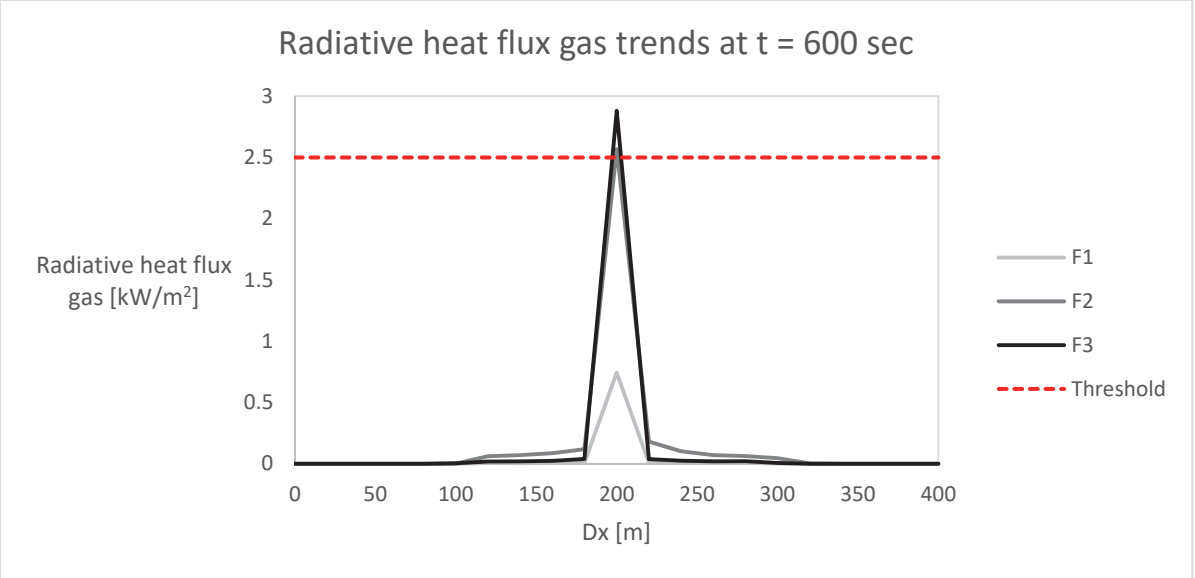

Figure 10.24. Radiative heat flux gas trends at z = 2 m for F1, F2 and F3 fire scenarios

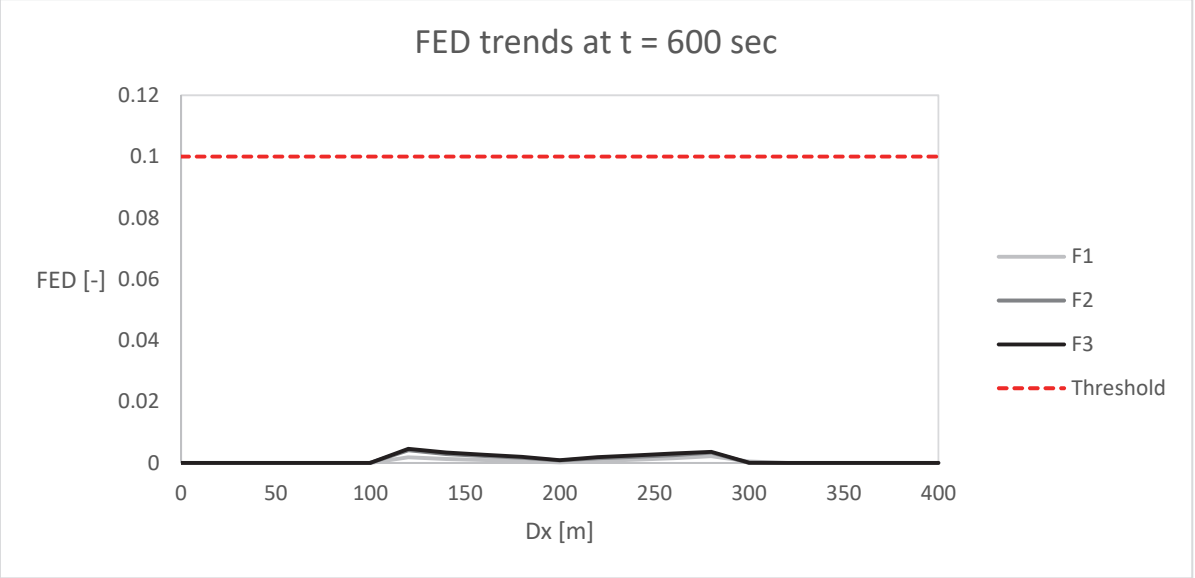

Figure 10.25. FED trends at z = 2 m for F1, F2 and F3 fire scenarios

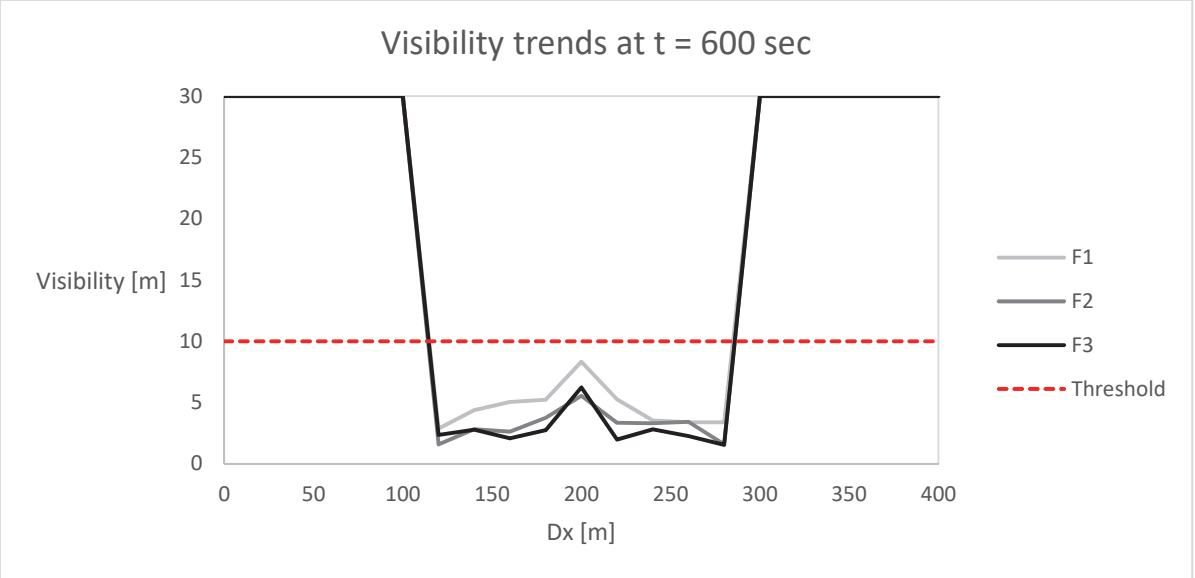

Figure 10.26. Visibility trends at z = 2 m for F1, F2 and F3 fire scenarios

Table 10.16. Results from fire modelling for the third alternative configuration of T1 and T5

Tunnel	Fire scenario		Ventilation system	ASET upwind t (sec) – x (m)		ASET downwind t (sec) – x (m)		Criteria
T1 1367 m	F1	X1	Success	363	120	311	1247	Visibility
	F1	X1	Failure	503	40	448	1327	Visibility
	F2	X1	Success	242	120	200	1247	Visibility
	F2	X1	Failure	332	80	290	1287	Visibility
	F3	X1	Success	320	120	286	1247	Visibility
	F3	X1	Failure	230	100	202	1267	Visibility
	F1	X2	Success	363	603.5	343	763.5	Visibility
	F1	X2	Failure	503	523.5	485	843.5	Visibility
	F2	X2	Success	242	603.5	187	763.5	Visibility
	F2	X2	Failure	332	563.5	314	803.5	Visibility
	F3	X2	Success	320	603.5	263	280	Visibility
	F3	X2	Failure	230	583.5	188	783.5	Visibility
	F1	X3	Success	363	1087	354	280	Visibility
	F1	X3	Failure	503	1007	459	360	Visibility
	F2	X3	Success	242	1087	224	280	Visibility
	F2	X3	Failure	332	1047	304	320	Visibility
	F3	X3	Success	320	1087	284	280	Visibility
	F3	X3	Failure	230	1067	212	300	Visibility
T5 605 m	F1	X1	Success	363	1925	353	2950	Visibility
	F1	X1	Failure	503	1845	484	2087.5	Visibility
	F2	X1	Success	242	1925	197	2950	Visibility
	F2	X1	Failure	332	1885	290	2067.5	Visibility
	F3	X1	Success	320	1925	311	2950	Visibility
	F3	X1	Failure	230	1905	221	2057.5	Visibility
	F1	X2	Success	363	2027.5	330	2708.25	Visibility
	F1	X2	Failure	503	1947.5	493	2036.25	Visibility
	F2	X2	Success	242	2027.5	224	2708.25	Visibility
	F2	X2	Failure	332	1987.5	283	2016.25	Visibility
	F3	X2	Success	320	2027.5	275	2708.25	Visibility
	F3	X2	Failure	230	2007.5	202	2006.25	Visibility
	F1	X3	Success	363	2130	353	2466.5	Visibility
	F1	X3	Failure	503	2050	489	1985	Visibility
	F2	X3	Success	242	2130	187	2466.5	Visibility
	F2	X3	Failure	332	2090	326	1965	Visibility
	F3	X3	Success	320	2130	304	2466.5	Visibility
	F3	X3	Failure	230	2110	219	1955	Visibility

10.5.3 Risk estimation

The risk estimation conducted on the configuration with a semi-transverse ventilation system is interesting in terms of FN curves. In fact, a significant reduction of the risk is obtained for both T1 and T5, whose FN curves almost lie in the ALARP zone.

The maximum number of fatalities is the same of the initial configuration, but the frequency associated to this number (which determines the recurrence of the event) is much lower and almost reaches the lower limit of the ALARP zone, which signs the passage to the zone at negligible risk. Instead, the initial part of the curve (which is the portion of the curve where all the frequencies are cumulated) is still slightly higher than the upper limit for T1 (Figure 10.27), whereas for T5 this happens in a much more reduced portion of the graph (Figure 10.28).

However, considering all the hypothesis made, which are on the safe side for the characteristics of the fire (polyurethane reaction, delay in the activation of the transverse ventilation) and also of the occupants (300 seconds as the maximum pre-evacuation time, 0.5 m/s as the minimum walking speed) the curves are considered meaningful and represent a good configuration from the engineering point of view.

The comparison in terms of Expected Value (required by the Legislative Decree) is verified, because the EV of the alternative configuration is lower or at least equal of the reference tunnel's. The slight difference for T1 (0.397 for the reference and 0.408 for the alternative) is not significant: the two values represent the same level of risk (Table 10.17).

Also in this case, the curves are calculated with QRAM and highlight an underestimation of both the cumulated frequency and the maximum number of fatalities.

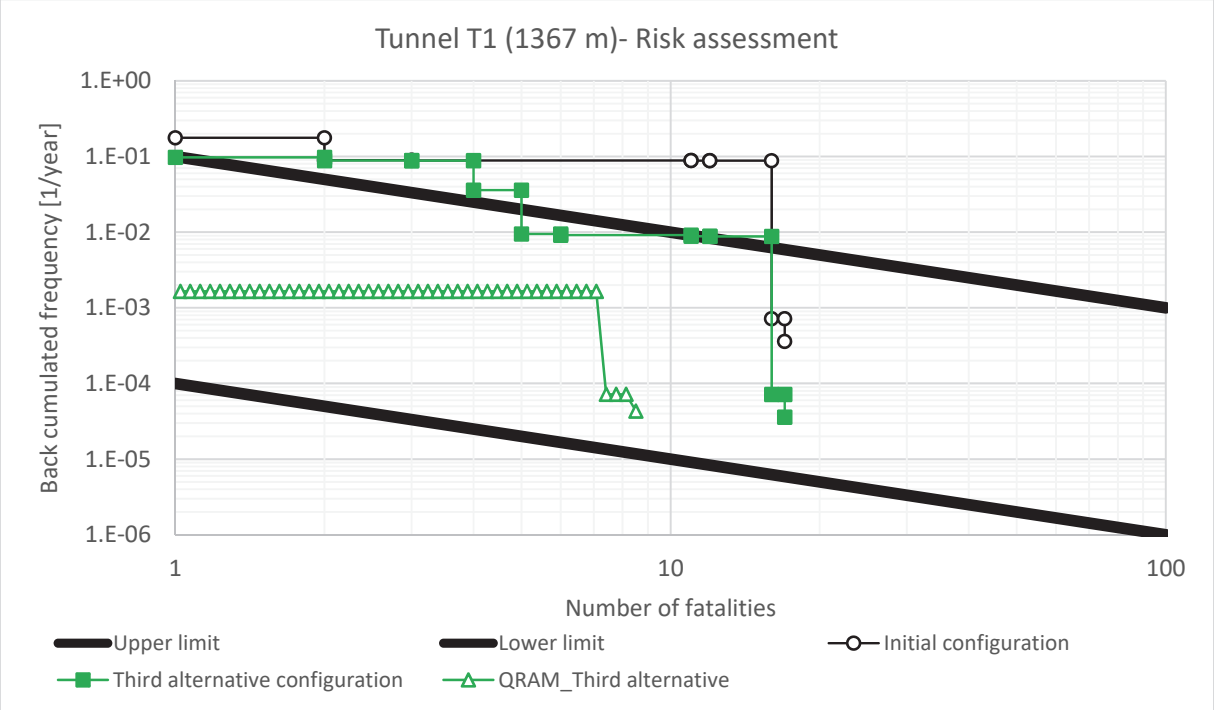

Figure 10.27. FN curve for T1 tunnel (3° alternative vs initial configuration)

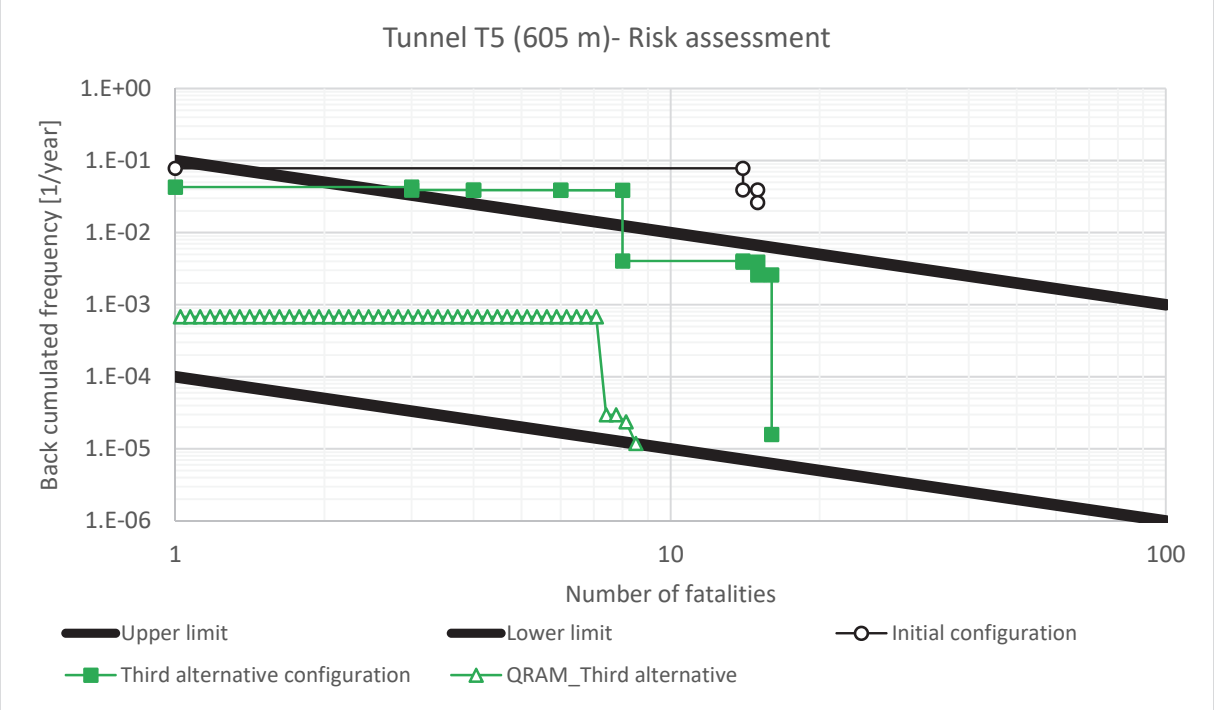

Figure 10.28. FN curve for T5 tunnel (3° alternative vs initial configuration)

Table10.17. Expected Value for the configuration

Tunnel configuration	Expected Value (fatalities/year)	
	T1	T5
Initial	1.409	0.689
Reference	0.397	0.418
Third alternative	0.408	0.311

10.6QRA for the fourth alternative configuration

Also in the case of semi-transverse ventilation system, a configuration with more reliable safety systems is proposed by modifying the probability of success and failure of both detection and ventilation systems, respectively to 0.95 and 0.05.

This fourth and final alternative configuration ideally represents a higher level of management (control centre, CCTV circuit, loudspeakers and lighting panels are added inside the tunnel). The QRA is conducted and risk is estimated also in this case.

10.6.1Fire scenarios

The fire simulations are the same of those contained in section 10.5.1.

10.6.2Evacuation scenarios

The evacuation scenarios are those reported in 10.3.2.

10.6.3Risk estimation

The FN curves (Figures 10.29 and 10.30) are very similar to those of the previous case, with a reduction of the frequency and the resulting Expected Value (Table 10.18).

There is still a portion of the tunnel exceeding the ALARP zone. However, in this case, the modification of the probability of success and failure of the safety systems contributes to the reduction of the risk under the threshold set by the reference tunnel, which makes the solution acceptable for both T1 and T5. The QRAM curve is not drawn because it is not possible to add this type of management measures in the input.

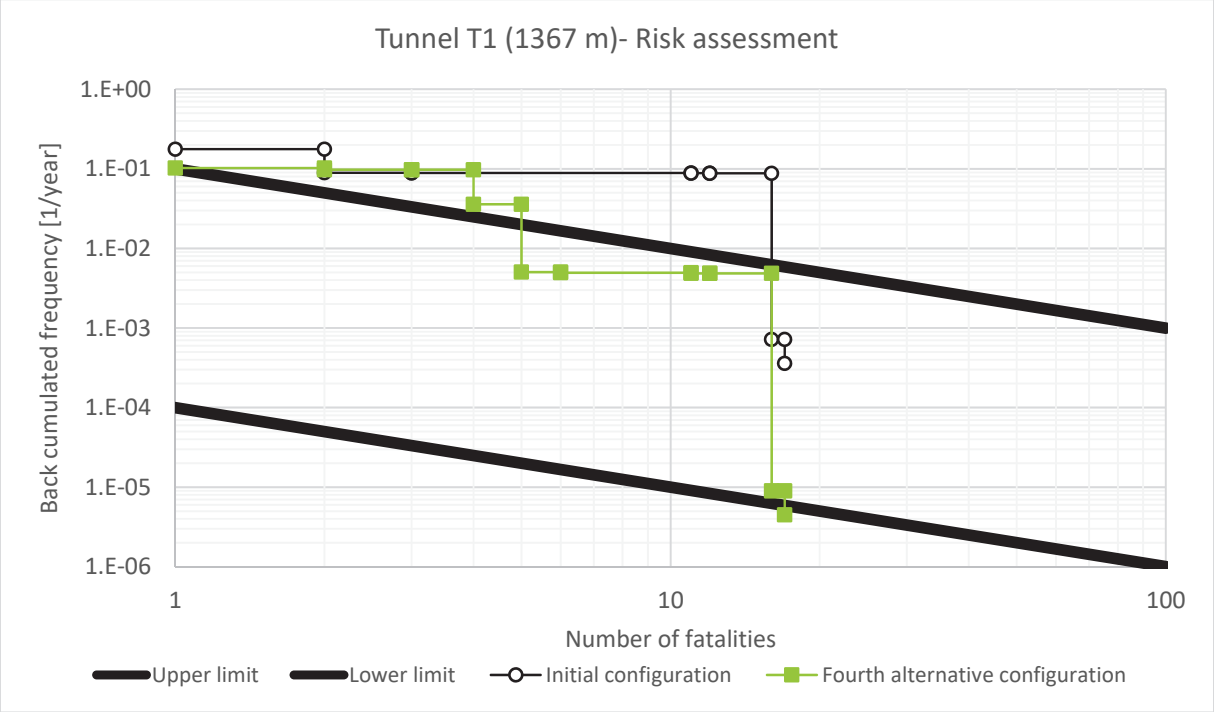

Figure 10.29. FN curve for T1 tunnel (4° alternative vs initial configuration)

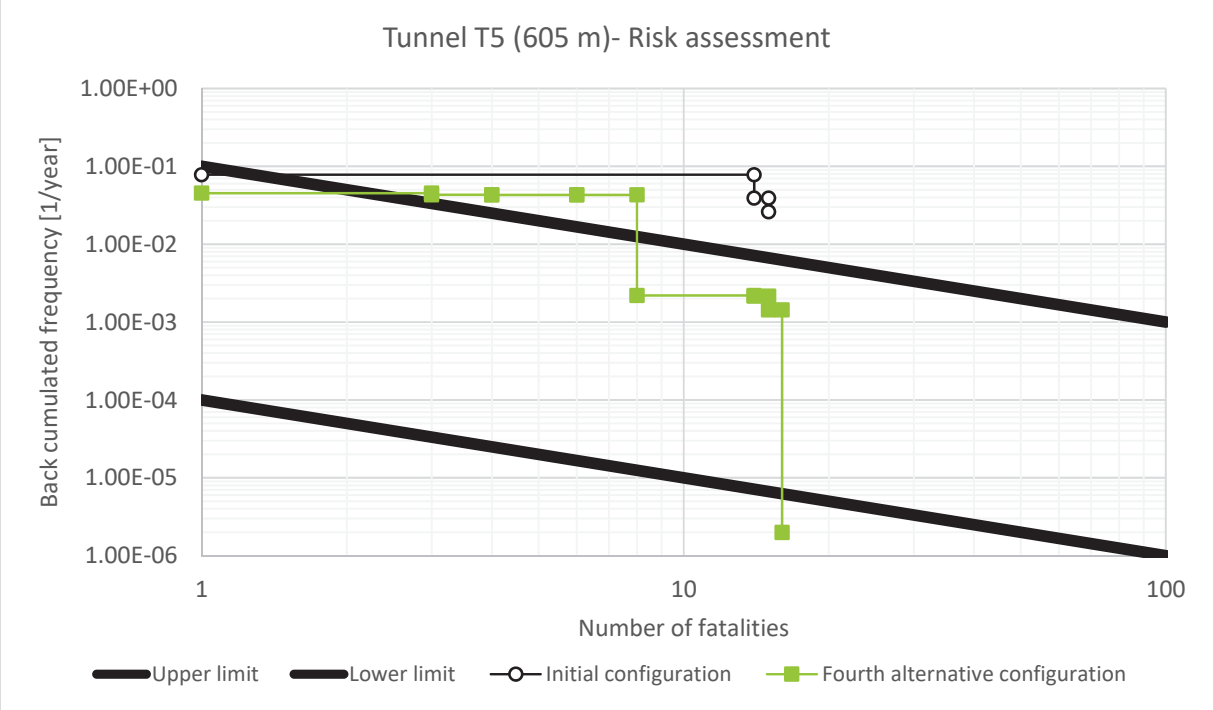

Figure 10.30. FN curve for T5 tunnel (4° alternative vs initial configuration)

Table 10.18. Expected Value for the configuration

Tunnel configuration	Expected Value (fatalities/year)	
	T1	T5
Initial	1.409	0.689
Reference	0.397	0.418
Fourth alternative	0.387	0.322

10.7 Comparisons and comments

The two indicators of risk (FN curves and EVs) are used for a final comparison among all the analysed configurations.

Firstly, considering the FN curves obtained by using the QRAM software, it can be noticed that there is a constant underestimation of the risk (already noticed for the case of unidirectional tunnel). The disadvantages of using an Excel-based approach increase with the complexity of the system. Fire dynamics in case of different ventilation strategies need a direct fluid-dynamics modelling of the area, allowing the risk analyst to really understand the magnitude of the risk, its causes and above all to design alternative measures and evaluate numerically the reduction of the risk. The following considerations are made on the curves obtained through advanced modelling, considered more reliable and on the safe side.

Considering tunnel T1 (figure 10.31 and 10.32), the initial configuration shows a non-acceptable risk. The FN curve, in fact, exceeds the upper limit of the ALARP zone and, for this reason, alternative configurations of the tunnel are proposed. The adopted procedure of QRA with advanced consequence analyses seems very precise to measure the difference of risk when alternative measures are inserted.

For example, the tenable conditions obtained by the adoption of a longitudinal ventilation system are worse compared to the initial configuration, where only natural ventilation is considered. Natural ventilation, in fact, is able to provide a stratification of smoke up to a certain distance from the fire source: then, basically when the

temperature of the smoke decreases, the two zones subdivision (upper zone with hot smoke, lower zone with fresh air) is not guaranteed anymore and destratification occurs. On the other hand, the longitudinal ventilation is very dangerous for those occupants that find themselves in the same direction of the jet fans. Jet fans, in fact, are effective in protecting the zone upwind the fire source and for this are normally implemented in unidirectional tubes, but for bidirectional cases they can expose people to smoke effluents, causing mainly a loss of visibility and an increment of temperature.

The semi transverse ventilation system instead provides a reduction of the risk: the related FN curve is slower than the initial configuration and the EV is even slower than the EV of the reference tunnel. This is very positive, because it implies that the adoption of a semi transverse ventilation system with smoke extractors can substitute the presence of emergency exits at the required distance of 500 m. The same conclusions can be drawn for tunnel T5 (Figures 10.33 and 10.34).

Comparing the EVs of the initial configurations of T1 and T5 tunnels it can be noticed that their ratio is almost a factor of two. This is because both tunnels have no ventilation nor means of egress system, but the length of T1 is double of T, and the length is computed in the procedure when the frequency of the initiating event is calculated (the set of values of CETU and the other standards are normalised to kilometres).

The EVs of the references configuration, instead, is the same for T1 and T5 and this ensures that the procedure is correctly working. In fact, the reference configuration is the one that complies with the minimum requirements of the European standards and, therefore, no matter what the length of the tunnel is, the risk for people driving is the same. The FN curves of the reference configurations are not identical because the minimum requirements depend on the length of the tunnel: therefore, T1 is equipped with a semi transverse ventilation system, whereas T5 has only natural ventilation.

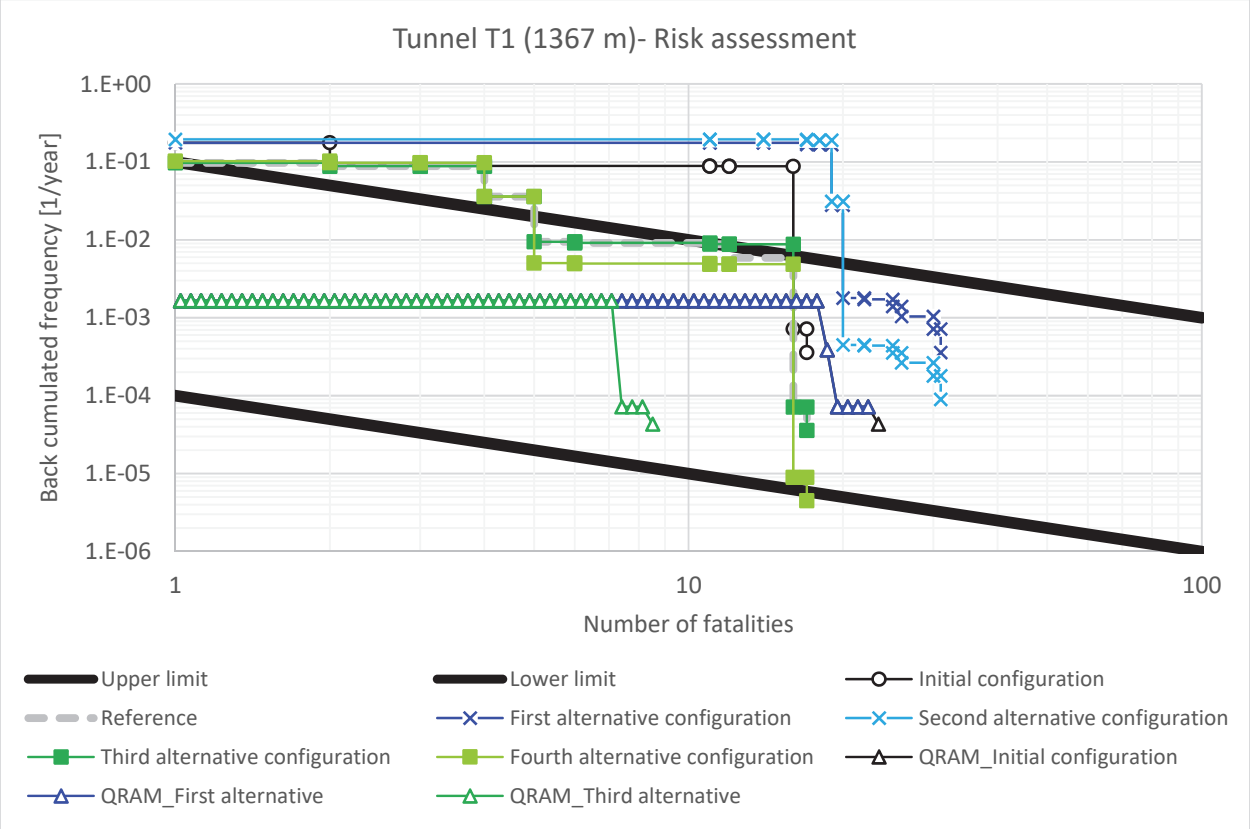

Figure 10.31. FN curve for T1 tunnel (all configurations)

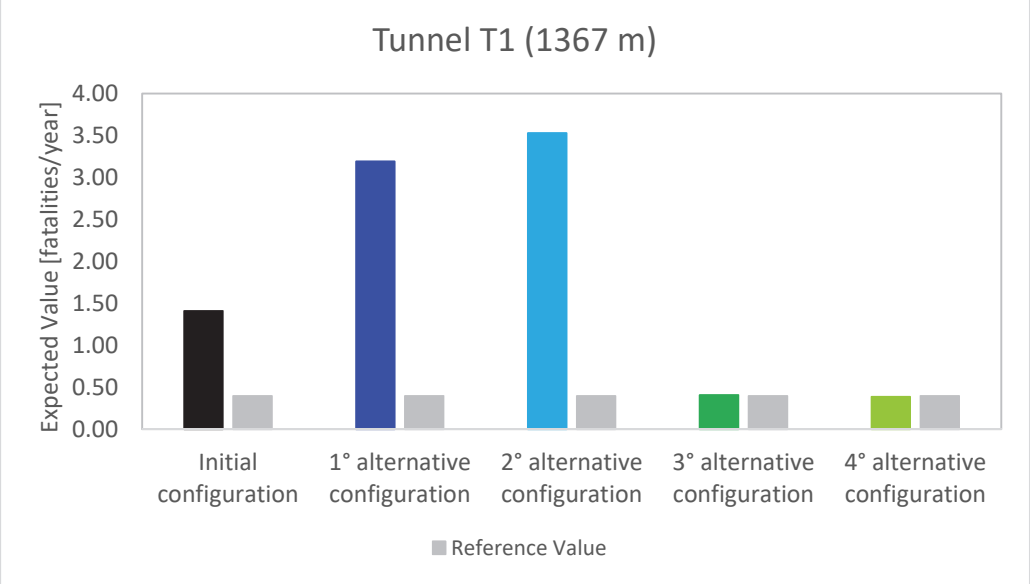

Figure 10.32. Expected Value for T1 tunnel (all configurations)

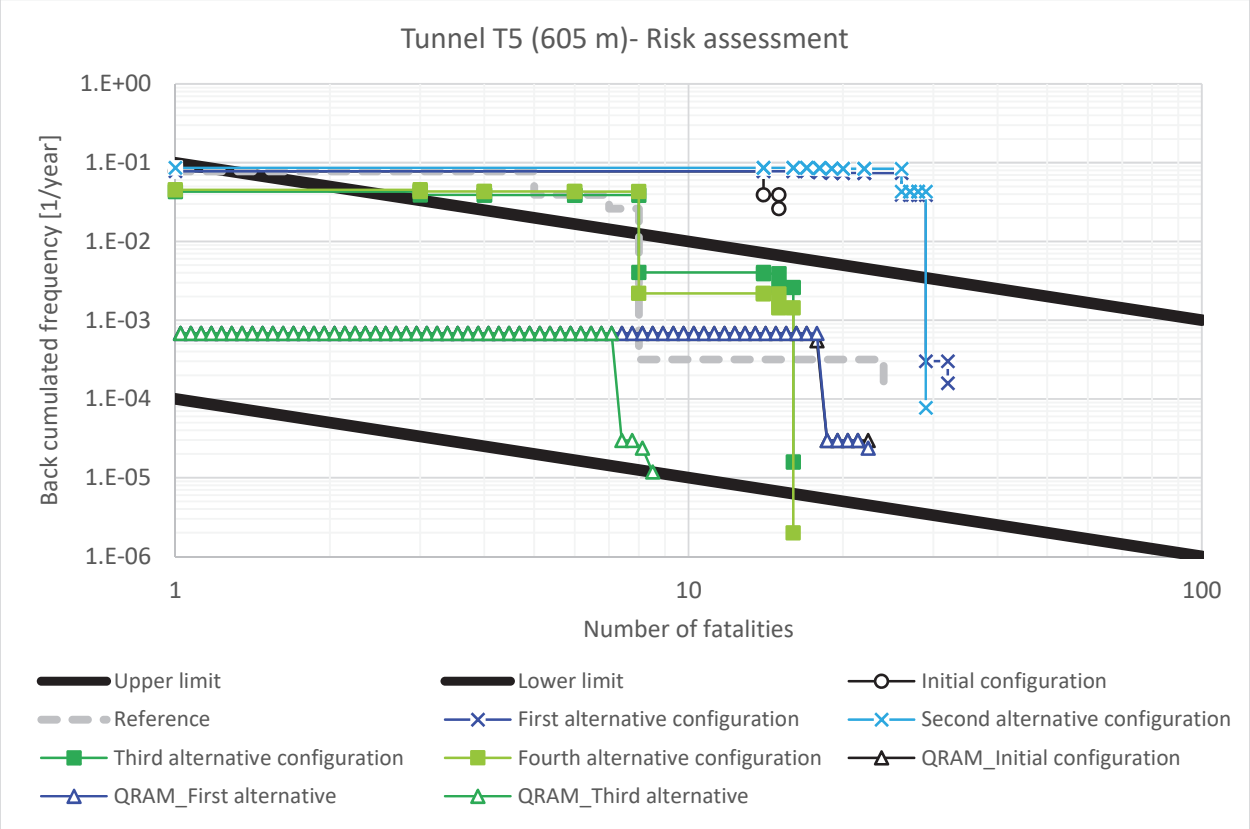

Figure 10.33. FN curve for T5 tunnel (all configurations)

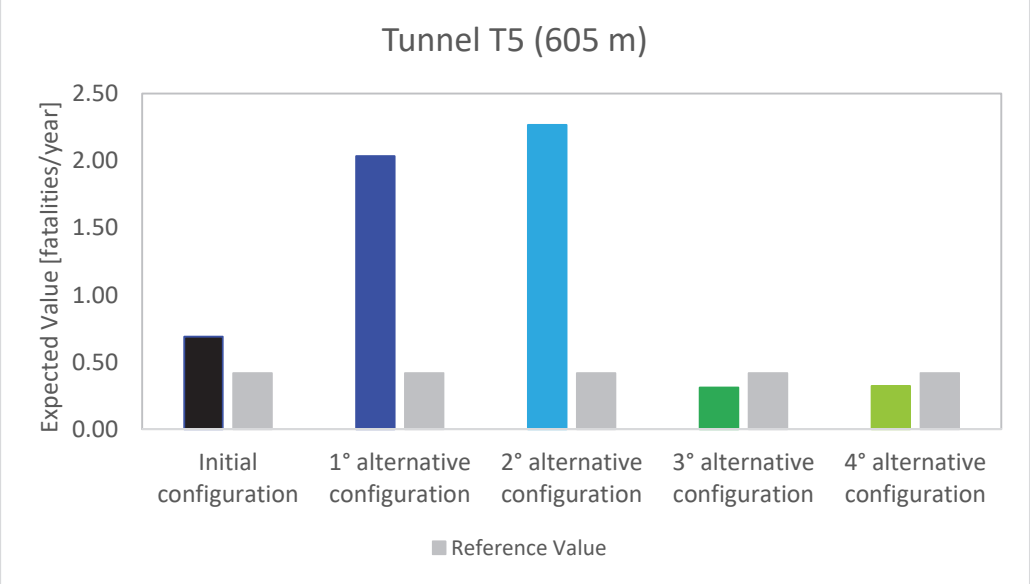

Figure 10.34. Expected Value for T5 tunnel (all configurations)

The choice of representing the increased level of reliability of the systems through a different level of probability of success and failure result in a decrement in the risk for semi transverse ventilation systems, but a slight increment occurs in the case of longitudinal ventilation systems. In other terms, the factors have different weight on the scenarios and probably if one wants to consider the effect of a higher level of management, the modifications of the probability must be coupled with new fire and evacuation scenarios (i.e. modifying the time to detect the fire and the occupants).

It must be admitted that the FN curves do not lie entirely in the ALARP zone. This can be due to many aspects: firstly, for both tunnels the conditions of traffic are very conservative, because a homogenous traffic volume for the two directions of travel is considered. In addition, the fatalities are calculated according to the visibility criterion, which appear to provide much more penalty compared to the other criteria of temperature, FED and radiative heat flux gas. However, it is worth remembering that the acceptability thresholds are absolutely in line with the state of the art in the fire safety field and are fixed according to the most recent fire prevention standard in Italy (2015) when FSE approach is used for life safety verifications.

Finally, among all the alternative strategies the effect due to the adoption of new emergency exits is not directly investigated in this Chapter as an alternative solution. This is because in case of bidirectional tunnels (single tube) that solution is often not practicable and is feasible because of an unbalanced cost benefit ratio (dedicated emergency tunnels can be very expensive). However, some results can be shown because the risk estimation of the reference configuration of T1 and T5 is made considering also the availability of emergency exits. The Figures 10.35 and 10.36 show the evacuation paths for the reference tunnels (equipped with emergency exits placed homogenously so as to not exceed 500 metres). The maximum evacuation time never exceeds 600 seconds, a very low value (similar to those generally found for building

compartments). Therefore, the solution is certainly the safest in terms of time to exit the area, but as it has been demonstrated in the Chapter, the adoption of alternative and correctly designed measures allows to mitigate the risk up to a tolerable level, as the regulations require.

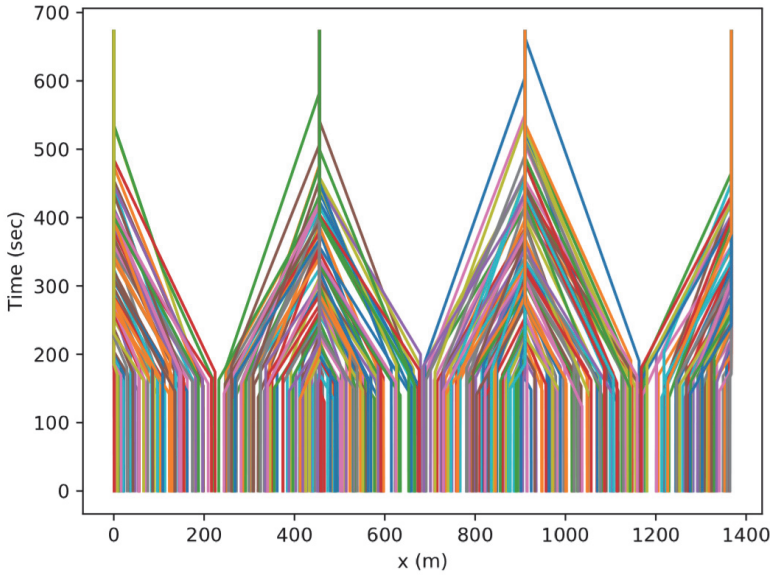

Figure10.35. Time-space evacuation paths for reference T1 configuration

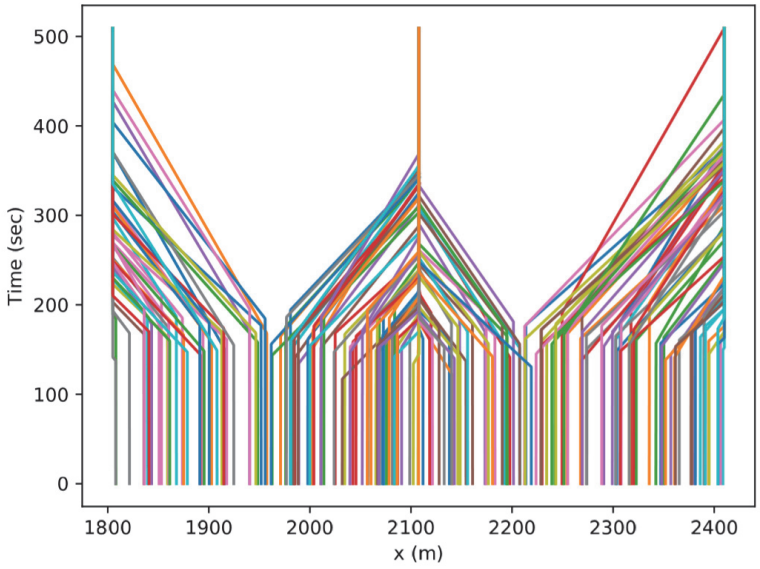

Figure 10.36. Time-space evacuation paths for reference T5 configuration

10.8 Assessment of the tenability conditions in the rockfall galleries

The risk analysis for tunnels T1 and T5 is carried out as they were isolated from the rest of the tunnel system. This implies that the extremities of tunnels T1 and T5 are considered a "safe place" in terms of tenable conditions, that is people who reach that location are accounted as they have been safely evacuated.

However, this is a simplified assumption. In fact, both tunnels have one of the extremities that is a rockfall gallery instead of an exit portal, with only one lateral wall equipped with vertical openings. Therefore, as the consequence analysis is carried out with the use of advanced models, it is reasonable to verify directly with CFD simulations if the tenability thresholds are not reached in those places.

A new model is considered: the overall length is still 400 metres, but 100 metres of this length is equipped with lateral openings, reproducing the rockfall section.

Two different ventilation conditions are analysed and both the extremities of the tunnels are considered:

- natural ventilation (according to the prevalent traffic flow, which is in the direction T1 → T5);
- longitudinal ventilation system, with jet fans in the direction T1→T5 (Figure 10.37).

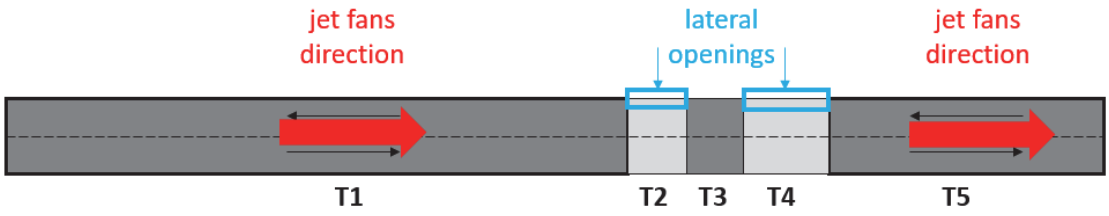

Figure 10.37. Sketch of the longitudinal ventilation system

The analysis is not conducted for the case of semi transverse ventilation system because it has been previously demonstrated that the smoke extractors are able to confine the smoke efficiently. Some results are reported in the following images in terms of visibility trends because the other quantities do not meet the limiting threshold.

10.8.1 Boundary between tunnel T1 and rockfall T2

The visibility in the rockfall section does not always exceed 10 m. When jet fans blow air in the rockfall's direction, the visibility drops under the threshold for F1, F2 and F3. In case of natural ventilation, instead, this happens for F2 and F3 scenarios.

However, the achievement of the untenable threshold is only related to visibility, whose drops are in the order of 1-2 metres. This is certainly not enough to orientate inside a building or a fire compartment, but is considered to be enough to wait for rescuers or at least to breathe fresh air while not moving (visibility is for orientation but you do not need to orientate if you are next to a window). See Figures 10.38-10.43.

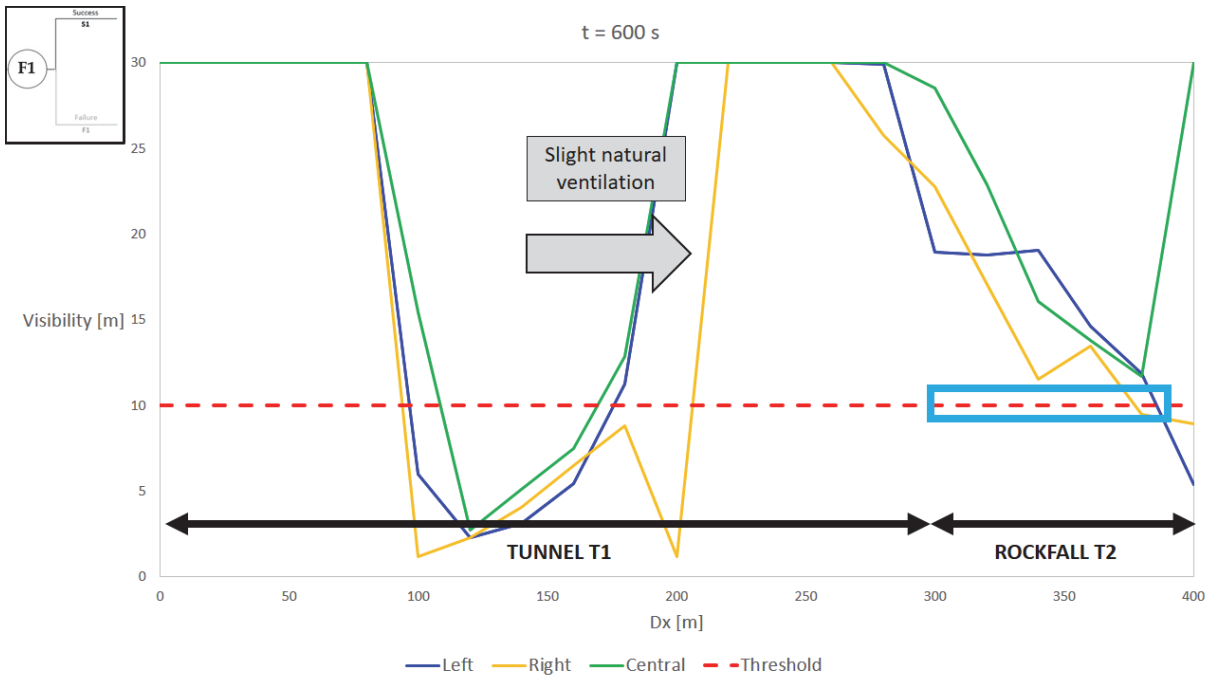

Figure 10.38. Visibility at z=2 m at the boundary T1-T2 for F1 and natural ventilation

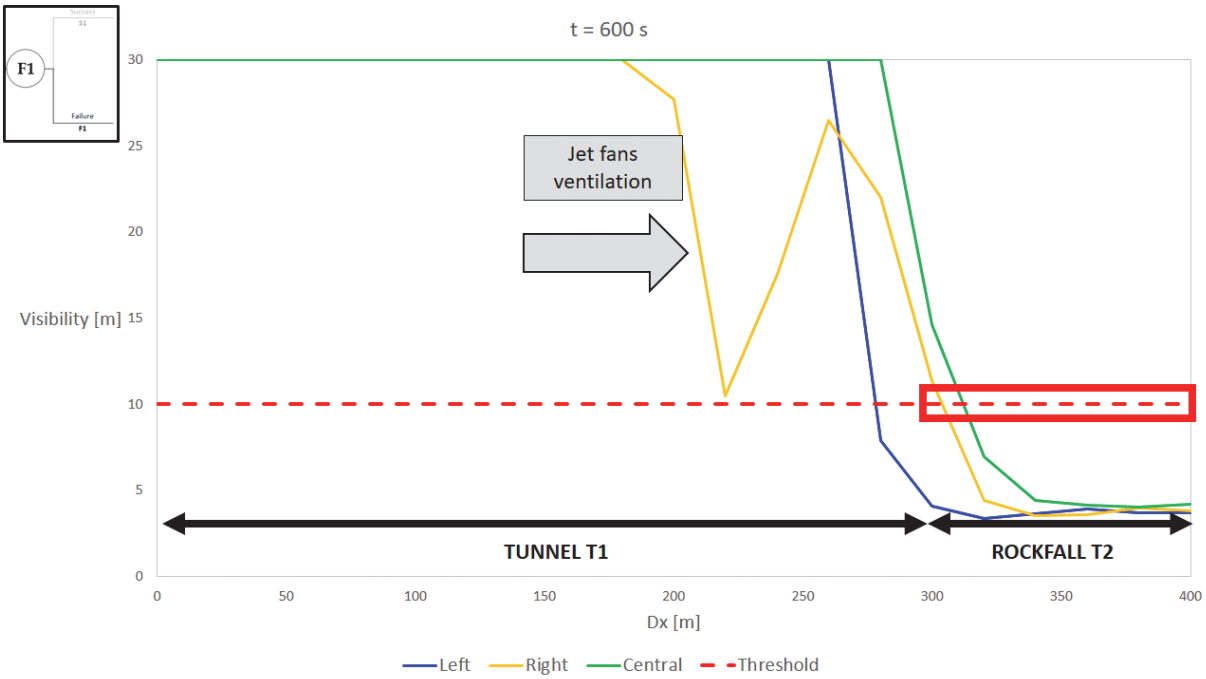

Figure 10.39. Visibility at z=2 m at the boundary T1-T2 for F1 and longitudinal ventilation

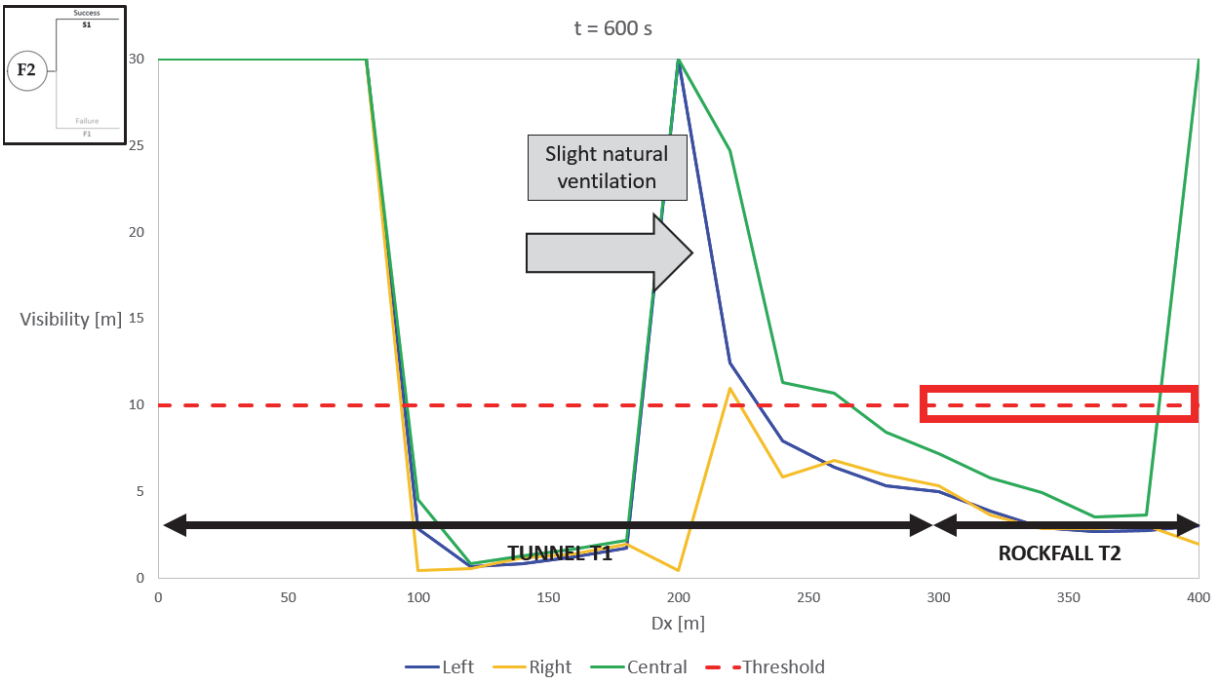

Figure 10.40. Visibility at z=2 m at the boundary T1-T2 for F2 and natural ventilation

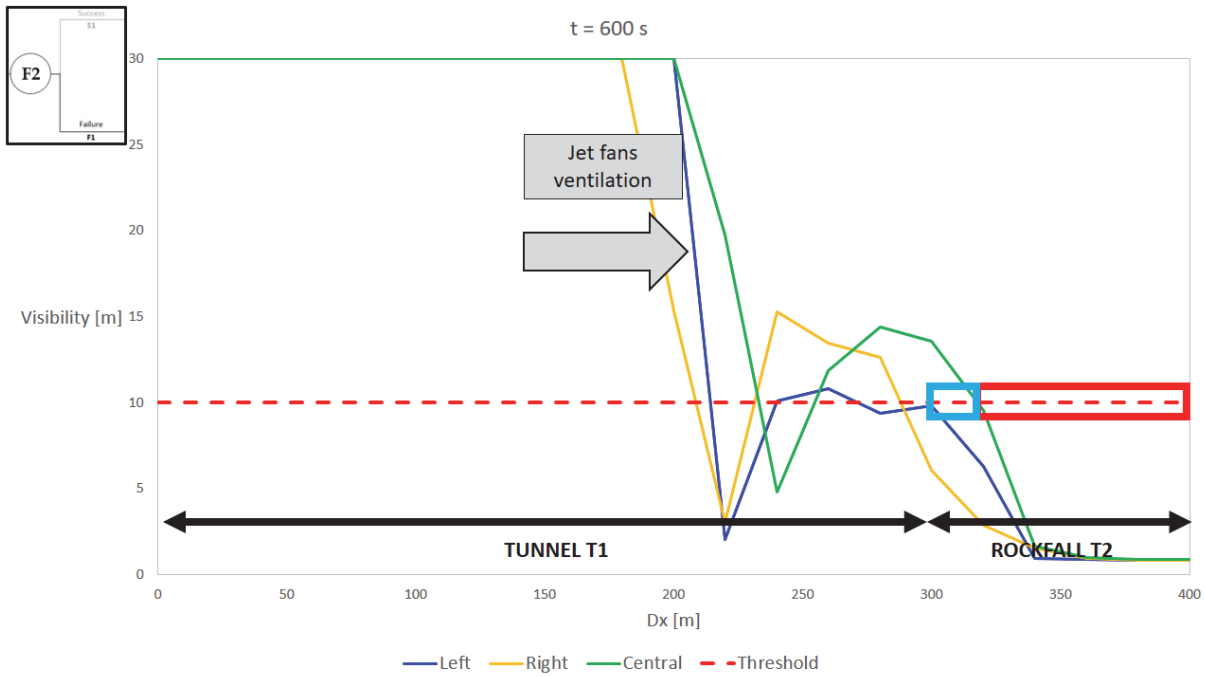

Figure 10.41. Visibility at z=2 m at the boundary T1-T2 for F2 and longitudinal ventilation

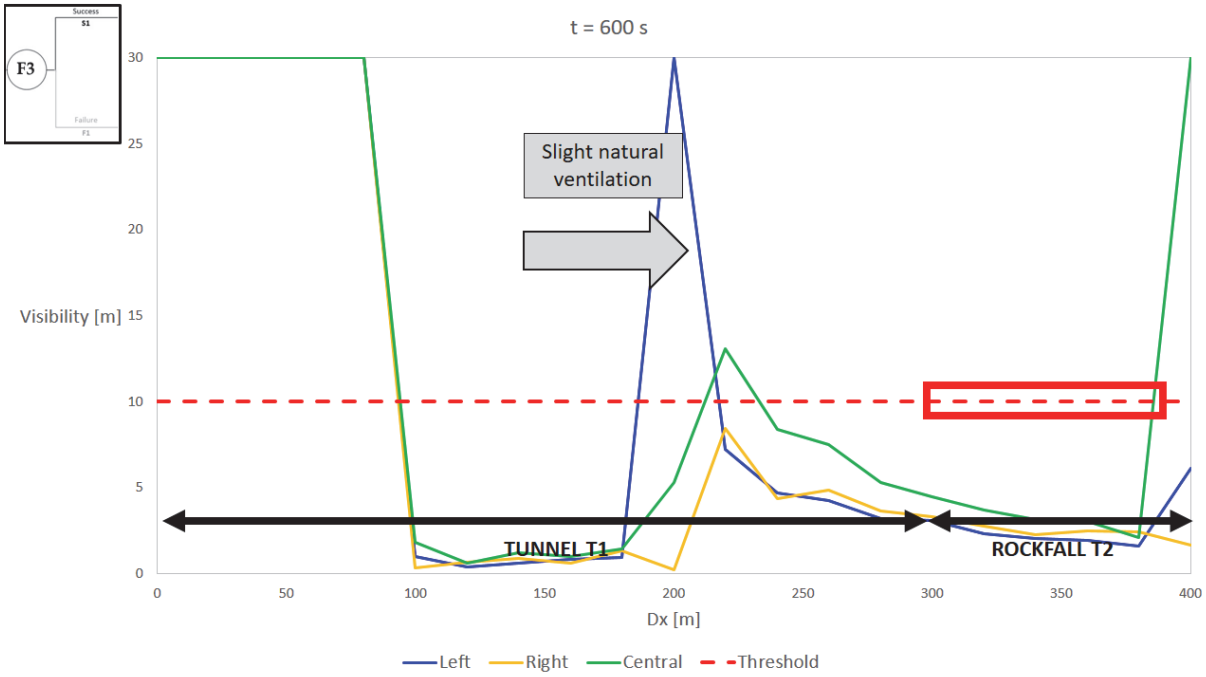

Figure 10.42. Visibility at z=2 m at the boundary T1-T2 for F3 and natural ventilation

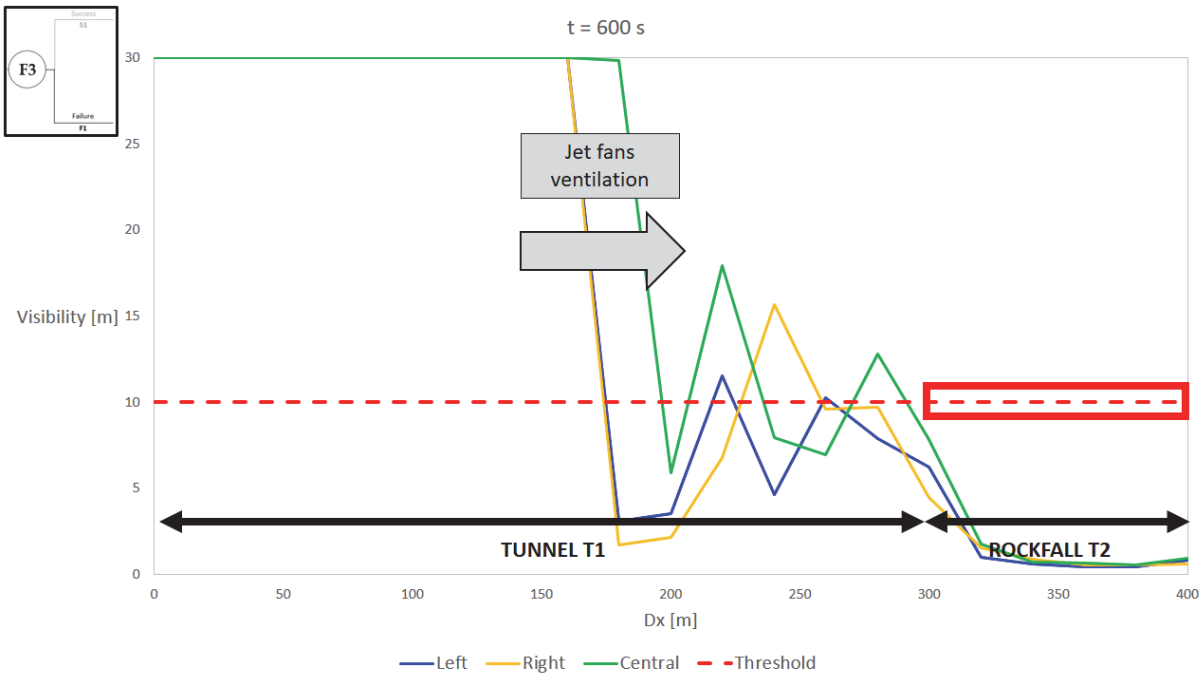

Figure 10.43. Visibility at z=2 m at the boundary T1-T2 for F3 and longitudinal ventilation

10.8.2 Boundary between rockfall T4 and tunnel T5

In this case, the longitudinal ventilation system blows air in the opposite direction of the rockfall tunnel (that is, towards T5) and coherently the rockfall tunnel T4 does not meet the tenability thresholds for the three selected scenarios.

On the other hand, in case of natural ventilation, as for the boundary between T1 and T2 the visibility criterion meets its threshold for F2 and F3. Even in this case the occupants who are in that location are not considered to be exposed to exaggerated risk because the toxicity level (which is actually lethal) is much lower than the threshold and the occupants do not need to orientate themselves to reach the exit because they are next to vertical openings. See Figures 10.44-10.49 for the various cases.

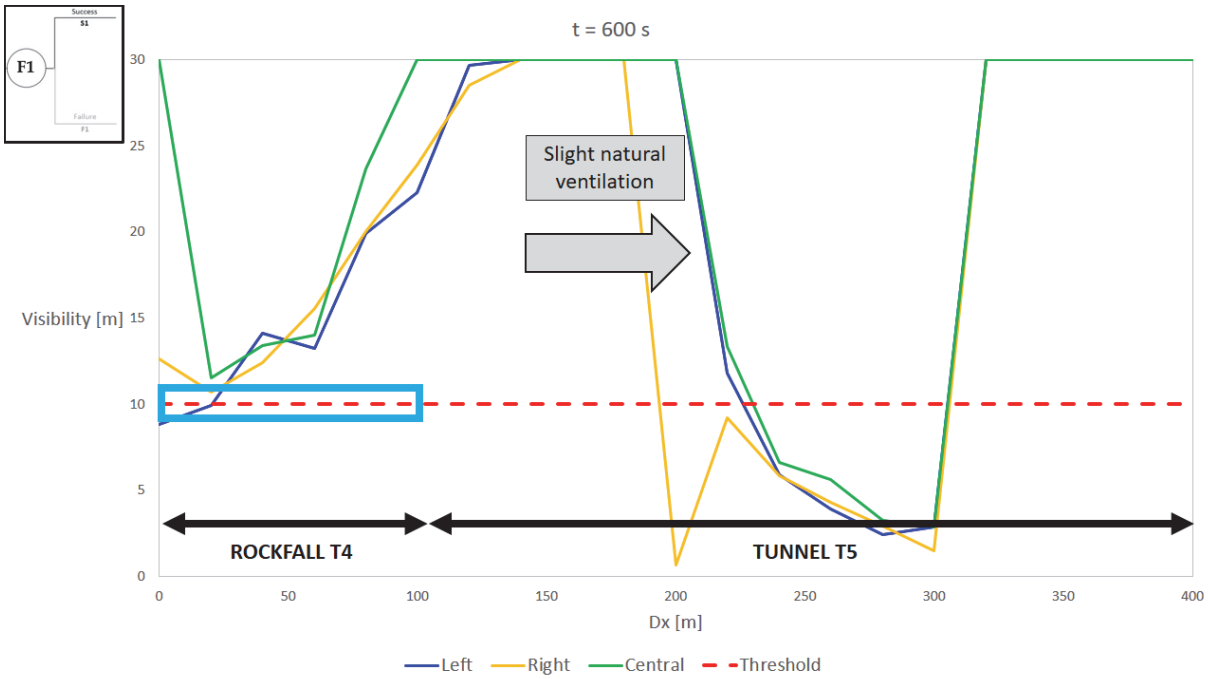

Figure 10.44. Visibility at z=2 m at the boundary T4-T5 for F1 and natural ventilation

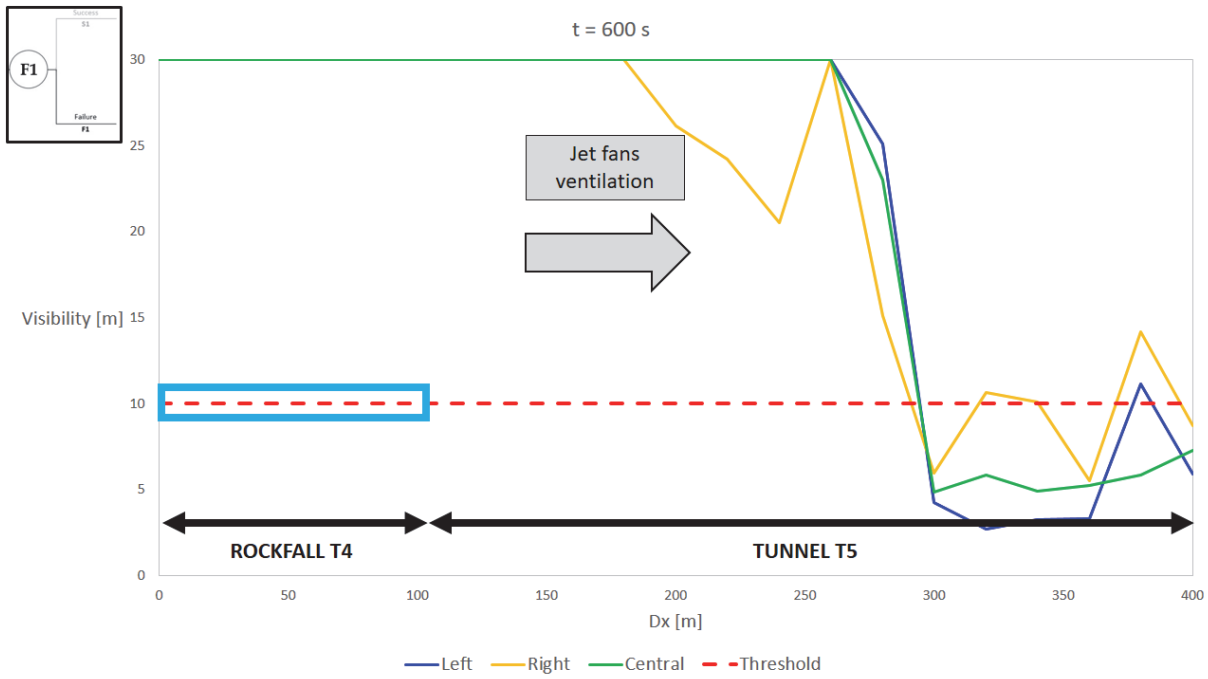

Figure 10.45. Visibility at z=2 m at the boundary T4-T5 for F1 and longitudinal ventilation

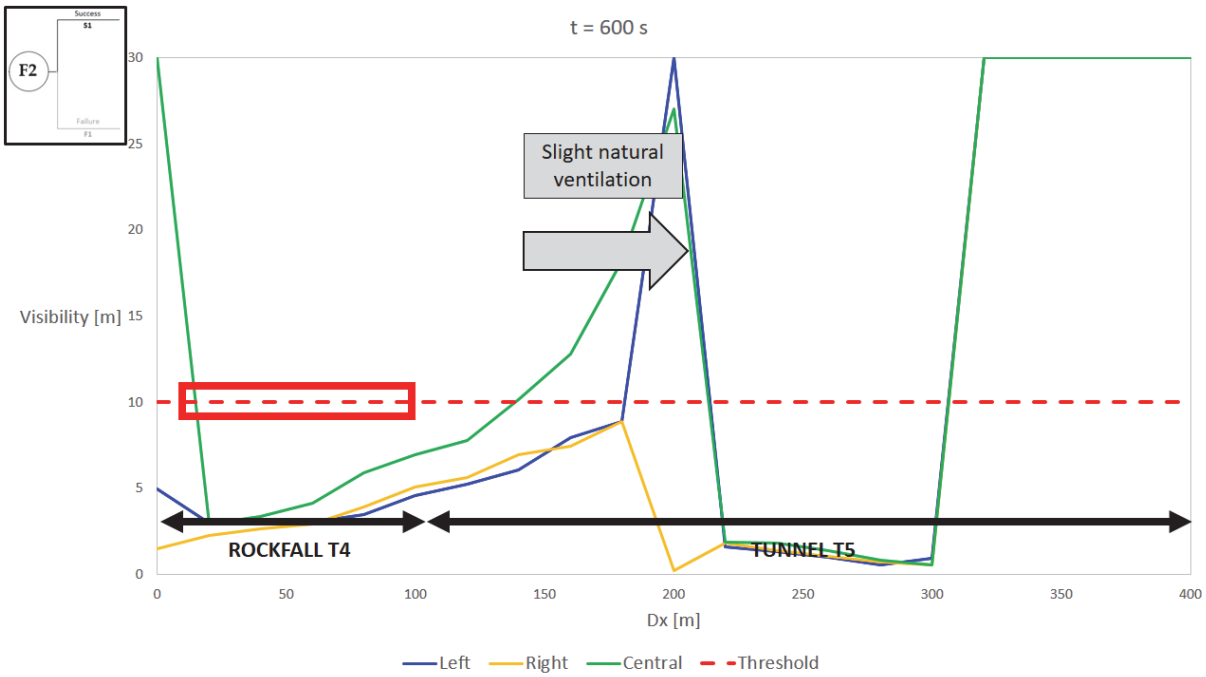

Figure 10.46. Visibility at z=2 m at the boundary T4-T5 for F2 and natural ventilation

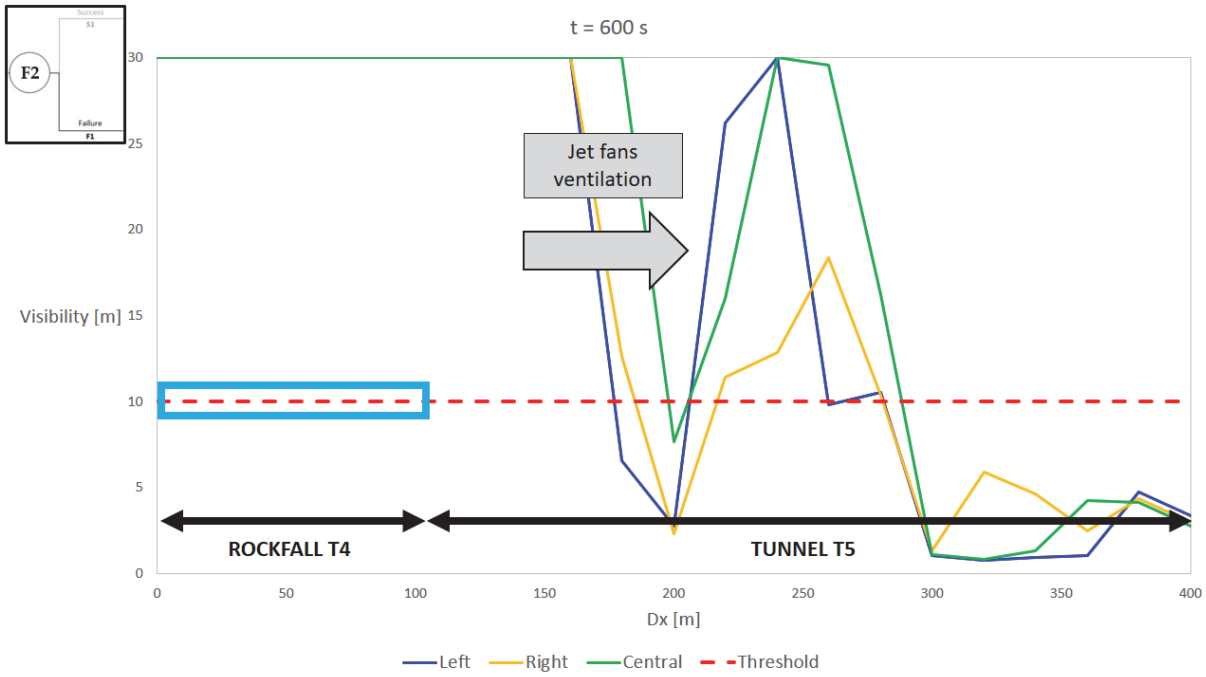

Figure 10.47. Visibility at z=2 m at the boundary T4-T5 for F2 and longitudinal ventilation

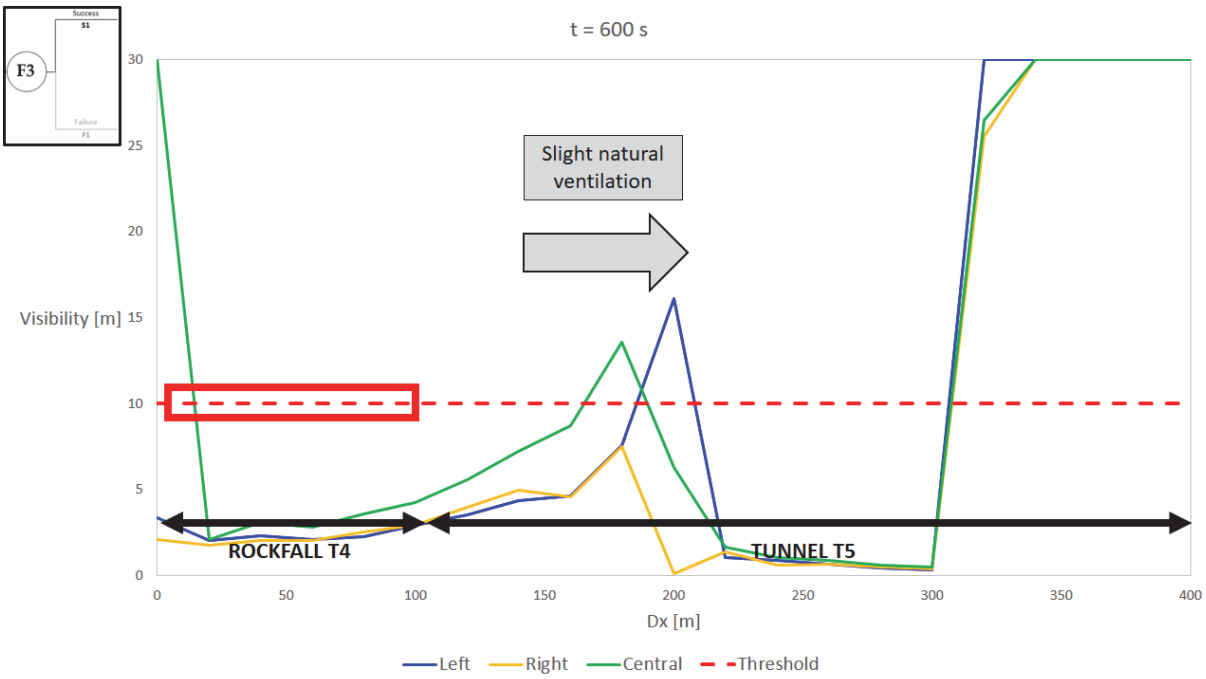

Figure 10.48. Visibility at z=2 m at the boundary T4-T5 for F3 and natural ventilation

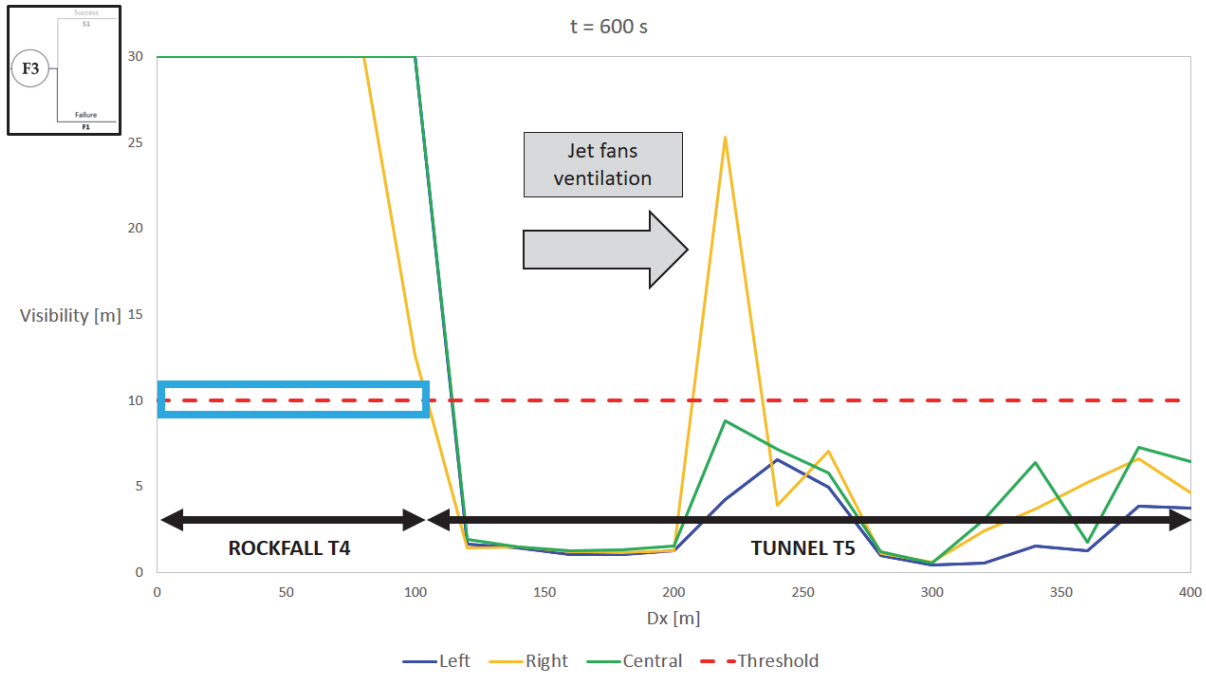

Figure 10.49. Visibility at z=2 m at the boundary T4-T5 for F3 and longitudinal ventilation

CONCLUSIONS

CONCLUSIONS

CONCLUSIONS

Conclusions

The thesis is focused on the fire risk of road tunnels and its assessment through advanced consequence analysis carried out with CFD and evacuation models. The attention is given to fire events due to light and heavy good vehicles' accidents in case of single or double direction of travel.

The case history of major fires tells us that road tunnels are particularly sensitive to fire accidents. The geometrical configuration of a confined and long structure facilitates the horizontal propagation of smoke effluents, which can be very rapid if the tunnel is not equipped with a proper mechanical ventilation. The backlayering phenomena and drops of the layer height can deteriorate the tenable conditions even hundreds of meters far from the fire source, causing injuries and fatalities if the occupants have not completed the evacuation yet.

The European Directive 2004/54/EC states the minimum requirements that road tunnels should have in order to reduce the risk under a tolerable level. However this path can be difficult, especially for existing road tunnels that need expensive and sometimes technically impracticable refurbishment. In that case, the jurisdictional authorities have to evaluate the proposal of alternative configurations of the given tunnel, equipped with additional measures to compensate the risk due to the non-conformity to the minimum requirements of the Directive. The modification of the initial level of risk associated to the choice of alternative configurations has to be numerically estimated through quantitative risk analysis (QRA), which is identified as the only tool able to

catch all the significant aspects that contribute to the overall complexity of road tunnels including, for example, geometry, traffic, HGVs percentage, safety systems. In the context of road tunnels, fire risk is a function of the frequency of the critical events (in the thesis, fires due to vehicles) and their consequences, expressed in terms of fatalities. Therefore, the risk is generally measured referring to indicators of societal risk: back-cumulated frequency-fatalities curve (FN) and Expected Value (EV) measured in fatalities/year.

The methodology of the QRA as well as the criteria for the risk acceptability are addressed by the Member States; in Italy, the Legislative Decree 2006/264 states life safety as the objective of the QRA and comparative criteria for the acceptability of the alternative configurations, defined in relation to the reference tunnel. However, the details of how to conduct the frequency and the consequence analysis for the numerical estimation of the risk indicators are not included. This is explicitly treated in the thesis, in which the detailed procedure of QRA where the consequence analysis is based on advanced fire and evacuation modelling is contained, including the basis for the selection of fire and evacuation scenarios appropriate for life safety verifications (Chapter 8).

The steps that compose the procedure of quantitative risk assessment for road tunnels are not new: the World Road Association (PIARC) has published lots of technical documents which act as a guide for the design, refurbishment and maintenance of road tunnels. However, it emerges that the current design practice is not homogenous among the Member States and sometimes is orientated towards a quick risk assessment that, however, does not deserve the appellative of quantitative risk assessment. In addition, considering all the uncertainties affecting the real tunnel system and its representation in terms of sub-systems, which represent the basis for the Fault Tree Analysis and Event Tree Analysis, it should, at least, be verified that the adopted numerical procedure gives

conservative results as outputs. For this reason, the QRAM software is reviewed in Appendix D and the results, limited to fire scenarios, highlight that despite its user friendly interface and fast calculations, it is not able to take into account the variation of some parameters, including, for example, the average distance among the exits and the volume flow provided by the longitudinal ventilation system. This implies that the software is not able to correctly assess the mitigating or deteriorating effect related to the adoption of alternative measures like additional emergency exits and increment of the number of jet fans.

The awareness of the need of a comprehensive approach, supported by reliable and accurate numerical tools able to quantify the effect of selected measures in terms of risk indicators, drives the attention to fire and evacuation models. They are considered advanced tools according to the state of the art in the fire prevention field, because they allow for the most detailed description of fire dynamics and evacuation patterns. They are systematically used in Northern Europe, but their use is increasing in Italy thanks to the recent evolution of fire regulations.

Before using these models for the risk estimation of road tunnels, independent parametric and sensitivity analysis are conducted on the fire model Fire Dynamics Simulator FDS (Chapter 5 and Appendix C) as well as the evacuation models Pathfinder and FDS+Evac (Chapter 7).

FDS is investigated in the case of a short tunnel (100 m), different levels of HRR and steady state conditions. The parametric analysis highlights that near the fire source the macroscopic quantities (temperature, radiative heat flux gas, visibility and FED) can be significantly affected by the modifications of the input parameters, but this effect rapidly decreases by furthering away from the fire source. Above all, it emerges that FDS model is sensitive to the parameters involved in the implementation of alternative measures of fire safety, aimed at reducing the initial risk. Pathfinder and FDS+Evac are

used to perform evacuation simulations for simple geometries and different initial densities. Pathfinder is considered more conservative, because it provides for slightly higher results with equal input values of the parameters. The other results of this part of the thesis are detailed in the body of the text.

The previous analysis on FDS and Pathfinder are used to support the proposed methodology, suitable for existing tunnels for which alternative measures are needed to mitigate the risk. The methodology, which is developed through the definition of the Event Tree, is finally applied to two case studies, based on real Italian tunnels.

Specifically, the first case study is a double bored unidirectional tunnel, where the initial configuration does not comply with the EU requirements because the average distance among the exits exceeds 500 m. The quantitative risk analysis is conducted firstly for the initial configuration and then for two alternative configurations equipped with more powerful mechanical ventilation and, in addition, management strategies to monitor and control the traffic in the tunnel. The FN curve related to the improved configurations are still in the ALARP zone of the FN diagram, but the EV is right under the threshold set by the reference configuration.

The second case study, instead, is a bidirectional tunnel system and highlights that the presence of a double direction of travel inside the same tube makes the overall system intrinsically riskier in terms of Expected Value compared to the previous unidirectional tunnel. The initial configuration (with no ventilation nor emergency exits) is in the non-acceptable zone (over the upper limit of the FN diagram) and mitigation strategies consisting of different ventilation systems are evaluated. In the case of symmetrical traffic conditions, the longitudinal ventilation system gives worse results in terms of risk indicators and is not acceptable also considering that the Expected Value is much higher than the referred tunnel's. On the contrary, the adoption of the semi transverse ventilation system with smoke extractors every 200 meters provides a significant

reduction of risk, with the resulting Expected Value decreasing under the referred tunnel's.

The case studies are single realisations of a large variety of cases that can be found in the European road network, but they are representative of the situation of many existing tunnels that do not comply with the minimum structural requirements of the correct average distance among the exits (European Directive 2004/54 EC).

The results cannot be generalised but demonstrate that the methodology is suitable for evaluating the improvement or the deterioration of the tenable conditions induced by the adoption of a certain measure in the tunnel system. The methodology is, in fact, based on models that are sensitive to the modifications of the conditions that determine the Available Safe Egress Time and the Required Safe Egress Time for the given tunnel.

The steps illustrated from the theoretical and practical point of view can be, therefore, a valid basis for the designers who have to propose and assess the effect of the alternative measures and, moreover, for the jurisdictional authorities who need to evaluate the proposal and approve the best alternative configuration in terms of risk reduction and cost-benefit ratio.

Appendix A

Pressurised enclosure: tests and CFD

Analytical design of pressurised systems

One of the first tasks in the design stage of a pressurisation system involves considerations of the minimum air supply for the maintenance of a specific performance requirement. For an enclosure provided with an air supply and separating two compartments, the first requirement is to maintain a minimum overpressure inside the internal volume; the second requirement is to obtain a minimum velocity of the air exiting from the enclosure when the door bounding with the fire floor is opened.

Usually the boundaries of the system may consist of walls, doors and windows: gaps around doors, unintentional cracks in walls and direct openings represent leakage paths. The desired overpressure is maintained by a properly designed ventilation system, conceived to achieve a given airflow compensation as determined through the leakage area.

The pressure criterion states that the air supply is a functional of the pressure differential between the internal enclosure and the external volumes, the cross sectional area of the leakage paths out of the enclosed space and their discharge coefficients. Butcher and Parnell (1979) give an equation based on the Bernoulli equation for steady and incompressible flow and standard air density (1) for the simplified pressure system design.

$$Q = KAP^{1/N} \tag{1}$$

where:

- Q (m^3/s) is the air supply;

- A (m^2) is the total cross sectional area of the leakage paths out of the enclosed space;

- P (Pa) is the pressure differential ($P = P_1 - P_2$) between the inside and outside of the enclosure;

- K is the discharge coefficient of the leakage paths of the barrier (= 0.827 for the units selected);

- N is a coefficient varying between 1 and 2 (usually set to 2 for doors and 1.6 for windows).

Since the leakage is expected to occur only along the perimeter of the doors, A is analytically calculated by multiplying the length of the edges for a discharge surface estimated as 0.0035 m^2/m for each enclosure door (usually discharge surface vary in the range 0.0017 and 0.0040 m^2/m (Butcher et al, 1979)).

It is worthwhile to note that a relation similar to (1) is included in the EN 12101-6 standard, where it is also recommended for design purpose of the air supply to apply a safety factor of 1.5. Regarding the leakage along the perimeter of the doors, the EN 12101-6 recommends higher values for the discharge surface: 0.01 or 0.02 m^2/m for doors opening respectively inwards or outwards the pressurised enclosure. However, considered the attention given to minimise the gaps through door sealing systems, the set of values recommended in (Butcher et al, 1979) seems to be a reasonable choice.

In this research, only the leakage through the edges of the doors is considered because the walls, ceiling and pavement of the experimental test rig are made of metal sheets and protected by cover plastic sheets, therefore it can be assumed that there are no gaps. Applying the relation (1) to the experimental test rig, the 30 Pa pressure differential (minimum level according to the Italian standard requirements) is reached by an airflow of about Q = 0.194 m^3/s (698.4 m^3/h), which applying a safety coefficient of 1.5, requires an air supply of about 1050 m^3/h. On this basis, it has been selected a commercial fan

(oversized with respect to the nominal calculated airflow) with variable manual speed selection and a maximum capacity of 1630 m^3/h, in order to pressurise the enclosure even at higher level of overpressure.

Since the experimental set up is not equipped with an automatic control system of the airflow with the pressure level, the velocity criterion across opened doors is not directly used for the design, as EN 12101-6 would require.

Velocity across the doors are intensively studied as a result of more advanced design. Other issues such as velocity profiles and measurement points appear of primary importance to deepen the understanding of the phenomena associated with the depressurisation of an enclosed space and assess different geometrical configurations of the space itself as well as the optimal position of the air inlet.

Experimental tests

The experimental tests have been carried out in the Hydraulic Laboratory of the Central Directorate for the Prevention and Technical Safety of the Italian National Fire Rescue and Service. The pressurised enclosure test rig is a 3.0 m side cube with two identical single leaf doors. Each door is 1.0 m wide and 2.1 m high and they are located on the front and the rear wall enclosure sides. The front door swings inwards the enclosure in overpressure while the back door opens outwards, coherently with the direction of the egress. Figure A.1 shows the experimental smokeproof enclosure, highlighting the front and back door positions.

Walls and doors are fire-resistant and ensure structural resistance and no spread of smoke and heat for 60 minutes ISO 834 standard curve. The enclosure structure is a steel frame construction with a wooden floor covered by a metal sheet and walls and ceiling composed by assembling self-supporting double skin metal faced insulating panels. Linear joints and gaps were sealed so that the air leakage is reasonably restricted through

the edges of the doors. Inside the compartment a helicoidal fan is placed at the left wall of the system (at height of 2.2 m from the floor and horizontal distance from the front wall of 2.1 m).

Due to geometrical constraints of actual smoke enclosure configurations, it is usually not possible to place the fan in a desired position, not even in a symmetric wall position. Therefore, the fan position has been chosen arbitrary and horizontally asymmetric on the side enclosure wall.

Considering the mechanical properties of the fan, five different levels of velocity can be manually selected for the fan and the as-built system is able to reach 50 Pa of overpressure with maximum airflow of 1630 m^3/h. The choice of the fan has been made according to the analytical design described in the previous section.

A testing campaign has been conducted to get functional information about the fluid dynamics behaviour in a controlled environment representing a typical setup adopted in the Italian fire engineering practice (i.e. an enclosure separating a stairwell part of an escape route). Several values of differential pressure up to 50 Pa in the enclosure have been generated varying the working fan velocity. As recommended in the NFPA 92, the tests are carried out without smoke, considering only fresh air. The first part of the experimental campaign consists of studying how the pressure varies in time, taking into account the decreasing and increasing pressure trends due to the opening and closing of entrance and exit doors. The pressure difference between the enclosure and the outside space is logged with a KIMO C310 data logger. A time step of 1 s is usually employed, unless an oscilloscope Tektronix TDS 210 is used to zoom in the transitory phenomena of the pressure variation when the doors are opened or closed. Then, velocities across the doors are collected with an anemometer.

Specifically, the experimental apparatus consists of two pressure differential sensors, one anemometer and an analogic oscilloscope. The pressure sensors measure the

overpressure between the inside and the outside; they were placed initially at z = 1 m near the right lateral wall enclosure at a distance of 1 meter among them (sufficiently far from local effects of sublayer near-wall as well as those caused by the air supply by the fan). During the experimental campaign, the position of the sensors was changed in order to verify the coherence of the pressure measurements.

The anemometer, instead, is fixed at different horizontal and vertical positions according to any interesting measurement. The measuring range of the instrument is 0-25 m/s, with a resolution of 0.1 m/s and an accuracy is ± 3% of the reading ± (0.1 m/s up to 3 m/s).

Initially the two doors are kept closed and the fan is activated to reach the desired pressure level inside the enclosure. After the system is stabilised, different sequences are investigated (Table A.1). In the first sequence, only the front door is opened and closed after 30 seconds, while in the second sequence, the back door is opened and closed after 30 seconds, with the aim of qualitatively investigate whether the exiting airflow was stable and sufficient. In the third and last sequence, in order to simulate the egress of an occupant, the front door is opened and closed after 4 seconds, then the back door is opened after 2 seconds and closed after 4 seconds. This sequence is considered as a reasonable time interval simulating the entering of an occupant inside the enclosure and of course in agreement with the automatic door closer systems commonly available. During each sequence the fan is always kept running at the high velocity in order to achieve the fastest system response during both opening and closing of the doors. In the Table A.1 *D*1 is the front door, *D*2 is the back door, *c* means door closed while *o* indicates an open door. No information about the pressure or the airflow is contained in the Table since several series of tests are done by varying the operating velocity of the fan, although most of the tests allow to reach 40 – 50 Pa inside the enclosure.

To sum up, pressure is measured with closed doors, while velocity (airflow) is measured with open doors.

Figure A.1A-B. Experimental smokeproof enclosure (front and back door opening respectively inwards and outwards)

Table A.1. Concise description of the tests (D1 is front door, D2 is back door, c is closed, o is opened)

	t = 0 s	t = 120 s	t = 124 s	t = 126 s	t = 130 s	t = 150 s
Test 1	D1 = c	D1 = o				D1 = c
	D2 = c	D2 = c				D2 = c
Test 2	D1 = c	D1 = c				D1 = c
	D2 = c	D2 = o				D2 = c
Test 3	D1 = c	D1 = o	D1 = c	D1 = c	D1 = c	
	D2 = c	D2 = c	D2 = c	D2 = o	D2 = c	

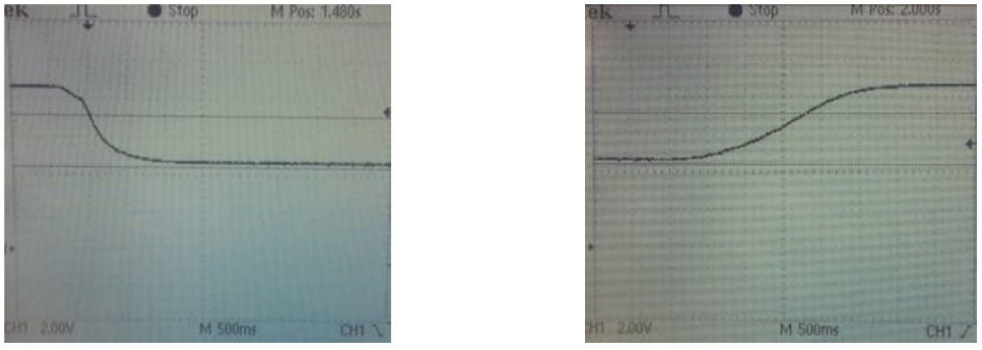

Figure A.2A-B. Relaxation pressure time logged during one door opening (A) and closing phase (B).

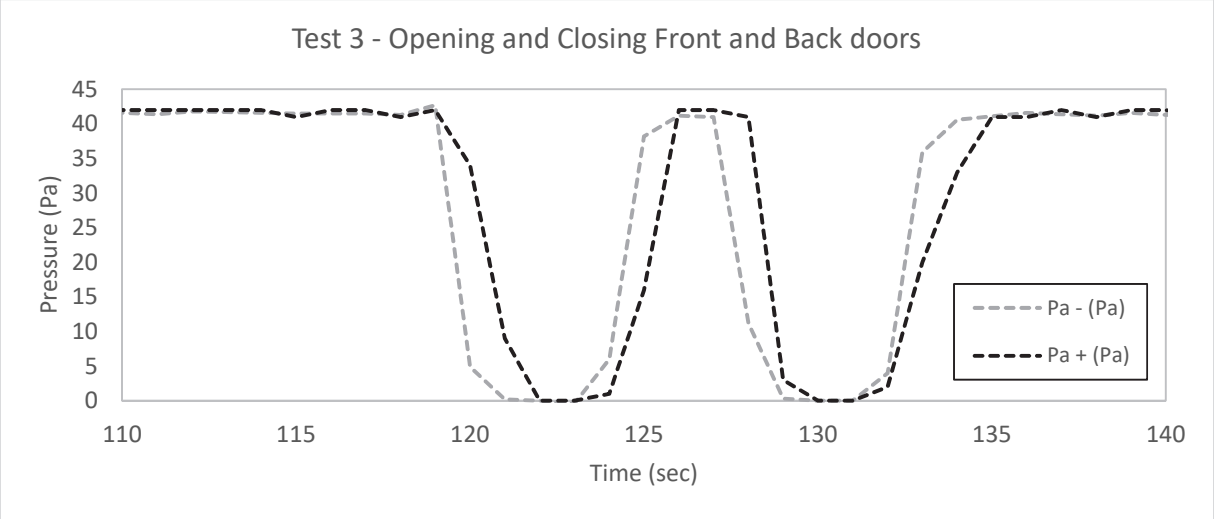

Figure A3. Pressure variation in Test 3

The Figure A.2 reports typical pressure profiles recorded by the oscilloscope during the transient phases. The oscilloscope is analogical and the pictures are not well visible; however the length scale of the signals on the screen is 500 ms and the ordinate value is the pressure (scaled based on the maximum value). The first screenshot (A) displays the logged signal of the pressure decay in one test carried out when the front door is opened while the pressure inside the enclosure is 40 Pa. It takes about 1 second for the pressure to be relaxed (with fan running). The second screenshot (B) displays the logged signal of the pressure rise in one test carried out when the back door is closed and fan is operating to establish a 40 Pa inside the enclosure. In this case, it takes about 2 seconds to restore the pressurisation.

For other tests with fan working at its maximum velocity, the internal overpressure reaches 50 Pa but the number of seconds to stabilise the system (both opening and closing the doors) do not change. As an example, the Figure A.3 depicts the pressure variation obtained performing the Test 3 described in the Table A.1. Two lines ("+" and "–") indicate the two sensors: the trend are essentially the same, only a slight delay can be noticed between them.

It is important to remark that pressurised enclosures are significantly different from pressurised stairwell for their strong sensitivity to the boundary conditions. The ratio pressurised volume/dimensions of the door is small and so are the decay to zero of the overpressure and its restoration to the original value. Looking at figure A.3, it is clear that this aspect is positive because in 2 seconds the overpressure reaches the maximum value starting from 0, but at the same time the decay at the opening of the door is almost instantaneous.

Regarding the velocity of the air across the doors, large variability is found out in the measurements caught by the anemometer. Firstly, due to the lateral position of the fan, the resulting velocities across the doors have strong directional components, sometimes fluctuating. Secondly, the distribution of the velocities is widely disperse, with higher values concentrated in the upper part of the door openings as well as in the lowest part very close to the floor, whereas in the central core of opening the air velocity is slower. The highest local values recorded are about 0.7-0.8 m/s, but most of the monitored points does not exceed 0.4 m/s. If the average velocity is compared with the threshold recommended in EN 12101-6 (0.75 m/s for application similar to the Italian fire engineering practice) the airflow requirement is not fulfilled.

CFD simulations

The same domain is studied by CFD simulations, with the aim of improving the knowledge about velocities and comparing the results gathered during the experimental tests. The numerical code used is Fire Dynamics Simulator (FDS) developed by NIST (National Institute of Standard and Technology) in the USA. The version 6.2.0 has been used for this work (Mc Grattan et al, 2014).

FDS works under the Low Mach number approximation, consistent with the range of pressure developing during fire conditions. According to this approximation, the total

pressure is considered to be composed of a background component p1 plus a perturbation component p2. Most often, p1 is just the hydrostatic pressure and p2 is the flow-induced spatially-resolved perturbation. The strength of the Low Mach approximation is that the solving equations are expressed only in terms of the background pressures, eliminating the need to solve detailed flow equations within the ventilation ducts that do not influence the overall behaviour of the phenomena.

For this kind of model, a number of pressure zones need to be specified (compartments within the computational domain with their own background pressure). These zones are connected via leakage and duct paths whose flow rates are tied to the pressure of the adjacent zones, giving good estimations in terms of dynamic pressure inside the domain.

Description of the model

The model is built keeping the same geometrical dimensions of the experimental enclosure, as shown in the Figure A.4. The dimensions of the model are 5x5x5 meters in the x, y and z directions. The grid size is cubic shaped 5 cm (commented below), with a total number of 100 cells in the three directions. Boundary conditions for the most external vertical planes are "open" at atmospheric pressure. Measurement points will be explicitly specified before each graph but are concentrated in the centre of the enclosure for the pressure and across the doors for the velocity.

Since the simulations provide the presence of neither the fire source nor hot smoke, thermal properties of materials are not significant for the results; however, the basic parameters are included in the model. Specific heat, conductivity and density are respectively 0.84 kJ/(kg K), 0.48 W/(m K) and 1440 kg/m^3 for obstructions (walls, including the doors, floor and roof).

The doors are modelled as obstructions. In FDS the action of opening the door becomes simply the removal of the obstruction from the domain. The two zones of pressure (inside

the compartment and external volume) are immediately connected and merged into a single zone but the time to reach the equilibrium is calibrated through the pressure relaxation time function, using the value obtained by the oscilloscope in the experimental test (Figure A.4). The same for the closing of the door: as the obstruction is inserted in the model, FDS reads two different pressure zones instead of one, with the consequence of instantaneous rise of the internal pressure (in this case FDS seems to be unable to slow down the transitory phase, even changing the value of the pressure relaxation time). Specifically, the pressure relaxation time in FDS is set to 1 second for the case in which the door is opened, while 2 seconds are chosen for the closing case (although irrelevant because it does not affect the output of the simulations).

Other way of removing the obstruction (partially, dividing the door in more sub-obstructions to be removed one at a time) would not have led to improvement of the results, since the behaviour of the model is linked to the "pressure zones" solver. Clearly, although a similar example is contained in the FDS User Guide the instantaneous removal of the obstruction seems to be quite different from the door swings open. On the other hand, the accuracy of this feature in terms of pressure is guaranteed through the calibration of the pressure relaxation time based on real data collected with the help of the oscilloscope.

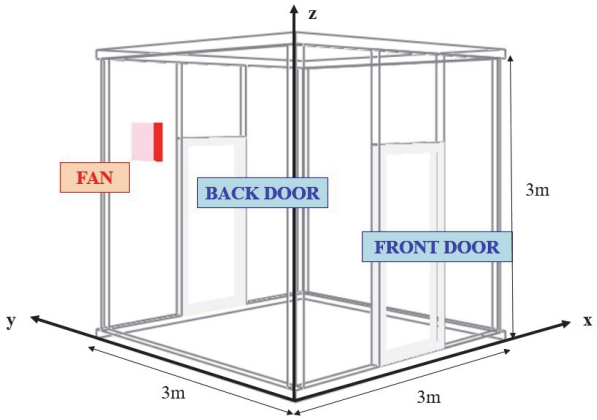

Figure A.4. Screenshot of the FDS model

The model of the fan is a simple air supply blowing air at constant rate as in the experimental enclosure, considering the nominal capacity. The work, in fact, does not take into account the hydraulic losses of the fan nor consider the actual "pressure versus air flow" fan curve.

The size of the mesh has been chosen after calibration and sensitivity analysis. Considering that the flow field originates from a 40x40cm inlet surface, a 5 cm side cubic mesh seems to be sufficiently fine to correctly predict the air movement in the domain. As the boundary conditions of the pressure are much more complicated than the usual features typical of FDS, the extension of the surrounding domain is investigated, in order to understand whether the cycle of opening and closing doors affects the results. Looking at the pressure reached inside and the distribution of the velocities across the doors, extending the limit of the model up to 1 meter more than the horizontal boundaries of the enclosure is a good compromise between the quality of the results and the computational effort. In the vertical direction the domain is extended up to 2 meters beyond the roof in order to keep an overall cubic domain with side of 5 meters.

The leakage through the doors is inserted in the model through a localised leakage function. The leakage through the edges of doors is a phenomenon whose order of magnitude is the millimetre. Therefore, indirect modelling through a HVAC function is used to represent airflow through a certain leakage area by explicitly defining internal and external vents; in this way, FDS identifies leak paths where the air flows until a dynamic equilibrium between the zones is reached. Therefore, for each edge two vents are defined (internal and external, respectively bounding with the inside and the outside of the enclosure, thus belonging to two different pressure zones) and linked through a HVAC function (TYPE_ID='LEAK') whose area is defined through calibration of the numerical results with trend obtained by experimental tests.

This function is inserted for both doors through the four boundaries of the obstructions: each door is bounded from thin vents (with thickness of 5 cm) along the perimeter and every vent (horizontal and vertical) identifies a leak path. The quantity of airflow lost through these vents depends on the area defined inside each vent, chosen so that the internal pressure stabilises at 50 Pa as in the final series of tests. This is an indirect way to consider the leakage but functional for the purpose of this study: as the leakage works only when doors are closed, the interest is maintaining the pressure at the required level and so the balance of the airflows (in and out) is used. The Figure A.5 depicts the calibration curves of the modelled leakage.

The series of tests considered for the calibration of the model are only those reaching 50 Pa, which are the only ones used for the comparison with numerical results, as is reported in the next section. The series reaching 40 Pa was initially used to run a preliminary set of experimental tests; the trends are actually very similar, because the dynamics of the system is quite fast, although the maximum overpressure is different due to the different working velocities of the fan.

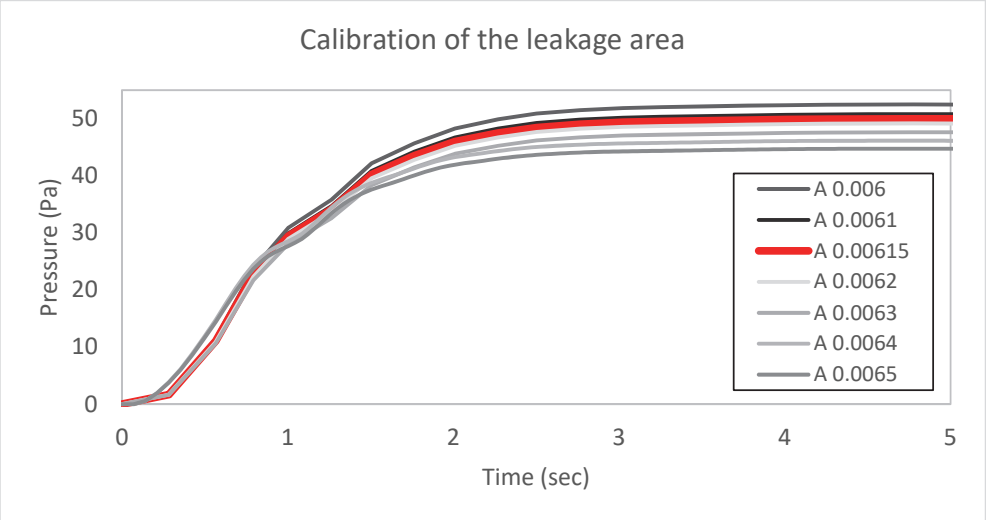

Figure A5. Calibration of the leakage (A is the leakage area expressed in m²)

Another hypothesis behind this approach is that the leakage is uniformly distributed through the external perimeter of the doors (other assumption could have been to localise all the leakage in the horizontal lowest part of the doors): as already stated before, detailed analysis of the leakage is beyond the scope of this study. In the Figure A.6 two slices (horizontal, crossing the lowest edge and vertical, crossing the right edge of the front door) of the velocity field are represented, showing also how the localised leakage function affects the field.

Comparison between numerical and experimental results

The fundamental three tests previously described are studied with FDS. Globally, the results of the numerical simulations seem to closely match the overall phenomenon, from the development of the air patterns inside the enclosure to the maximum overpressure and distribution of velocities across the doors.

In the Figure A.7 the trends of the pressure in time are represented both for the numerical simulation and actual data recorded during the Test 1. The lines overlap during all the phases, apart from the very last 20 seconds of the test, probably because of a fluctuation in the working conditions of the fan. There are two dashed lines ("+" and "-") for the experimental trend because there are two pressure differential sensors; however, in line with the scalar nature of the pressure, the recorded values are the same.

Coherently in the Figure A.8 the contour of the pressure along a slice of the FDS simulation shows a homogeneous pressure for all the domain. As previously stated, the homogeneity is due to the pressure modelling implemented in FDS. The slice is taken with closed doors, after the pressure is stabilised.

Then the working of the system from the point of view of the velocity of the air is investigated. Firstly, in the Figure A.9, an instantaneous screenshot of the velocity field caused by the air supply is shown. The slice cuts the domain at z = 2.2 m (the middle

height of the fan): the air is pushed with a maximum velocity of 3 m/s to the opposite wall, where the flow slips along the walls until it reaches the doors (and so the leak paths). Due to the horizontally asymmetric position of the fan, higher velocities are concentrated close to the back door, especially in the upper part (at the level of the fan). Aware of this effect, since the study is intended to assess the operational conditions of the pressurised smokeproof enclosure, attention is mostly given to what happens on the front door, from which the smoke could enter in case of fire.

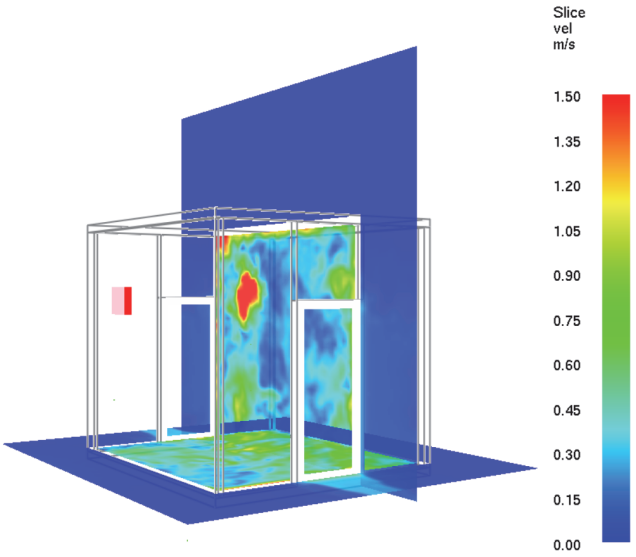

Figure A.6. Vertical and horizontal velocity slices showing localised leakage through the front door

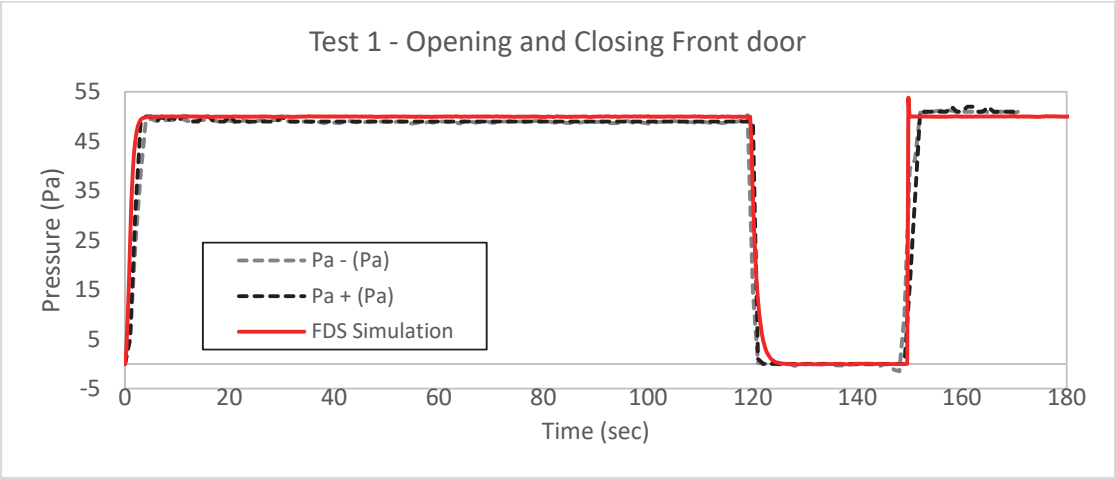

Figure A.7. Trend of the pressure in time during Test 1

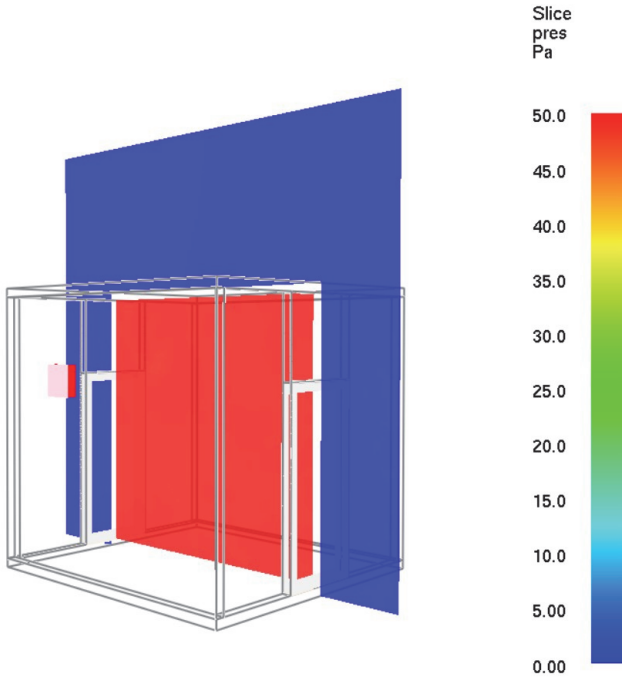

Figure A.8. Pressure contours in the central vertical plane (closed doors)

The numerical simulation confirms the main findings of the experimental tests: large variability affects the velocity distribution across the front door, with values not satisfying the requirement of EN12101-6. In the Figure A.10 the velocity slice (located at the cross section of the front door as view by an incoming occupant) shows that velocities are far from being uniform both in the modules and in the directions. Values are low, especially in the centre of the door, while a sort of slip along the internal walls makes the air exit mostly from the right side of the door itself.

Considering the central axis of the cross section across the front door, a velocity profile built-up by interpolating FDS punctual numerical measurements is drawn in the Figure A.11. Only FDS predicted velocities are shown because experimental measurements were too close to the resolution of the anemometer and are not reported. Since the velocities are highly fluctuant as typical of LES solver and fine mesh, each represented value is obtained by an average of three different close monitored points (at a relative distance of 5 cm in the thickness of the door). As velocity is a vector, according to the axis definition

shown in the Figure A.4, negative and positive values in the profile are meaningful in understanding if the airflow is actually exiting the door or ineffectively recirculating into the enclosure. The continuous line is the normal component of the velocity (called "V-Velocity", negative in the outwards direction), while the dotted line is the whole velocity (called simply "Velocity", that is the module ||v|| but preserving the sign of the normal component to facilitate the reading). The difference between them is a measure of how much of the airflow is directed orthogonally to the door section. In fact, the EN12101-6 does not specify whether the minimum velocity requirement is related to the total or normal component of the velocity, but the normal component should be the most efficient to contrast the entrance of smoke compared to the transversal and longitudinal components. However, the limit of 0.75 m/s is not reached: higher velocities are concentrated at the boundaries while between z = 1.5 m and z = 1.9 m there is also an internal circulation of air.

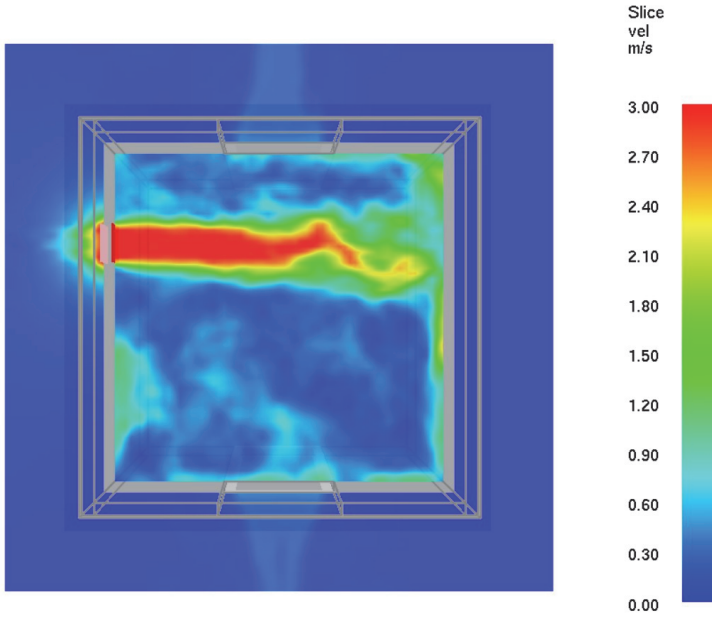

Figure A.9. Velocity slice at z = 2.2 m (closed doors)

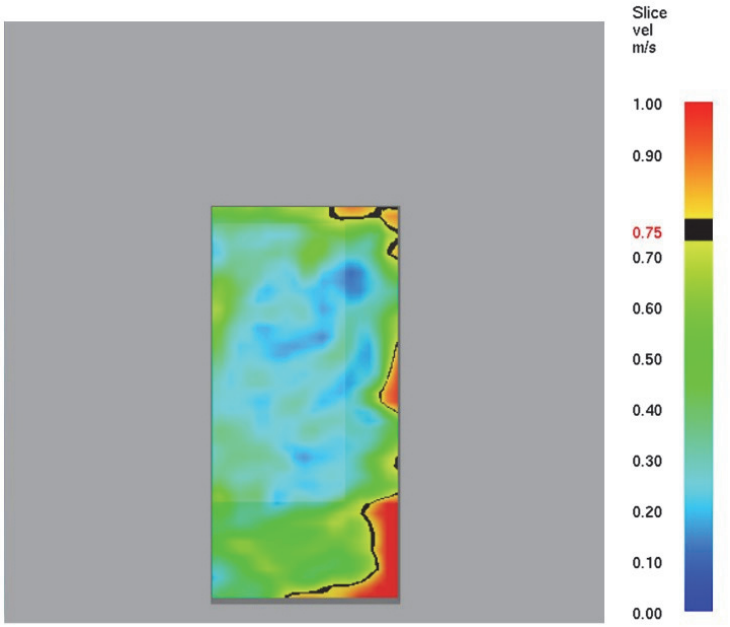

Figure A.10. Velocity slice across the front door at t=130sec during test 1 (front door opened)

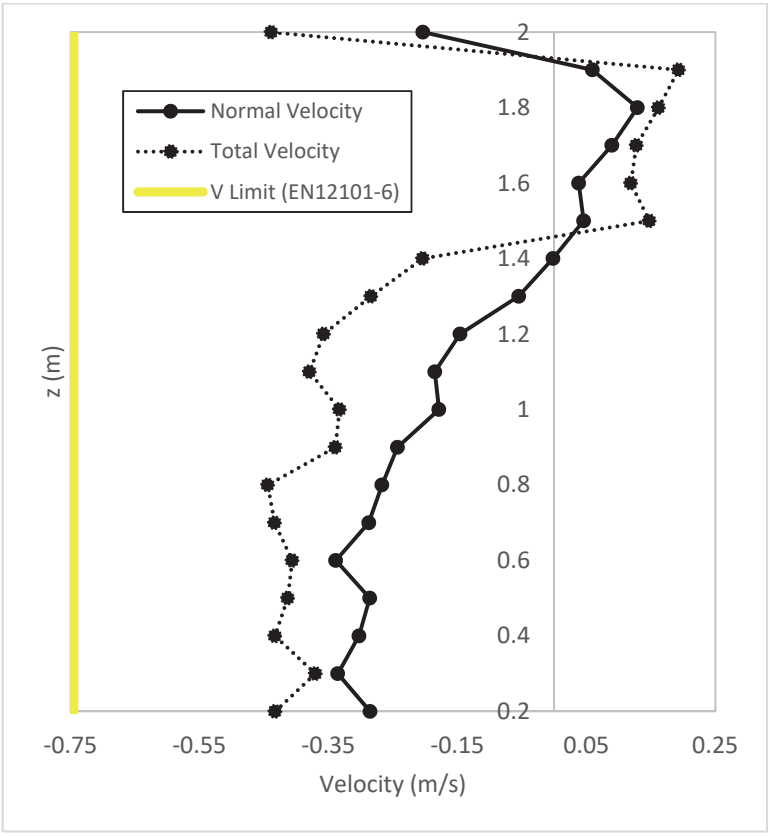

Figure A.11. Velocity profile in the centreline of the door at t=145sec (Test 1, front door opened).

Considerations

Based on the FDS simulations, the following considerations can be done.

Firstly, as expected, the system does not comply the EN12101-6 requirements because the velocity requirement is not fulfilled. This is not a surprise: the fan has been designed and chosen only considering the pressure criterion. Even if the installed (and thus modelled) fan is oversized in terms of airflow (1630 m^3/h instead of 1050 m^3/h), the simulation results confirm that this is not enough to guarantee an acceptable average velocity through open doors.

Secondly, the absence of symmetry in the horizontal position of the fan has significant effect on the distribution of the velocities. Furthermore, since the fan is placed in the left lateral wall of the enclosure, it blows air towards the right wall instead of being directed towards the front door, causing internal circulation of the air and unavoidable loss of the efficiency of the system.

Lastly, the fan is not equipped with the control system to adjust the air supply according to the operational conditions. The consequence of the constant air supply is that when doors are closed the airflow is more than the strictly necessary to reach the minimum design pressure, whereas when one door is opened the airflow is not enough to guarantee the desired level of velocity across the doors.

Following the previous considerations, some possible alternative solutions have been studied from the numerical point of view, trying to identify which are the negative aspects of the experimental enclosure that mostly influence the non-uniform distribution of the velocity: position of the fan or insufficient airflow when doors are opened. The results are exposed in the papers (Ponziani, 2016; Gai, 2017).

Appendix B

Fire Dynamics Simulator (FDS)

Generalities

FDS (McGrattan et al, 2014) is designed in such a way that the users have to specify a small number of numerical parameters, focusing instead on the physical description of the problem. The grid is rectilinear: the only numerical parameters chosen by the user are the three dimensions of the grid. Then, the objects are defined as rectangular obstructions that define the geometry to the level of resolution determined by the grid (these obstructions snap to the grid).

The governing equations are approximated using second-order accurate finite differences on the uniformly spaced three-dimensional grid. Scalar quantities are assigned to the center of each grid cell; vector components are assigned at the appropriate cell faces (this is what is commonly referred to as a "staggered grid").

LES and Low-Mach approximation

The equations for large eddy simulation (LES) are derived by applying a filter, parameterized by a width Δ, to the transport equations for mass, momentum and energy. In FDS, the filter width Δ is equivalent to the local cell size δx (implicit filtering).

For low speed applications like fire, the spatially and temporally resolved pressure, p, can be decomposed into a background pressure $p(z,t)$ plus a perturbation $p(x,y,z,t)$. The equation of state (ideal gas law) can be written in function of the only background pressure:

$$\bar{p} = \rho T R \sum_{\alpha} \frac{Z_\alpha}{W_\alpha} \equiv \frac{\rho R T}{\bar{W}} \tag{B.1}$$

Note that z is the spatial coordinate in the direction of gravity; thus, the stratification of the atmosphere is included in the background pressure. The perturbation $\bar{p}$ drives the fluid motion.

The first consequence is that, by considering a HVAC system, the air flowing between compartments can be described in terms of the difference of the background pressures, eliminating the need to solve detailed flow equations within the ventilation ducts.

The second consequence of the low Mach number approximation is that the internal energy, e, and enthalpy, h, may be related in terms of the thermodynamic (background) pressure:

$$h = e + \bar{p}/\rho \tag{B.2}$$

The energy conservation equation may then be written in terms of the sensible enthalpy, h_s:

$$\frac{\partial}{\partial t}(\rho h_s) + \nabla \cdot (\rho h_s \boldsymbol{u}) = \frac{D\bar{p}}{Dt} + \dot{q}''' + \dot{q}_b''' - \nabla \cdot \dot{\boldsymbol{q}}''' \tag{B.3}$$

The term $\dot{q}'''$ is the heat release rate per unit volume from a chemical reaction (HRRPUV), while $\dot{q}_b'''$ represents the energy transferred to subgrid-scale droplets and particles.

The term $\dot{\boldsymbol{q}}'''$ is the conductive, diffusive and radiative heat fluxes: it depends on the thermal conductivity k and the D_α diffusivity of species α.

$$\dot{\boldsymbol{q}}''' = -k\nabla T - \sum_{\alpha} h_{s,\alpha} \rho D_\alpha \nabla Z_\alpha + \dot{\boldsymbol{q}}_r''' \tag{B.4}$$

The velocity divergence can be written as follows:

$$\nabla \cdot \boldsymbol{u} = \frac{1}{\rho h_s}\left[\frac{D}{Dt}(\bar{p} - \rho h_s) + \dot{q}''' + \dot{q}_b''' - \nabla \cdot \dot{\boldsymbol{q}}'''\right] \tag{B.5}$$

The hydrodynamics solver guarantees that this divergence is verified: if this is true the energy is conserved.

Mass and species transport

The most basic description of the chemistry of fire is a reaction of a hydrocarbon fuel with oxygen that produces carbon dioxide and water vapour. Because fire is a relatively inefficient combustion process involving multiple fuel gases that contain more than just carbon and hydrogen atoms, the number of gas species reacting in the simulation is almost limitless. However, to make the simulations tractable, FDS normally limits the number of fuels to one and the number of reactions to just one or two. FDS also leaves the possibility that the reaction may not proceed for lack of sufficient oxygen in the incoming air stream, as when a fire in a closed compartment extinguishes itself. Even with this simplified approach to the chemistry, we still need to track at least six gas species (Fuel, O_2, CO_2, H_2O, CO, N_2) plus soot particulate. If a single – step reaction is assumed, only two transport equations (instead of seven) need to be solved: one for the fuel and one for the products. The air is everything that is neither fuel nor products. Whereas the fuel is a single gas species, the air and products are what are often referred to as "lumped species ". A lumped species represents a mixture of gas species that transport together and react together and, from the point of view of the numerical model, a lumped species can be treated as a single species. In fact, the mass transport equations make no distinction between a single or lumped species.

If ρ is the density and u is the velocity vector, the equation for total mass is written as:

$$\frac{\partial \rho}{\partial t} + \nabla \cdot (\rho \boldsymbol{u}) = \dot{m}_b'' \tag{B.6}$$

where the source term on the right hand side represents the addition of mass from evaporating droplets or other subgrid – scale particles, that can represent sprinkler and fuel sprays, vegetation, etc.; otherwise is zero.

Momentum transport

Noting the vector identity

$$(\boldsymbol{u}\cdot\nabla)\boldsymbol{u}=\frac{\nabla|\boldsymbol{u}|^2}{2}-\boldsymbol{u}\times\omega \tag{B.7}$$

and defining the stagnation energy per unit mass

$$H\equiv\frac{|\boldsymbol{u}|^2}{2}+\frac{\tilde{p}}{\rho} \tag{B.8}$$

the momentum equation can be written

$$\frac{\partial\boldsymbol{u}}{\partial t}-\boldsymbol{u}\times\omega+\nabla H+\tilde{p}\nabla\left(\frac{1}{\rho}\right)=\frac{1}{\rho}[(\rho-\rho_0)\mathbf{g}+\mathbf{f}_b+\nabla\cdot\tau] \tag{B.9}$$

The term, $\mathbf{f}_b$, represents the drag force exerted by the subgrid – scale particles and droplets. The viscous stress, τ, is closed via gradient diffusion with the turbulent viscosity obtained from the Deardorff eddy viscosity model.

If the equation is written in the form

$$\frac{\partial\boldsymbol{u}}{\partial t}+\boldsymbol{F}+\nabla H=0 \tag{B.10}$$

a Poisson equation for the pressure is obtained by considering the following divergence

$$\nabla^2 H=-\left[\frac{\partial}{\partial t}(\nabla\cdot\boldsymbol{u})+\nabla\cdot\boldsymbol{F}\right] \tag{B.11}$$

Combustion

Combustion and radiation are introduced into the governing equations via the source terms in the energy transport equation. Since the energy equation is not solved explicitly, these terms find their way into the expression for the divergence.

For most applications, FDS uses a combustion model based on the mixing – limited, infinitely fast reaction of lumped species: reactant species in a given grid cell are converted to product species at a rate determined by a characteristic mixing time, τ_{mix}. The heat release rate per unit volume is defined by summing the lumped species mass production rates multiplied for their respective heats of formation.

$$\dot{q}''' = -\sum_{\alpha} \dot{m}_{\alpha}''' \Delta h_{f,\alpha} \tag{B.12}$$

Radiation

The net contribution from thermal radiation in the energy equation is defined by:

$$\dot{q}_r''' \equiv -\nabla \cdot \dot{\boldsymbol{q}}_r''(\boldsymbol{x}) = k(\boldsymbol{x})[U(\boldsymbol{x}) - 4\pi I_b(\boldsymbol{x})], \quad U(\boldsymbol{x}) = \int_{4\pi} I(\boldsymbol{x}, \boldsymbol{s}')d\boldsymbol{s}' \tag{B.13}$$

Where $k(\boldsymbol{x})$ is the absorption coefficient, $I_b(\boldsymbol{x})$ is the source term and $I(\boldsymbol{x}, \boldsymbol{s}')$ is the solution of the radiation transport equation (RTE) for a non – scattering gray gas.

The radiation equation is solved using a technique similar to a finite volume method for convective transport, thus the name given to it is the Finite Volume Method (FVM). Using approximately 100 discrete angles which are updated over multiple time steps, the finite volume solver requires about 20% of the total CPU time of a calculation, a modest cost given the complexity of the radiation heat transfer.

Solution procedure

The solution procedure is based on two main features: a predictor and a corrector. There are 13 steps in the solution procedures, 6 for the predictor and 7 for the corrector. In a given cell of a grid and at a given time step (for example, the n_{th}) the software starts from the following quantities: ρ (density), $Z_{n\alpha}$ (lumped species mass fractions), $\boldsymbol{u_n}$ (velocity vector) and H_n (fluctuating stagnation energy per unit mass). Moreover, each compartment has associated a background pressure denoted with $\bar{p}_n$. The advancing in time of these quantities is described using a second order explicit scheme called predictor – corrector, based on the features mentioned above.

The predictor:

1. estimates , $Z\alpha$, $\bar{p}$ at the next time step with a first order accuracy. Usually first order accuracy quantities are denoted with an asterisk; for example, ρ is calculated as

$$\rho \approx \frac{\rho^* - \rho^n}{\delta t} + \boldsymbol{\nabla} \cdot \rho^n \boldsymbol{u} = 0 \tag{B.14}$$

2. computes T* from the equation of state

3. computes the divergence $(\nabla \cdot \boldsymbol{u})^*$ from the estimated thermodynamics quantities. Note that the velocity has not been calculated yet at the next time step, but only its divergence

4. solves the Poisson's Equation for pressure

$$\rho \nabla^2 H^n = -\frac{(\nabla \cdot \boldsymbol{u})^* - \nabla \cdot u}{\delta t} - \nabla \cdot F^n \tag{B.15}$$

5. estimates the velocity at the next time step

$$\frac{u^* - u^*}{\delta t} + F^n + \nabla H^n \tag{B.16}$$

6. checks that the time – lapse δt satisfies the CLF stability condition (the time step must be lower than the time required for one particle of fluid to span a cell in one of the three main directions)

$$\delta t = \max\left(\frac{|u|}{\delta x}, \frac{|v|}{\delta y}, \frac{|w|}{\delta z}\right) < 1 \tag{B.17}$$

7. if the time step is too large, δt is reduced to satisfy the mentioned condition (procedure back to step 1); if the time step is ok, then the solution proceeds with the corrector phase.

The corrector:

1. corrects the density, the lumped species concentrations and the background pressure at the next time step; for the density, for example, it is

$$\rho \approx \frac{\rho^* - \rho^n}{\delta t} + \boldsymbol{\nabla} \cdot \rho^n \boldsymbol{u} = 0 \tag{B.18}$$

2. computes T* from the equation of state

3. splits time for the mass source terms; these terms are applied to the scalars (both chemical reactions and Lagrangian particles; they are calculated using the results of the corrected scalar transport scheme)

4. computes the final T^{n+1} from the equation of state with the updated density and composition

5. calculates the divergence of the velocity on the basis of the corrected thermodynamics quantities $\nabla \cdot u^{n+1}$

6. calculates the pressure

$$\nabla^2 H^n = \frac{\nabla \cdot u^{n+1} - \frac{1}{2}(\nabla \cdot u^* + \nabla \cdot u^n)}{\delta t/2} \tag{B.19}$$

7. corrects the velocity of the next time step, integrating the previous one

$$\frac{u^{n+1} - \frac{1}{2}(u^* + u^n)}{\delta t/2} + F^* + \nabla H^* = 0 \tag{B.20}$$

APPENDIX B

Appendix C

Parametric study of FDS

Generalities

A parametric study has been carried out on a short tunnel (100m x 10 m x 5 m) with the objective of identifying the most influential parameters on the macroscopic quantities that are generally used for life safety assessment: temperature, radiative heat flux gas, visibility and FED (Table C.1). The tunnel has a central burner, positioned in the middle of the length and only natural ventilation is taken into account. Six sections are considered (Figure C.1). A 30 MW fire is chosen for cases with $3 \leq i \leq 10$.

Table C.1. Synthesis of the parametric study

i	Parameter		Unit	Run 1	Run 2	Run 3
1	Grid resolution		cm	Coarse	Medium	Fine
2	Heat release rate	Coarse Medium Fine	MW	5	30	100
3	Fire source. Area		m^2	1	2	4
4	Fire source. B/W		-	1/1	2/1	4/1
5	Soot yield		g/g	0.05	0.10	0.20
6	Material behaviour		-	Inert	Concrete	Adiabatic
7	Presence of vehicles		-	No vehicles	Low traffic	Queue
8	External boundary. L_{ext}		m	3/5 Ht	Ht	2Ht
9	Longitudinal inclination		%	- 5 %	0 %	+ 5 %
10	Initial temperature		°C	10	20	30

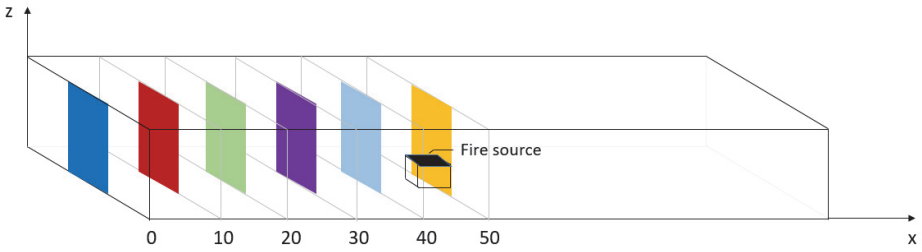

Figure C.1. Scheme of the tunnel

The following results are reported:

- differences (%) for single quantities Qi (temperature, radiative heat flux gas, visibility and FED) by varying one parameter Pi at a time. The differences are calculated at the upper layer (UL, z=4 m) and lower layer (LL, z=2) by selecting the minimum and maximum value of the quantity Qi at fixed locations (X=0,..50 m) among the three runs (run 1, run 2 and run 3) and evaluating their maximum, minimum and average difference (%). This gives an idea of the effect of the selected input parameter (Pi) on the four output quantities.
- profiles of the quantities Qi (temperature, radiative heat flux gas, visibility and FED) along the centerline of a given section by varying a single parameter Pi (only for the cases in which significant variations occur). Refer to Table C.1 for the colors of the lines related to the run 1, 2 and 3.
- slices with Smokeview, when relevant.

Comments and considerations on the results are contained in the Chapter 5 where the parametric study is discussed.

The FED quantity has often very low values (10^{-3}-10^{-4}) and this is responsible for apparently large differences (over 100 %), which however are not significant and alarming.

Parameter: Grid resolution

Table C.2. Difference (%), 5 MW, UL, grid resolution

<table>
<tr><th colspan="2">UPPER LAYER – 5 MW - GRID RESOLUTION (Coarse-Medium-Fine)</th></tr>
<tr><td>TEMPERATURE
 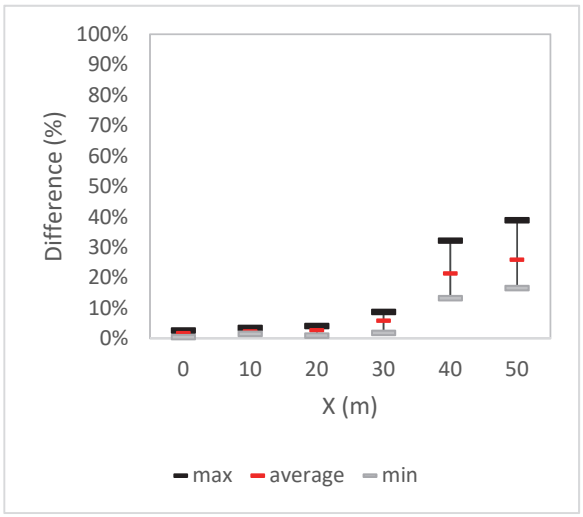
</td><td>RADIATIVE HEAT FLUX GAS
 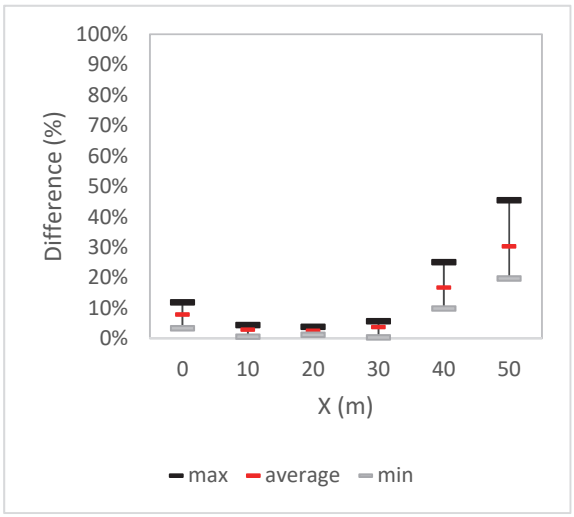
</td></tr>
<tr><td>VISIBILITY
 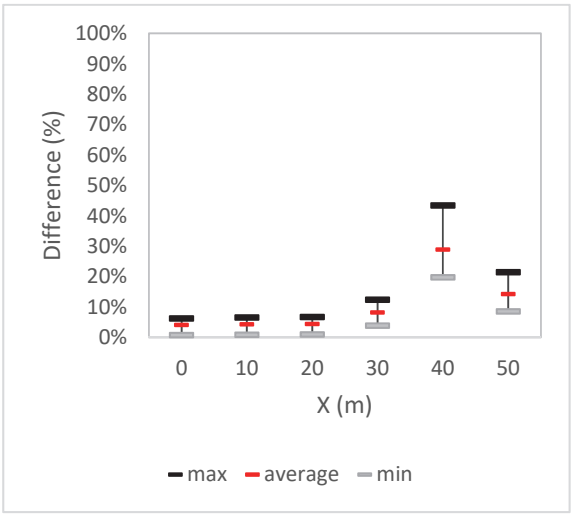
</td><td>FED
 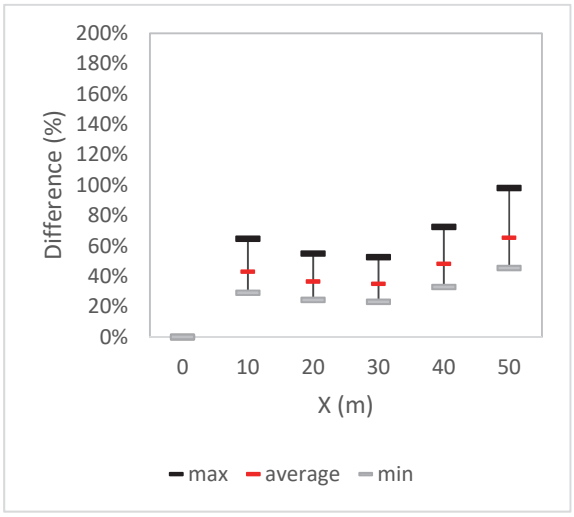
</td></tr>
</table>

Table C.3. Difference (%), 5 MW, LL, grid resolution

<table>
<tr><th colspan="2">LOWER LAYER – 5 MW - GRID RESOLUTION (Coarse-Medium -Fine)</th></tr>
<tr><td>TEMPERATURE
 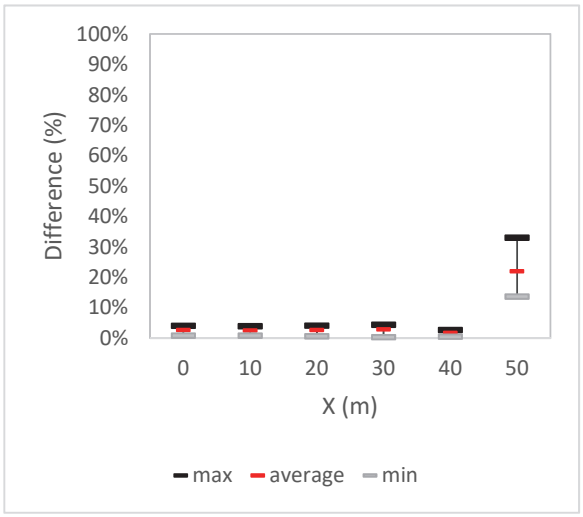
</td><td>RADIATIVE HEAT FLUX GAS
 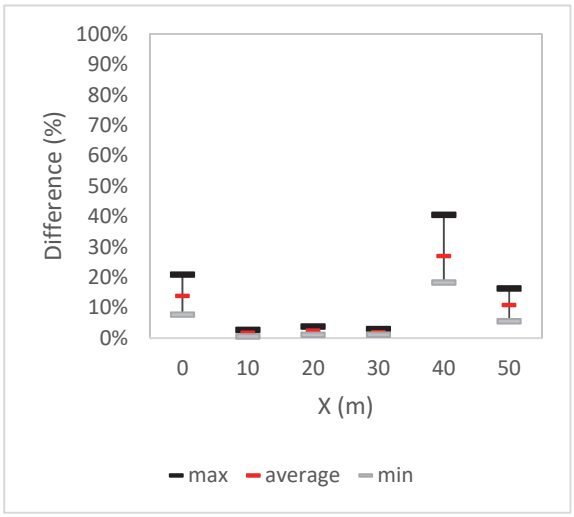
</td></tr>
<tr><td>VISIBILITY
 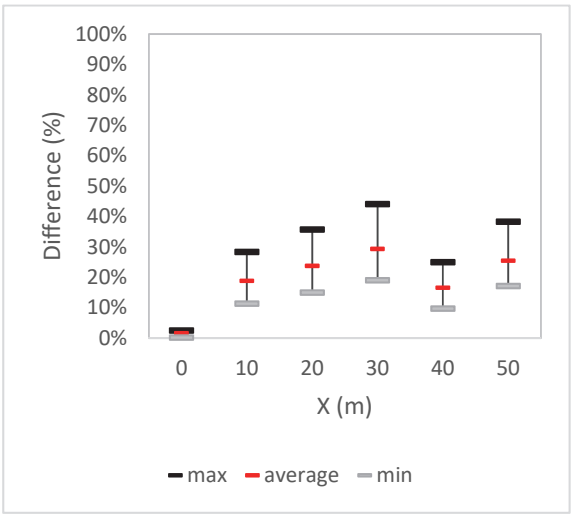
</td><td>FED
 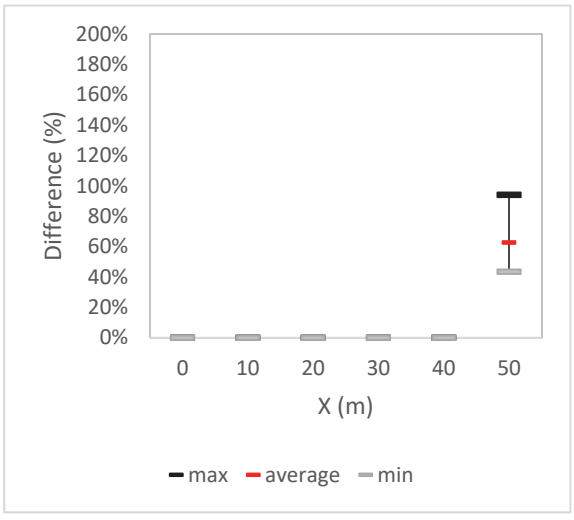
</td></tr>
</table>

Table C.4. Difference (%), 30 MW, UL, grid resolution

<table>
<tr><th colspan="2">UPPER LAYER – 30 MW - GRID RESOLUTION (Coarse-Medium -Fine)</th></tr>
<tr><td>TEMPERATURE
 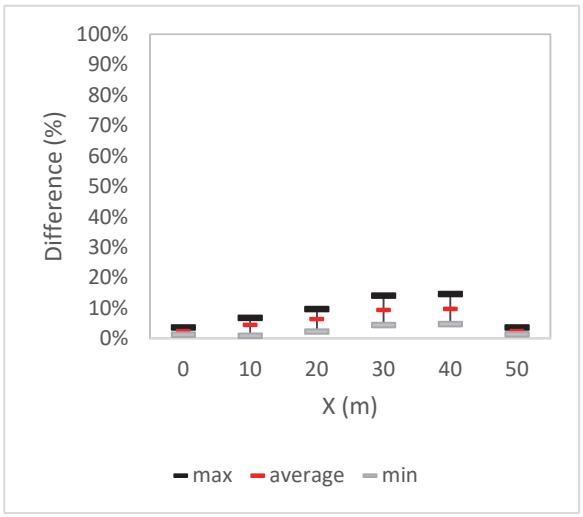
</td><td>RADIATIVE HEAT FLUX GAS
 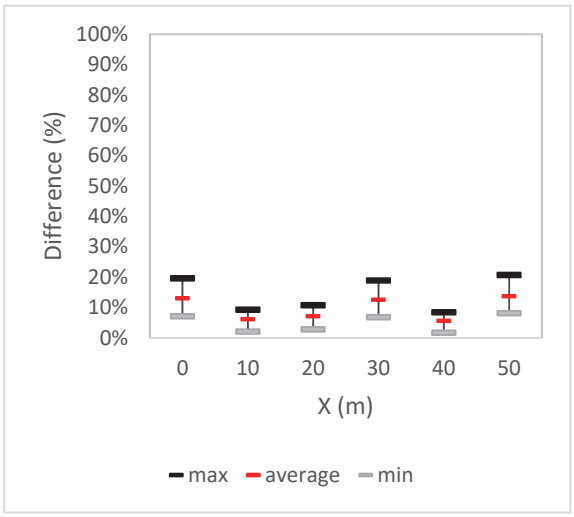
</td></tr>
<tr><td>VISIBILITY
 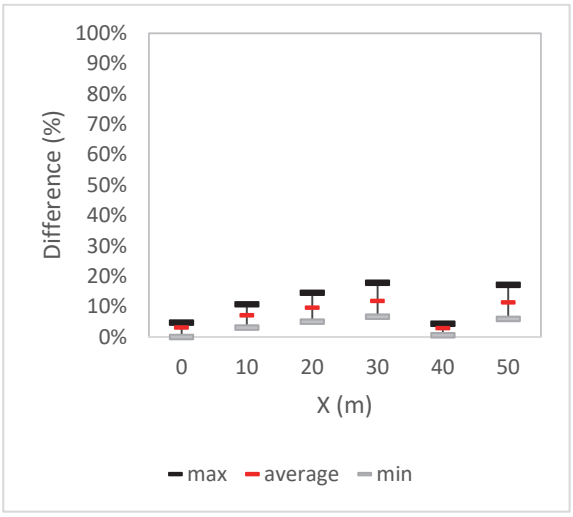
</td><td>FED
 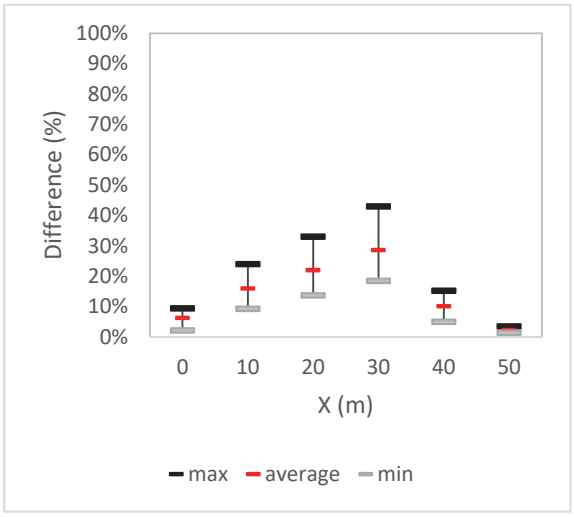
</td></tr>
</table>

Table C.5. Difference (%), 30 MW, LL, grid resolution

LOWER LAYER – 30 MW - GRID RESOLUTION (Coarse-Medium -Fine)

TEMPERATURE

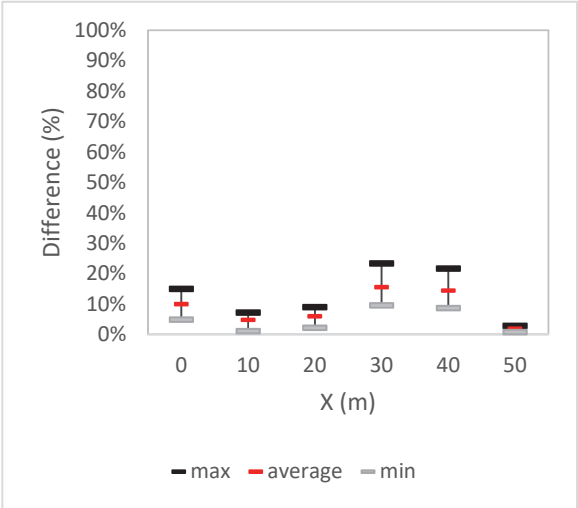

RADIATIVE HEAT FLUX GAS

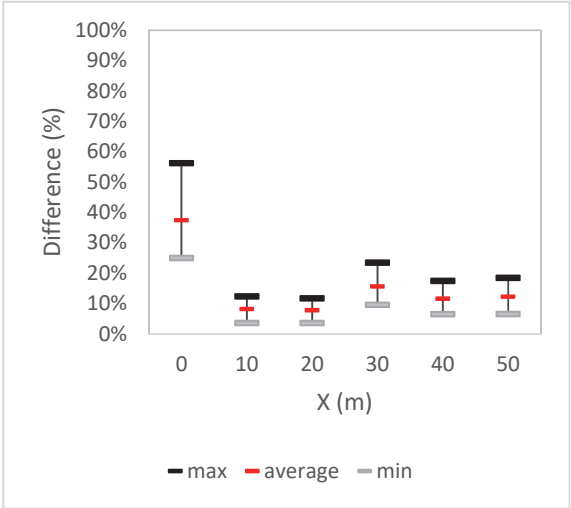

VISIBILITY

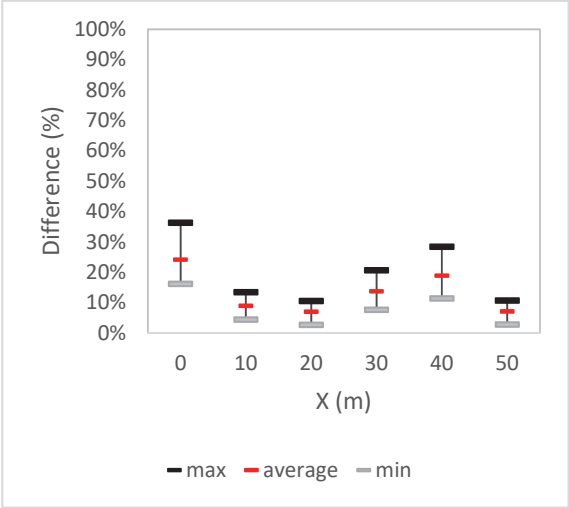

FED

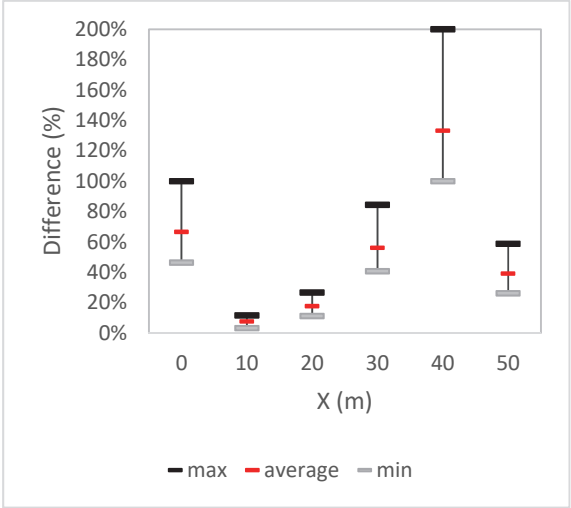

Table C.6. Difference (%), 100 MW, UL, grid resolution

UPPER LAYER – 100 MW - GRID RESOLUTION (Coarse-Medium -Fine)

TEMPERATURE

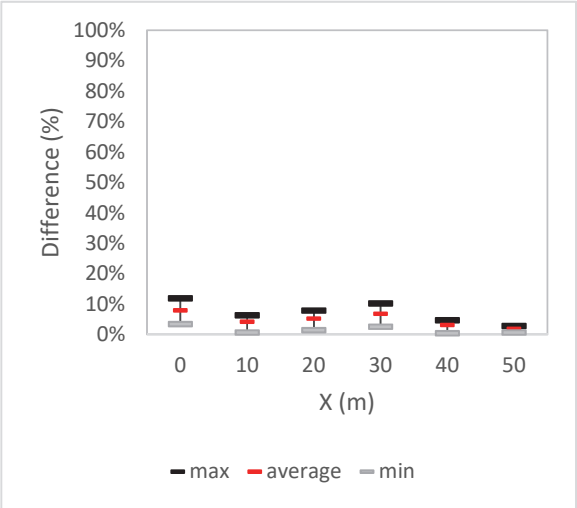

RADIATIVE HEAT FLUX GAS

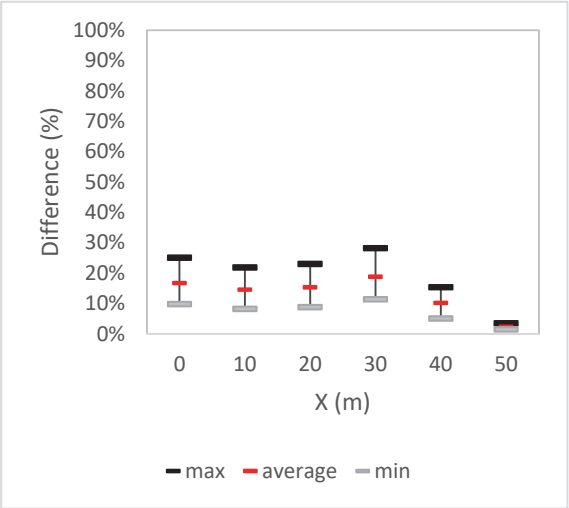

VISIBILITY

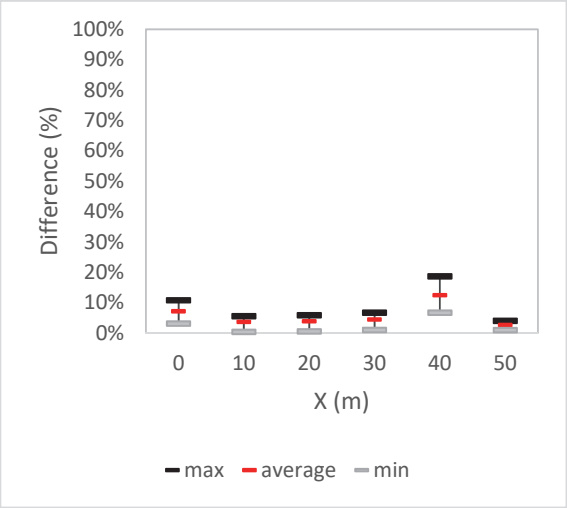

FED

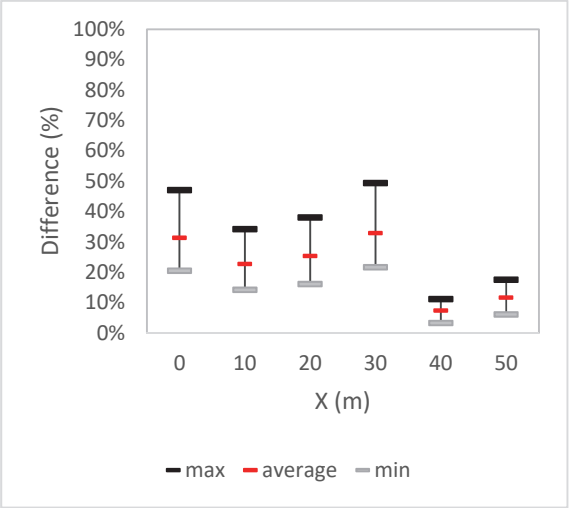

Table C.7. Difference (%), 100 MW, LL, grid resolution

<table>
<tr><th colspan="2">LOWER LAYER – 100 MW - GRID RESOLUTION (Coarse-Medium -Fine)</th></tr>
<tr><td>TEMPERATURE
 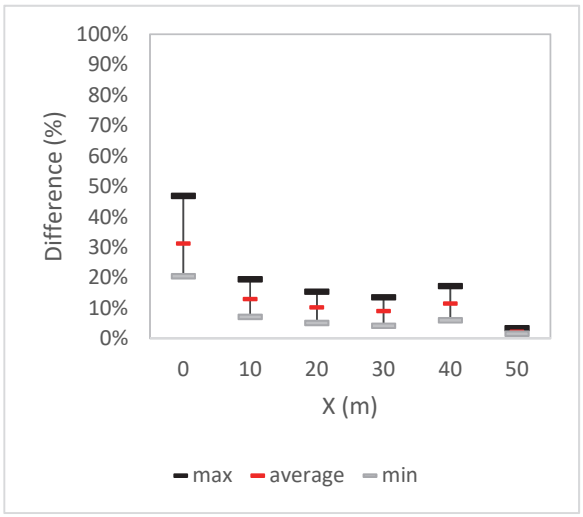
</td><td>RADIATIVE HEAT FLUX GAS
 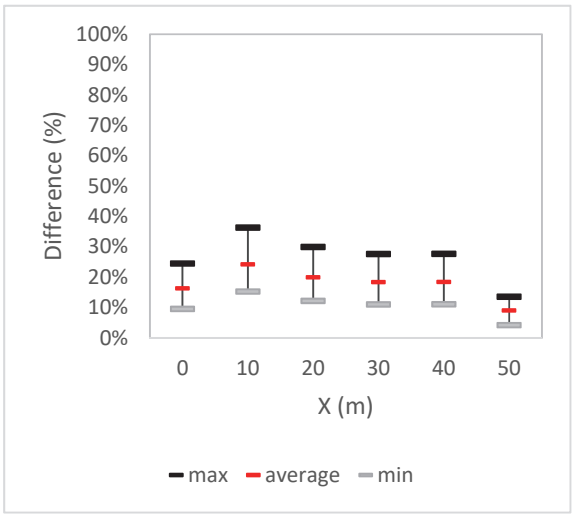
</td></tr>
<tr><td>VISIBILITY
 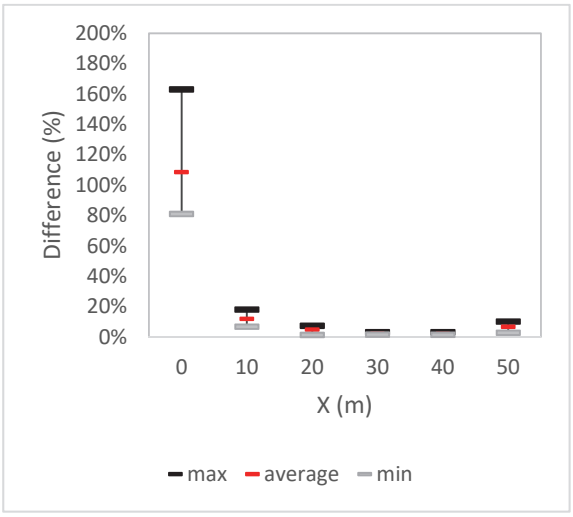
</td><td>FED
 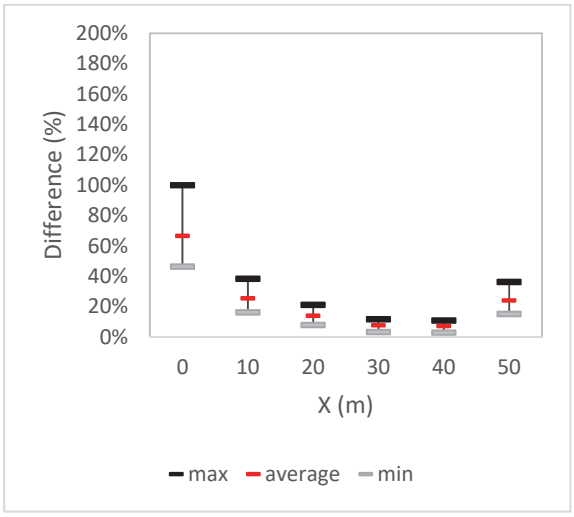
</td></tr>
</table>

Parameter: HRR

Table C.8. Difference (%), UL, HRR

UPPER LAYER – HRR VARIATION (5-100 MW)

TEMPERATURE

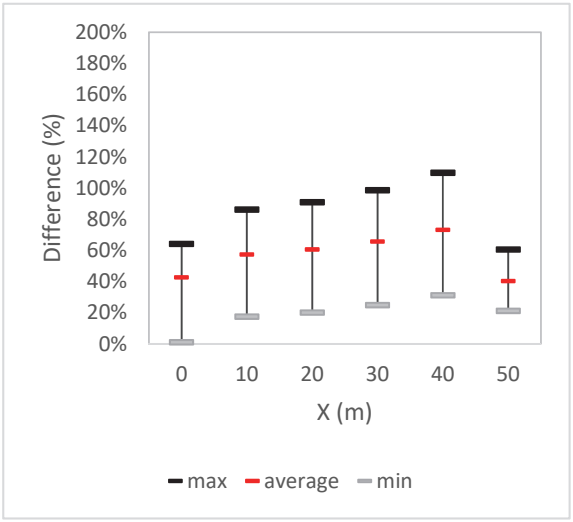

RADIATIVE HEAT FLUX GAS

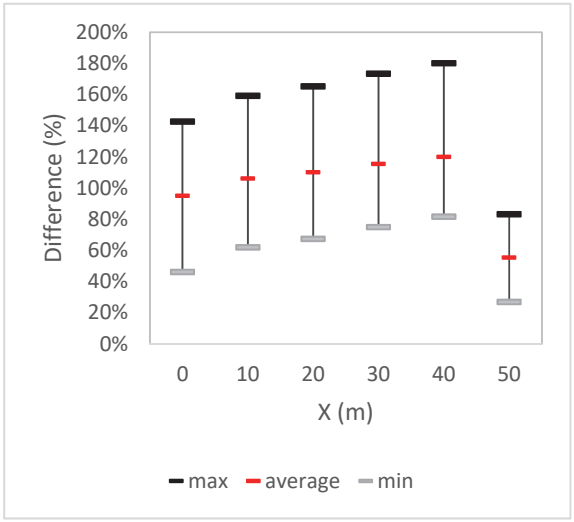

VISIBILITY

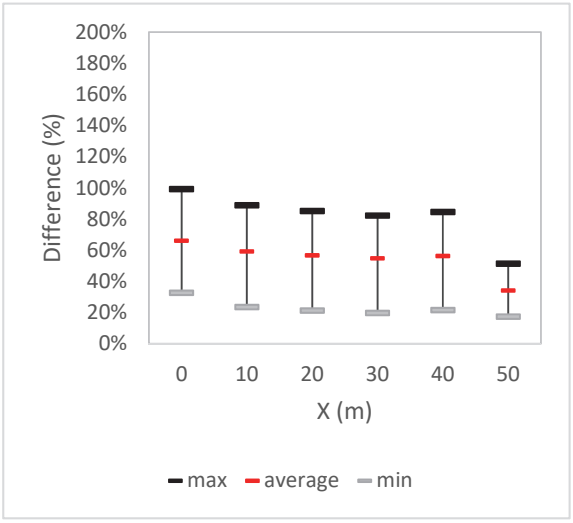

FED

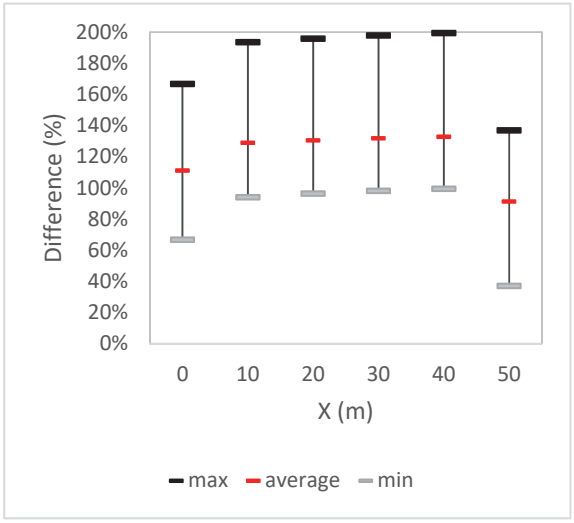

Table C.9. Difference (%), LL, HRR

LOWER LAYER – HRR VARIATION (5-100 MW)

TEMPERATURE

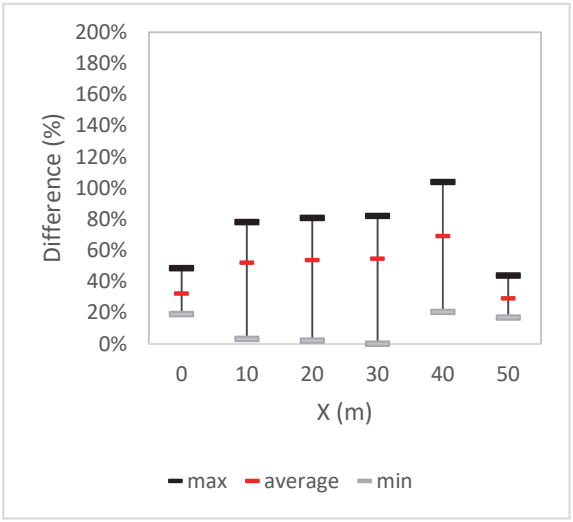

RADIATIVE HEAT FLUX GAS

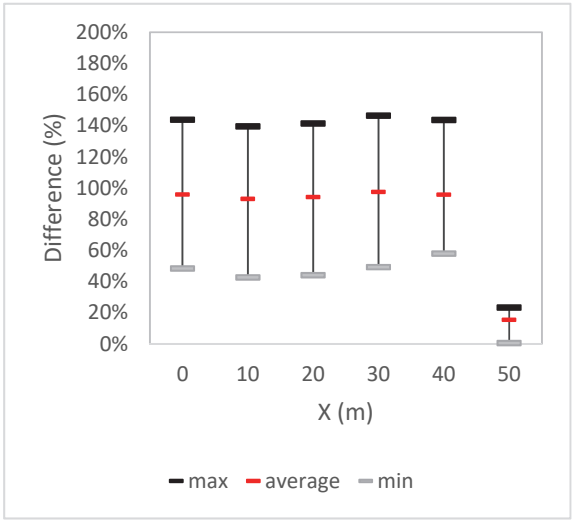

VISIBILITY

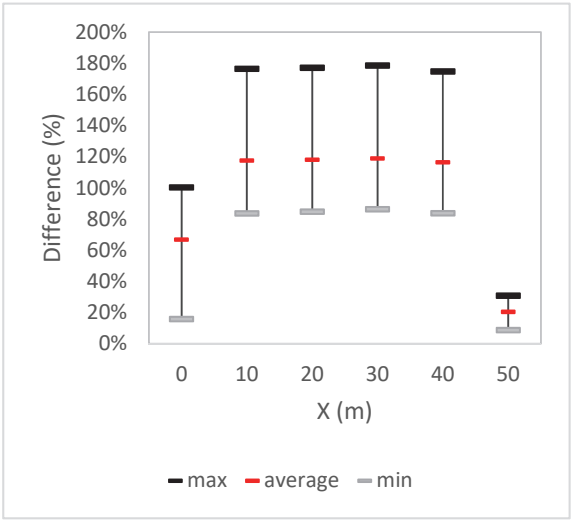

FED

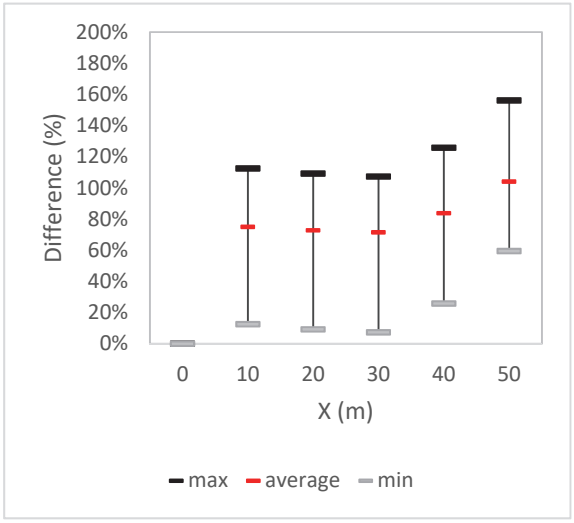

Parameter: Fire source. Area

Table C.10. Difference (%), UL, Fire source. Area

UPPER LAYER – FIRE SOURCE. AREA (1-4 m)	
TEMPERATURE	RADIATIVE HEAT FLUX GAS
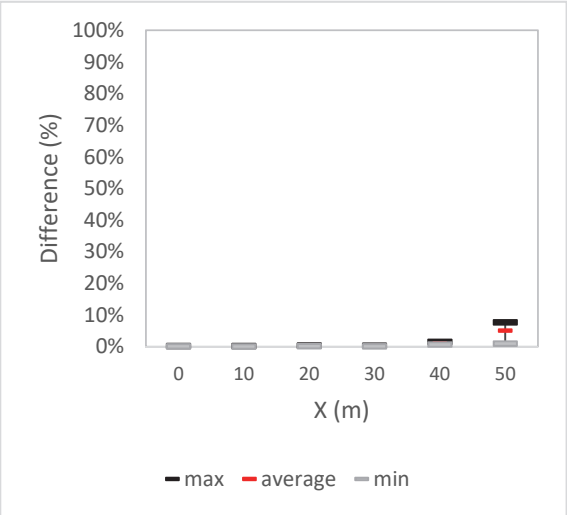	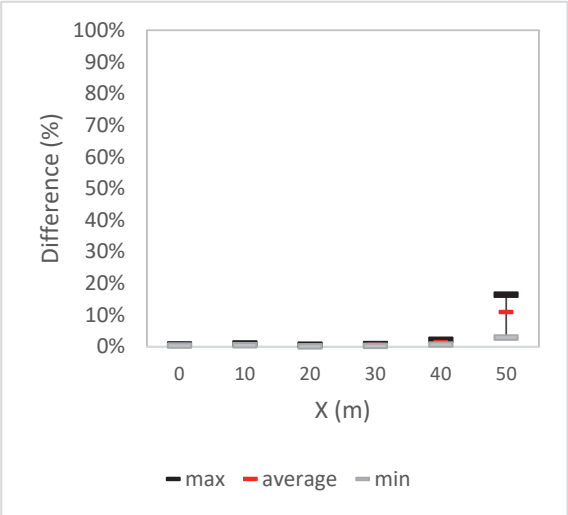
VISIBILITY	FED
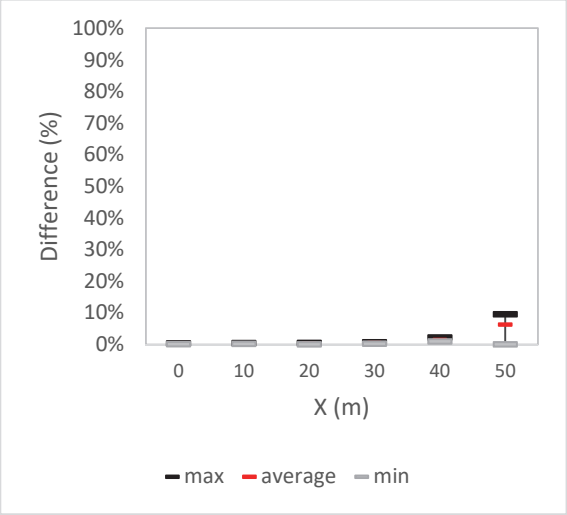	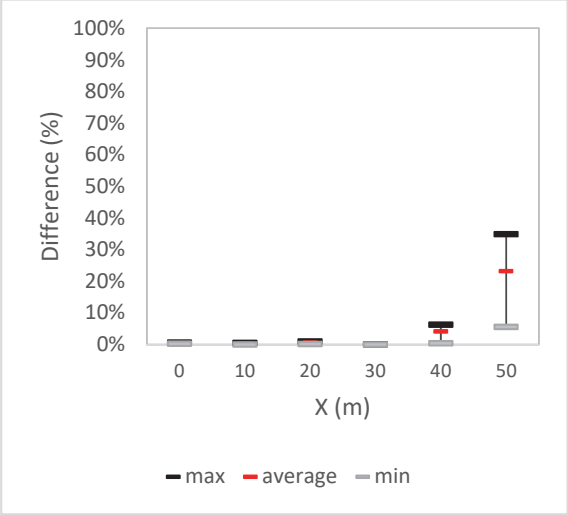

Table C.11. Difference (%), LL, Fire source. Area

LOWER LAYER – FIRE SOURCE. AREA (1-4 m)	
TEMPERATURE	RADIATIVE HEAT FLUX GAS
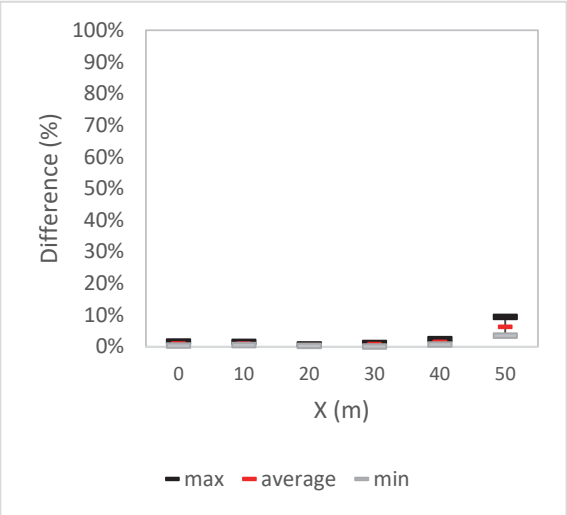	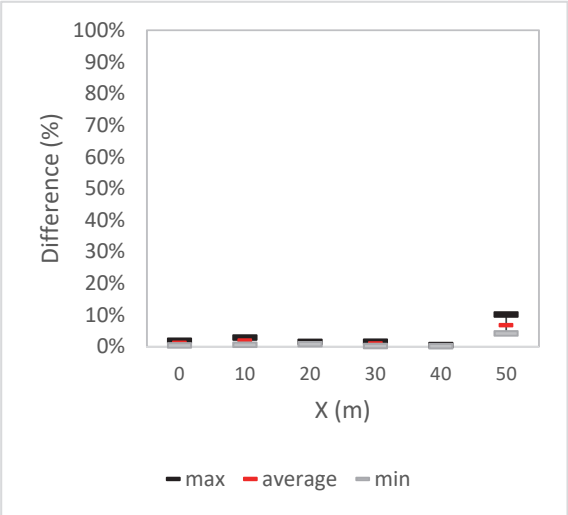
VISIBILITY	FED
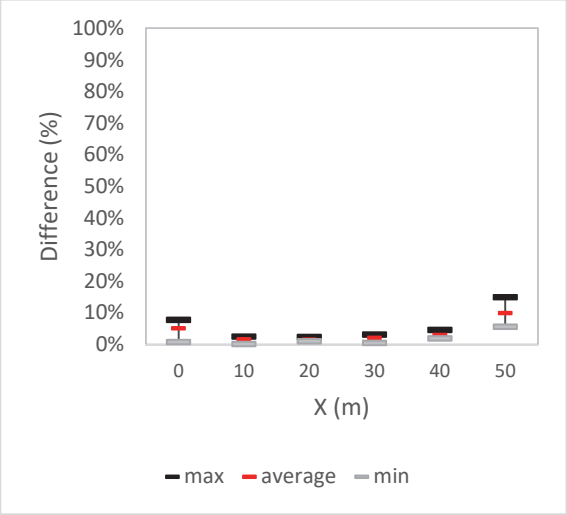	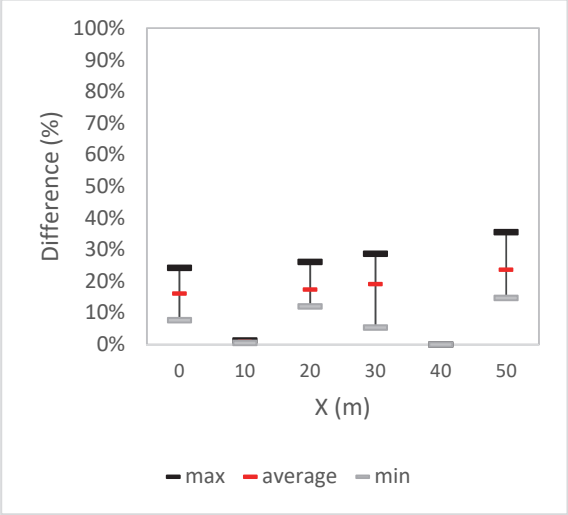

Table C.12. Profiles of the quantities X=40 m, Fire source. Area

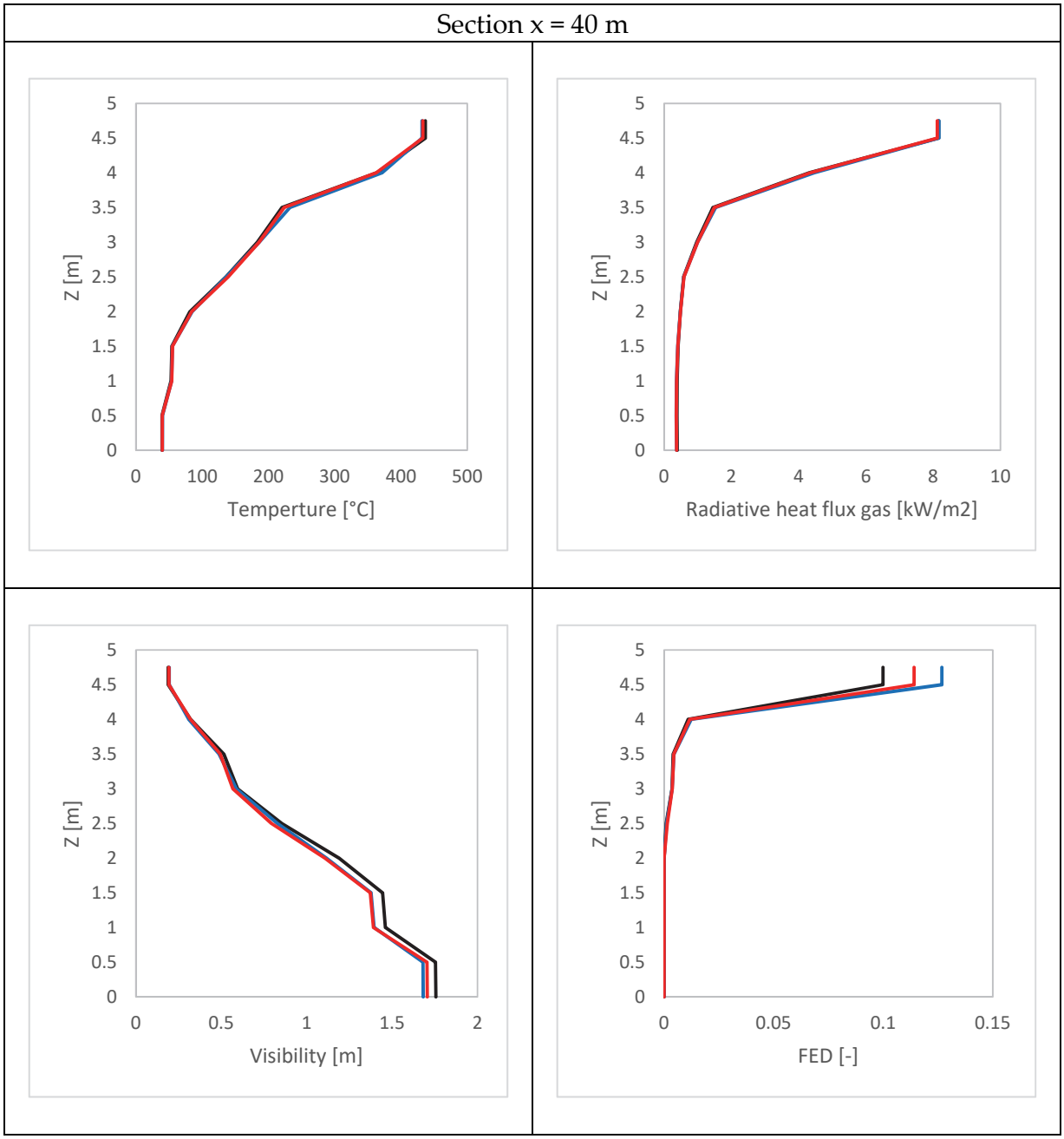

Red is 4 m², blue is 2 m²and black is 1 m² of fire source area.

Table C.13. Difference (%), UL, Fire source. B/W

<table>
<tr><th colspan="2">UPPER LAYER – FIRE SOURCE. B/W (1/1-4/1)</th></tr>
<tr><td>TEMPERATURE
 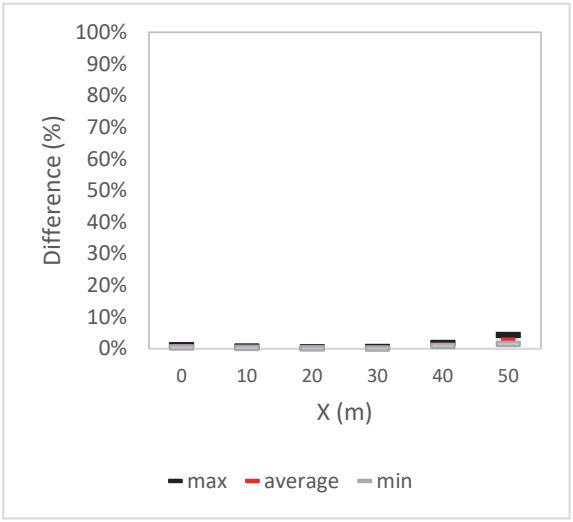
</td><td>RADIATIVE HEAT FLUX GAS
 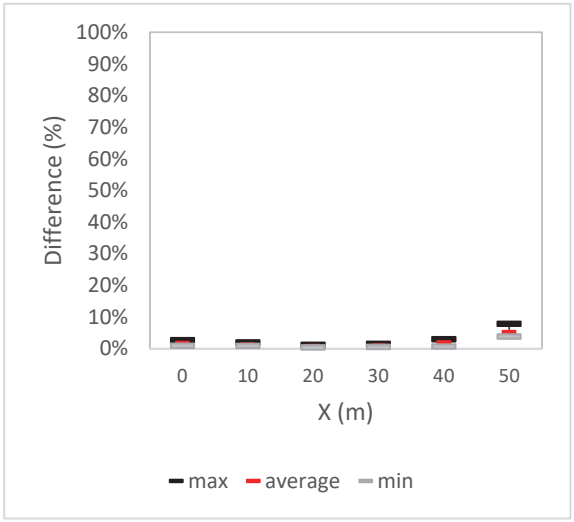
</td></tr>
<tr><td>VISIBILITY
 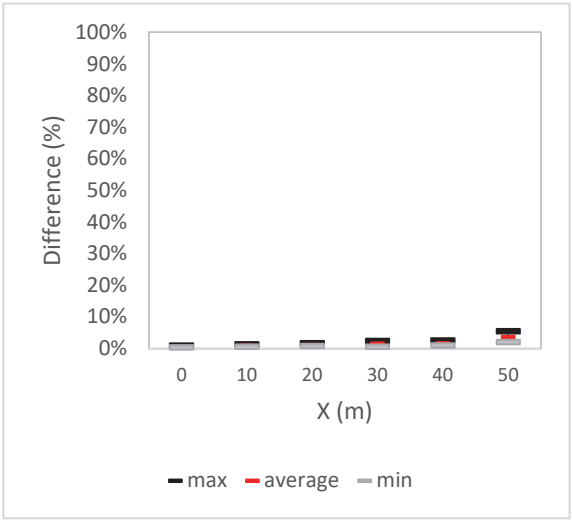
</td><td>FED
 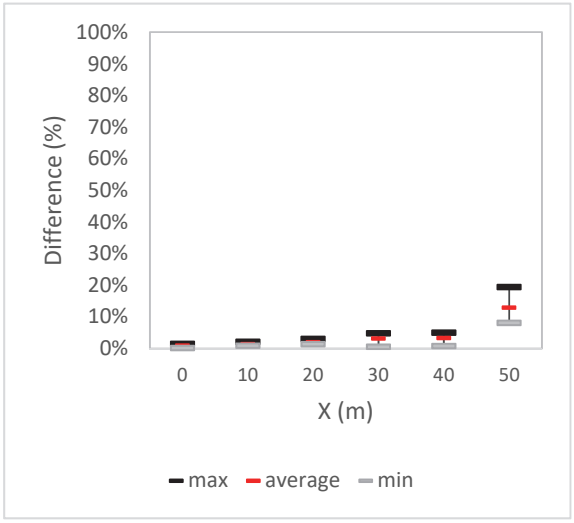
</td></tr>
</table>

Table C.14. Difference (%), LL, Fire source. B/W

LOWER LAYER – FIRE SOURCE. B/W (1/1-4/1)

TEMPERATURE

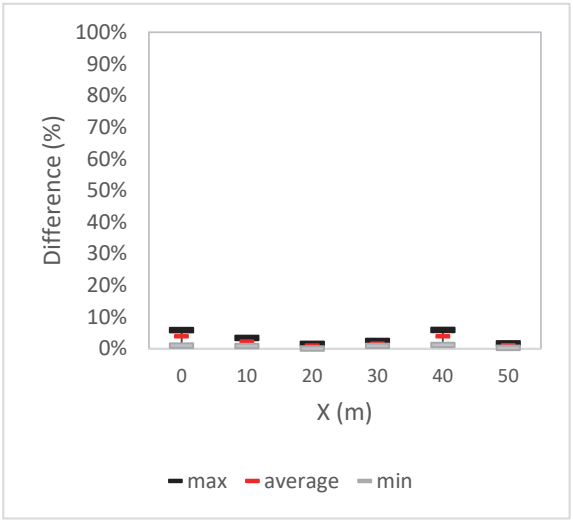

RADIATIVE HEAT FLUX GAS

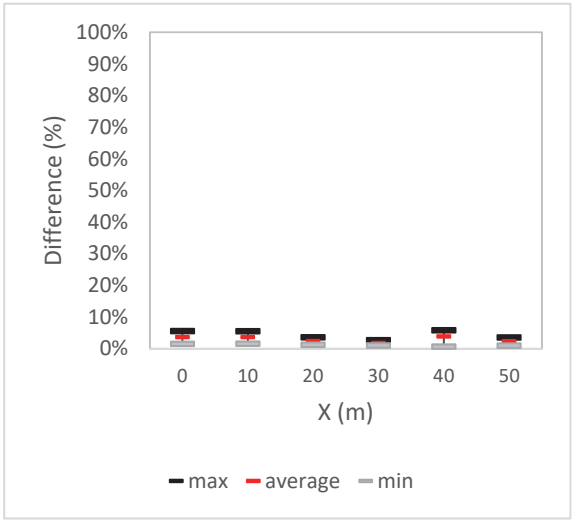

VISIBILITY

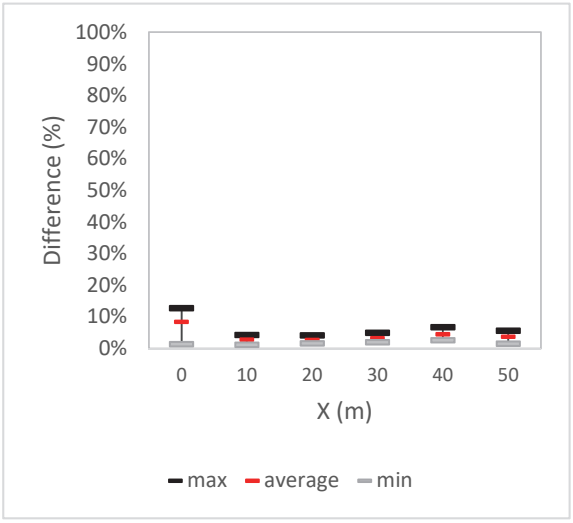

FED

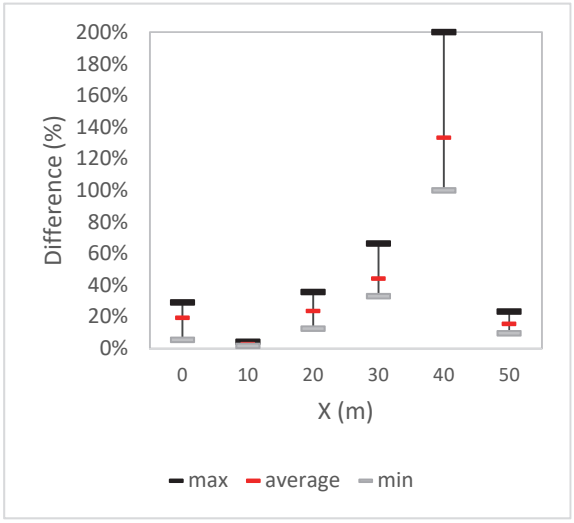

Table C.15. Profiles of the quantities X=40 m, Fire source. B/W

Section x = 40 m	
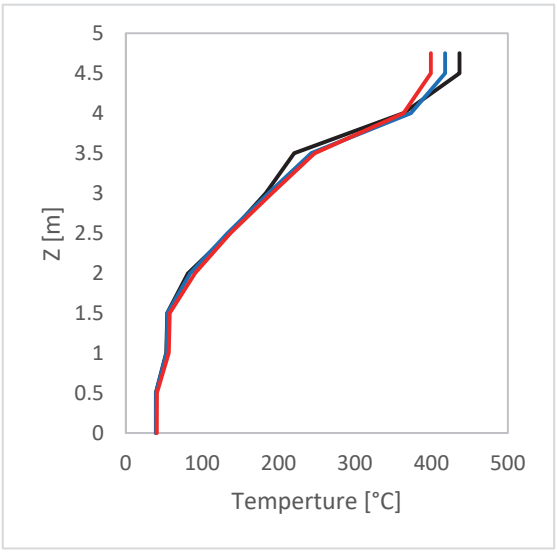	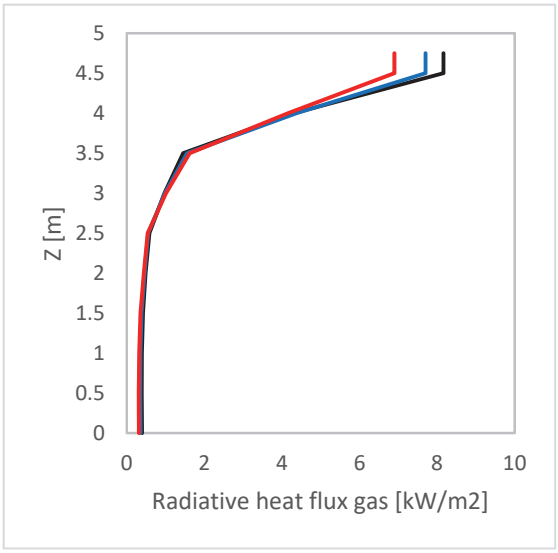
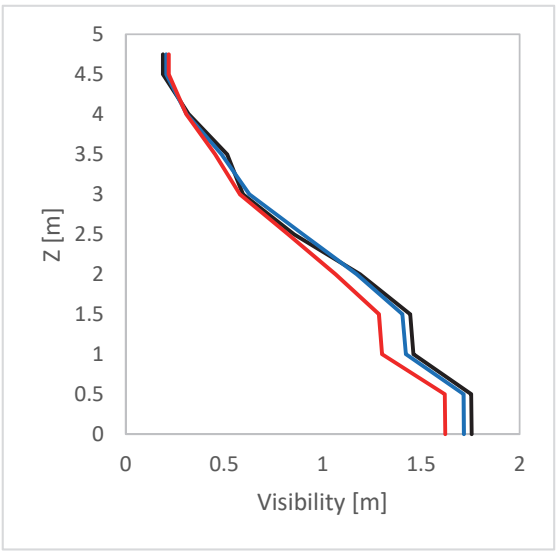	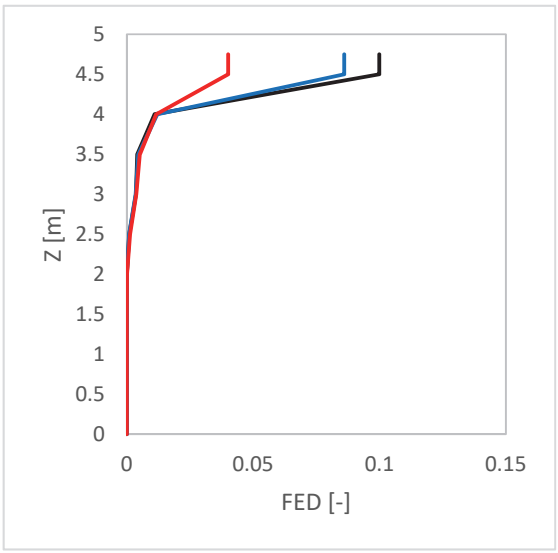

Red is 4/1, blue is 2/1 and black is 1/1 of B/W ratio.

Table C.16. Difference (%), UL, Soot yield

<table>
<tr><th colspan="2">UPPER LAYER – SOOT VARIATION (0.05-0.2 g/g)</th></tr>
<tr><td>TEMPERATURE
 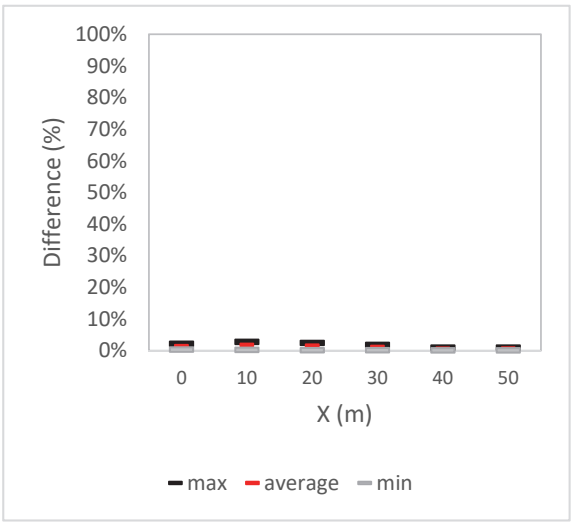
</td><td>RADIATIVE HEAT FLUX GAS
 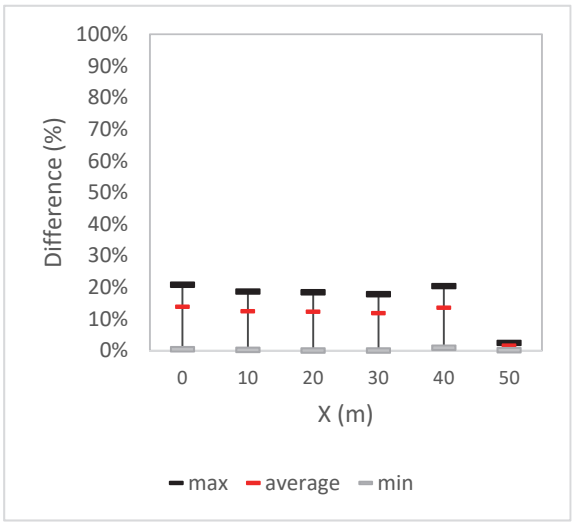
</td></tr>
<tr><td>VISIBILITY
 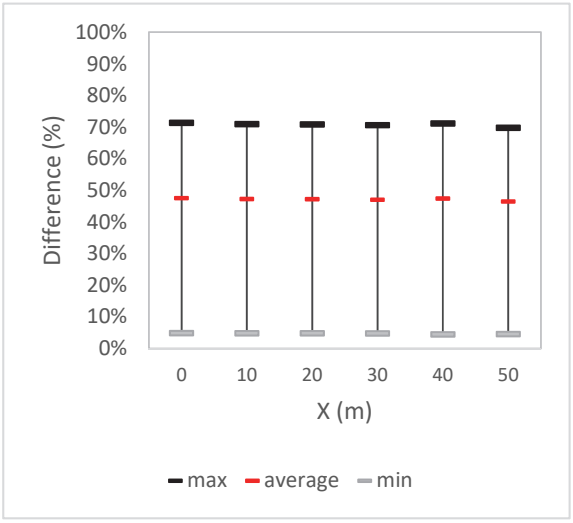
</td><td>FED
 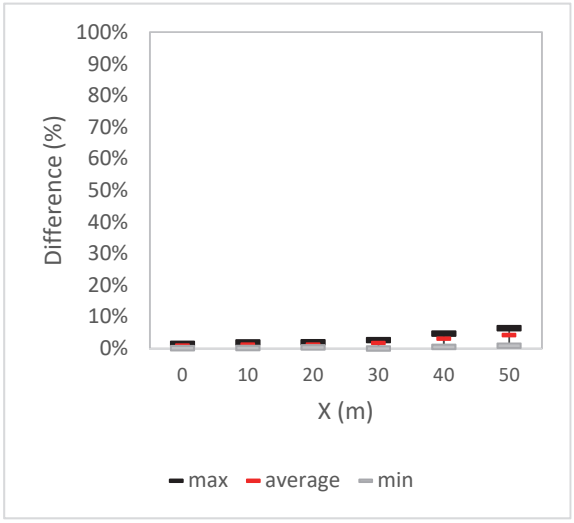
</td></tr>
</table>

Table C.17. Difference (%), LL, Soot yield

<table>
<tr><th colspan="2">LOWER LAYER – SOOT VARIATION (0.05-0.2 g/g)</th></tr>
<tr><td>TEMPERATURE
 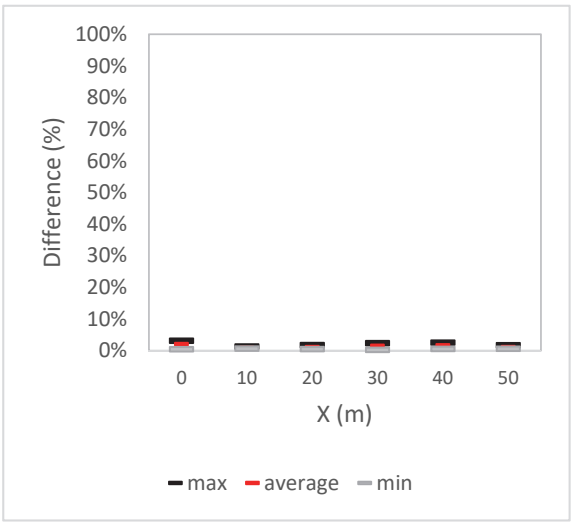
</td><td>RADIATIVE HEAT FLUX GAS
 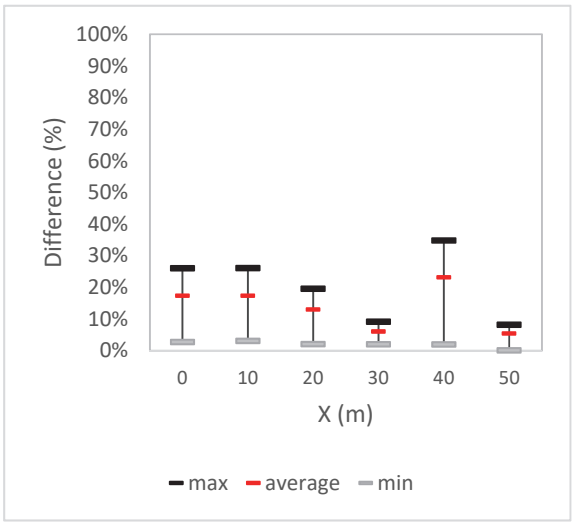
</td></tr>
<tr><td>VISIBILITY
 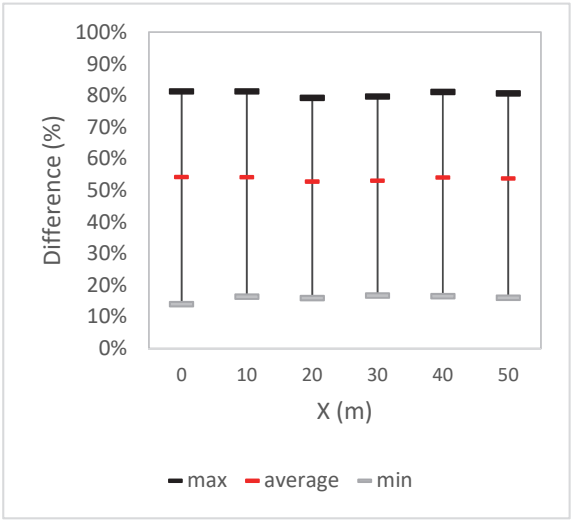
</td><td>FED
 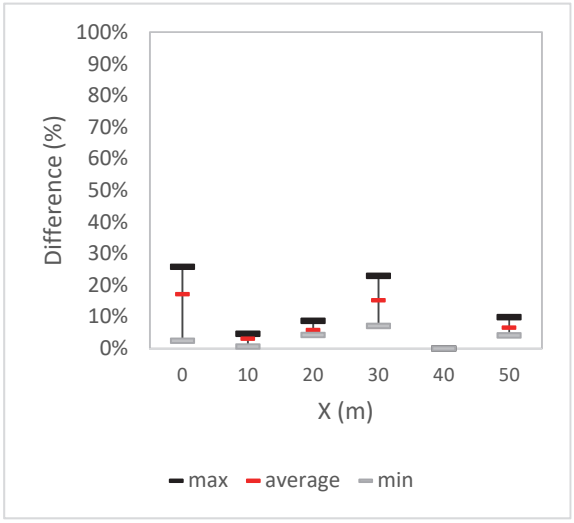
</td></tr>
</table>

Table C.18. Difference (%), UL, Material

UPPER LAYER – MATERIAL (INERT-CONCRETE-ADIABATIC)

TEMPERATURE

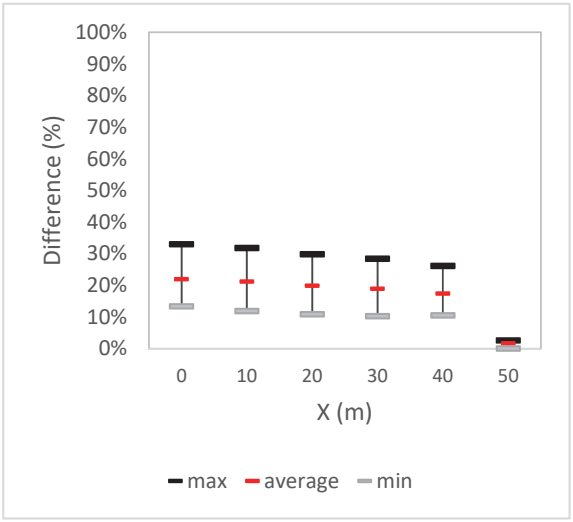

RADIATIVE HEAT FLUX GAS

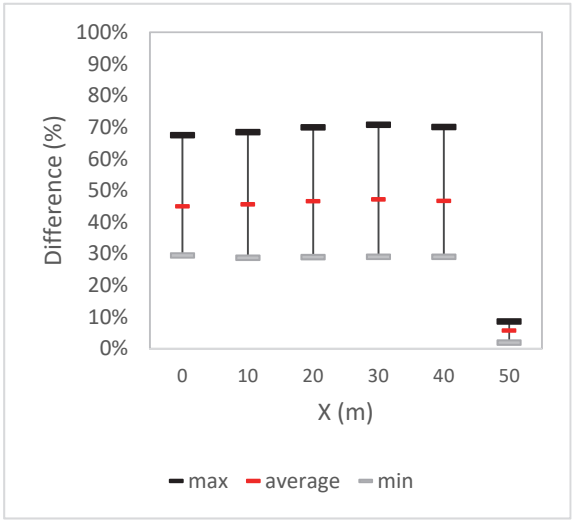

VISIBILITY

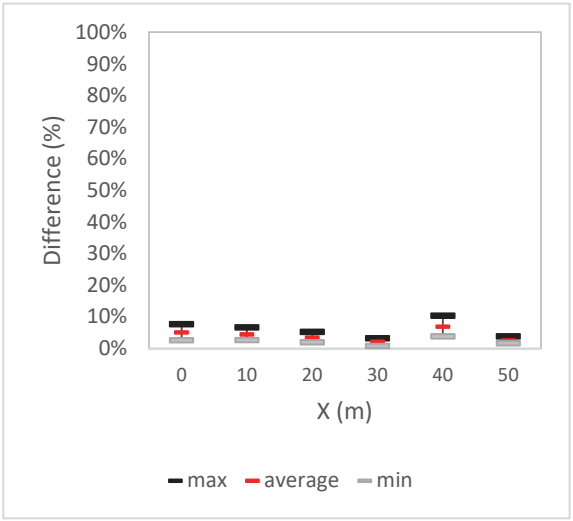

FED

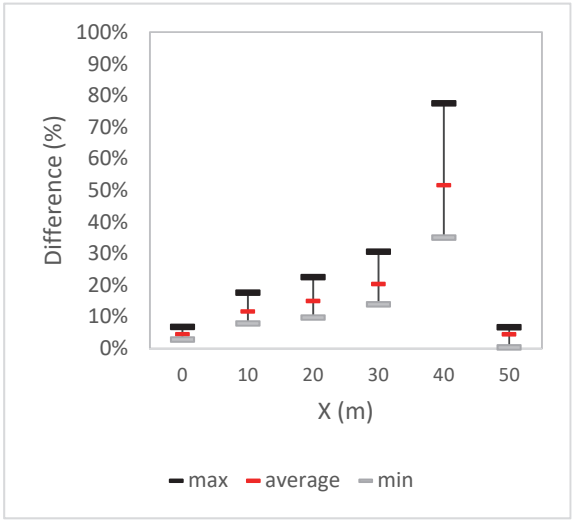

Table C.19. Difference (%), LL, Material

<table>
<tr><th colspan="2">LOWER LAYER – MATERIAL (INERT-CONCRETE-ADIABATIC)</th></tr>
<tr><td>TEMPERATURE
 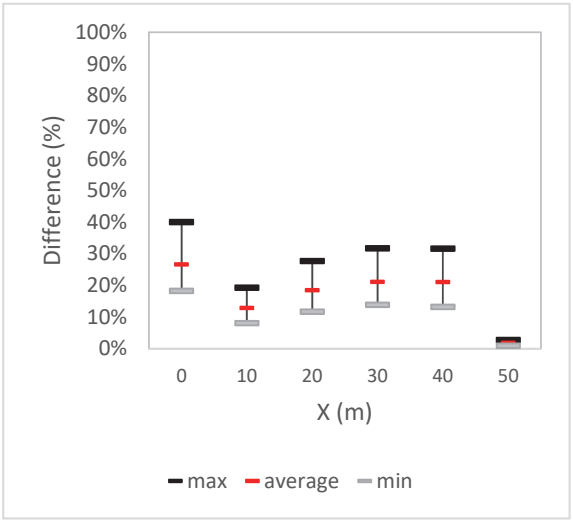
</td><td>RADIATIVE HEAT FLUX GAS
 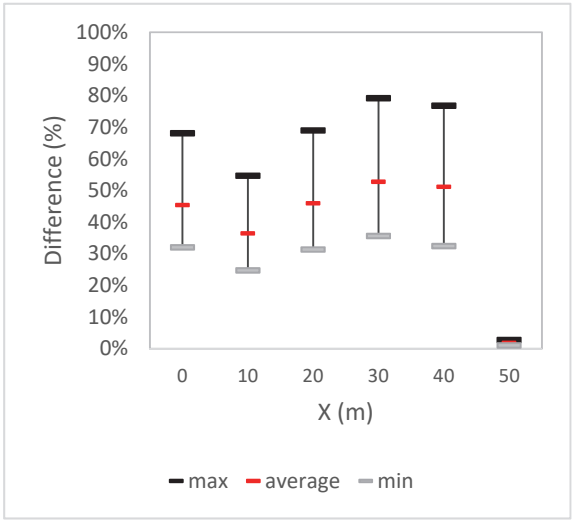
</td></tr>
<tr><td>VISIBILITY
 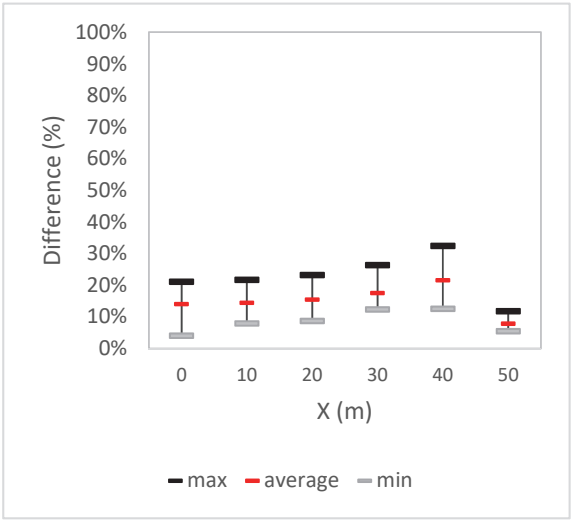
</td><td>FED
 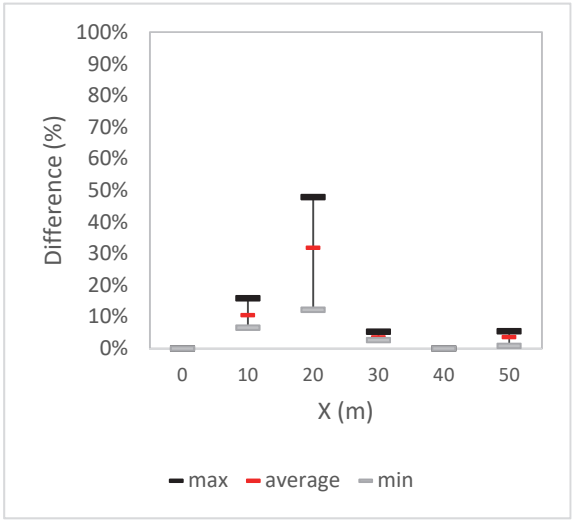
</td></tr>
</table>

Table C.20. Profiles of the quantities X=30 m, Material

Section x = 30 m	
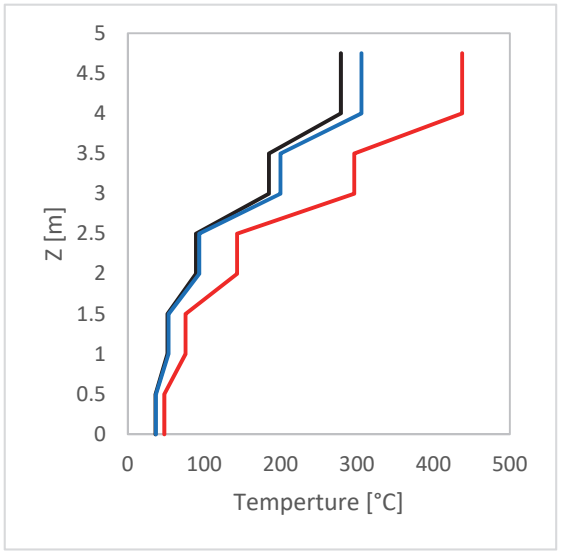	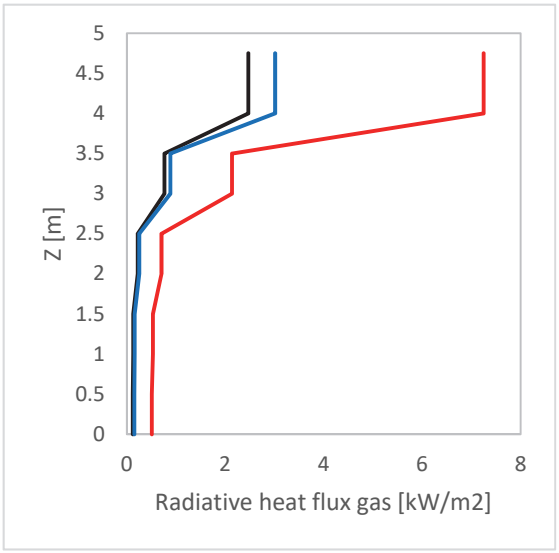
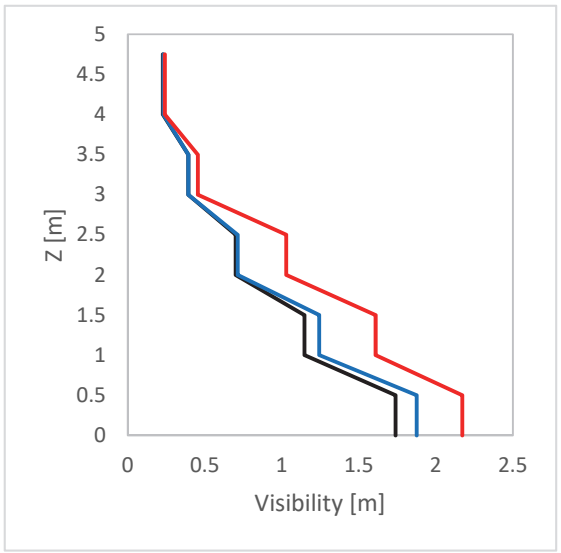	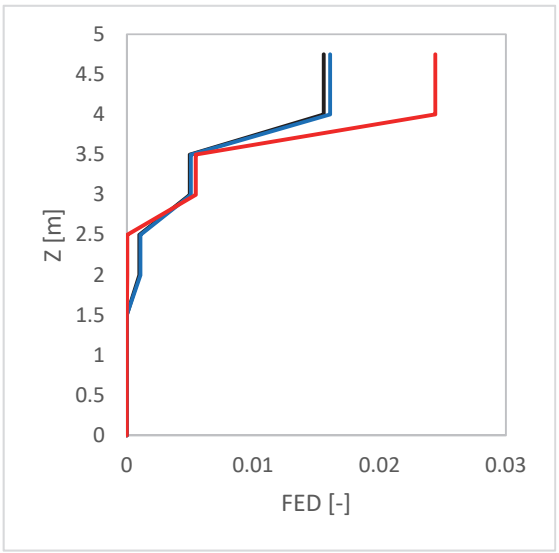

Red is adiabatic, blue is concrete and black is inert material.

Table C.21. Difference (%), UL, Presence of vehicles

<table>
<tr><th colspan="2">UPPER LAYER – PRESENCE OF VEHICLES AS OBSTRUCTIONS</th></tr>
<tr><td>TEMPERATURE
 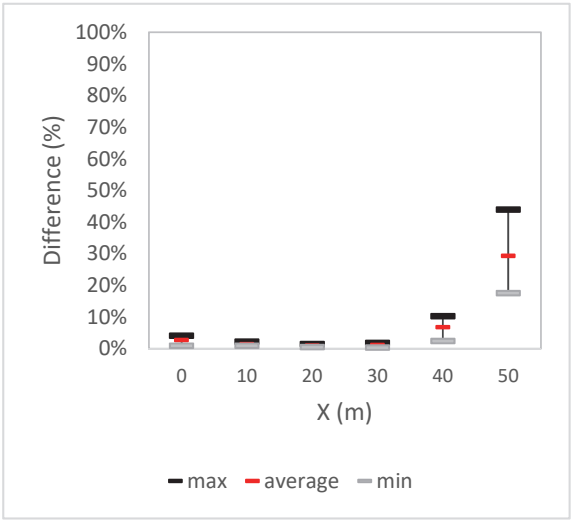
</td><td>RADIATIVE HEAT FLUX GAS
 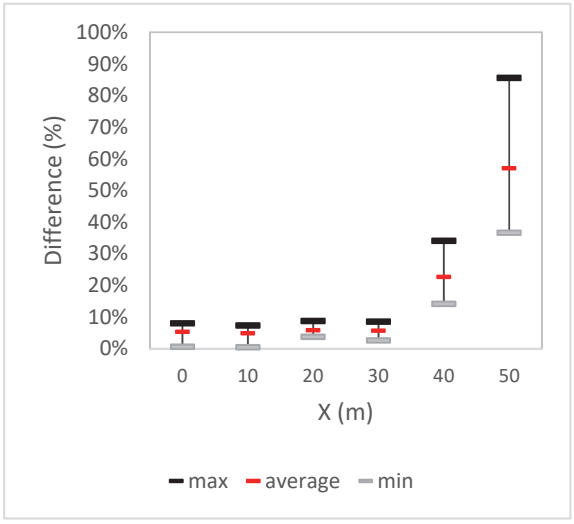
</td></tr>
<tr><td>VISIBILITY
 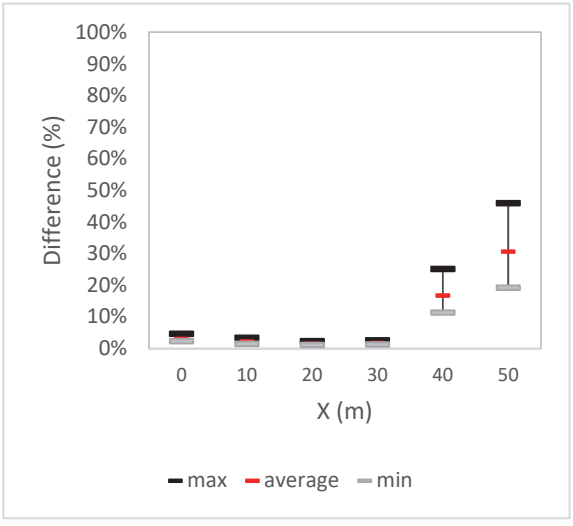
</td><td>FED
 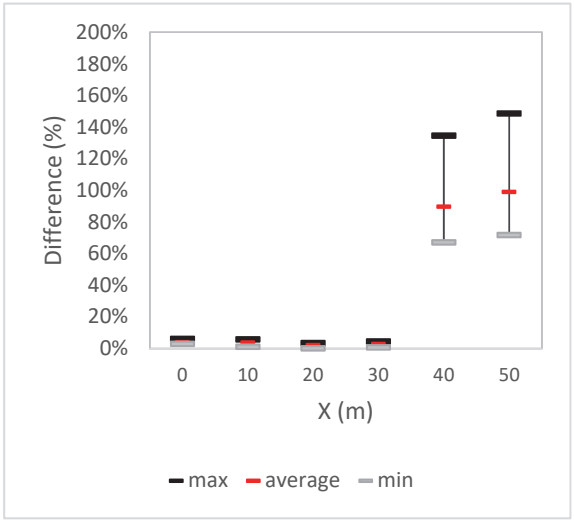
</td></tr>
</table>

Table C.22. Difference (%), LL, Presence of vehicles

<table>
<tr><th colspan="2">LOWER LAYER – PRESENCE OF VEHICLES AS OBSTRUCTIONS</th></tr>
<tr><td>TEMPERATURE
 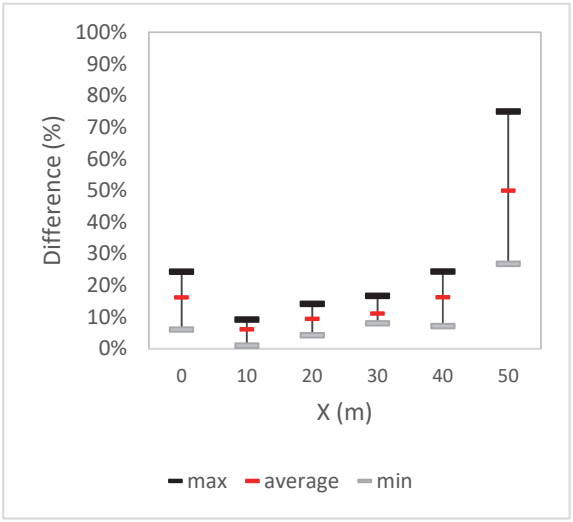
</td><td>RADIATIVE HEAT FLUX GAS
 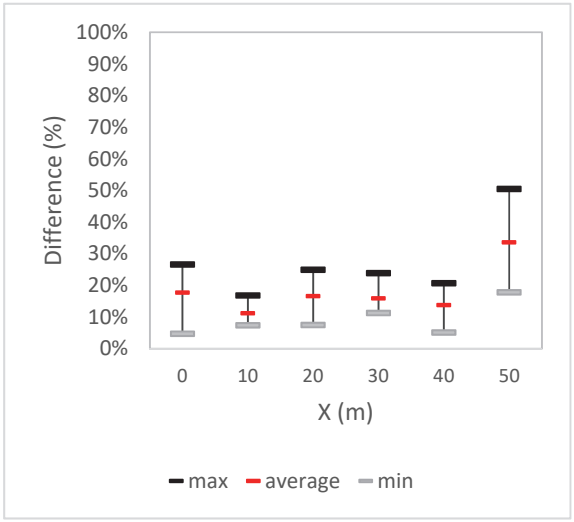
</td></tr>
<tr><td>VISIBILITY
 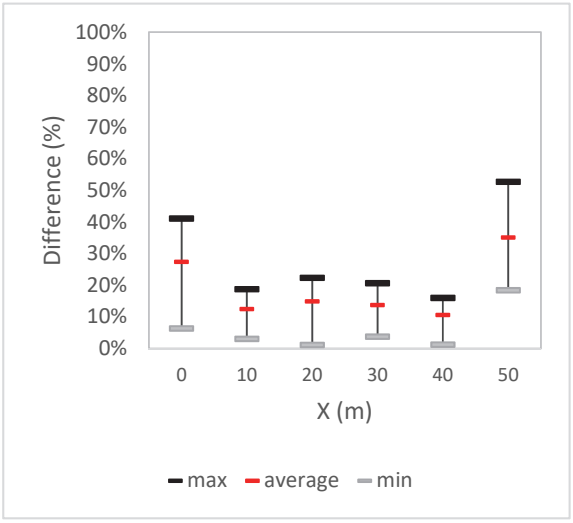
</td><td>FED
 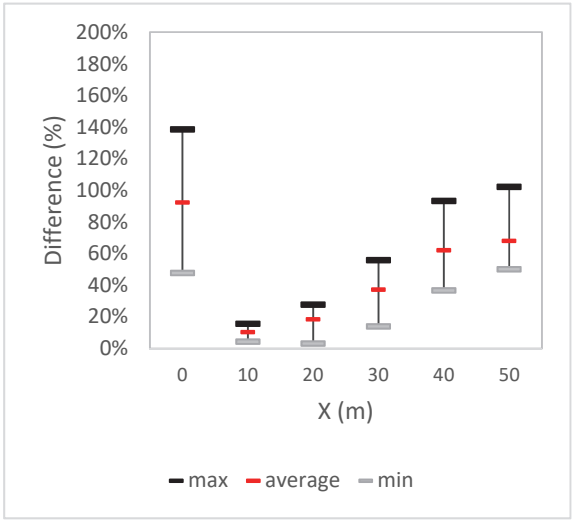
</td></tr>
</table>

Table C.23. Profiles of the quantities, X=30m, Presence of vehicles

Section x = 30 m

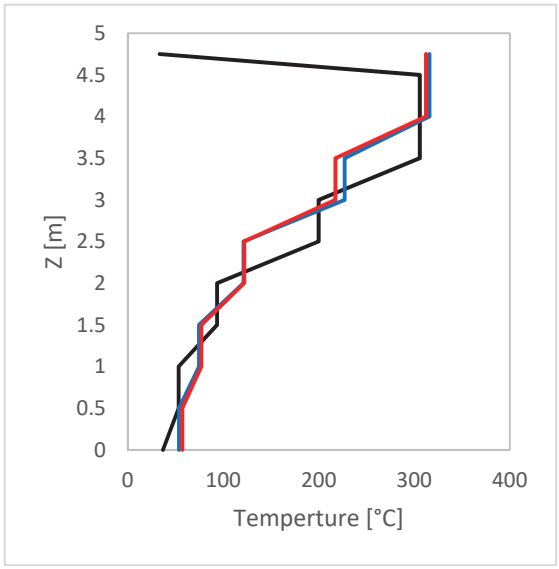

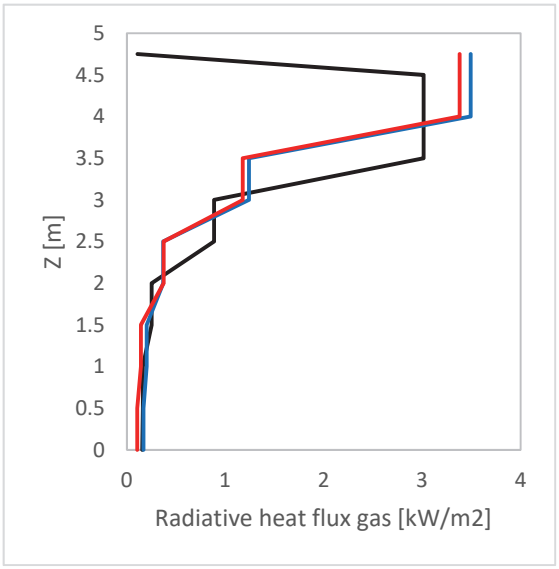

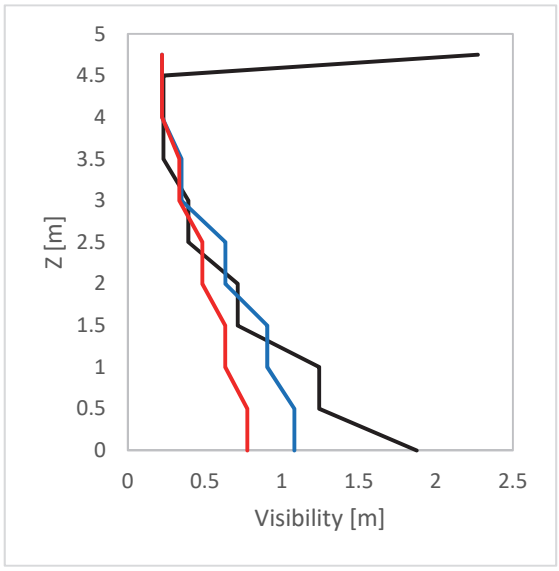

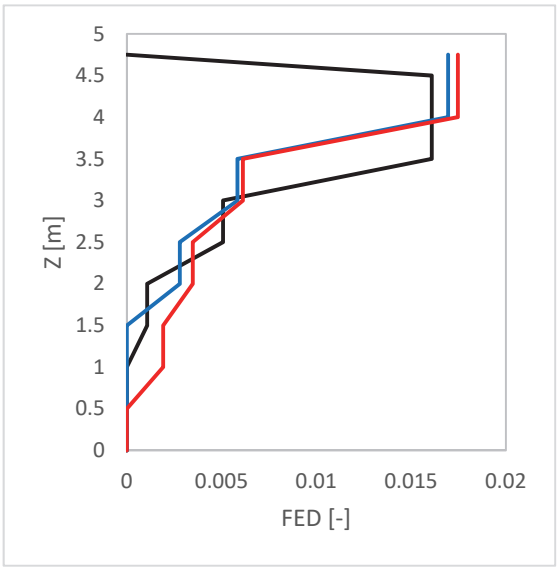

Red is queue of vehicles, blue is low traffic vehicles and black is zero vehicles.

Table C.24. Difference (%), UL, External boundary

UPPER LAYER – EXTERNAL BOUNDARY Lext (3/5H-2H m)	
TEMPERATURE	RADIATIVE HEAT FLUX GAS
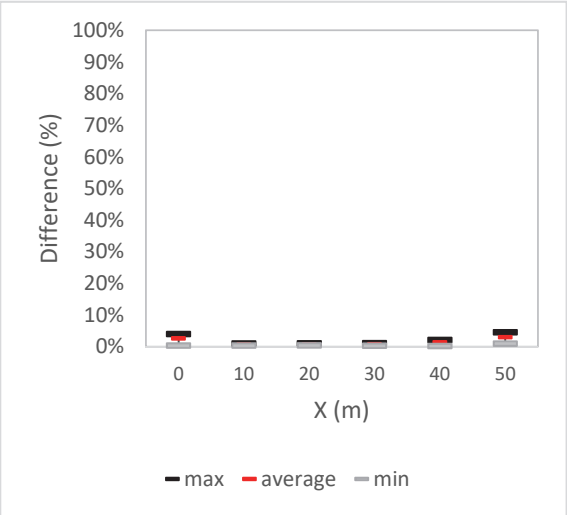	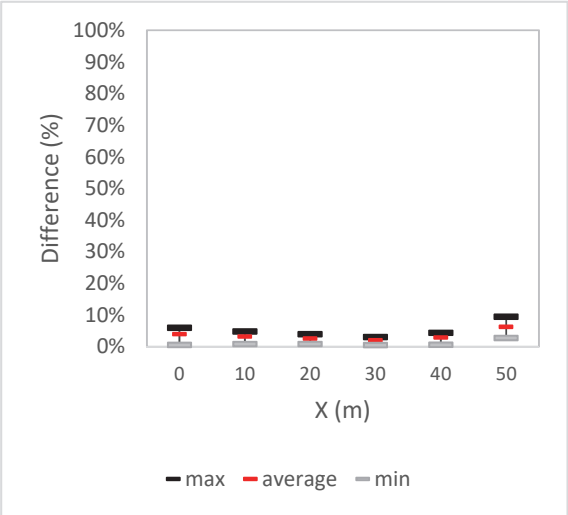
VISIBILITY	FED
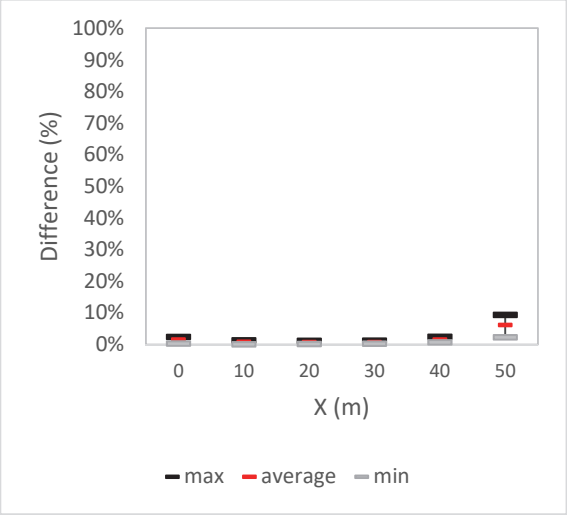	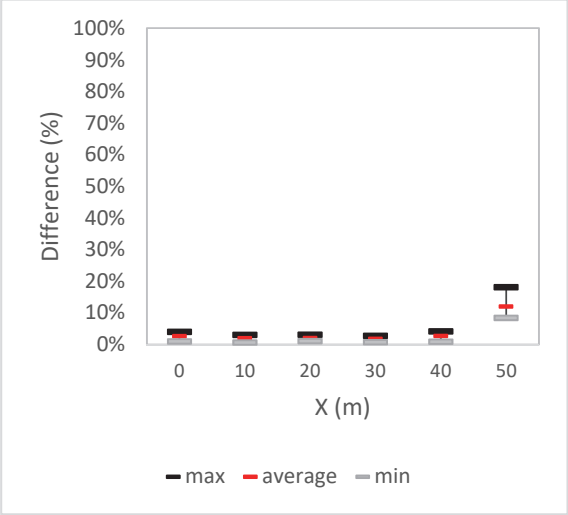

Table C.25. Difference (%), LL, External boundary

<table>
<tr><th colspan="2">LOWER LAYER – EXTERNAL BOUNDARY Lext (3/5H-2H m)</th></tr>
<tr><td>TEMPERATURE
 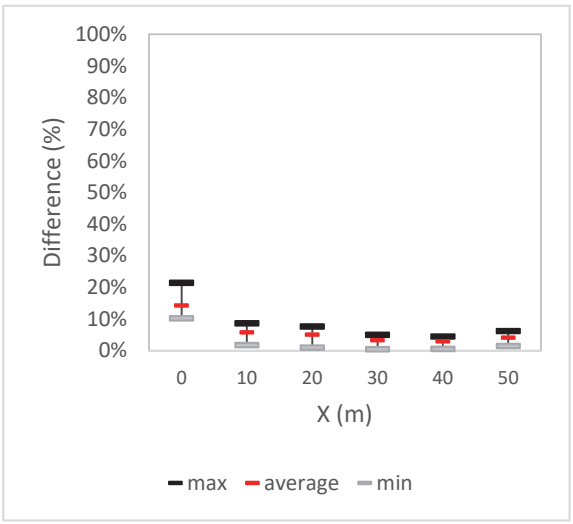
</td><td>RADIATIVE HEAT FLUX GAS
 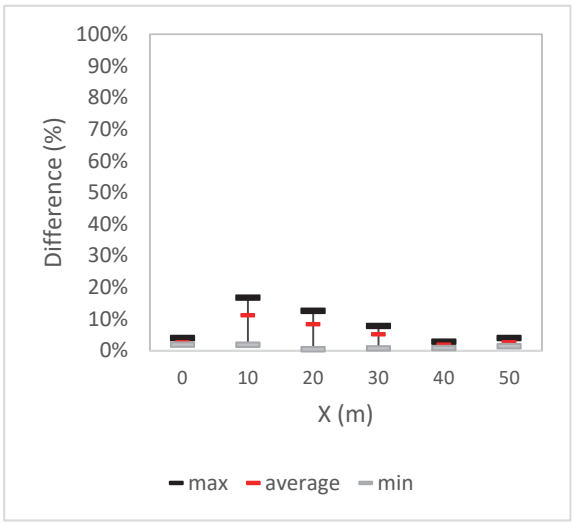
</td></tr>
<tr><td>VISIBILITY
 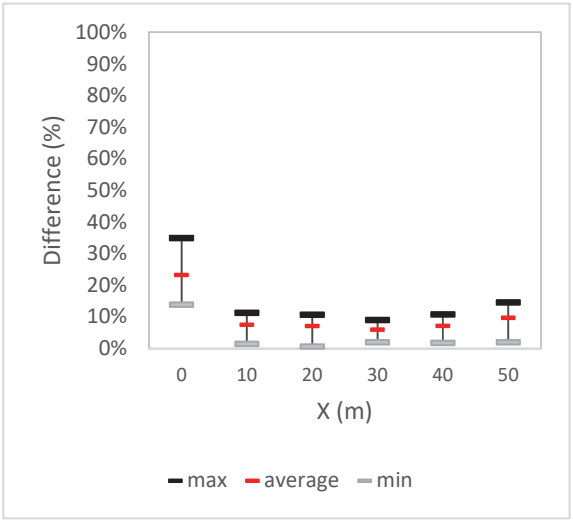
</td><td>FED
 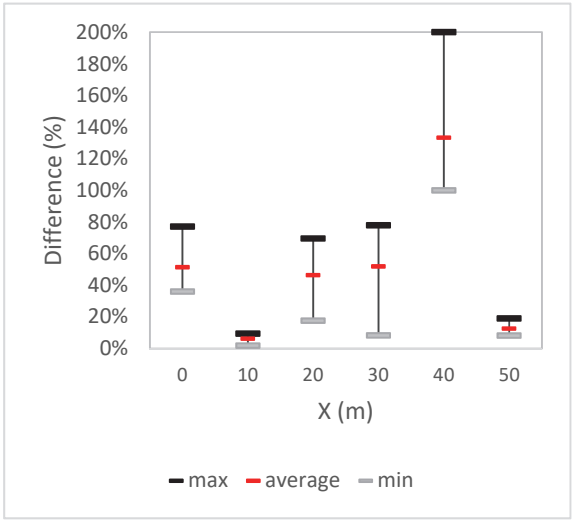
</td></tr>
</table>

Table C.26. Profiles of the quantities, X=10m, External boundary

Section x = 10 m	
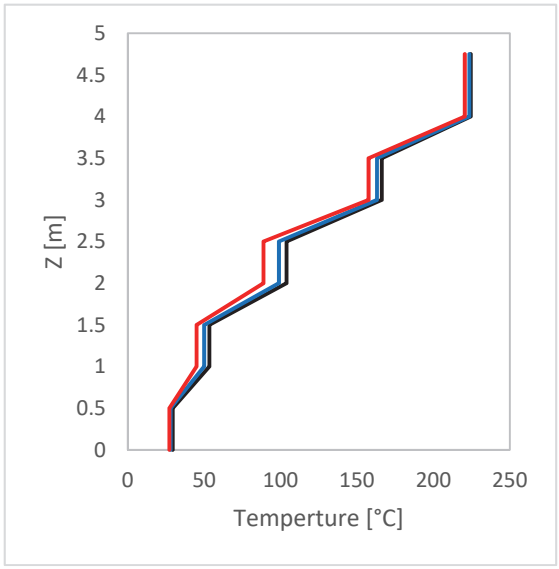	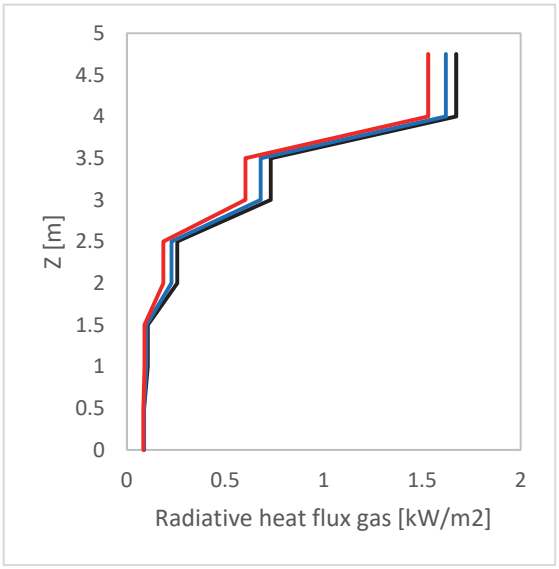
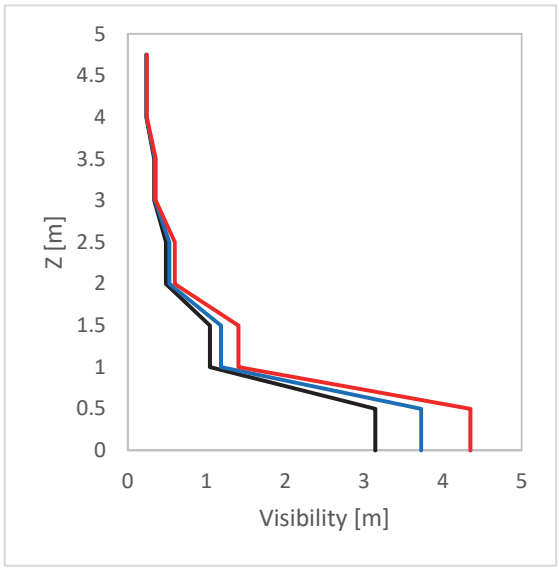	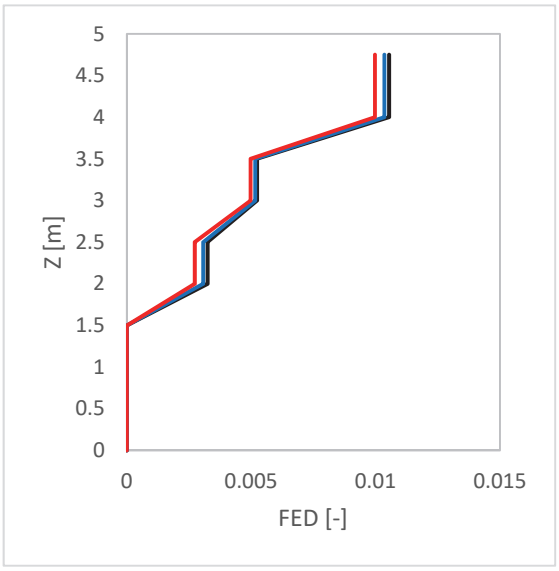

Red is $2H_t$, blue is $1H_t$ and black is $3/5H_t$ of external length (H_t = tunnel height).

Table C.27. Difference (%), UL, Longitudinal inclination

<table>
<tr><th colspan="2">UPPER LAYER – LONGIDUTINAL INCLINATION (-5%,+5%)</th></tr>
<tr><td>TEMPERATURE
 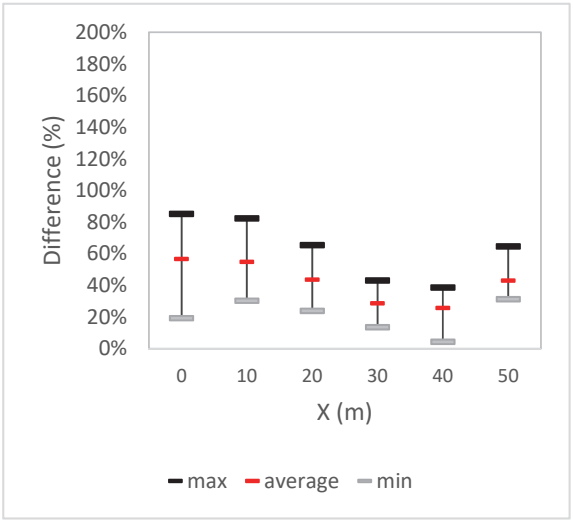
</td><td>RADIATIVE HEAT FLUX GAS
 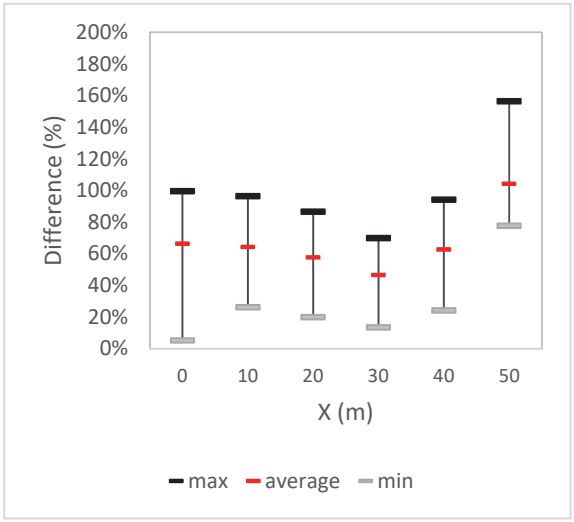
</td></tr>
<tr><td>VISIBILITY
 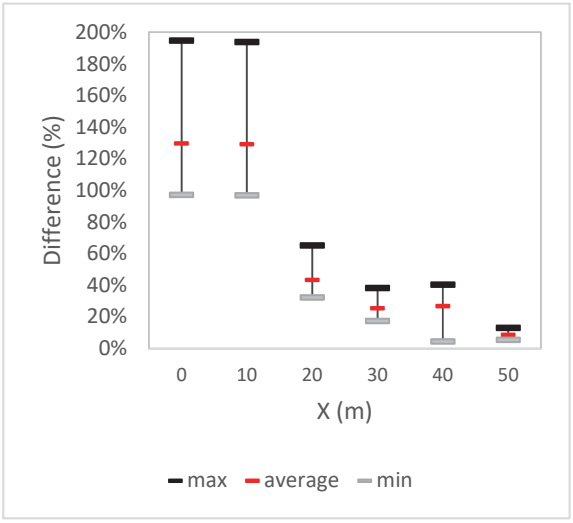
</td><td>FED
 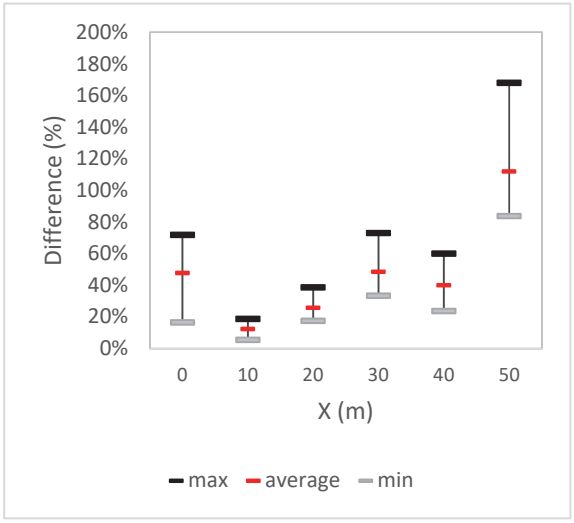
</td></tr>
</table>

Table C.28. Difference (%), LL, Longitudinal inclination

<table>
<tr><th colspan="2">LOWER LAYER – LONGIDUTINAL INCLINATION (-5%,+5%)</th></tr>
<tr><td>TEMPERATURE
 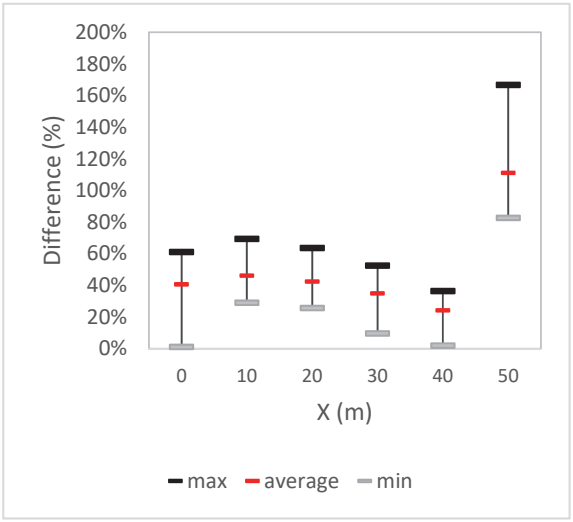
</td><td>RADIATIVE HEAT FLUX GAS
 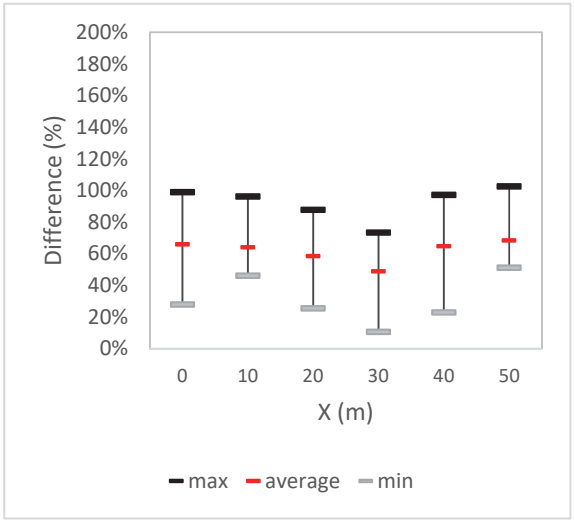
</td></tr>
<tr><td>VISIBILITY
 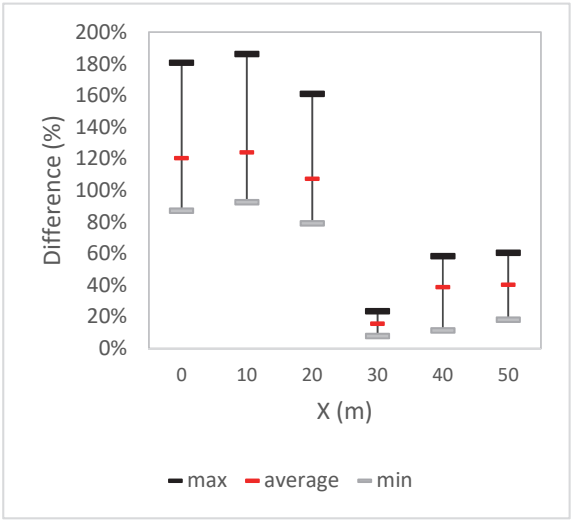
</td><td>FED
 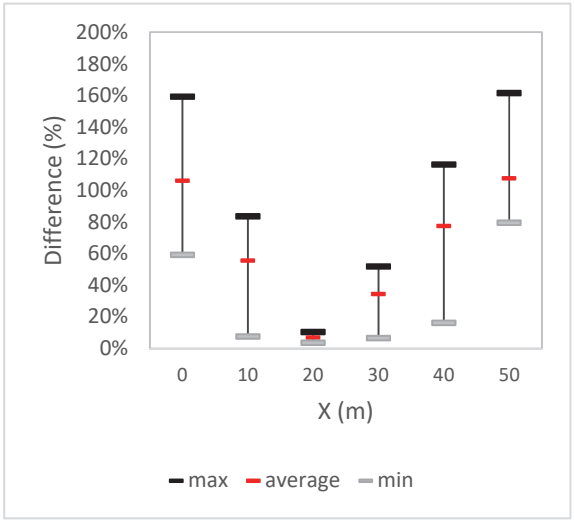
</td></tr>
</table>

Table C.29. Profiles of the quantities, X=20m, Longitudinal inclination

Section x = 20 m	
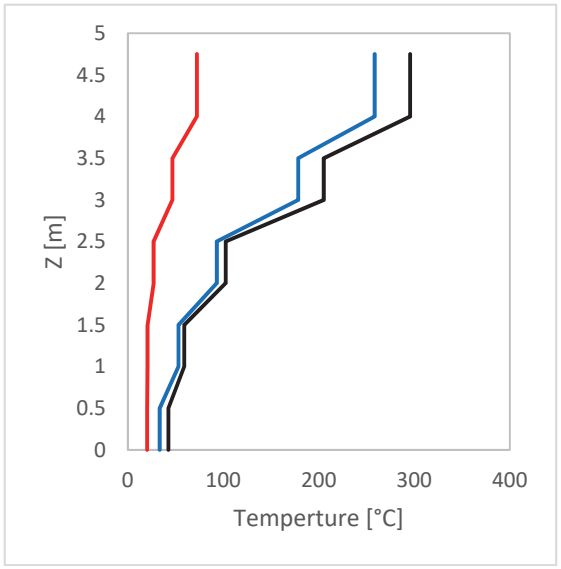	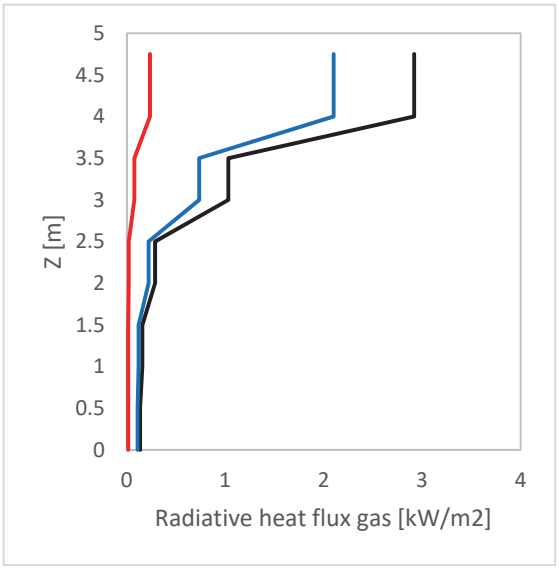
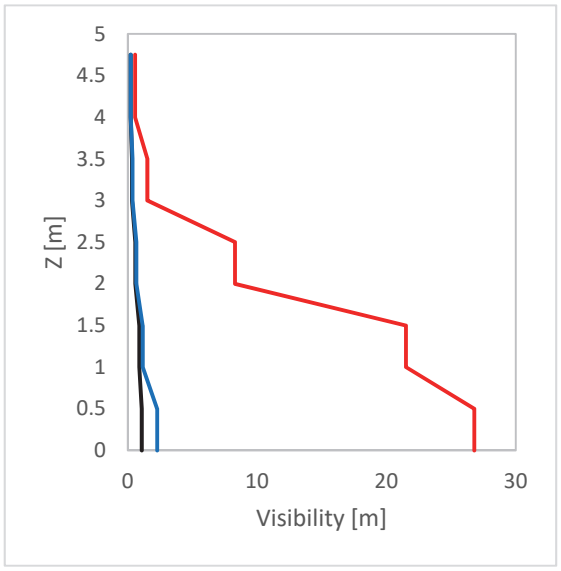	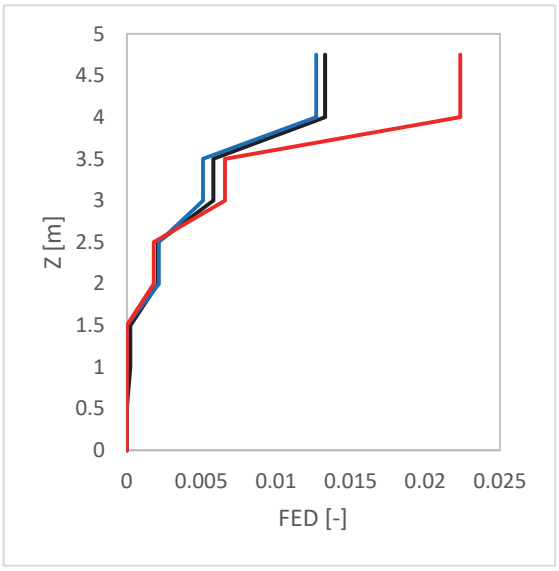

Red is downwards, blue is upwards and black is zero inclination.

Table C.30. Difference (%), UL, Initial temperature

UPPER LAYER –INITIAL TEMPERATURE (10-30°C)	
TEMPERATURE	RADIATIVE HEAT FLUX GAS
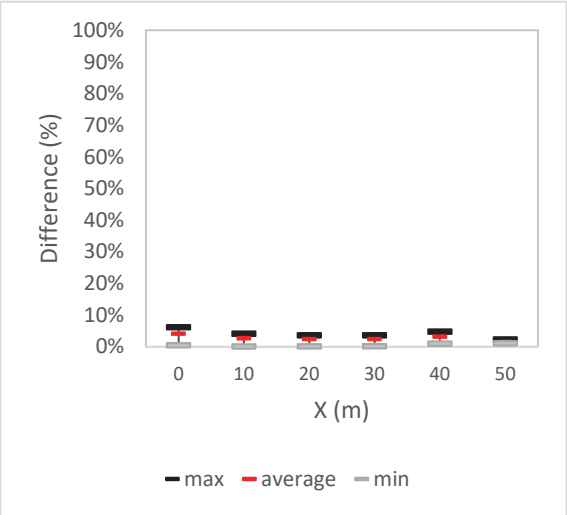	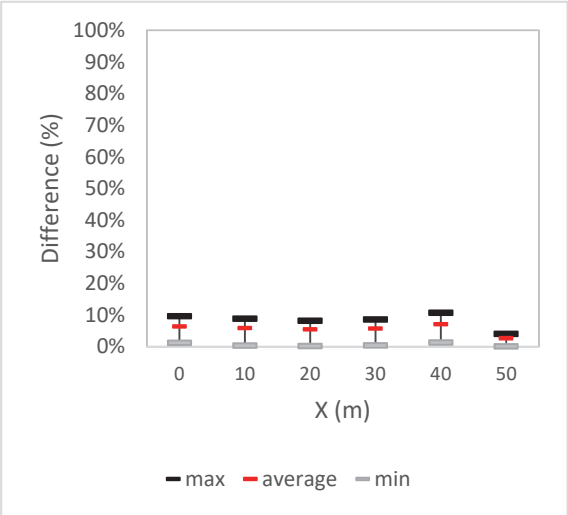
VISIBILITY	FED
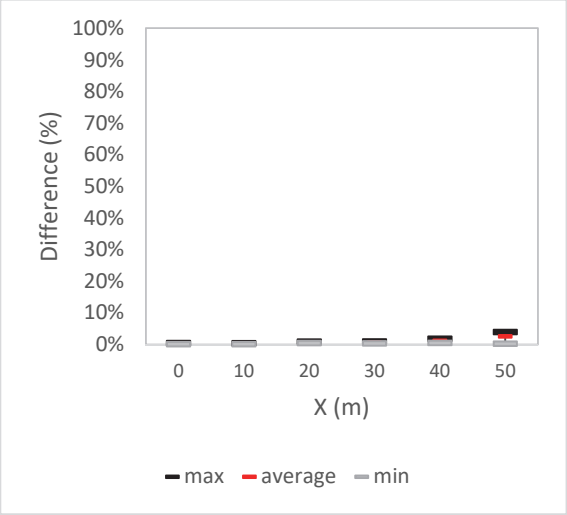	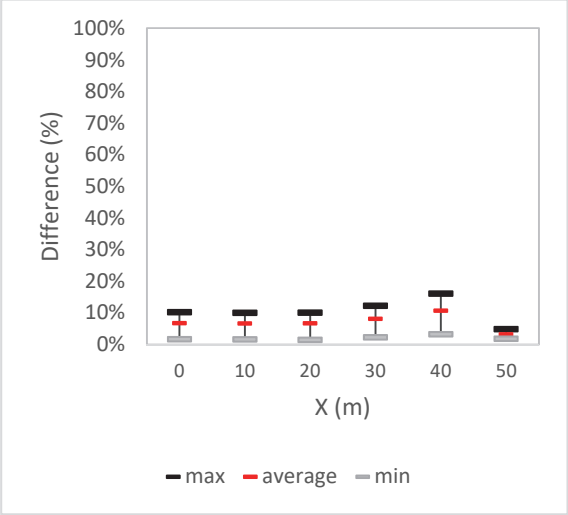

Table C.31. Difference (%), LL, Initial temperature

<table>
<tr><th colspan="2">LOWER LAYER – INITIAL TEMPERATURE (10-30°C)</th></tr>
<tr><td>TEMPERATURE
 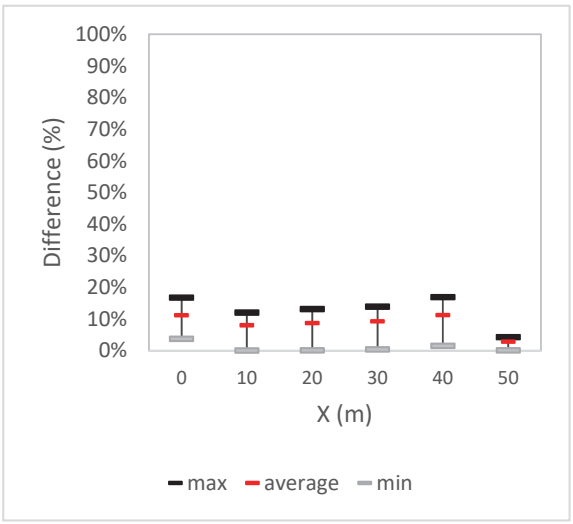
</td><td>RADIATIVE HEAT FLUX GAS
 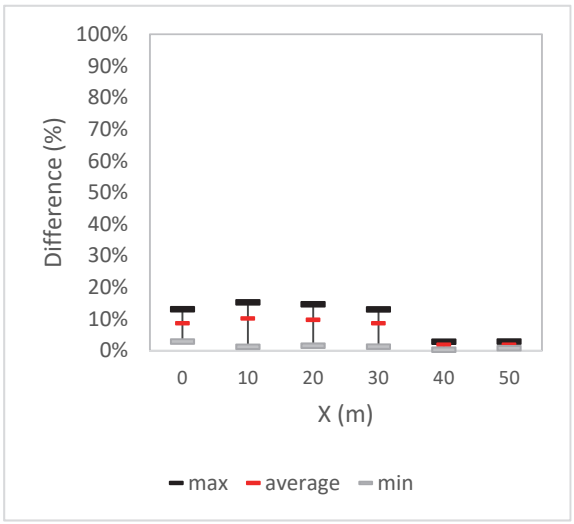
</td></tr>
<tr><td>VISIBILITY
 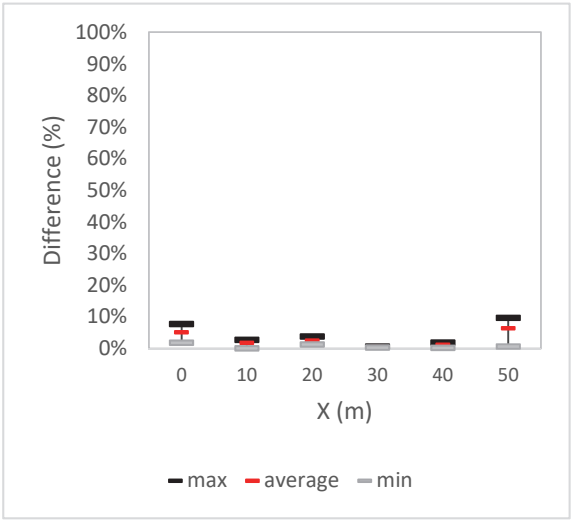
</td><td>FED
 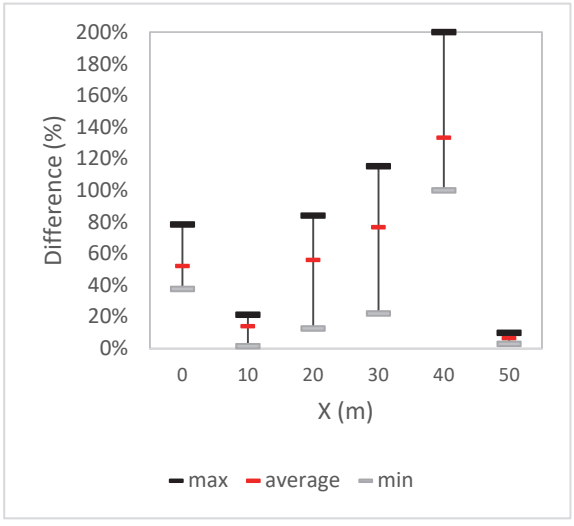
</td></tr>
</table>

Table C.32. Profiles of the quantities, X=20m, Initial temperature

Section x = 20 m	
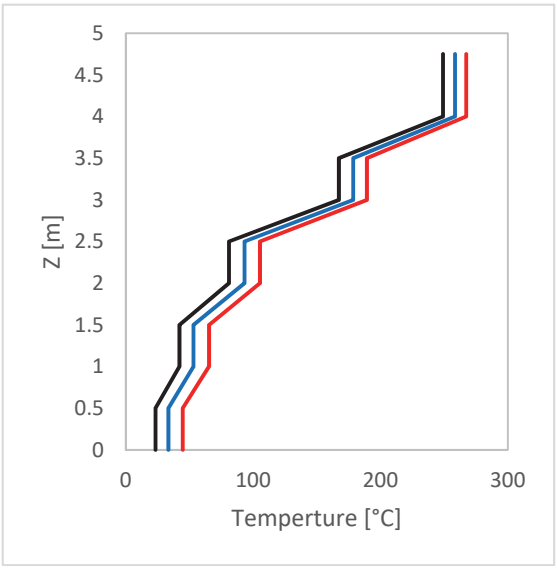	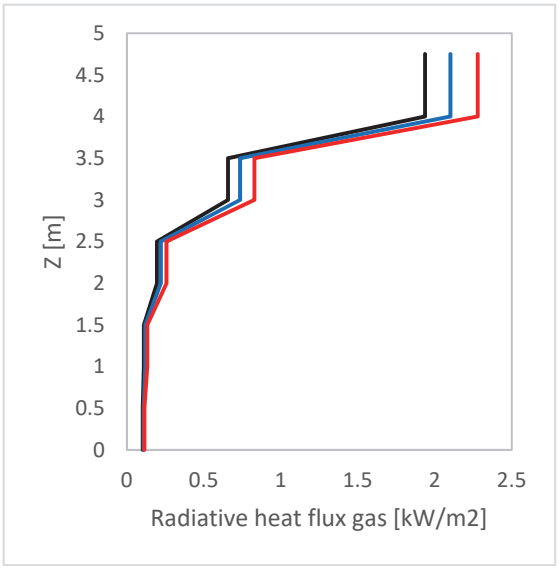
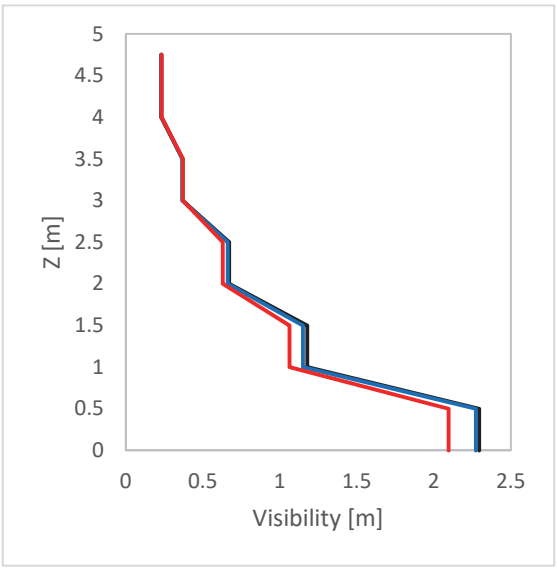	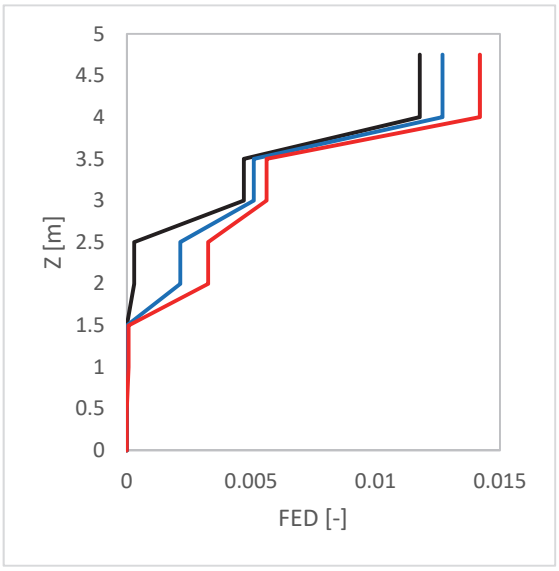

Red is 30°C, blue is 10°C and black is 20°C of initial temperature.

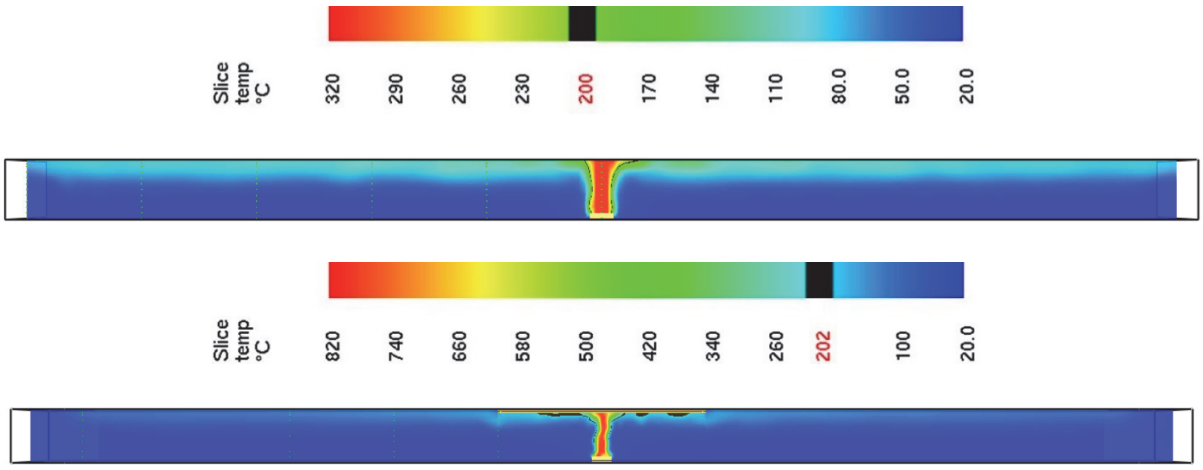

Figure C.2. 5 MW fire scenario for coarse and centered-medium grid resolution

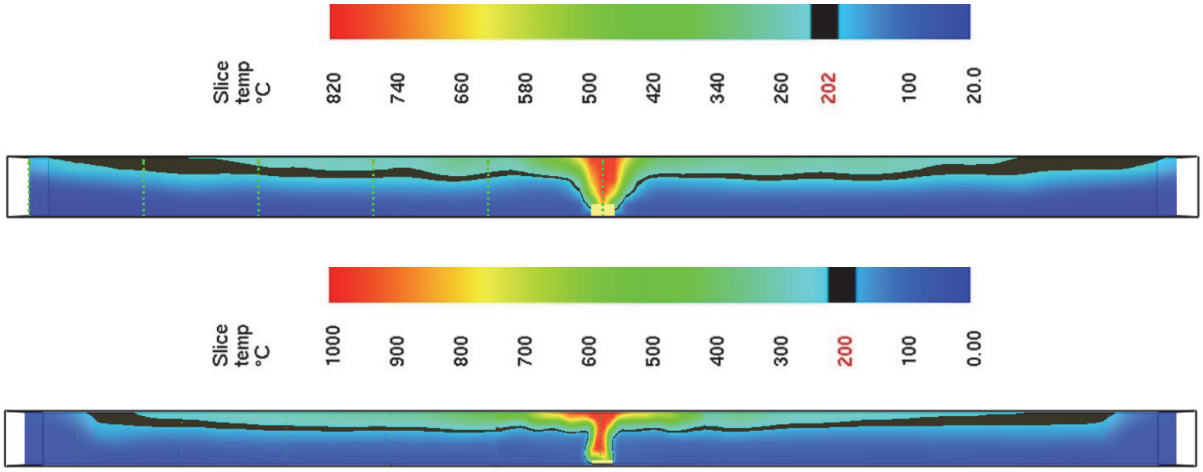

Figure C.3. 30 MW fire scenario for coarse and centered-medium grid resolution

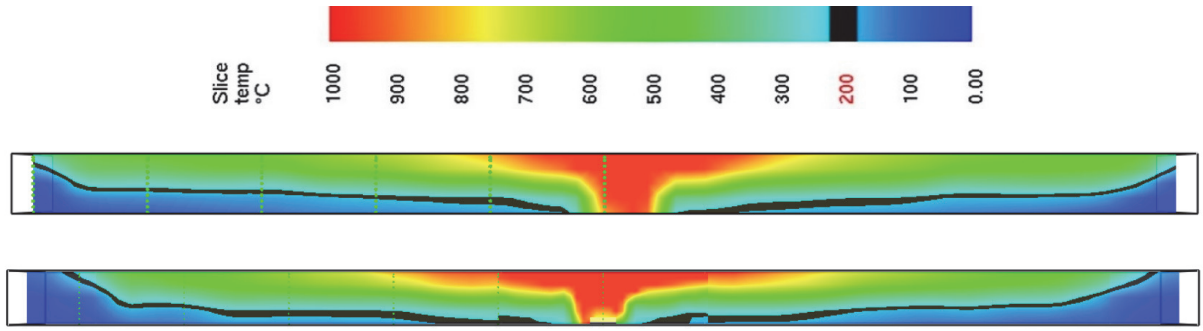

Figure C.4. 100 MW fire scenario for coarse and centered-medium grid resolution

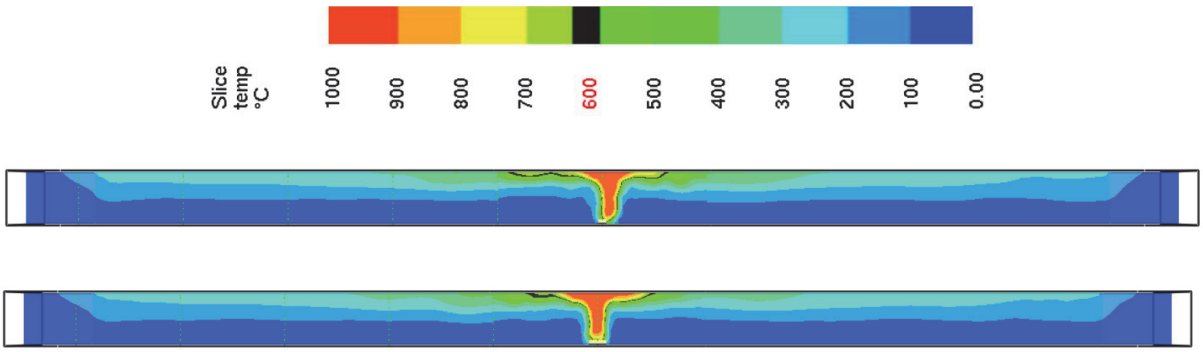

Figure C.5. Temperature slice for fire source area as 0.8 m² and 2.4 m²

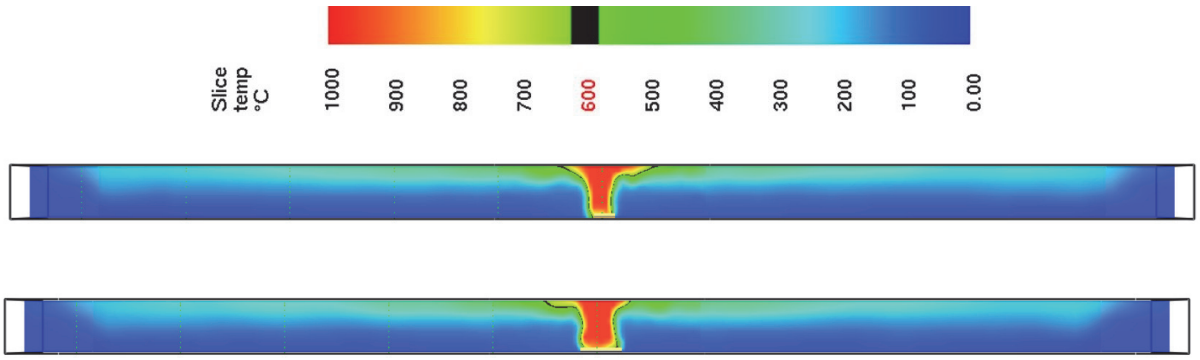

Figure C.6. Temperature slice for B/W as 2 and 4

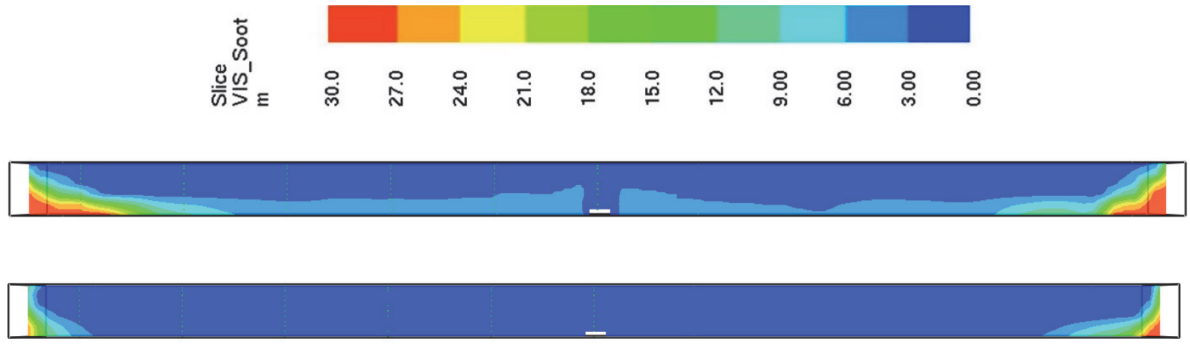

Figure C.7. Visibility slice for soot yield 0.05 g/g (top) and 0.20 g/g (bottom)

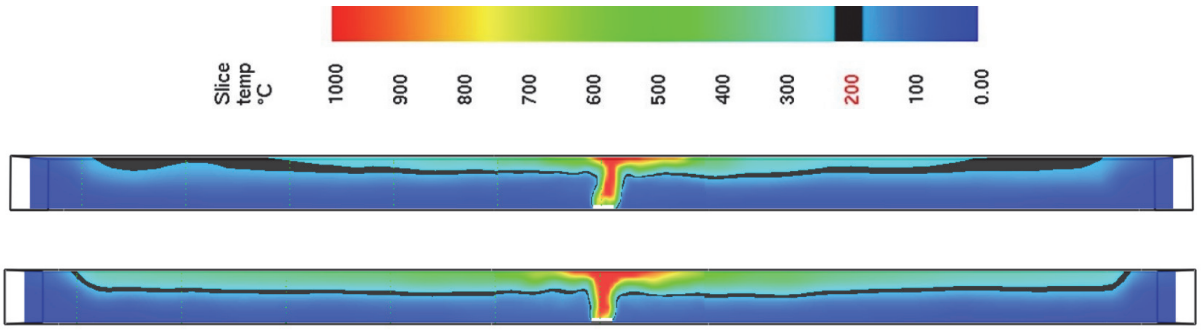

Figure C.8. Temperature slice for inert and adiabatic material

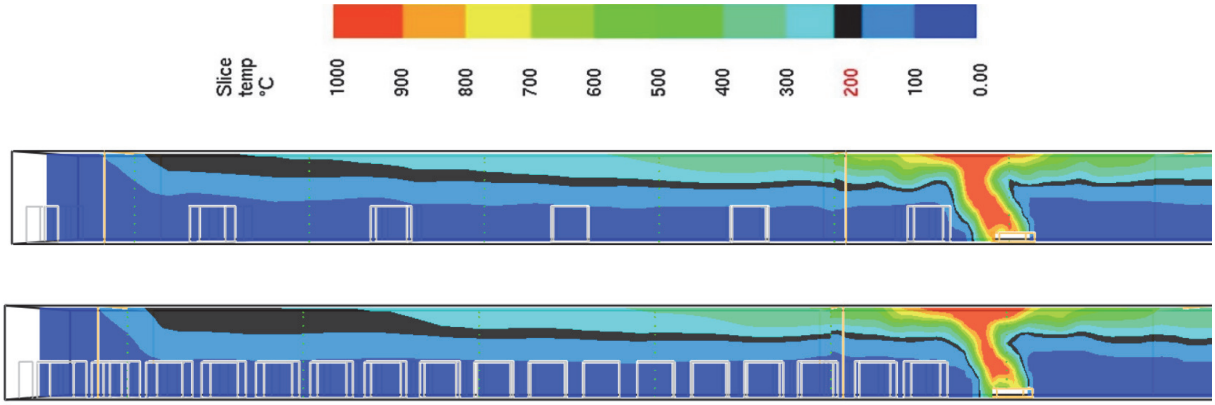

Figure C.9. Temperature slice for low and high traffic volume

Figure C.10. Smoke distribution for L_{ext} = 3 m and L_{ext} = 10 m

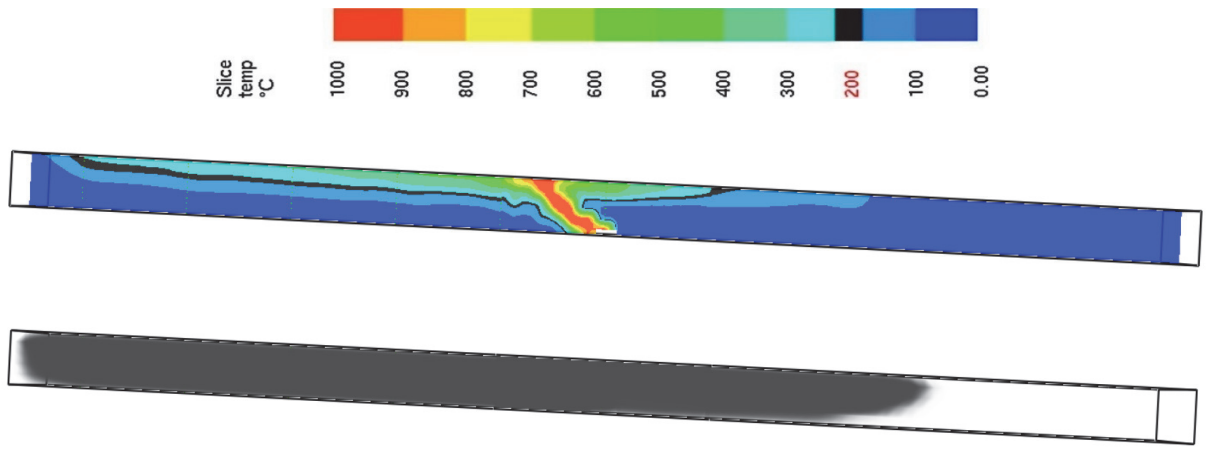

Figure C.11. Temperature and smoke distribution for downwards tunnel

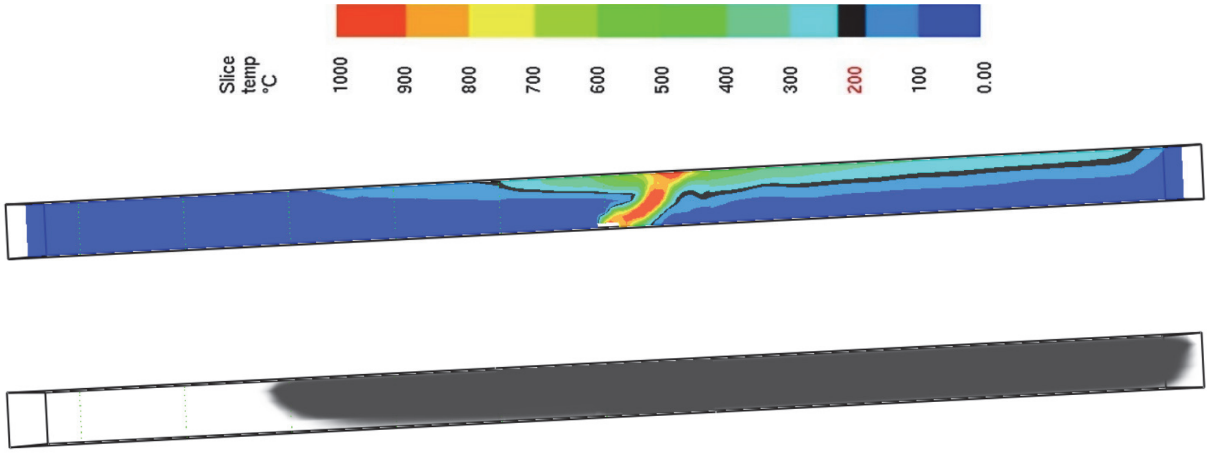

Figure C.12. Temperature and smoke distribution for upwards tunnel

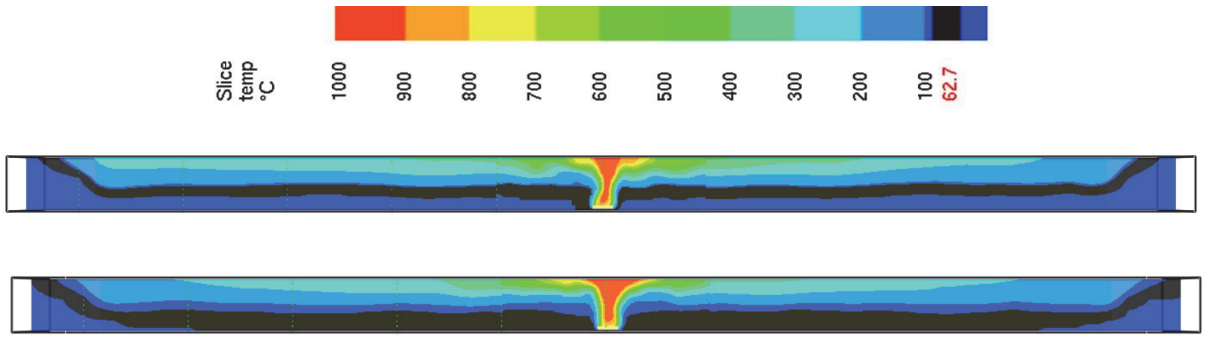

Figure C.13. Temperature slice for ambient temperature of 10°C and 30°C

APPENDIX C

Appendix D

QRAM software

Description of the model

The QRAM software is a quantitative risk analysis tool developed jointly by PIARC (World Road Association) and OECD (Organization of Economic Cooperation and Development) as part of the ERS2 project (1997-2001). Thanks to its simple user interface and well-structured internal database, the software has been widely used in several countries.

The software (3.61 version) is based on Microsoft Excel 2003 and conceived to work on PC equipped with 32bits Windows OS up to Windows XP. However, with some adaptations, it can work properly also on more recent operating systems.

The main limitation of the software is that it should be used for the transport of dangerous goods only, although among the default array of scenarios two are explicitly related to non-DG HGV fires. In addition, there is a series of bugs when calculations are run.

Depending on the type of analysis that need to be performed (tunnel and/or open sections), the user is asked to appropriately define the following characteristics of the road network:

- routes, defined in sections (each tunnel is a single section);
- tunnel geometry, ventilation, drainage, warning systems, spacing of exits, etc.;
- traffic characteristics (vehicle mix, speeds) for each route section and traffic direction;
- population along the route.

The QRAM software considers 13 accident scenarios listed in the Table D.1, which are representative of key dangerous goods groupings (the user can add others).

Table D.1. Classification of accident scenarios (Di Santo, 2014)

No.	Scenario	DG	Mode of containment	Diameter release hole	Mass flow rate
1	20 MW HGV Fire	Non-DG	-	-	-
2	100 MW HGV Fire	Non-DG	-	-	-
3	BLEVE	Liquefied Petroleum Gas (LPG)	Cylinder (50 kg)	-	-
7	BLEVE	Liquefied Petroleum Gas (LPG)	Bulk (18 t)	-	-
8	VCE	Liquefied Petroleum Gas (LPG)	Bulk (18 t)	50 mm	36 kg/s
9	Torch Fire	Liquefied Petroleum Gas (LPG)	Bulk (18 t)	50 mm	36 kg/s
4	Pool Fire	Motor Spirit	Bulk (18 t)	100 mm	20.6 kg/s
5	VCE	Motor Spirit	Bulk (18 t)	100 mm	20.6 kg/s
11	Toxic Liquid Release	Acrolein (toxic liquid)	Bulk (30000 litres)	50 mm	24.8 kg/s
12	Toxic Liquid Release	Acrolein (toxic liquid)	Cylinder (100 litres)	4 mm	0.02 kg/s
6	Toxic Gas Release	Chlorine (toxic gas)	Bulk (20 t)	50 mm	45 kg/s
10	Toxic Gas Release	Ammonia (toxic gas)	Bulk (20 t)	50 mm	36 kg/s
13	BLEVE	Liquefied CO_2	Bulk (20 t)	-	-

The combination of frequency and consequence analysis allows the calculation of the societal risk, expressed in FN curves and Expected Value (EV). Another outcome available from the calculation concerns the individual risk indicators, but they will not be considered in this study.

How the software works

Frequency analysis

The fundamental parameter of the frequency analysis is the accident rates on each section (tunnel or open). The user must define the accident rate (in terms of accidents per vehicles

km) based on national statistics and default values (for the design phase) or observations and reports (for in-service tunnels).

The accident rates is used by the QRAM software to calculate the frequency of the consequence scenarios, expressed in terms of conditional probabilities that the initial event (accident or breakdown) can run into each end-branch of the event tree. The software is provided with a table, which is coupled with different boundary conditions and used to automatically perform the calculation.

Consequence analysis

The consequence analysis is based on pre-determined calculations of physical and physiological consequences of scenarios in open and tunnel sections (respectively 2D and 1D tool). The consequence analysis can be expressed in terms of fatalities or fatalities plus injuries, considering only road users or near population.

Physical effects (i.e. thermal and pressure) are calculated through several models considering the main hazards (fire and smoke for non-DG HGV scenarios) depending on the phenomena (fire, BLEVE, etc.) and the domain (tunnel or open section).

Physiological effects (fatalities and injuries) are obtained from physical effects through Probit functions (Table D.2). The Probit Analysis originates in the field of entomology (Bliss, 1934) from the need to linearize the relationships between dose and response. It allows indeed to transform the nonlinear dose-response curve into a straight trend that can be analysed by regression. Probit functions have been introduced after having experienced that the susceptibilities of a group exposed to lethal loads (for example toxic or radiative) is often lognormal. Thus, a straight trend is obtained when expressing the probabilities of killing a given number of individuals within the exposed group in terms of units of standard deviation and related to a mean of five (probits), and representing it versus the logarithm of the load (Finney, 1980).

The adopted expression for a probit function is:

$$\Pr = a + b \ln(L)$$

Where a and b are constants and L is the load related to the specific physical effect.

The Mortality Rate is then derived from the Probit functions through a statistical transformation or using a table given by Finney (1971).

$$R = h(Pr) = \int_{-\infty}^{Pr-5} e^{(-\frac{1}{2}u^2)} du$$

Table D.2. Probit equations for lethality (QRAM Reference Manual, 2001)

Effect	Probit equations in the open	Probit equations in tunnel
Fires/BLEVE - Thermal	$\Pr = -14.9 + 2.56 * \ln q^{4/3} t$	$\Pr = -14.9 + 2.56 * \ln q^{4/3} t$
Fires - Smoke		$\Pr = -37.98 + 3.7 * \ln C_{co} t$
VCE	$\Pr = 5 - 8.49 \ln S_i$	$\Pr = -77.1 + 6.91 \ln p^{\circ}$
Toxic release - Chlorine	$\Pr = -5 + 0.5 * \ln C^{2.75} t$	
Toxic release - Ammonia	$\Pr = -35.95 + 1.85 * \ln C^{2} t$	
Toxic release - Acrolein	$\Pr = -3.18 + \ln(Ct)$	

The QRAM software performs automatically this part of the calculation and significantly reduces the work of the risk analyst that otherwise should consider well-established thresholds of tenability criteria like those explained in the Chapter 8.

Parametric study for two-tubes unidirectional tunnel

The QRAM software has a large number of parameters to be defined as input before running a calculation. Starting from an example contained in the User Guide, a case study is selected to run a sensitivity analysis of the software, considering fixed geometrical conditions (Figure D.1 and Table D.3) and changing one parameter at a time. Most of the parameters considered in the analysis are related to the case study discussed in Chapter 9.

The aim of the study is to assess the capabilities of the software limited to the fire risk. Therefore, the sensitivity analysis is focused only on the non-DG HGV scenarios, which represent 20 MW and 100 MW fires. For ease of reading, the results are expressed in terms of Expected Value, which is the most synthetic risk indicator given by the software.

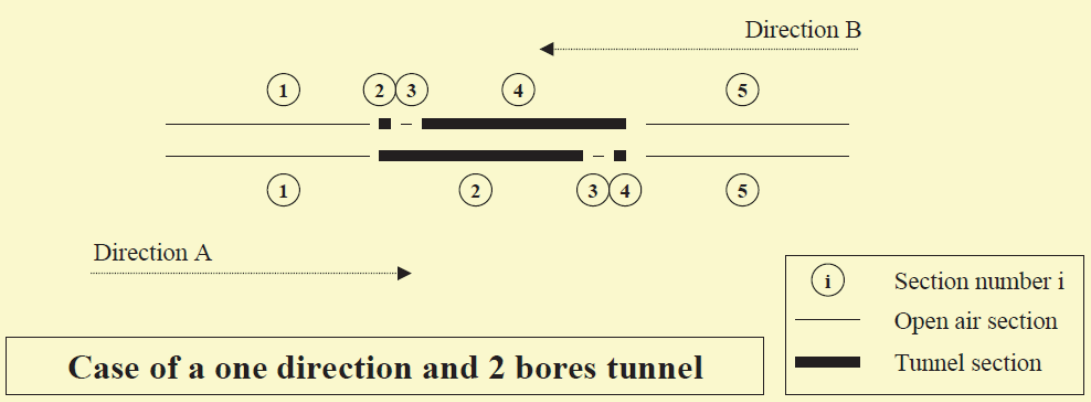

Figure D.1. Sketch of the layout selected for the SA

Table D.3. Length of the sections

Section	Direction AB	Direction BA
1	100 m	100 m
2	2695 m	0 m
3	0 m	0 m
4	0 m	2695 m
5	100 m	100 m

The parameters P_i selected for the sensitivity analysis are:

- P_1: total traffic (vehicles/day);
- P_2: HGV percentage in the total traffic (%);
- P_3: delay for stopping approaching traffic (seconds);
- P_4: light vehicles speed (km/h);
- P_5: HGV speed (km/h);
- P_6: accident frequency (accidents/vehicles km);
- P_7: number of segments;

- P_8: average distance among exits (meters);
- P_9: volume flow of the ventilation system (m^3/s).

The results are reported below in terms of histograms (Figures A2-A19), where the Expected Values for scenarios 1 and 2 are reported in the abscissa axis as a function of the selected parameter. As the total traffic significantly affects the EV, the effect of the parameters has been investigated under low and high traffic conditions. When they do not change, the values of the parameters are reported in the Table D.4.

Table D.4. Basic values of the model

Total traffic	2000 (low), 20000 (high) veh/day
HGV percentage	30 % (P_1 and P_3), 15 % (other cases)
Delay for stopping approaching traffic	300 sec
Light vehicles speed	100 km/h
HGV speed	70 km/h
Accident frequency	French default database
Segments	4
Average distance among exits	700 m
Ventilation system	Longitudinal, 120 m^3/s at nodes

Total traffic

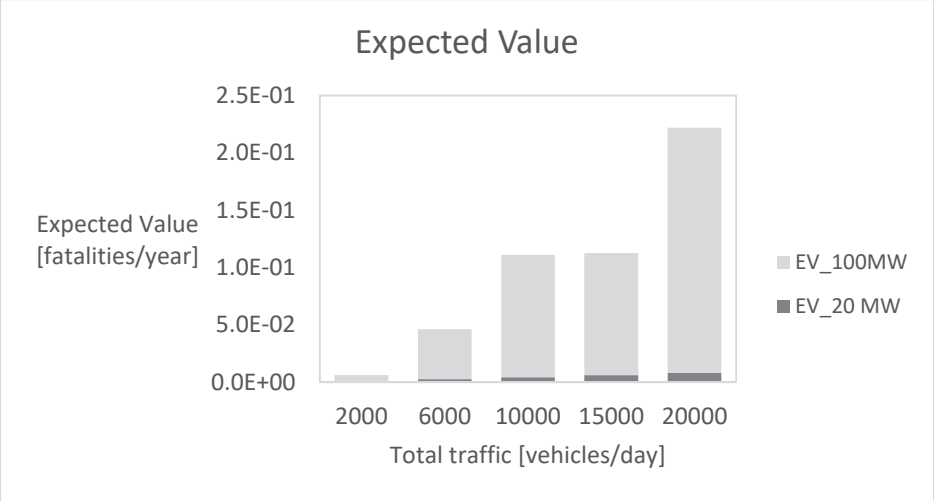

Figure D.2. Unidirectional EV tot, Traffic variation

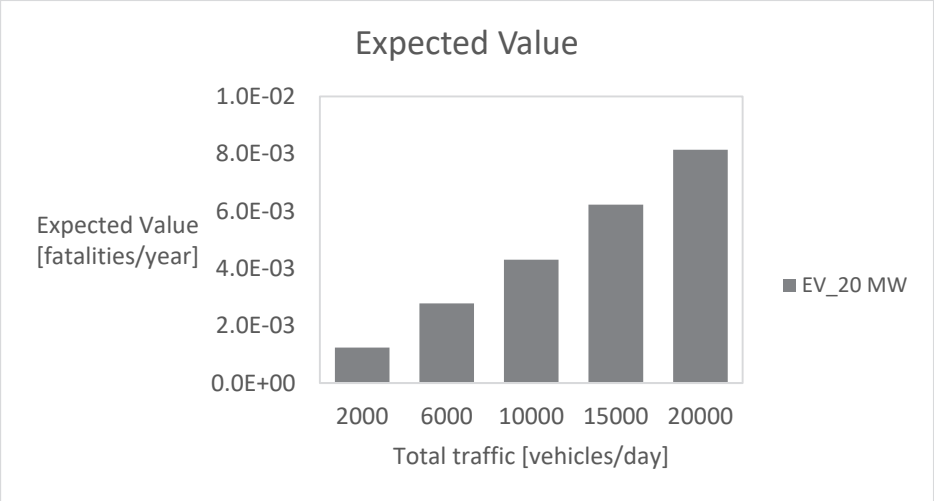

Figure D.3. Unidirectional EV 20 MW, Traffic variation

HGV percentage

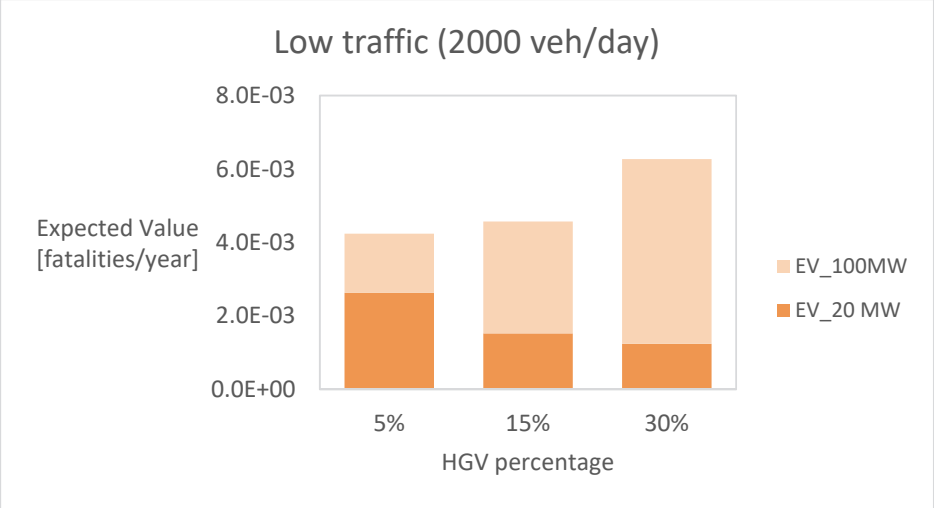

Figure D.4. Unidirectional EV tot, Low traffic, HGV percentage variation

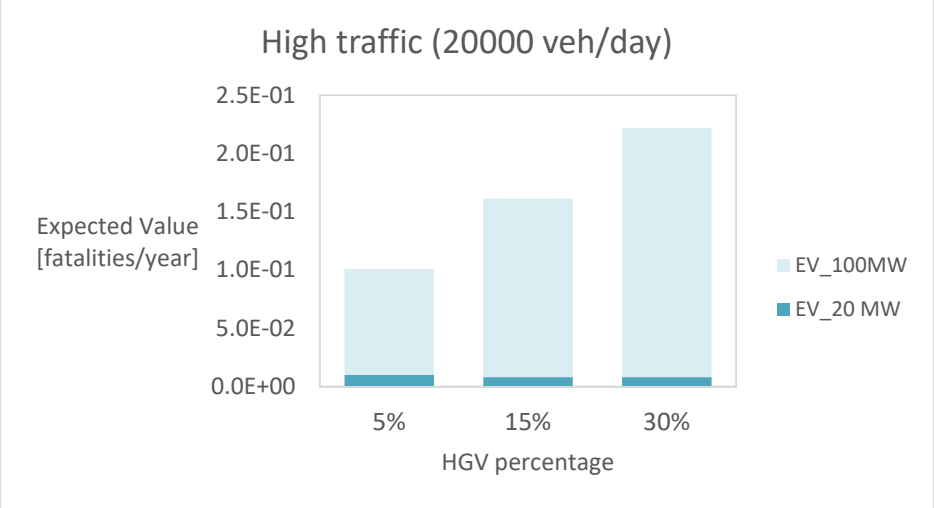

Figure D.5. Unidirectional EV tot, High traffic, HGV percentage variation

Delay for stopping approaching traffic

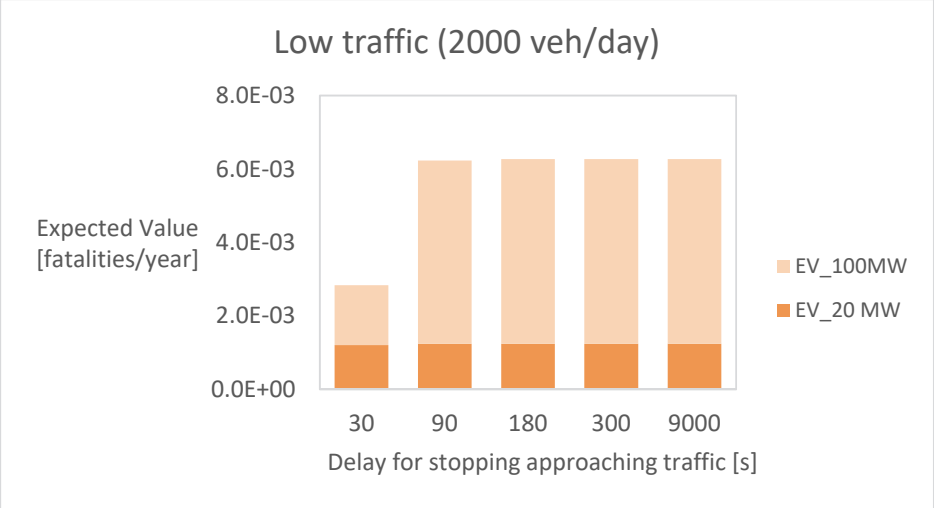

Figure D.6. Unidirectional EV tot, Low traffic, delay variation

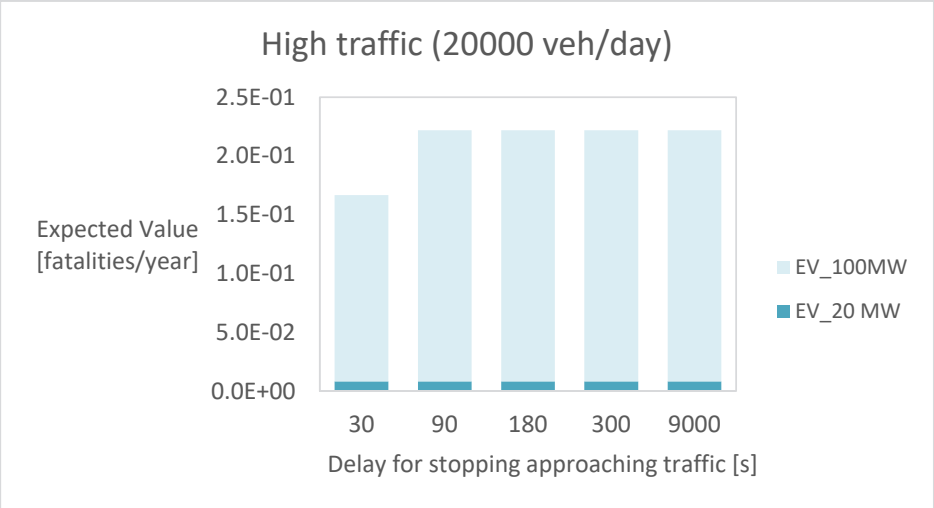

Figure D.7. Unidirectional EV tot, High traffic, delay variation

Light vehicles speed

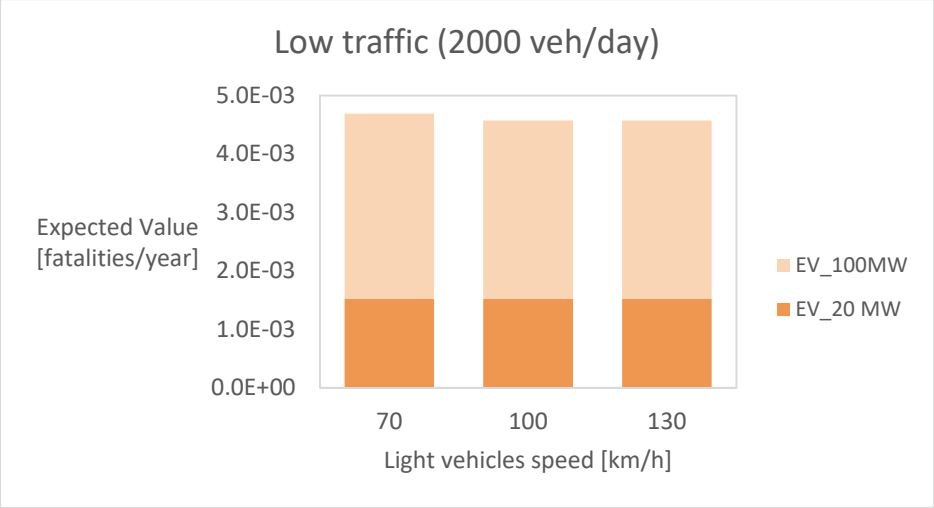

Figure D.8. Unidirectional EV tot, Low traffic, light vehicles speed variation

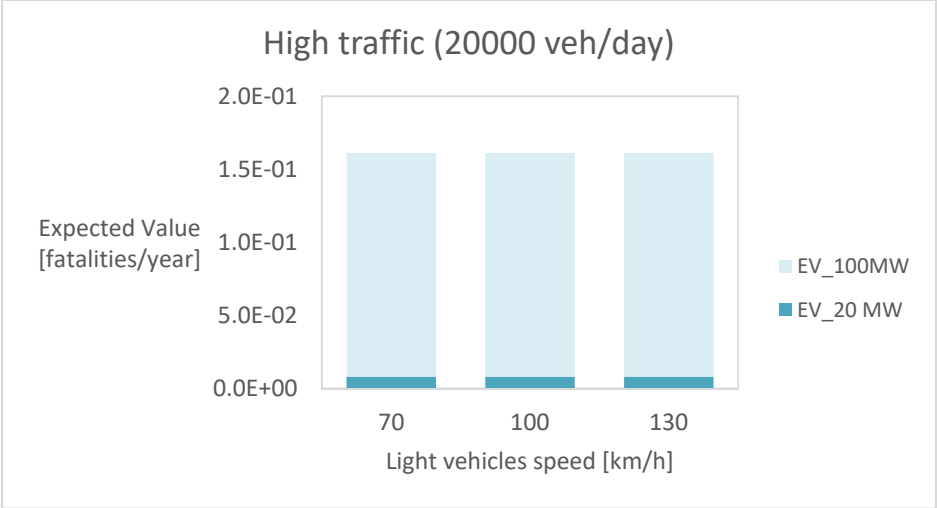

Figure D.9. Unidirectional EV tot, High traffic, light vehicles speed variation

HGV speed

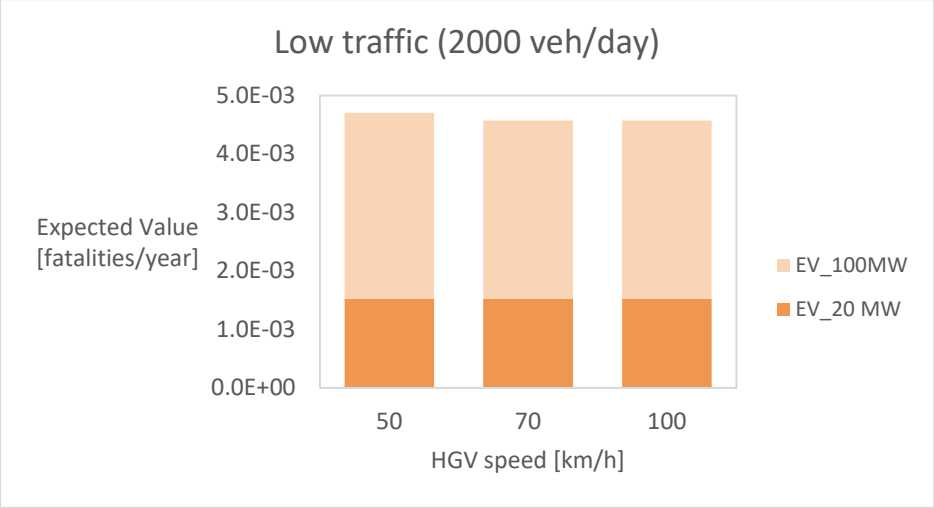

Figure D.10. Unidirectional EV tot, Low traffic, HGV speed variation

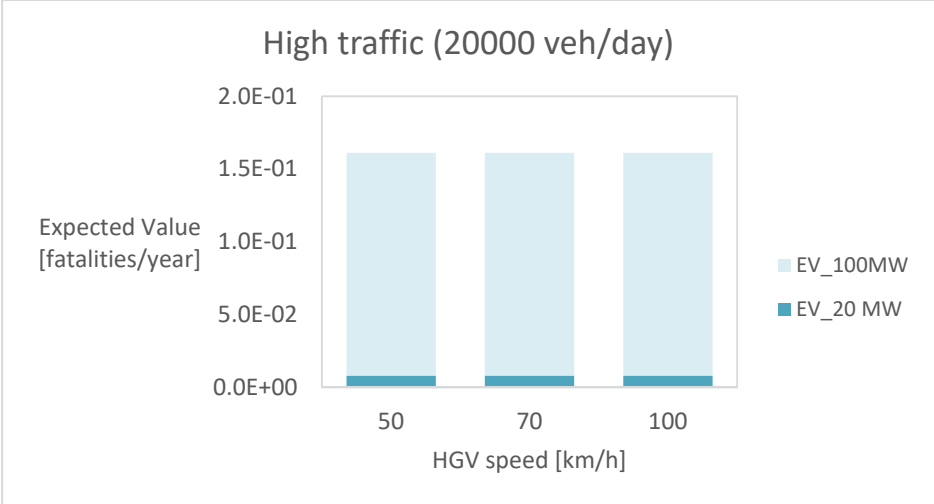

Figure D.11. Unidirectional EV tot, High traffic, HGV speed variation

Accident frequency

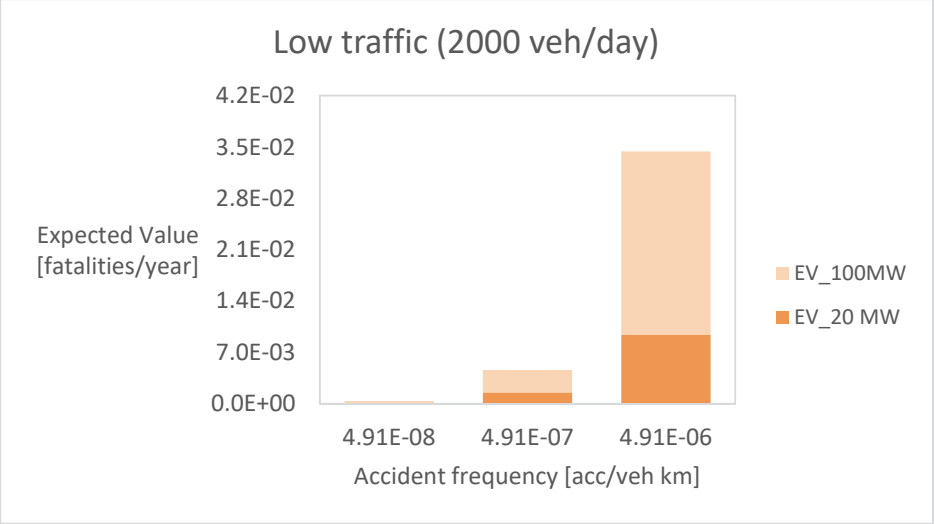

Figure D.12. Unidirectional EV tot, Low traffic, accident frequency variation

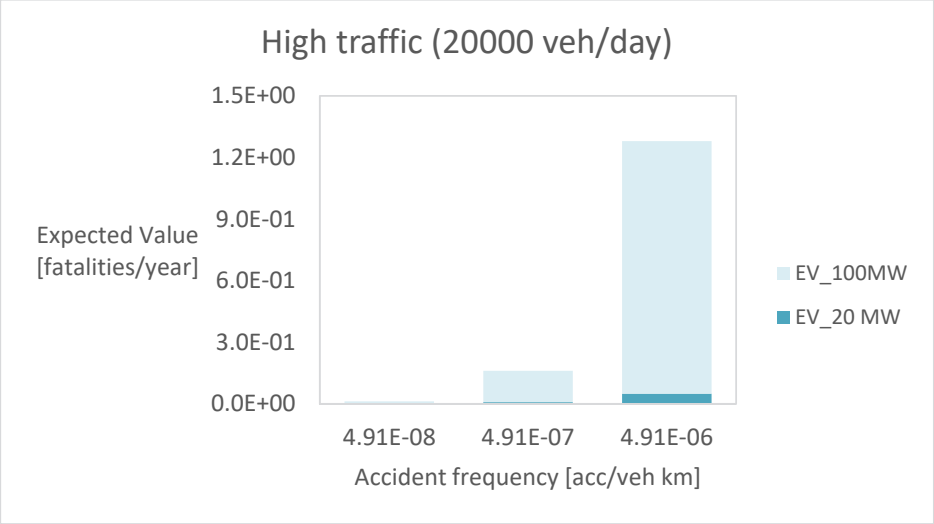

Figure D.13. Unidirectional EV tot, High traffic, accident frequency variation

Segments

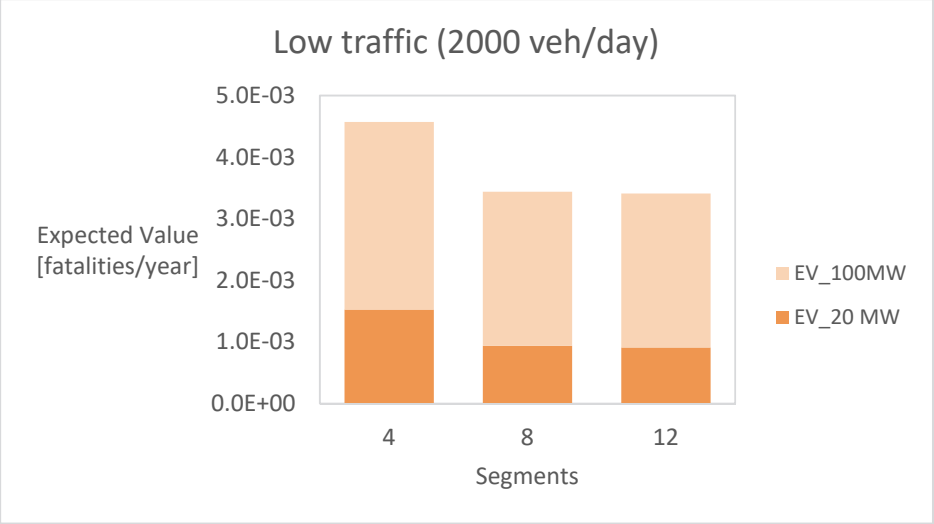

Figure D.14. Unidirectional EV tot, Low traffic, segments variation

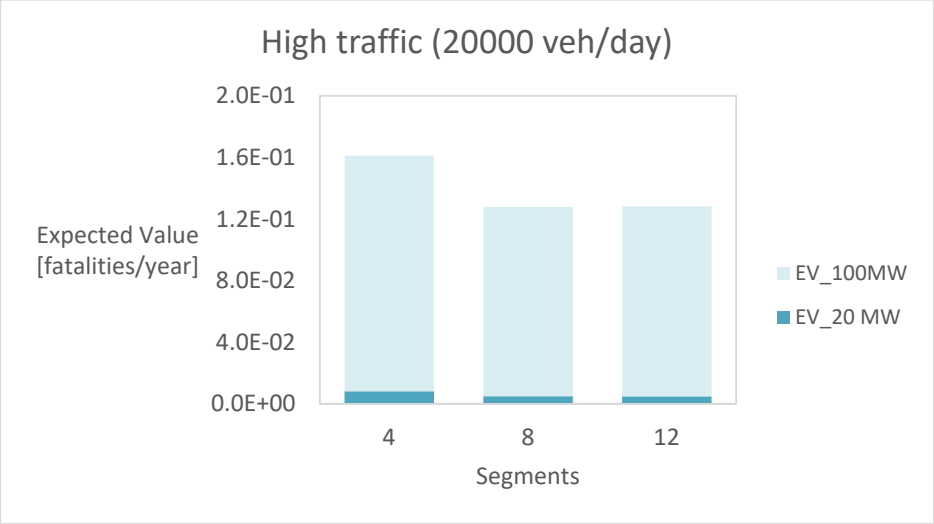

Figure D.15. Unidirectional EV tot, High traffic, segments variation

Average distance among exits

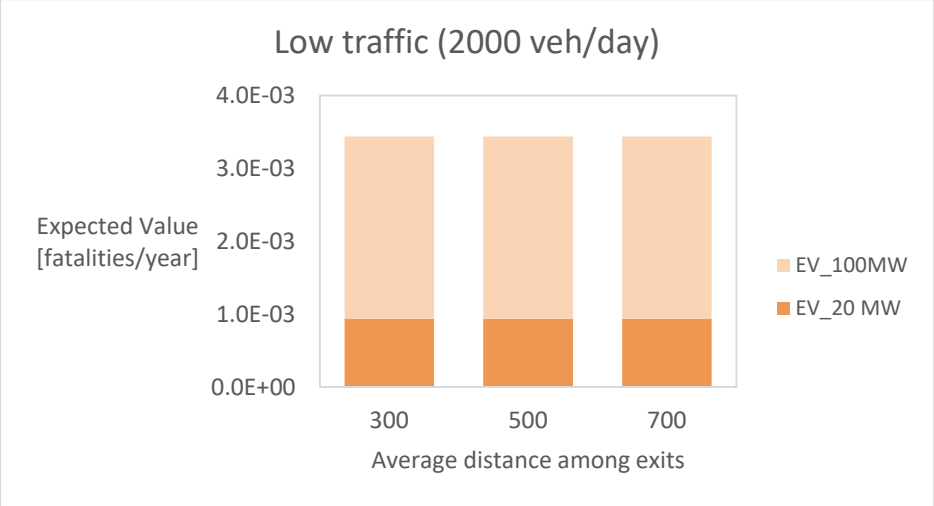

Figure D.16. Unidirectional EV tot, Low traffic, distance among the exits variation

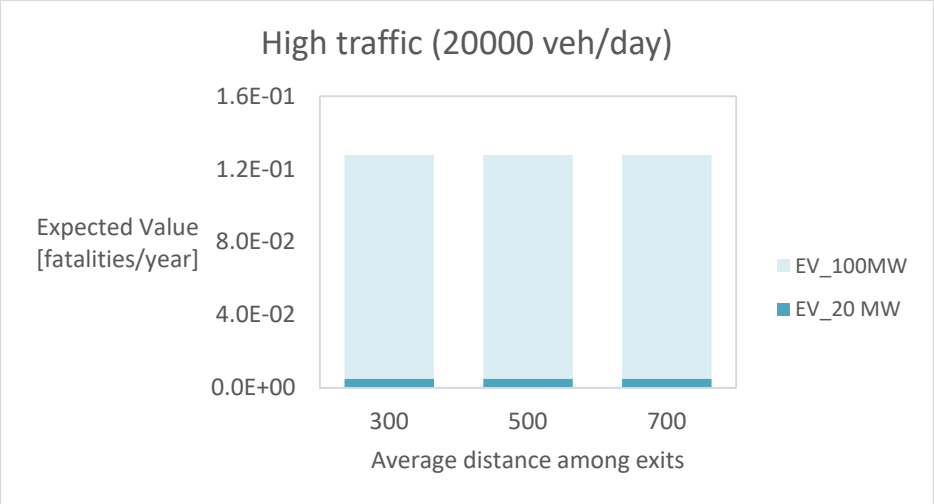

Figure D.17. Unidirectional EV tot, High traffic, distance among the exits variation

Ventilation system

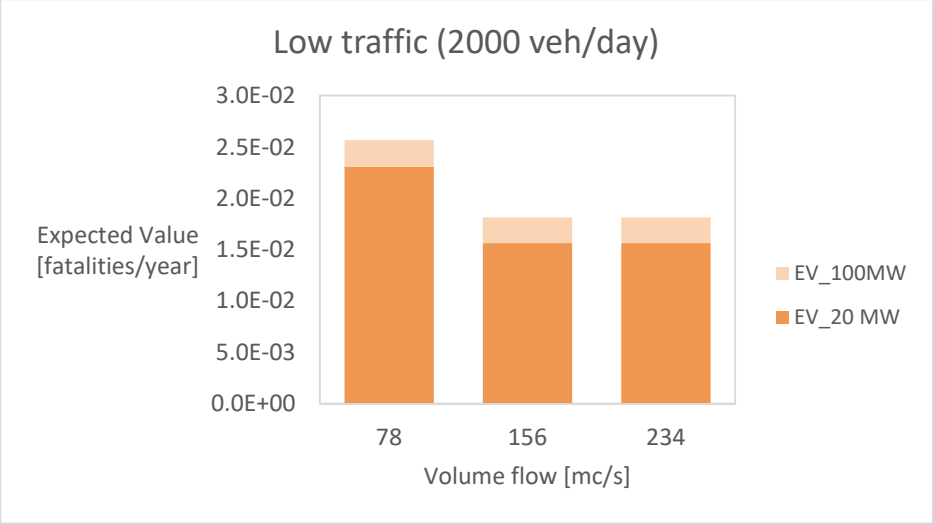

Figure D.18. Unidirectional EV tot, Low traffic, ventilation volume flow variation

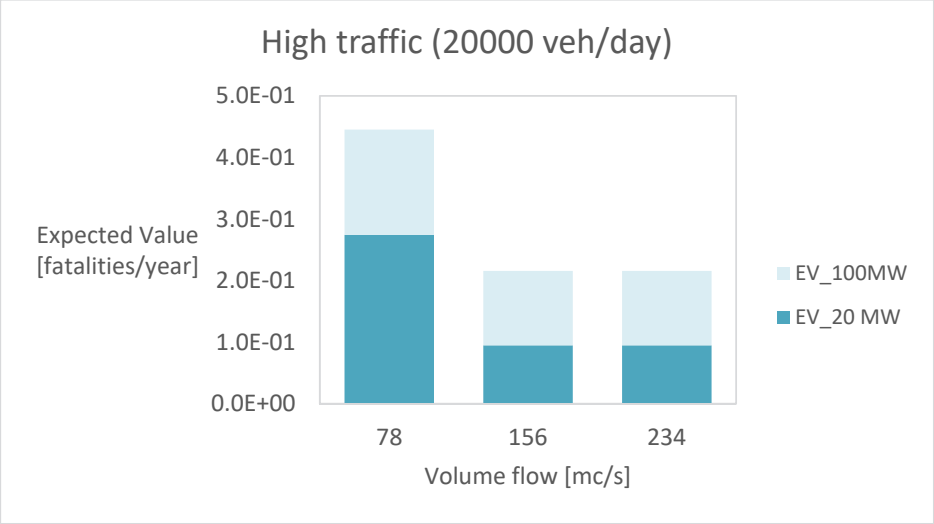

Figure D.19. Unidirectional EV tot, High traffic, ventilation volume flow variation

Parametric study for single tube bidirectional tunnel

An analogous study is carried out for a bidirectional tunnel, with a single tube and the same characteristics for direction AB and BA. Starting from an example contained in the User Guide, a case study is selected to run a sensitivity analysis of the software, considering fixed geometrical conditions (Figure D.20 and Table D.5) and changing one parameter at a time. Most of the parameters considered in the analysis are related to the case study discussed in Chapter 10.

Like in the previous case, the analysis is focused only on the non-DG HGV scenarios, which represent 20 MW and 100 MW fires. For ease of reading, the results are expressed in terms of Expected Value.

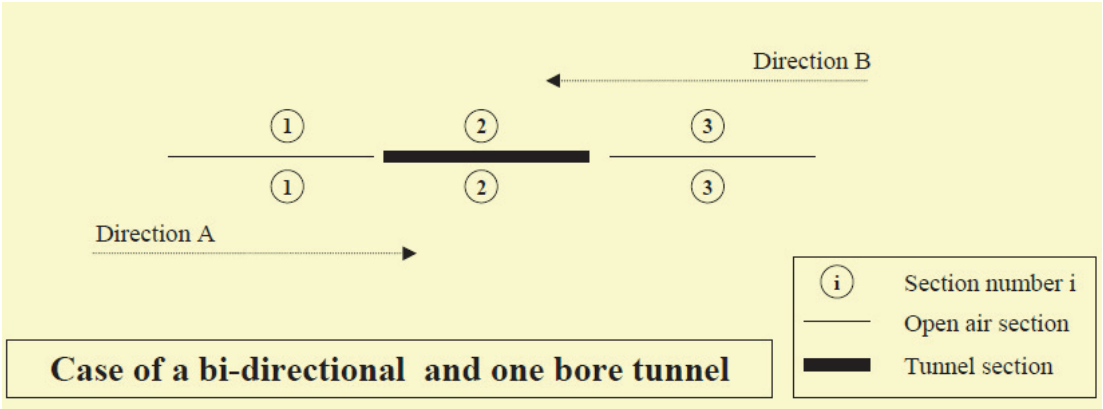

Figure D.20. Sketch of the layout selected for the SA

Table D.5. Length of the sections

Section	Direction AB
1	100 m
2	2500 m
3	100 m

The parameters P_i selected for the sensitivity analysis are:

- P_1: total traffic (vehicles/day);
- P_2: HGV percentage in the total traffic (%);

- P_3: delay for stopping approaching traffic (seconds);
- P_4: light vehicles speed (km/h);
- P_5: HGV speed (km/h);
- P_6: accident frequency (accidents/vehicles km);
- P_7: number of segments;
- P_8: average distance among exits (meters);
- P_9: extraction flow of the ventilation system (m^3/s).

The results are reported below in terms of histograms (Figures A21-A38), where the Expected Values for scenarios 1 and 2 are reported in the abscissa axis as a function of the selected parameter. As the total traffic significantly affects the EV, the effect of the parameters has been investigated under low and high traffic conditions. When they do not change, the values of the parameters are reported in the Table D.6.

Table D.6. Basic values of the model

Total traffic	2000 (low), 20000 (high) veh/day
HGV percentage	30 % (P_1 and P_3), 15 % (other cases)
Delay for stopping approaching traffic	300 sec
Light vehicles speed	100 km/h
HGV speed	70 km/h
Accident frequency	French default database
Segments	7
Average distance among exits	700 m
Ventilation system	Semi-transverse, extraction of 110 m^3/s for emergency mode

Total traffic

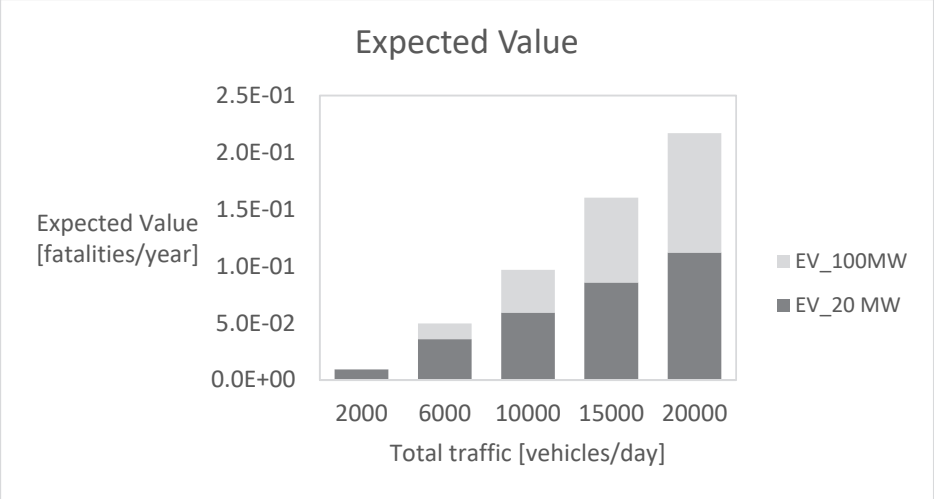

Figure D.21. Bidirectional EV tot, traffic variation

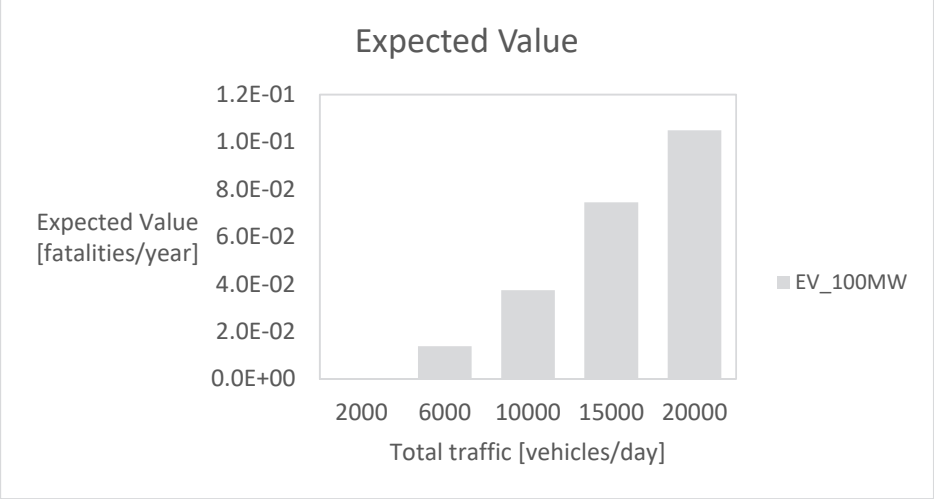

Figure D.22. Bidirectional EV 100 MW, traffic variation

HGV percentage

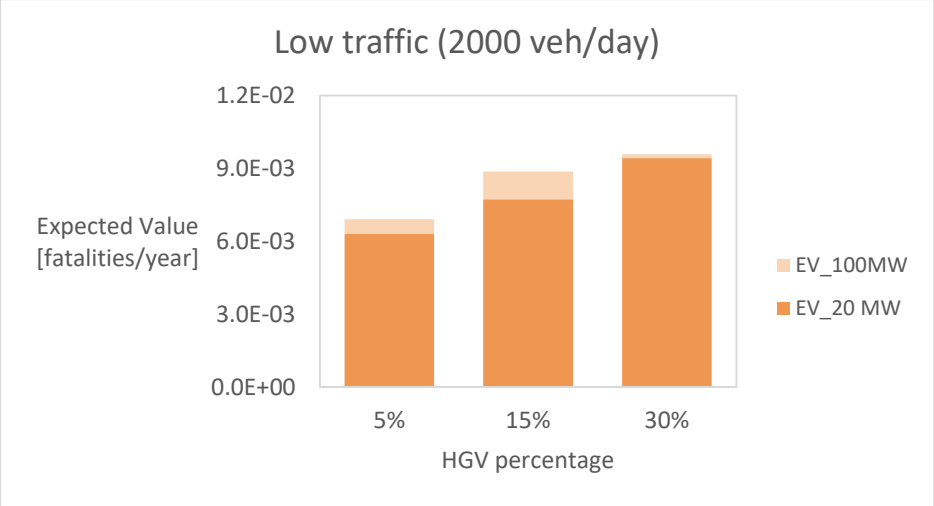

Figure D.23. Bidirectional EV tot, Low traffic, HGV variation

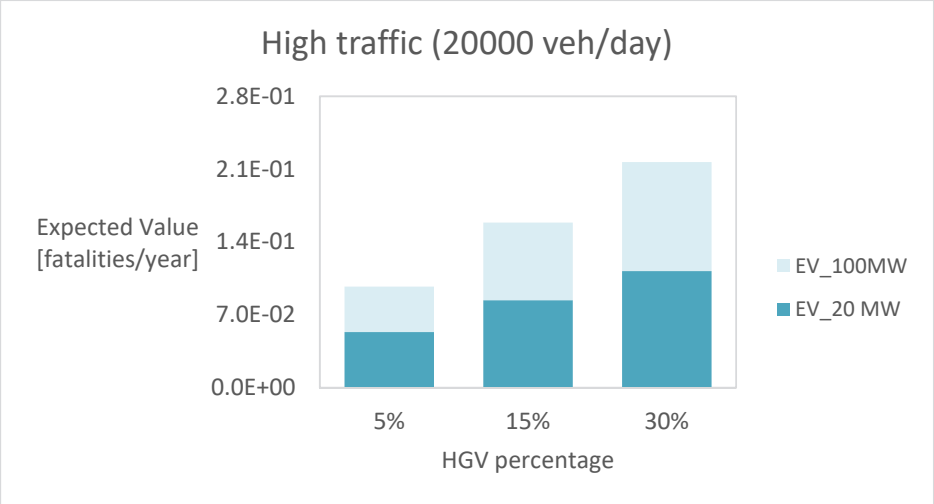

Figure D.24. Bidirectional EV tot, High traffic, HGV variation

Delay for stopping approaching traffic

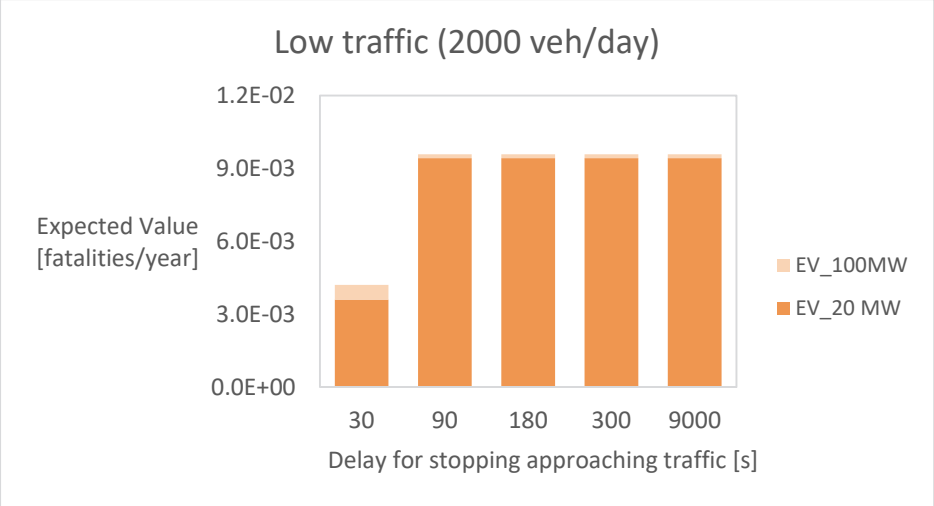

Figure D.25. Bidirectional EV tot, Low traffic, delay variation

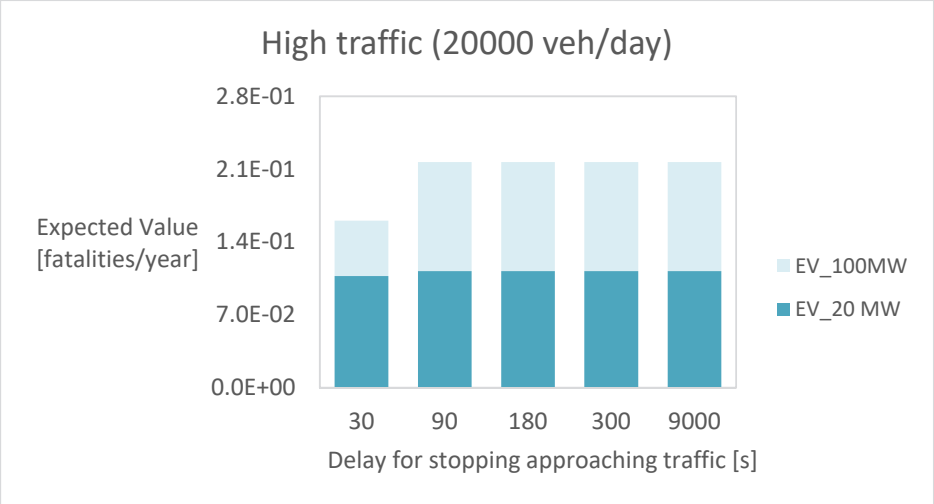

Figure D.26. Bidirectional EV tot, High traffic, delay variation

Light vehicles speed

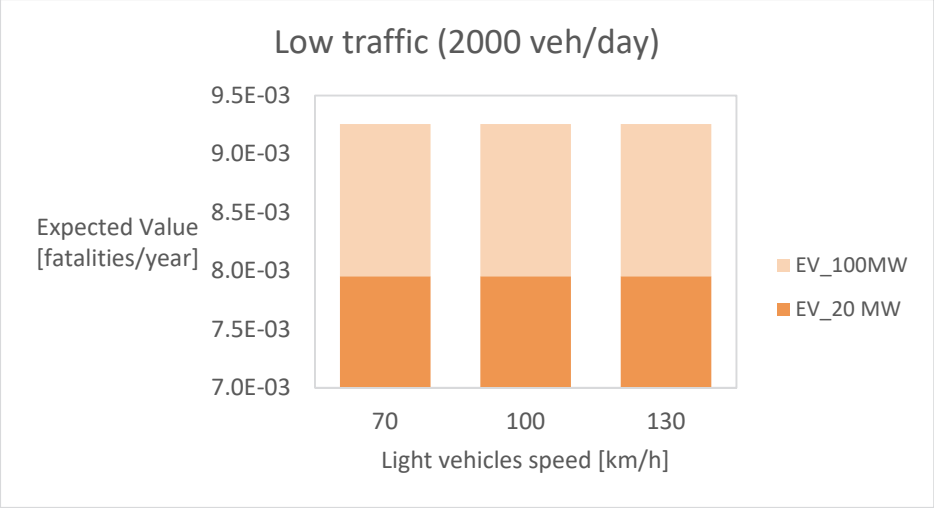

Figure D.27. Bidirectional EV tot, Low traffic, ligh vehicles speed variation

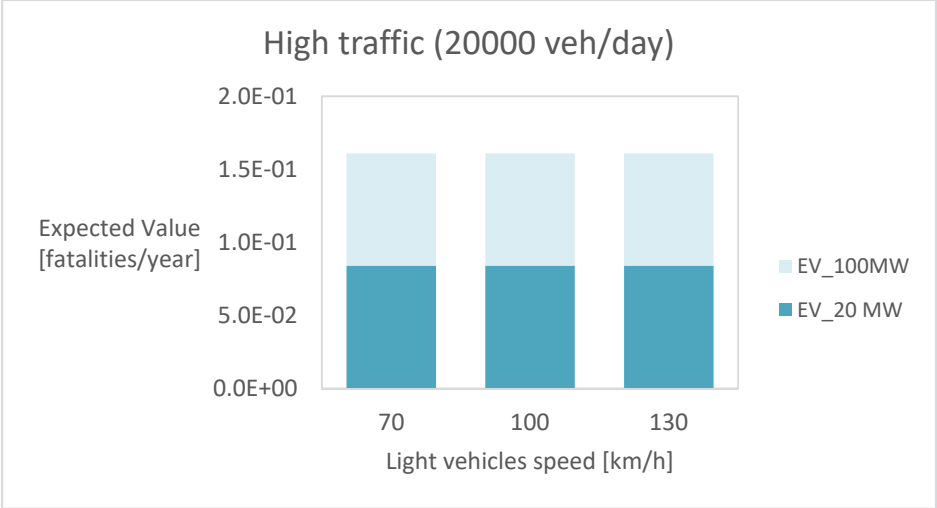

Figure D.28. Bidirectional EV tot, High traffic, light vehicles speed variation

HGV speed

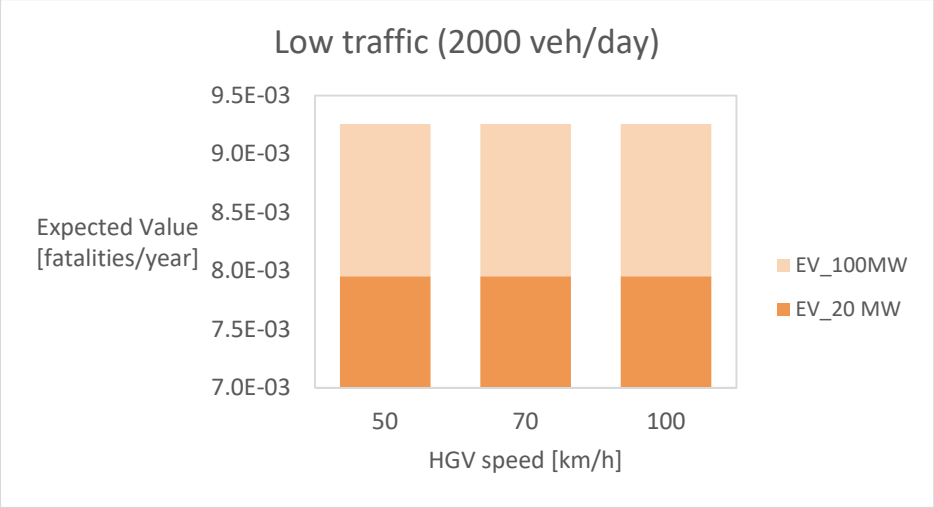

Figure D.29. Bidirectional EV tot, Low traffic, HGV speed variation

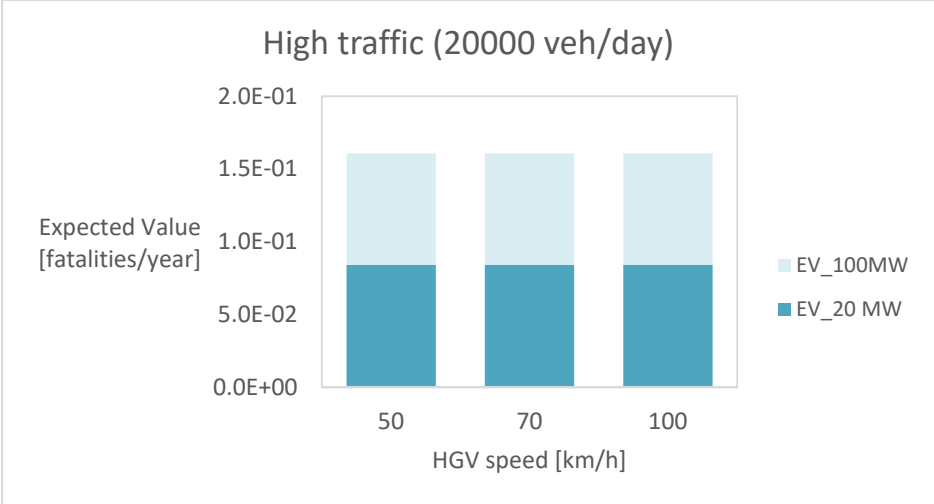

Figure D.30. Bidirectional EV tot, High traffic, HGV speed variation

Accident frequency

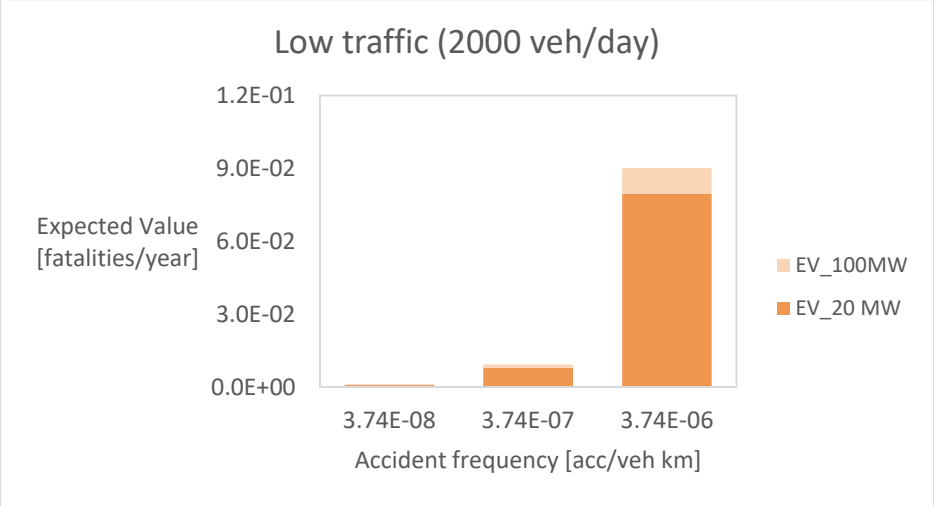

Figure D.31. Bidirectional EV tot, Low traffic, accident frequency variation

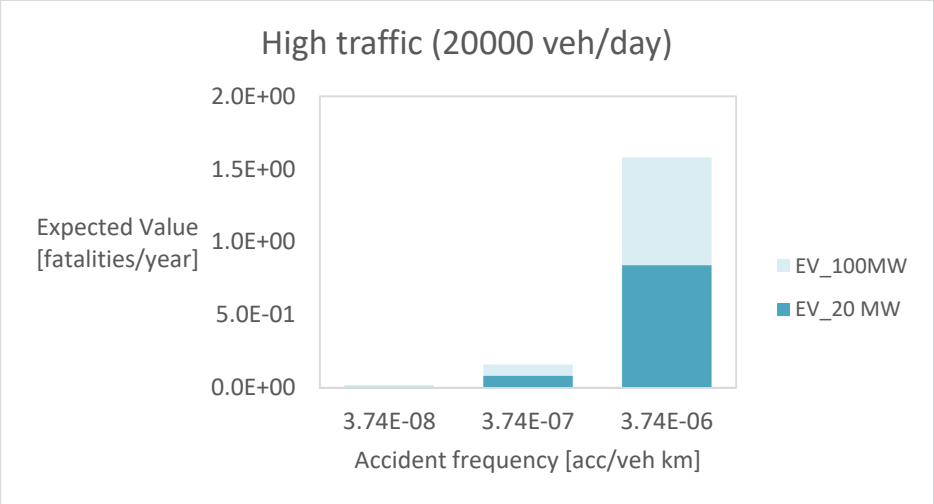

Figure D.32. Bidirectional EV tot, High traffic, accident frequency variation

Segments

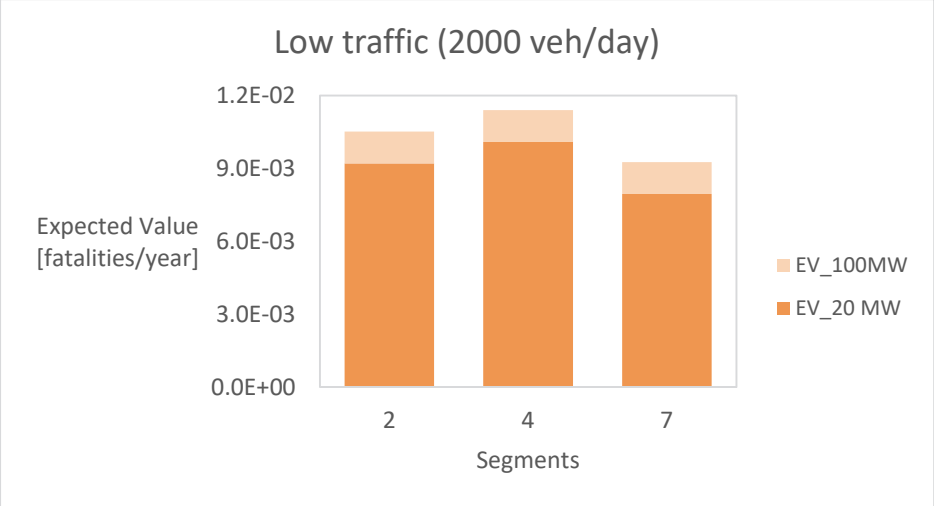

Figure D.33. Bidirectional EV tot, Low traffic, segments variation

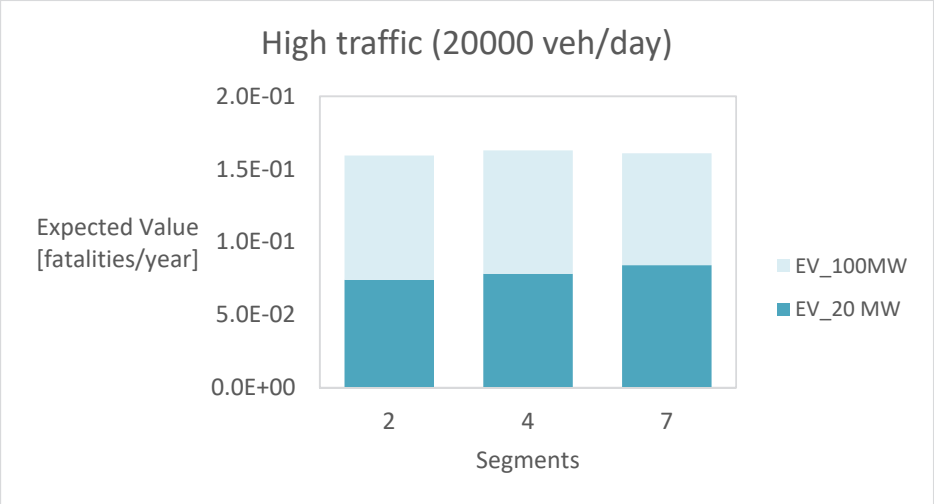

Figure D.34. Bidirectional EV tot, High traffic, segments variation

Average distance among exits

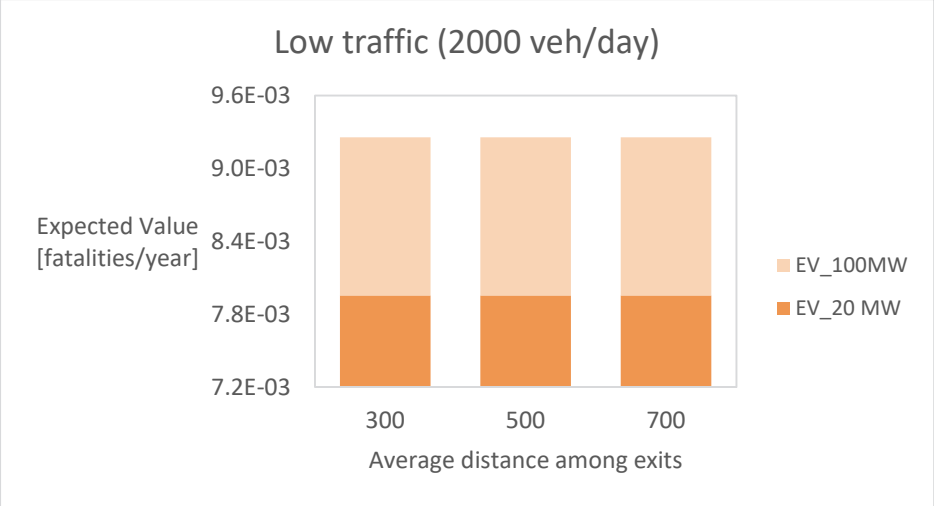

Figure D.35. Bidirectional EV tot, Low traffic, distance among the exits variation

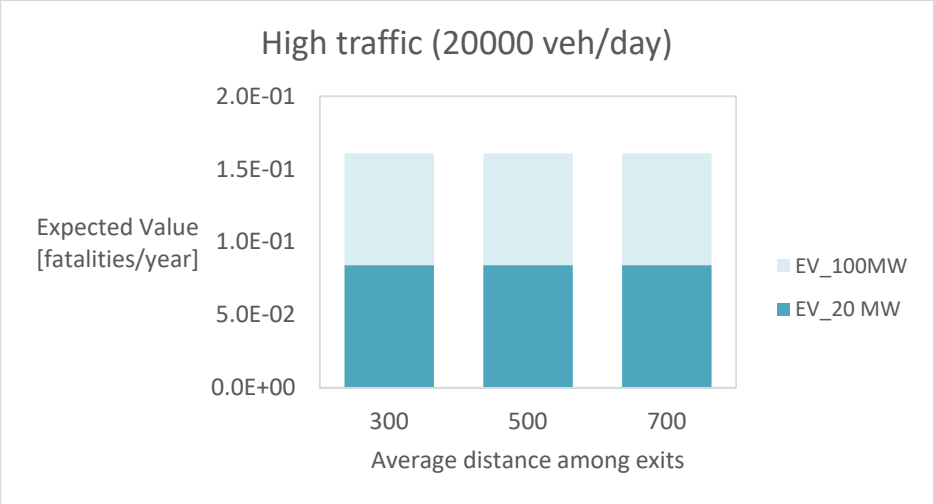

Figure D.36. Bidirectional EV tot, High traffic, distance among the exits variation

Ventilation system

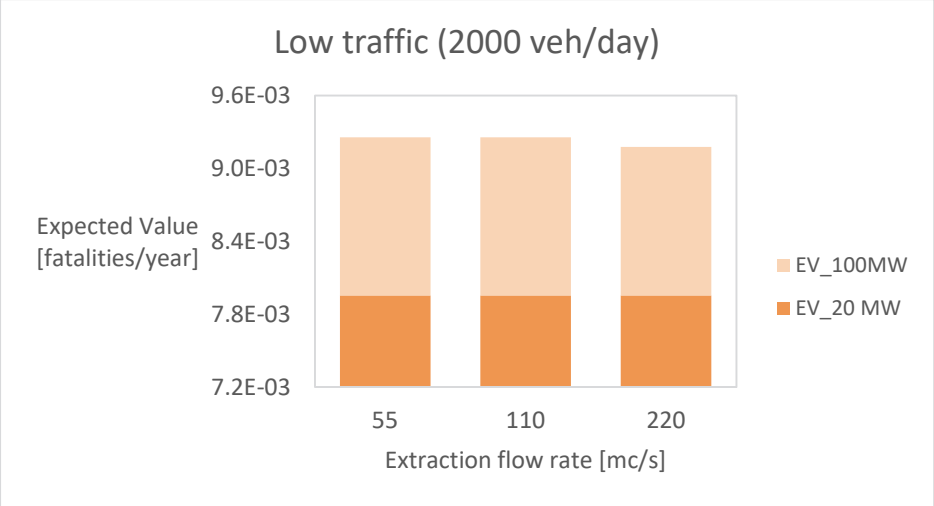

Figure D.37. Bidirectional EV tot, Low traffic, ventilation extraction flow variation

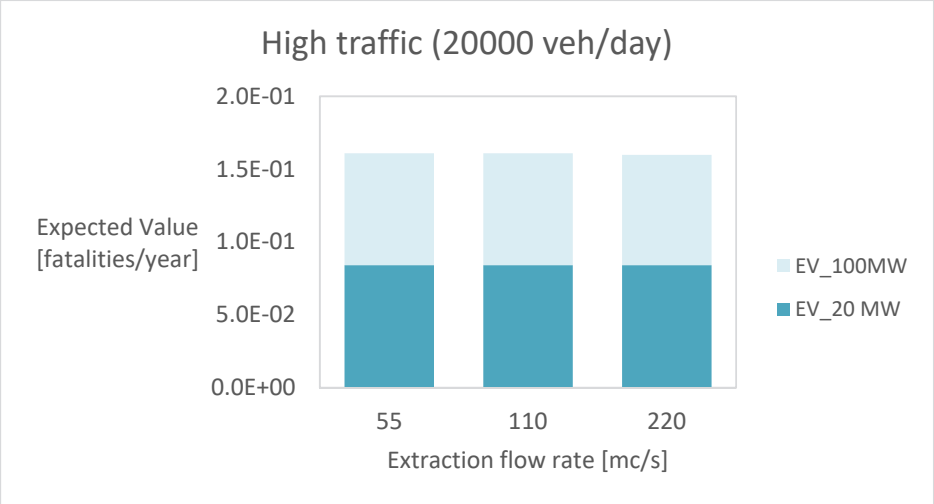

Figure D.38. Bidirectional EV tot, High traffic, ventilation extraction flow variation

Considerations and final remarks

The sensitivity analysis highlights that:

- some parameters have no influence at all on the EV;
- some parameters slightly influence the EV;
- some parameters significantly influence the EV.

Two tubes unidirectional tunnel

Among all the graphs related to this case study, the EV associated to 100 MW fire scenario is higher than that related to 20 MW fire scenario: this is due to the higher number of expected fatalities caused by the former.

The light vehicles and HGVs speed (Figures A8-A11) as well as the average distance among the exits (Figures A16-A17) do not affect the EV. This implies that, for instance, the presence of escape routes and by-passes cannot be verified by the QRAM software.

The delay for stopping approaching traffic (Figures A6-A7), the number of segments (Figures A14-A15) and the volume flow of the emergency ventilation system (Figures A18-A19) slightly affect the EV. Specifically, their effect is limited to a range of values up to a certain threshold, after which the EV is not influenced any more.

Specifically, considering the ventilation system, the calculation of the EV is influenced by the volume flow of the emergency mode only up to an average velocity across the cross section of 3 m/s, implicitly assumed as the critical velocity of all tunnels. However, the critical velocity cannot be fixed a priori, because it is dependent on the geometrical layout of the tunnel and the specific characteristics of the ventilation system.

Finally, the total traffic (Figures A2-A3), the HGV percentage (Figures A4-A5) and the accident frequency (Figures A12-A13) significantly contribute to the EV over a wide range of values.

Single tube bidirectional tunnel

For this case study, it is worth to notice that the share of EV related to 100 MW scenario is generally lower than the one of 20 MW scenario, in contrast with the previous case. This is probably an effect of the adoption of a semi-transverse ventilation system, which is able to confine the untenable zone both for 20 and 100 MW, whereas for tunnels equipped with longitudinal ventilation the backlayering phenomenon, responsible for fatalities, is much more evident for 100 MW scenarios. In addition, considering that the probability of having 100 MW fire is lower than that of 20 MW fire, the share of 20 MW is higher in this case study.

By looking at the graphs, very similar considerations can be drawn out for the parameters. The light vehicles and HGVs speed (Figures A27-A30), the average distance among the exits (Figures A35-A36) and the extraction flow rate (Figures A37-A38) do not affect the EV. The delay for stopping approaching traffic (Figures A25-A26) affects the EV only for low values (30-90 seconds), whereas the number of segments (Figures A33-A34) appears to slightly affect the EV only in case of low traffic conditions.

Finally, also for this case study the total traffic (Figures A21-A22), the HGV percentage (Figures A23-A24) and the accident frequency (Figures A31-A32) significantly contribute to the EV over a wide range of values.

Overall, in agreement with the accident statistics, the EV of bidirectional tunnel is higher compared to the EV of unidirectional tunnel.

It is worth to notice again that the study is limited to non-DG HGV scenarios because the thesis is focused on the fire risk and quantitative risk estimation of fires related to light vehicles and HGVs. Therefore, the considerations of the presented study cannot be extended to DG scenarios and their EV.

INDICES AND REFERENCES

List of figures

List of tables

References

AIChE (American Institute of Chemical Engineers), *Guidelines for Chemical Process Quantitative Risk Analysis*. Center for Chemical Process Safety, New York, 1989.

Ale, BJM, Lahey, GMH, & Uijt de Haag, PAM, "Zoning instruments for major accident prevention". *Proceedings of the International Conference on Probabilistic Safety Assessment and Management*, pp. 2191–2196. Crete, 1996.

Amundsen, FH, *Studies on the Norwegian Road Tunnels II. An analysis on traffic accidents in road tunnels 2001-2006*. Vegdirectoratet, Road and Traffic Department, Traffic Safety Section, 2009.

ANAS, Direzione Progettazione ANAS, *Italian Guidelines for Road Tunnel Safety*. Second edition, 2009.

Anderberg, Y & Thelandersson, S, "Stress and deformation characteristics of concrete at high temperatures, 2- Experimental investigation and material behaviour model" in: *Bulletin 54*, Lund Institute of Technology, Sweden, 1976.

API (American Petroleum Institute), *Risk-based Inspection Methodology - Recommended Practice 581*. Third Edition, April 2016.

Arhens, M, U.S. Vehicle Fire Trends and Patterns. NFPA Fire Analysis and Research Division, 2010.

Babrauskas, V, "Estimating Room Flashover Potential", *Fire Technology*, Vol. 16, no. 2, pp.94-104, 1980.

Beard, A & Carvel, R, *Handbook of Tunnel Fire Safety*. Second edition. ICE Publishing, London, 2012.

Bedford, T & Cooke, RM, *Probabilistic Risk Analysis: Foundations and Methods*. Cambridge University Press, New York, 2001.

Beitel, J, *Analysis of Needs and Existing Capabilities for Full-Scale Fire Resistance Testing*. NIST GCR 02-843-1, 2008.

Beitel, J & Iwankiw, N, *Analysis of Needs and Existing Capabilities for Full-Scale Fire Resistance Testing*. NIST GCR 02-843-1 (Revision), October 2008.

BMVBS/BAST (German Federal Ministry of Transport, Building and Urban Development/Federal Highway Research Institute), "Verfahren zur Kategorisierung von Strassentunnel gemass ADR 2007", BUNG Ingenierure AG, Ernst Basler+Partner, PTV AG, 2009 (in German).

Borchiellini, R, Verda, V, "A fuzzy logic procedure for ventilation control in case of fire in long tunnels", *Fire Safety Journal*, Vol. 44, pp. 612-621, ISSN: 0379-7112, 2009.

Bottelberghs, PH, Risk analysis and safety policy developments in The Netherlands, *Journal of Hazardous Material*, Vol. 71, pp. 59–84, 2000.

British Standards. BS EN 12101-6: Smoke and Heat Control Systems - Specification for Pressure Differential Systems-Kits, 2005.

Butcher, EG & Parnell, AC, *Smoke Control in Fire Safety Design*, E. and F.N. Spon Ltd, London, UK, 1979.

Caliendo, C & De Guglielmo, ML, "Accident Rates in road Tunnels and social Cost Evaluation", *Procedia: social & behavioral sciences*. Vol. 53, pp. 166-177. ISSN: 1877-0428, 2012.

Caliendo, C & De Guglielmo, ML, "A crash-prediction model for road tunnels", *Accident analysis and prevention*, Vol. 55, pp. 107-115. ISSN: 0001-4575, 2013.

Carvel R, *Fire size in tunnels*, PhD Dissertation, University of Edinburgh, UK, 2004.

Carvel, RO, Beard, AN & Jowitt, PW, "Fire Spread Between Vehicles in Tunnels: Effects of Tunnel Size, Longitudinal Ventilation and Vehicle Spacing". *Fire Technology*, Vol. 41, pp.271–304, 2005.

Carvel, R & Ingason, H, "Fires in vehicle tunnel". In: Hurley M.J. et al. (eds), *SFPE Handbook of Fire Protection Engineering*. Springer, New York, NY, 2016.

CETU, *Guide des dossiers de securitè des tunnels routiers-Fascicule 4: Les ètudes speécifiques des dangers*, 2003.

CETU, *Thematic Network Fire In Tunnels. Technical Report - Part 2*. Fire Safe Design, 2005.

Colella, F, Verda, V, Borchiellini R & Rein, G, "One-dimensional and multi-scale modelling of tunnel ventilation and fires". In: Carvel, R, Beard, A (eds) *Handbook of Tunnel Fire Safety*, Second edition. ICE Publishing, London, 2012.

Collier, PCR, *Car Parks-Fires involving modern cars and stacking systems*. BRANZ Study Report 255, BRANZ Ltd, Judgeford, New Zealand, 2011.

Commissione Permanente Gallerie, Consiglio Superiore dei Lavori Pubblico. *Relazione annuale al Parlamento – Interventi di adeguamento delle gallerie stradali realizzati nell'anno 2011 e previsti per l'anno 2012*. Rome, June 30th 2012.

Cosentino, S, Borchiellini, R, Lupinacci, F, Mejias, J & Verda, V, "Integrating 1D and 3D modeling for the analysis of ventilation control in tunnels", *ICHMT International Symposium on Advances in Computational Heat Transfer*, 28 May-01 June, Naples, 2017.

De Guglielmo, ML, *Rischio di incidente nelle gallerie stradali: applicazioni della Probabilistic Risk Analysis*. PhD Dissertation, University of Naples Federico II, Italy, 2007.

Decree of the Minister of the Interior 03 August 2015 Approval of Fire Prevention Technical Standards, 2015.

Decree of the President of the Republic August 1, 2011, no. 151. Regulations for simplified application of the discipline procedures relating to fire prevention activities (in Italian).

Directive 2004/54/EC on minimum safety requirements for tunnels in the trans-European road network. Official Journal of the European Union L 167, Brussels.

Di Santo, C, Risk Analysis for severe traffic accidents in road tunnels. Thesis Dissertation, Sapienza University of Rome, Italy, 2014.

Domenichini, L & Caputo, FJ, *Sicurezza in galleria*. Egaf, 2016.

Dwaikat, MB & Kodur ,VKR, "Hydrothermal model for predicting fire-induced spalling in concrete structural systems", *Fire Safety Journal* Vol. 44, no. 3, pp. 425–434, 2009.

EN 1992-1-2. Design of concrete structures. Part 1-2: general rules—structural fire design," Eurocode 2, European Committee for Standardization, Brussels, Belgium, 2004.

Federation International du Beton. Bulletin 38. Fire design of concrete structures- materials, structures and modelling.April 2007.

Federation International du Beton. Bulletin 46. Fire design of concrete structures- structural behavior and assessment.July 2008.

Focaracci A, "Italian Risk Analysis Method", *International Conference of Underground Construction*, Prague, 2010.

Frantzich, H, *Uncertainty and Risk Analysis in Fire Safety Engineering Department of Fire Safety Engineering and Systems Safety*, PhD Dissertation, Lund University, Sweden, 1998.

Frantzich, H & Nilsson, D, "Evacuation experiments in a road tunnel: A study of Human Behaviour and technical installations", *Fire Safety Journal*, Vol. 44, pp. 458-468, 2009.

Fruin J, *Pedestrian planning and design*. Metropolitan Association of Urban Designers and Environmental Planners, 1971.

FSV (Austrian Research Association Road-Rail-Traffic). Guideline RVS 09.03.1012. Risk Assessment of Dangerous Goods Transports in Road Tunnels, 2010.

Galea, ER, Xie, H & Lawrence, PJ, "Experimental and Survey Studies on the Effectiveness of Dynamic Signage Systems", *Proceedings of the 11th International Symposium on Fire Safety Science*, 2014.

Galea, ER, Sauter, G, Deere, S & Filippidis, L, "Investigating the impact of culture on evacuation response behavior", *Proceedings of 6th International Symposium of Human Behaviour in Fire*, London, UK, 2015.

Gehandler, J, "Road tunnel safety and risk: a review", *Fire Science Review* Vol. 4(2), 2015.

Grewolls, G & Grewolls, K, "Sensitivity analysis of evacuation simulations", *Process Engineering*, Issue 2, 2014.

Gross, H, "High-temperature creep of concrete", *Nuclear Engineering and Design*,Vol. 32, no. 1, pp. 129–147, 1975.

Hasemi, Y & Tokunaga, T, "Flame geometry effects on the buoyant plumes from turbulent diffusion flames". *Fire Science and Technology*, Vol.4, Issue 1, pp.15-26, 1984.

Helbing, D, Farkas, I & Vicsek, T, "Simulating dynamical features of escape panic", *Nature*, Vol. 407, September 2000.

Helbing, D & Molnar, P, "Social force model for pedestrian dynamics", *Physical Review E*., Vol.51, May 1995.

Hertz, K, *Simple temperature calculations of fire exposed concrete constructions.* Report n°159, Institute of Building and Design, Technical University of Denmark, 1981.

Heskestad, G, "Fire Plume Behaviour in Temperature-Stratified Ambients", *Combustion Science and Technology*. Vol. 106, Issue 4-6, pp. 207-228, 1995.

Hostikka, S, Paloposki, T, Rinne, T, Saari, JM & Korhonen, T, *Evacuation experiments in offices and public buildings*. VTT Working Papers no. 85, 2007.

HSE (Health and Safety Executive), *Risk criteria for land use planning in the vicinity of major industrial hazards.* HSE Books ISBN 0-11-885491-7, UK, 1989.

Ingason, H, "State of the Art of Tunnel Fire Research", *Fire Safety Science,* Vol. 9, pp. 33–48, 2008.

Institute of Chemical Engineering, *Nomenclature for hazard and risk assessment in the process industries*, Rugby, England: The Institution, 1985.

ITA-COSUF, *Updated survey of existing regulations and recognised recommendations (operation and safety of road tunnels)*, August 2011.

Italian Ministry of the Interior, Legislative Decree 2006/264 (Italian).

ISO 13571:2012. *Life-threatening components of fire -- Guidelines for the estimation of time to compromised tenability in fires*.

ISO 16733:2009. *Fire safety engineering — Selection of design fire scenarios and design fires — Part 1: Selection of design fire scenarios.*

ISO 16738:2009. *Fire-safety engineering — Technical information on methods for evaluating behaviour and movement of people*.

Jin, T, "Studies on Human Behaviour and Tenability in Fire Smoke", *Proceedings of the 5th International Symposium on Fire Safety Science*, pp. 3-21, 1997.

Jonkman, SN, van Gelder, PHAJM & Vrikling JK, "An overview of quantitative risk measures for loss of life and economic damage", *Journal of Hazardous Materials* Vol. 99, Issue 1, pp 1-30, 2003.

Khoury, GA, *Transient thermal creep of nuclear reactor concrete pressure vessel type concretes*, PhD Dissertation, University of London, UK, 1983.

Khoury, GA, Grainger, BN & Sullivan, PJ, "Strain of concrete during fire heating to 600°C", *Magazine of Concrete Research*, Vol. 37, no. 133, pp. 195–215, 1985.

Kodur V, "Properties of concrete at high temperatures", *Civil Engineering*, 2014. http://dx.doi.org/10.1155/2014/468510.

Korhonen, T & Hostikka, S, *Fire Dynamics Simulator with Evacuation: FDS+Evac. Techinical Reference and User's Guide*, VTT Technical Research Centre of Finland, 2009.

Krajewki, G &Wegrzynski, W, "Air curtain as a barrier for smoke in case of fire: numerical modelling", *Bulletin of the Polish Academy of Sciences, Technical Sciences*, Vol. 63, Issue 1, 2015. DOI: 10.1515/bpasts-2015-0016

Kuligowski, ED, Peacock, RD & Hoskins, BL, A *review of building evacuation models*. Second Edition. NIST Technical Note 1680, 2010.

Laheij, GMH, Post, JG & Ale, BJM, "Standard methods for land-use planning to determine the effects on societal risk", *Journal of Hazardous Material*, Vol. 71, pp. 269–282, 2000.

Lay, S, "Pressurization systems do not work and present a risk to life safety", *Case Studies in Fire Safety*, Vol. 1, pp. 13-17, 2014.

Lemke, K, "Road Safety in Tunnel", *Transportation Research Record: Journal of the Transportation Research Board*, Vol. 1740, 2000.

Maries, A, Haque, MA, Yilmaz, SL, Nik, MB & Marai, GE, "Interactive Exploration of Stress Tensors Used in Computational Turbulent Combustion", *New Developments in the Visualization and Processing of Tensor Fields*, Springer, pp. 137-156, D. Laidlaw, A. Villanova (editors), 2012.

McCaffrey, BJ, Quintiere, JG & Harkleroad, MF, "Estimating room fire temperatures and the likelihood of flashover using fire test data correlations". *Fire Technology*, Vol. 17, Issue 2, pp. 98-119, 1981.

McConnell, N & Boyce K, "Individual and group response behaviours during evacuation of a public house", *Proceedings of Interflam 2016*, Windsor, UK, 2016.

McGrattan, KB, et al, *Fire Dynamics Simulator (Version 6) Technical Reference Guide*, NIST Special Publication 1018-5, National Institute of Standards and Technology, Gaithersburg, USA, 2014.

McGrattan, KB, et al, *Fire Dynamics Simulator (Version 6) Users Guide*, NIST Special Publication 1019-5, National Institute of Standards and Technology, Gaithersburg, USA, 2014.

Meyer-Ottens, C, *The question of spalling of concrete structural elements of standard concrete under fire loading.* PhD Dissertation, Technical University of Braunschweig, Germany, 1972.

SRA (Society for Risk Analysis), *Glossary of Risk Analysis Terms*, McLean, VA, 2000.

Meng, Q & Qu, X, "Quantitative Risk Assessment Model for Fire in Road tunnels with parameter Uncertainty". *4th International Workshop of Reliable Engineering Computing*, 2010.

METRO Project, *Final Report*, Malardalen University Press, 2012.

Mokhatari, K, Ren, J, Roberts, C & Wang, L, "Application of a generic bow-tie based risk analysis framework on risk management of sea ports and offshore terminals", *Journal of Hazardous Materials*, Vol. 192(2), pp. 465-475, 2011.

NCHRP Synthesis 415, "Design Fires in Road Tunnels, A synthesis of highway practice", *Transportation Research Boards*, Washington 2011.

NFPA 101. Life Safety Code. National Fire Protection Association, Quincy, MA, 2015.

NFPA 502. Standard for Road Tunnels, Bridges and other Limited Access Highways. National Fire Protection Association, Quincy, MA, 2014.

NFPA 551. Guide for the evaluation of fire risk assessment, National Fire Protection Association, Quincy, MA, 2012.

NFPA 92. Standard for Control Smoke Systems, National Fire Protection Association, Quincy, USA, 2015.

Nigro, E, Pustorino, S, Cefarelli, G & Princi, P, *Progettazione di strutture in acciaio e composte acciaio-calcestruzzo in caso di incendio*, ISBN: 9788820344009, Hoepli, 2009.

Nussbaumer, C, "Comparative analysis of safety in tunnels", *Young Researchers Seminar*, Brno, 2007.

Persson, M. *Quantitative risk analysis procedure for the fire evacuation from a road tunnel-An illustrative example*. Report 5096, Lund 2002.

PIARC. Integrated approach to road tunnel safety. World Road Association. France, 2007.

PIARC. Risk analysis for road tunnels. World Road Association, France, 2008.

PIARC, Committee on Road Tunnels. "Road Safety in Tunnels", World Road Association. France, 1995.

PIARC, Technical Committee 3.3, Design Fire Characteristics for Road Tunnels, World Road Association. France, 2017.

PIARC, Technical Committee C.4, Current practice for risk evaluation for road tunnels, World Road Association. France, 2012.

PIARC, Technical Committee C.4, Road tunnels: vehicles emissions and air demand for ventilation, World Road Association. France, 2012.

Petelin, S, Luin, B & Vidmar P, "Risk analysis methodology for road tunnels and alternative routes", *Journal of Mechanical Engineering* Vol. 56, pp. 41-51, 2010.

Pope, SB. "Ten questions concerning the large-eddy simulation of turbulent flows", *New Journal of Physics*, Vol. 6, Issue 1, pp. 35, 2004.

Purser, D, "Application of human behaviour and toxic hazard analysis to the validation of CFD Modelling for the Mont Blanc Tunnel fire incident", *Proceedings of the Fire Protection and Life Safety In Buildings and Transportation Systems Workshop 2009*, Santander, SP, p23-p57, 2009.

Purser, DA, "Dependence of modelled evacuation times on key parameters and interactions", *Fire Safety Science*, 2008.

Purser, DA, "The Effects Of Fire Products On Capability In Primates And Human Fire Victims", *Fire Safety Science*, 1986.

QRAM Reference Manual, OECD/PIARC/EU, *Transport of Dangerous goods through road tunnels Quantitative Risk Assessment Model (v. 3.60 and v. 3.61). User's Guide*, Research Report n. 20504, December 2005.

Qu, X & Meng Q, "Quantitative Risk Assessment Modeling for Nonhomogeneous Urban Road Tunnels", *Risk Analysis*, October 2010.

RABT - FGSV (German Research Association for roads and traffic), Guidelines for Equipment and Operation of Road Tunnels, 2006.

Report DCPST, Corpo Nazionale dei Vigili del Fuoco, 2016.

Report DCPST, Corpo Nazionale dei Vigili del Fuoco, 2017.

Rinne, T, Tillander, K & Grönberg, P, *Data collection and analysis of evacuation situations*. VTT Research Note 2562, 2010.

Riva, P, "Nonlinear and Plastic Analysis of RC Concrete Beams", *Proceedings Workshop Fire Design of Concrete Structures: What not? What next?,* Milan, 2-4 December 2004.

Ronchi, E, Alvear, D, Berloco, N, Capote, J, Colonna, P & Cuesta, A, "Human behaviour in road tunnel fires: comparison between egress models (FDS+Evac, Steps, Pathfinder)", *Proceedings of 12th Interflam Conference*, Nottingham, UK, 2010.

Ronchi, E, Kuligowski, E, Reneke, PA, Peacock, RD & Nilsson D, *The process of verification and validation of building fire evacuation models*. NIST Technical Note 1822, November 2013.

Ronchi, E, "Testing the predictive capabilities of evacuation models for tunnel safety analysis", *Safety Science*, Vol. 59, pp. 141-153, 2013.

Ronchi, E, "A research roadmap for evacuation models used in fire safety engineering", *Proceedings of Fire and Evacuation Modeling Technical Conference 2016,* Torremolinos, Spain, 2016.

SAFESTAR, *Safety Standards for Road Design and Redesign*, Final Report. 2002.

Salvisberg, U, Allenbach, R, Hubacher, M, Cavegn, M &Siegrist, S, *Report UPI n. 51*, Ufficio Svizzero per la prevenzione degli Infortuni, Berna 2004.

Sargant, T., Nightingale, S, Young, OD & Ganeshalingam, J, "Evacuation modelling in road tunnel fire events, CFD influencing evacuation results", *Proceedings of Fire and Evacuation Modeling Technical Conference 2014*, Gaithersburg, Maryland, September 8-10, 2014.

Schröder, B, *Multivariate Methods for Life Safety Analysis in Case of Fire*, PhD Dissertation, Wuppertal University, Germany, 2016.

SFPE Handbook of Fire Protection Engineering, Fifth Edition, 2016.

Shields, J, "Human behaviour during tunnel fires". In: Carvel R, Beard A (eds) *Handbook of Tunnel Fire Safety, 2nd edition*. ICE Publishing, London, pp. 399–420, 2012.

Soons, CJ, Bosch, JW, van Gelder, PHAJM & Vrijling, JK, Improvement of QRA for tunnel safety by comparing QRA used in other engineering fields. *Safety and Reliability for Managing Risk*, Guedes Soares & Zio (eds), 2006.

SWOV, Institute for Road Safety Research, *The road safety of motorways tunnels*. Swov Fact Sheet. Netherlands, 2009.

Thomas, PH, "Testing Products and Materials for their contribution to flashover in rooms". *Fire and Materials*, Vol. 5, Issue 3, pp. 103-111, 1981.

Thompson, P, Nilsson, D, Boyce, K, McGrath, D & Molloy, M, "Exploring the biomechanics of walking and crowd flow". *Proceedings of Human Behaviour in Fire 2015*, Cambridge (UK), September 2015.

Thunderhead Engineering, *Pathfinder Technical References*, 2016.

Thunderhead Engineering, *Pathfinder User Manual*, 2016.

Van Dyke, M, *An album of fluid motion*, Stanford University, 1982.

Vrijling, jk, van Gelder, phajm, "Societal risk and the concept of risk aversion", In: C. Guedes Soares (Ed.), *Advances in Safety and Reliability*, Vol. 1, Lisbon, pp. 45–52, 1997.

Watts Jr., JM & Hall Jr, JR, "Introduction to Fire Risk Analysis". In: *SFPE Handbook of Fire Protection Engineering 2016*, Fifth Edition, 2016.

Xie, H, Filippidis, L, Galea, ER, Blackshields, D, Lawrence, PJ, "Experimental analysis of the effectiveness of emergency signage and its implementation in evacuation simulation", *Fire and Materials*, Vol. 36, pp. 367-382, 2012.

Zhang, J & Seyfried, A, "Empirical characteristics of different types of pedestrian streams", *Procedia Engineering* Vol. 62, 655-662, 2012.